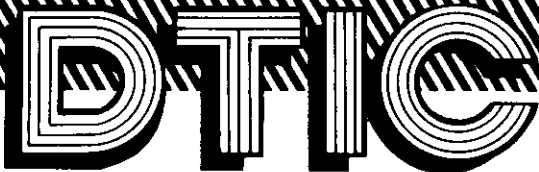


Doc  
FAA  
AM  
79  
17

UNCLASSIFIED



# Technical Report

distributed by



**Defense Technical Information Center  
DEFENSE LOGISTICS AGENCY**

Cameron Station • Alexandria, Virginia 22314

UNCLASSIFIED

# **NOTICE**

We are pleased to supply this document in response to your request.

The acquisition of technical reports, notes, memorandums, etc., is an active, ongoing program at the Defense Technical Information Center (DTIC) that depends, in part, on the efforts and interests of users and contributors.

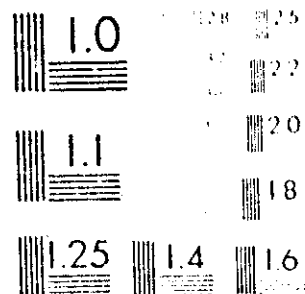
Therefore, if you know of the existence of any significant reports, etc., that are not in the DTIC collection, we would appreciate receiving copies or information related to their sources and availability.

The appropriate regulations are Department of Defense Instruction 5100.38, Defense Technical Information Center for Scientific and Technical Information (DTIC); Department of Defense Instruction 5129.43, Assignment of Functions for the Defense Scientific and Technical Information Program; Department of Defense Directive 5200.20, Distribution Statements on Technical Documents; Military Standard (MIL-STD) 847-A, Format Requirements for Scientific and Technical Reports Prepared by or for the Department of Defense; Department of Defense Regulation 5200.1-R, Information Security Program Regulation.

Our Acquisition Section, DTIC-DDA-1, will assist in resolving any questions you may have. Telephone numbers of that office are: (202) 274-6847, 274-6874 or Autovon 284-6847, 284-6874.

1 OF 3

AD  
A074 881



WILFRED A. GOLDBECK, INC., 1968

DOC FILE COPY

AD-A074881

FAA-AM-79-17

LEVEL

B.S.

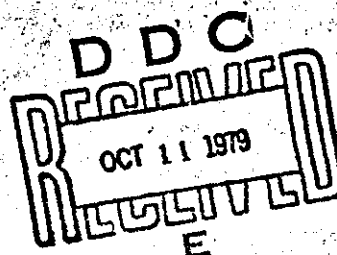
EVALUATION OF SEATING AND RESTRAINT SYSTEMS  
CONDUCTED DURING FISCAL YEAR 1978

Richard F. Chandler

and

Edwin M. Trout

FAA Civil Aeromedical Institute  
Oklahoma City, Oklahoma



June 1979

Document is available to the public through the  
National Technical Information Service,  
Springfield, Virginia 22131.

Prepared for  
U.S. DEPARTMENT OF TRANSPORTATION  
Federal Aviation Administration  
Office of Aviation Medicine  
Washington, D.C. 20591

NOTICE

This document is disseminated under the sponsorship of the Department of Transportation in the interest of information exchange. The United States Government assumes no liability for its contents or use thereof.

(11) 77-17

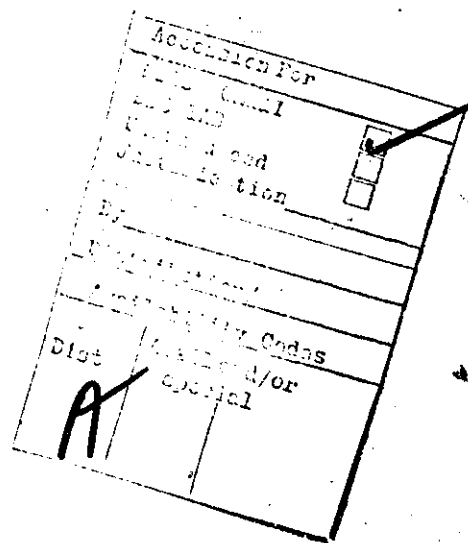
Technical Report Documentation Page

|  |  |   |           |
|--|--|---|-----------|
| 1. Report No.<br>FAA-AM-79-17  | 2. Government Accession No.                          | 3. Recipient's Catalog No.  |           |
| 4. Title and Subtitle<br><b>EVALUATION OF SEATING AND RESTRAINT SYSTEMS CONDUCTED DURING FISCAL YEAR 1978</b>  |  | 5. Report Date  |           |
| 6. Author(s)<br>Richard F. Chandler and Edwin M. Trout   |  | 6. Performing Organization Code   |           |
| 7. Performing Organization Name and Address<br>FAA Civil Aeromedical Institute<br>P.O. Box 25082<br>Oklahoma City, Oklahoma 73125  |  | 8. Performing Organization Report No.   |           |
| 9. Sponsoring Agency Name and Address<br>Office of Aviation Medicine<br>Federal Aviation Administration<br>800 Independence Avenue, S.W.<br>Washington, D.C. 20591   |  | 10. Work Unit No. (TRAIL)   |           |
| 11. Contract or Grant No.  |  | 12. Type of Report and Period Covered   |           |
| 13. Supplementary Notes<br>Research reported was conducted under Task AM-B-78-PRS-47.  |  | 14. Sponsoring Agency Code  |           |
| 15. Abstract<br><p>This report summarizes the results of test programs conducted by the Protection and Survival Laboratory to investigate the performance of prototype or operational seating and restraint systems relative to their ability to provide protection against crash injury and to validate the performance of the FAA Seat Occupant Model: Light Aircraft (SOMLA).</p> <p>Most of the data in this report were previously presented as the final quarterly progress report for Task AM-B-78-PRS-47 and are subject to additional evaluation or change on review, conduct of additional testing, or receipt of additional facts.</p> <p>(11) JUN 1978</p> |  |   |           |
| 17. Key Words<br>Seats<br>Restraints<br>Aircraft<br>Anthropomorphic dummies  |  | 18. Distribution Statement<br>Document is available to the U.S. public through the National Technical Information Service, Springfield, Virginia 22161. |           |
| 19. Security Classif. (of this report)<br>Unclassified   | 20. Security Classif. (of this page)<br>Unclassified | 21. No. of Pages<br>225   | 22. Price |

024 030

TABLE OF CONTENTS

|  | <u>Page</u> |
|--|-------------|
| INTRODUCTION   | 1           |
| METHOD   | 1           |
| ELECTRONICS INSTRUMENTATION  | 2           |
| PHOTOGRAPHIC INSTRUMENTATION   | 2           |
| SEAT OCCUPANT MODEL: LIGHT AIRCRAFT (SOMLA)  | 4           |
| AFTERMARKET TYPE UPPER TORSO RESTRAINT SYSTEM  | 5           |
| LOW-ELONGATION WEBBING   | 9           |
| ARMY ENERGY-ABSORBING SEAT   | 10          |
| REFERENCES   | 11          |
| <b>APPENDIX A. RESULTS OF STATIC AND DYNAMIC TESTS FOR VALIDATION<br/>OF THE FAA SEAT OCCUPANT MODEL: LIGHT AIRCRAFT<br/>(SOMLA) - SERIES I.</b> | 12          |
| RESULTS OF STATIC AND DYNAMIC TESTS FOR VALIDATION<br>OF THE FAA SEAT OCCUPANT MODEL: LIGHT AIRCRAFT<br>(SOMLA) - SERIES II.                     | 57          |
| <b>APPENDIX B. RESULTS OF DYNAMIC TESTS OF AN AFTERMARKET SHOULDER<br/>HARNESS</b>   | 101         |
| <b>APPENDIX C. RESULTS OF LOW-ELONGATION WEBBING EVALUATIONS</b>   | 150         |



EVALUATION OF SEATING AND RESTRAINT SYSTEMS  
CONDUCTED DURING FISCAL YEAR 1978

INTRODUCTION

This report summarizes the results of test programs conducted by the Protection and Survival Laboratory to investigate the performance of prototype or operational seating and restraint systems relative to their ability to provide protection against crash injury and to validate the performance of the Seat Occupant Model: Light Aircraft (SOMLA).

METHOD

The system evaluations were conducted on the Civil Aeromedical Institute (CAMI) test track. This is an impact test device capable of producing a controlled deceleration pulse that can be programmed to produce decelerations between 2 and 50 g, as required for a specific test. The device consists of a test sled that carries the test item along two 150-ft-long (46-m) horizontal rails, an accelerating device that brings the sled up to the desired impact velocity, and a sled braking device that produces the desired impact pulse. Modifications to the facility completed in FY-78 increased the maximum energy that can be imparted to the sled by about 68 percent, from 108,000 ft-lb to 182,400 ft-lb (153 kJ to 250 kJ).

The sled is a flat-topped steel truss on which the test item is mounted. By the use of adapters, a variety of test items can be attached to the sled so that the impact vector, which lies in a horizontal plane, can act on the test item in the desired direction. The sled is equipped with low-friction rollers that guide it along the rails of the track with minimal energy loss.

Velocity is imparted to the sled by an accelerating device that includes a 6,500-lb (2,900-kg) weight, a cable system with a 4-to-1 mechanical advantage attached between the sled and the weight, and a winch cart that can be positioned and locked at any point along the track. The winch cart retracts the sled and locks it into the "ready" position just prior to the test and, simultaneously, it lifts the weight. As the weight is lifted, potential energy is stored in the system and is subsequently used to accelerate the sled and test item to the desired impact velocity. A maximum of 182,000 ft-lb (250 kJ) of energy can be stored that can accelerate the sled and payload to velocities of up to 50 mi/h (80 km/h), depending on the payload weight. To accomplish the test, the sled is released from its locked position, is accelerated along the track by the falling weight, is allowed to coast without acceleration for a predetermined distance after the weight is stopped, and then contacts the braking device which produces the desired impact pulse.

The braking device is a "metal bender" form of energy absorber. This device uses two layers of No. 3 gage wires that are plastically deformed as

they are pulled over rollers by the sled and thus absorb energy to provide the required braking force. The wires are cut to length with sufficient allowance to provide a safety factor above displacement required by the sled during the impact. The wire size and the diameter of the rollers over which it passes were selected to generate a nominally required force of 2,500 lb (11 k N) to pull the wire through the rollers. The braking device holds two layers of 43 wires and is thus capable of generating a maximum braking force of 215,000 lb (940 k N). The deceleration-time history of the sled can be precisely controlled by selecting the number of wires placed in the braking device and adjusting the position at which they are contacted by the sled. The total deceleration distance is not limited by this braking device.

Component evaluations were conducted on specially built equipment that met the provisions of the specifications describing those tests.

#### ELECTRONICS INSTRUMENTATION

The electronics instrumentation system used by the Protection and Survival Laboratory for dynamic testing was designed for maximum versatility and reliability. Special provisions have been made for using strain gage bridge-type transducers. This type of transducer is available in many models and has proved to be reliable for measuring strain, acceleration, pressure, forces, and low frequency vibrations.

Signals are transmitted from transducers on the sled or test item to signal conditioners through a loose, flexible cable that is attached at one end to the sled. The signal conditioners (Endevco model 4470/4476.2) provide excitation to the transducers (3 to 10 V dc), amplify the signal, provide low-pass filtering if required, and provide resistance shunt calibration for each transducer through the entire data-recording system.

Outputs from the signal conditioners modulate subcarrier oscillators of a constant-bandwidth high frequency multiplexer system. The composite output from the multiplexer system is recorded on wideband analog tape that serves as primary data storage. The magnetic tape data are then reproduced through appropriate discriminators for recording on an oscillographic recorder (for quick-look analysis) or digitized and recorded on high-density digital tape for automatic data processing. Final data are processed in accordance with the requirements of Society of Automotive Engineers (SAE) Recommended Practice J211b, Instrumentation for Impact Tests, unless a specialized requirement exists.

#### PHOTOGRAPHIC INSTRUMENTATION

All dynamic tests are photographically recorded for technical documentation and for data collection. Instrumentation-quality 16-mm cameras of various types are operated with film speeds of 500 pictures/s (pps) or 1,000 pps to provide the necessary coverage with the required fields of view.

Color film is used in all cameras and processed at CAMI for maximum picture quality. Synchronization of all cameras with the electronics instrumentation system and timing of all film is provided; both serial-coded pulses (IRIG-A or IRIG-B\*) and numerical display are available on the film edge. Cameras and lighting are controlled by a 42-channel programing system that enables obtaining optimum frame rates during the impact event and prevents damage to the test specimen by the high-intensity lighting necessary for proper exposure. Film data are extracted and analyzed by using a Hewlett-Packard 9820 data system to digitize, store, analyze, and plot data as required.

\*Inter-Range Instrumentation Group

STATIC AND DYNAMIC TESTS FOR VALIDATION OF THE  
FAA SEAT OCCUPANT MODEL: LIGHT AIRCRAFT

The second series of tests to validate the Seat Occupant Model: Light Aircraft (SOMLA) program was accomplished using a rigid seat with deformable tubular legs. The purpose of this test series was to evaluate the ability of the model to predict seat structural response in the presence of localized deformation that changed the cross section of critical structural elements. To achieve this goal, the rigid test seat was constructed so that the tubular legs were fixed in place with a clamping system that provided a high "end fixity." The foot end of the legs was pin-joined to the floor structure to provide low "end fixity" in the x-z plane of the tests. Because the technique of clamping the legs in place used precision draw collets, it was not possible to control the length of the leg to a predrilled pinhole. Consequently the pinholes were located and drilled after the legs were clamped in place, using special tooling and the pin fittings on the sled for control. In this manner it was possible to achieve a seat structure that was not prestressed by the installation on the sled.

Eight static tests and 58 dynamic tests were completed in the forward-facing (-G<sub>x</sub>) orientations and with the floor angled at 60° to provide a downward and forward occupant reaction. Deceleration levels of 5.4 g and 9.5 g provided minimal plastic deformation (without significant cross section change) and marked plastic deformation (with localized buckling and cross section change at the fixed end), respectively, in the -G<sub>x</sub> orientation. In the tests with the floor angled, deceleration levels of 13.5 g and 22 g were required to produce similar results. Each test was repeated 10 times so that the results could be combined to yield a mean and standard deviation time history. Measurements of head, chest, and pelvis acceleration; seatbelt and shoulder belt loads; floor loads; and seat displacement were obtained. The results are presented in Appendix A, Figures A-1 through A-8.

## PERFORMANCE OF AN AFTERMARKET SHOULDER HARNESS

Owners of general aviation aircraft are sometimes reluctant to install a shoulder harness (upper torso restraint) in their aircraft because of the cost and complexity associated with modifying the airframe to provide an attachment point for the shoulder harness. Thus they do not benefit from the well-documented advantages of upper torso restraint during a crash. This problem could be alleviated if a proper shoulder harness could be installed without modifying the aircraft. One approach to this solution consists of a V-type shoulder harness with sewn loops at the apex and tips of the V. The rear seatbelt is passed through the loop at the apex of the V to secure the shoulder harness in the aircraft. The front (occupant) seatbelt is passed through the loops at the tips of the V and is then latched and adjusted in the normal manner. Adjusters are provided in each strap of the shoulder harness system so that it may be adjusted independently of the front or rear seatbelts.

Two aspects of this system warranted study. As in all systems in which the shoulder belts are attached near the center of the seatbelt (without negative "g" strap), the possibility exists that the seatbelt may be pulled from the pelvic skeleton into the abdominal area (submarining) with resultant soft tissue and spinal column injury. Also, if the downward angle of the shoulder harness causes compressive loads that act on the spinal column, vertebral fracture may occur. The importance of these two aspects depends on several factors of system installation and usage and on the events of the crash. In general, the potential for submarining may be influenced by seatbelt angles, softness or deformation of the seat structure or cushion under load, the lengths of belt webbing that stretch under load and can alter the geometry of the installation, and the positioning and adjustment of the restraint system by the user. In addition to the angle of the shoulder belt, vertebral column loading can be influenced by the above factors as well as the ability of the seat back to absorb the vertical component of the shoulder belt load, the tendency of the body to flex under the restraint, and the magnitude of the vertical component of loading that exists in the crash. Human tolerance to vertebral injury is influenced by age and spinal abnormalities that may exist.

To evaluate the performance and potential problems that might exist with this restraint, a brief series of controlled impact tests were completed. The tests were accomplished in a forward-facing (-Gx) orientation, using a general aviation (Piper) seat mounted on a rigid framework that not only supported the seat but provided attachment points for an aft seatbelt. A 50th-percentile anthropomorphic dummy weighing approximately 170 lb was used in all tests. The feet of the dummy rested on a flat plywood floor and were unrestrained. Instrumentation included accelerometers in the dummy and on the test sled and webbing load cells on the webbing of the restraint system. The general arrangement for these tests is shown in Figure 1. Three conditions of the restraint were evaluated in this series. Tests 059, 060, and 061 considered

the condition where the front seatbelt was short and attached to the seat frame. This created a seatbelt loop length of about 39 in when the webbing was snugly adjusted against the dummy.

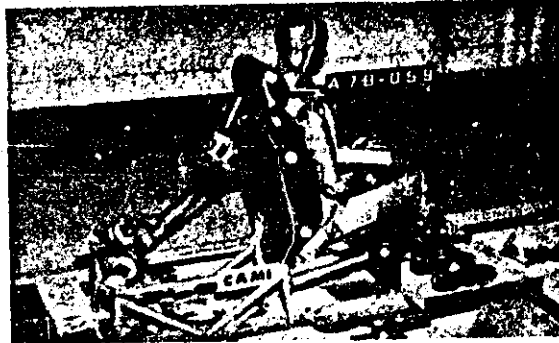


Figure 1. General test arrangement.

Tests 062 and 063 maintained the same general configuration but attached the seatbelt to the floor so as to provide a seatbelt loop length of about 70 in. The rear seatbelt attachment was unchanged. These tests were included to evaluate the effect of the longer seatbelt used in some aircraft. Finally, Tests 064, 065, and 066 evaluated this same configuration but with a somewhat loose restraint system (76-in seatbelt loop length). These tests were included to evaluate the effect of a slack restraint system, often encountered in the field even though it is generally considered to increase the potential of injury in a crash.

The seat pan membrane was found to be torn after Test 060. This membrane consisted of a thin moulded rubber sheet attached to the seat frame by hooks fitted into reinforced holes in the sheet. The membrane was replaced by a web of nylon seatbelt webbing attached to the hoods via anchor fittings and tensioned by a webbing adjuster mechanism. The webbing was brought sufficiently tight so that no subject difference was noted when compared to the moulded membrane (Figure 2).

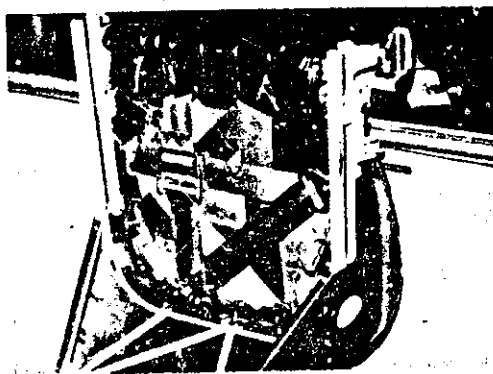


Figure 2. View of seat pan showing webbing which replaced seat pan membrane after Test 060.

The results of these tests are shown in Table 1.

TABLE 1. Test Results

| Test No. | G  | Lapbelt Load (lb) | Shoulder Belt Load (lb) | Head Forward (in) |
|----------|----|-------------------|-------------------------|-------------------|
| 059      | 6  | 950               | 700                     | 18                |
| 060      | 10 | 1,750             | 1,450                   | 18                |
| 061      | 14 | 2,200             | 1,800                   | 21                |
| 062      | 10 | 1,800             | 1,400                   | 21                |
| 063      | 14 | 2,200             | 1,900                   | 21                |
| 064      | 6  | 1,100             | 900                     | 24                |
| 065      | 10 | 1,850             | 1,550                   | 28                |
| 066      | 14 | 2,200             | 2,050                   | 25                |

The results of these tests indicate that 18 to 28 in of forward head motion could be expected when the restraint is used under the conditions of the test. During this movement the head bowed forward and down. The motion was most severe with the loose restraint system. Submarining also appeared imminent at the higher impact loads when the restraint was loose.

The spinal column load generated by the downward angle of the shoulder belt attachment to the lapbelt was estimated using the high-speed motion picture coverage of the tests. The angle between the shoulder belt and the estimated position of the spinal column was measured and used to calculate the component of belt load which would be generated along the axis of the spinal column. Since the seat back folded forward in the tests, it did not carry significant loading from the shoulder belt and was ignored for these computations. The results of these computations are shown in Figure 3. The open symbols in this figure refer to the component of spinal compressive load resulting from the aft portion of the shoulder belt; the closed symbols indicate the maximum total spinal compressive load that would exist if the shoulder belt load were carried, without frictional loss, over the shoulder to the lapbelt, and if that load were parallel to the spinal column. This condition was approximated during the tests. The actual spinal compressive load should fall between these extremes.

The ability of the spinal column to carry compressive load is dependent on several factors influenced by both human and crash conditions. A complete discussion of these conditions can be found in the references, but for the purpose of this report it is sufficient to note that the compressive strength varies from about 300 to 2,800 lb if normal spinal curvature is maintained. This is a severe limiting condition and was not attained in these tests. If the spinal column is flexed, the ability to carry load is greatly reduced. Although quantitative data are not generally available, best estimates indicate that the ability of the spinal column to carry compressive loading will be reduced by a factor of 3 to 5 if the column is flexed (1). Thus,

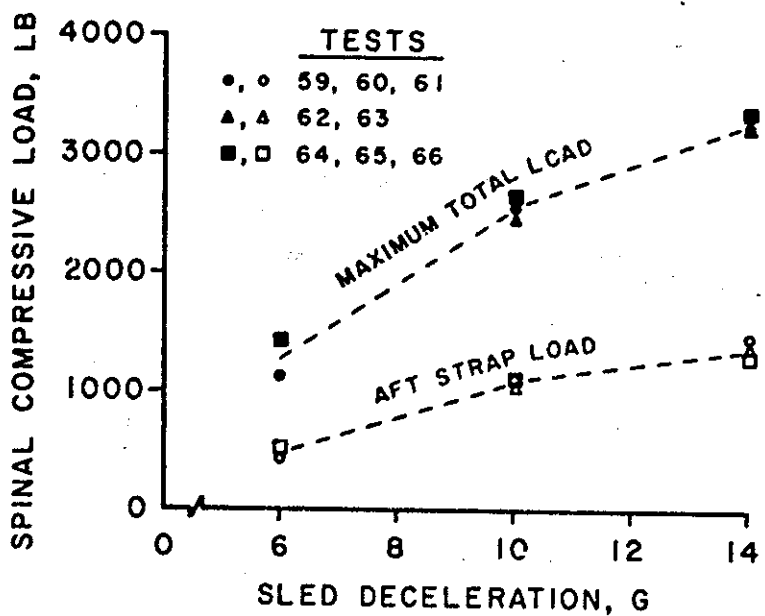


Figure 3. Results of computations of test results.

under the conditions of the tests, the spinal column could be expected to carry a compressive load, without fracture, which varies from a low tolerance of 60 lb to a maximum tolerance of 930 lb. It would be expected that elderly users of the restraint system would be most subject to injury (2,3). It should be noted that a vertical component of direct crash loading, not present in our tests but commonly present in aircraft crashes, would make injury even more likely.

Use of this restraint system should be judged on the availability of sufficient clearance in front of the body for head motion and on the option of possibly reducing head and facial injury at the expense of increasing the probability of vertebral fracture. Both of these injuries could be life-threatening or, if survivable, may cause lasting impairment.

The results of these tests are presented graphically in Appendix B, Figures B-1 through B-8.

#### EVALUATION OF THE PERFORMANCE OF LOW-ELONGATION WEBBING

Samples of 2-in-wide Kevlar webbing and low-elongation polyester webbing were used to construct a four-point restraint system. This system was then tested in a rigid seat with 90° seat back angle (4). Both static webbing and dynamic restraint system tests were conducted. Although these stiffer webbing systems performed well in the dynamic tests, an unusually severe cyclic pattern was noted in the restraint webbing load data with two pronounced load peaks of almost equal magnitude. This was confirmed by high-speed photoinstrumentation, which showed two obvious displacement cycles of the upper torso relative to the seat. The reason for this unusual performance is not yet known but may be related to the high spring constant provided by the webbing, especially when coupled to a rigid seat.

Fabrication and use problems were noted with the Kevlar webbing. This material was found to be relatively difficult to cut as it was being fabricated and slippage was noted in the webbing adjuster mechanism. This last problem may be rectified by the use of adjusters designed specifically for the Kevlar material, rather than the standard assemblies used for these tests. Inasmuch as there is no significant difference in performance between the low-elongation polyester webbing and the Kevlar webbing, the polyester webbing, which permits the use of conventional hardware and can be fabricated by conventional methods, holds greater potential for further development.

The results of these tests are presented in Appendix C, Figures C-1 through C-3.

#### USAARL ENERGY-ABSORBING HELICOPTER SEAT TESTS

Two tests were conducted on the fourth evaluation of a prototype two-passenger helicopter seat in cooperation with the U.S. Army Aeromedical Research Laboratory (USAARL) (3). Tests were conducted in the lateral orientation at 16 g and in the 30° yaw orientation at 24 g. Failures occurred under both conditions, the most serious of which was the failure of the stock floor anchorage fittings on the seats. These fittings use a ring of "fingers" which grasp a "button head" mounted on the floor. The fingers are locked in place by a spring-loaded collar, arranged so that lifting the collar releases the fingers so that the seat can be removed. The fingers failed while under load. These failures may have been aggravated by slack in the stainless steel cable system that goes between the seat back and the floor and is designed to absorb the lateral component of the seat load. One of these cables also failed during the 30° yaw test.

#### REFERENCES

1. Kazarian, L., and G. A. Graves, Jr.: Compressive Strength Characteristics of the Human Vertebral Column, SPINE, Vol. 2, No. 1, March 1977.
2. Henzel, J. H.: The Human Spinal Column and Upward Ejection Acceleration: An Appraisal of Biodynamic Implications. AMRL-TR-66-233, Wright-Patterson AFB, Ohio, September 1967.
3. Perey, Olaf: Fracture of the Vertebral End Plate in the Lumbar Spine, ACTA ORTHOP. SCAND., Supplement No. SSV, 1957.
4. Chandler, R. F., and E. M. Trout: Evaluation of Seating and Restraint Systems and Anthropomorphic Dummies Conducted During Fiscal Year 1977. FAA Office of Aviation Medicine Report No. FAA-AM-78-24, June 1978.

## APPENDIX A.

### RESULTS OF STATIC AND DYNAMIC TESTS FOR VALIDATION OF THE FAA SEAT OCCUPANT MODEL: LIGHT AIRCRAFT (SOMLA) - SERIES I AND II.

#### Figure No.

|           | <u>page</u>                                  |    |
|-----------|--|----|
| Series I  |  |    |
| A-1       | Forward-facing, low-deceleration tests.      | 13 |
| A-2       | Forward-facing, higher deceleration tests.   | 24 |
| A-3       | Combined loading, low-deceleration tests.    | 35 |
| A-4       | Combined loading, higher deceleration tests. | 46 |
| Series II |  |    |
| A-5       | Forward-facing, low-deceleration tests.      | 57 |
| A-6       | Forward-facing, higher deceleration tests.   | 68 |
| A-7       | Combined loading, low-deceleration tests.    | 79 |
| A-8       | Combined loading, higher deceleration tests. | 90 |

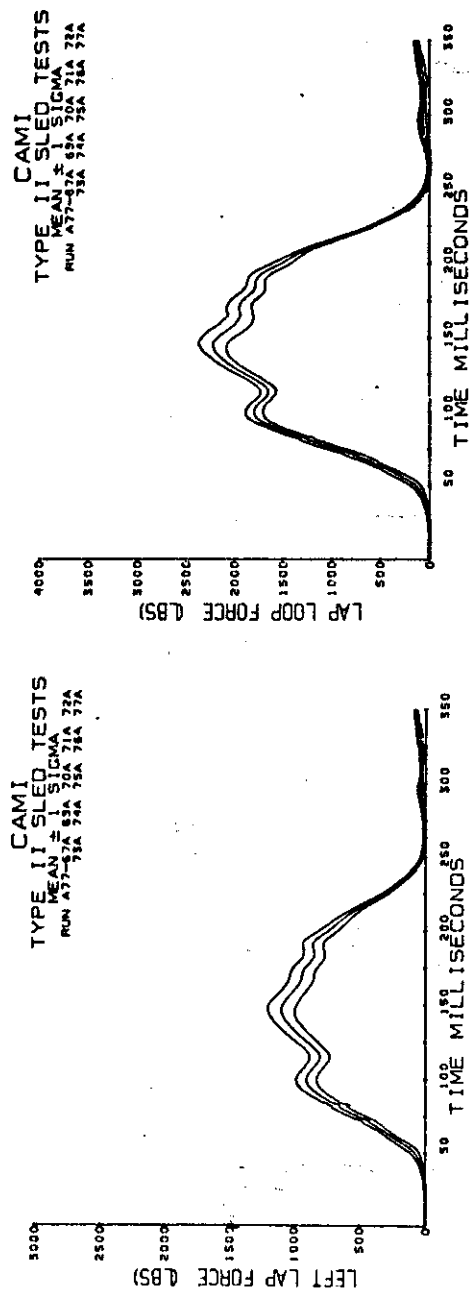
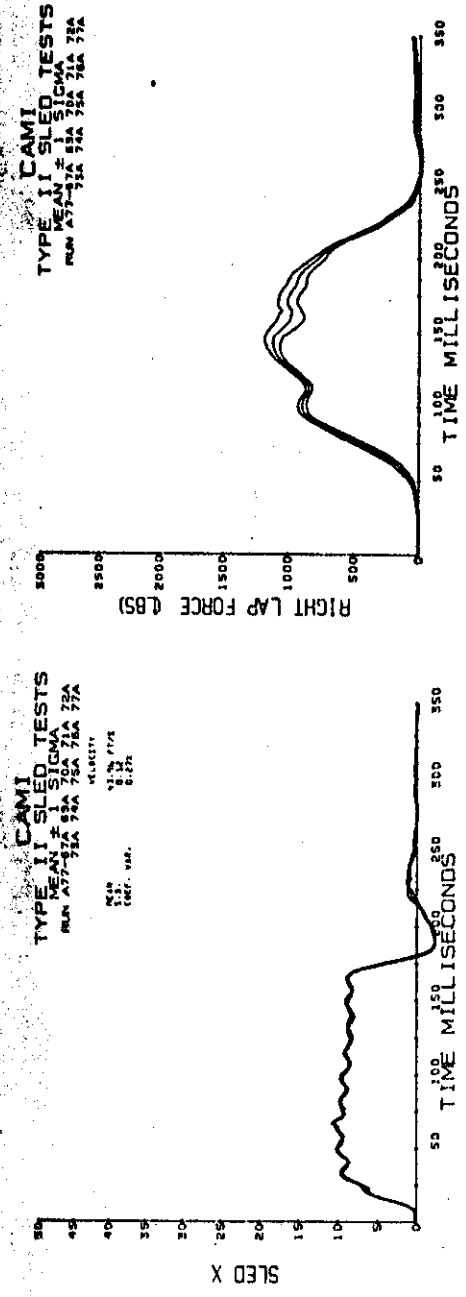


**Figure A-1.** Forward-facing, low deceleration tests.  
Sled deceleration and lapbelt loads.

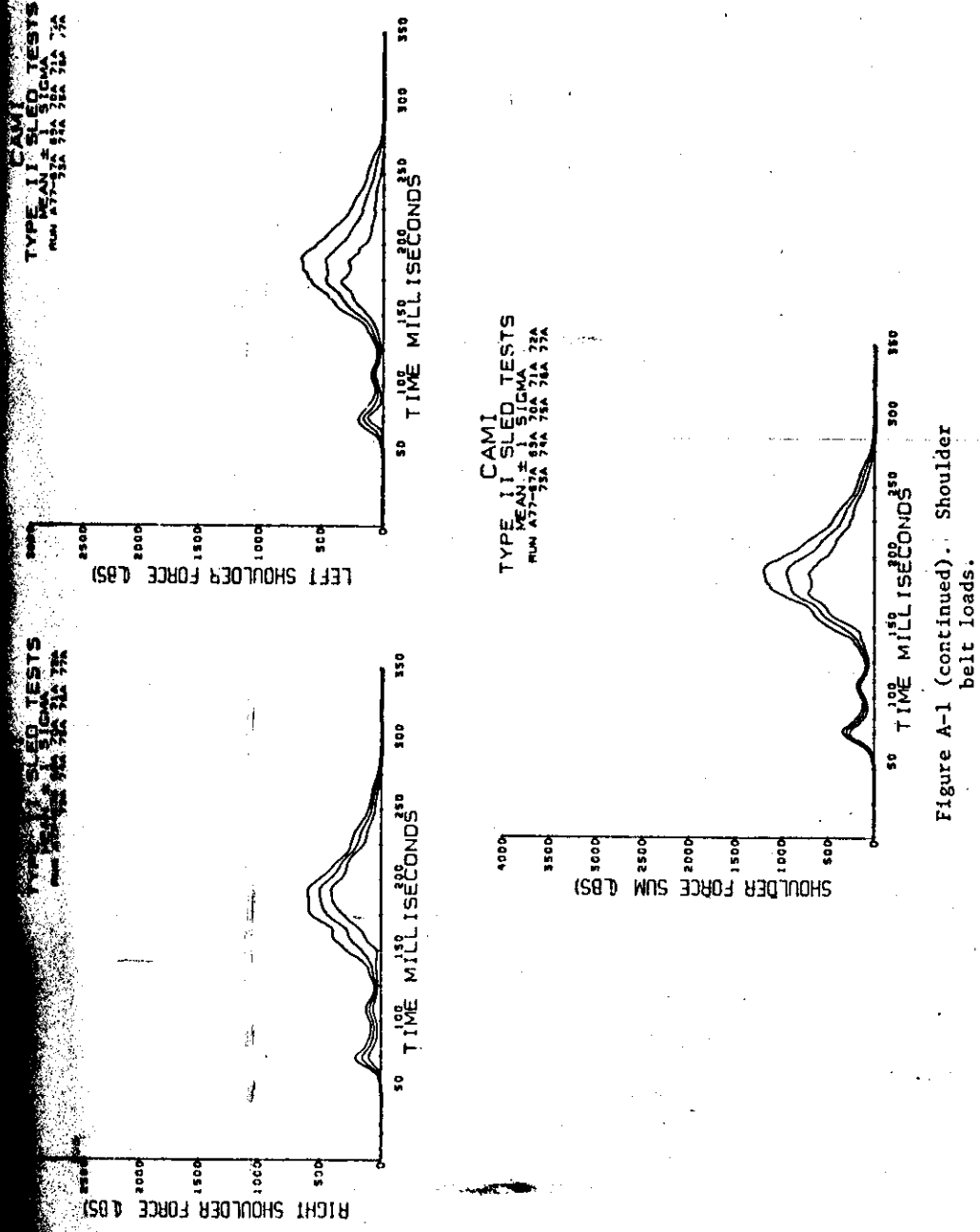


Figure A-1 (continued). Shoulder belt loads.

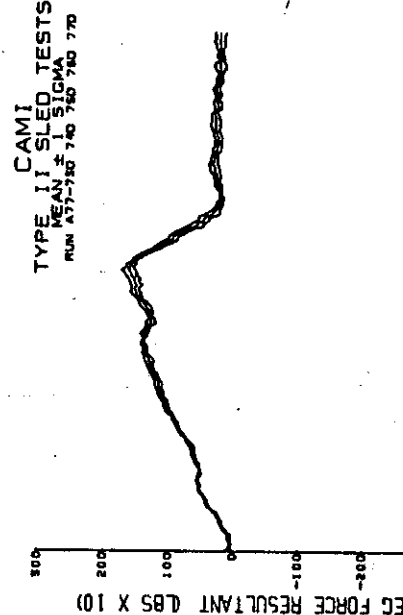
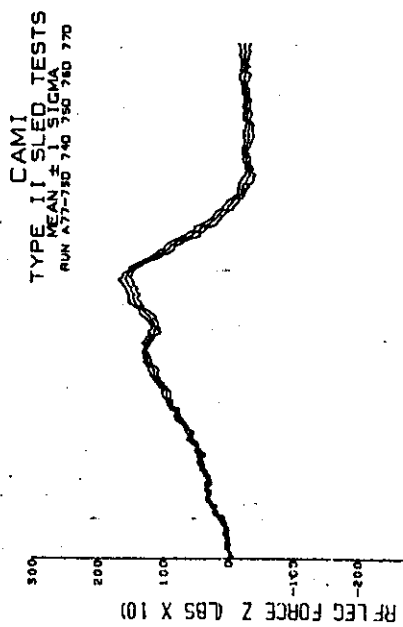
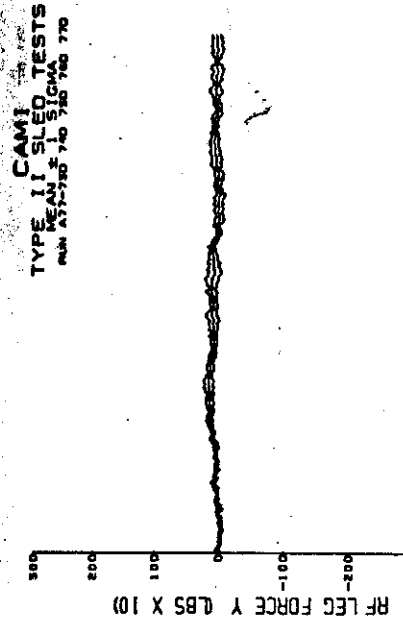
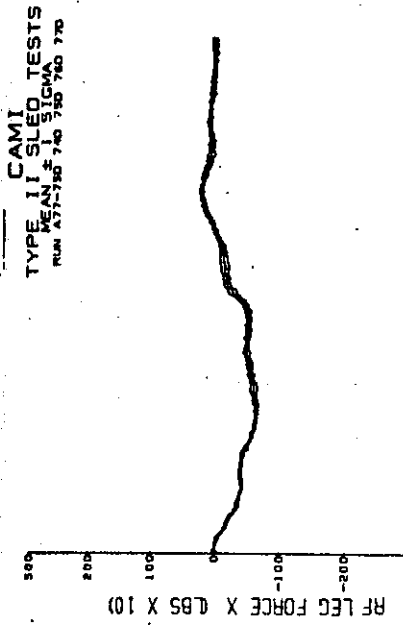


Figure A-1 (continued). Right front seat leg loads.

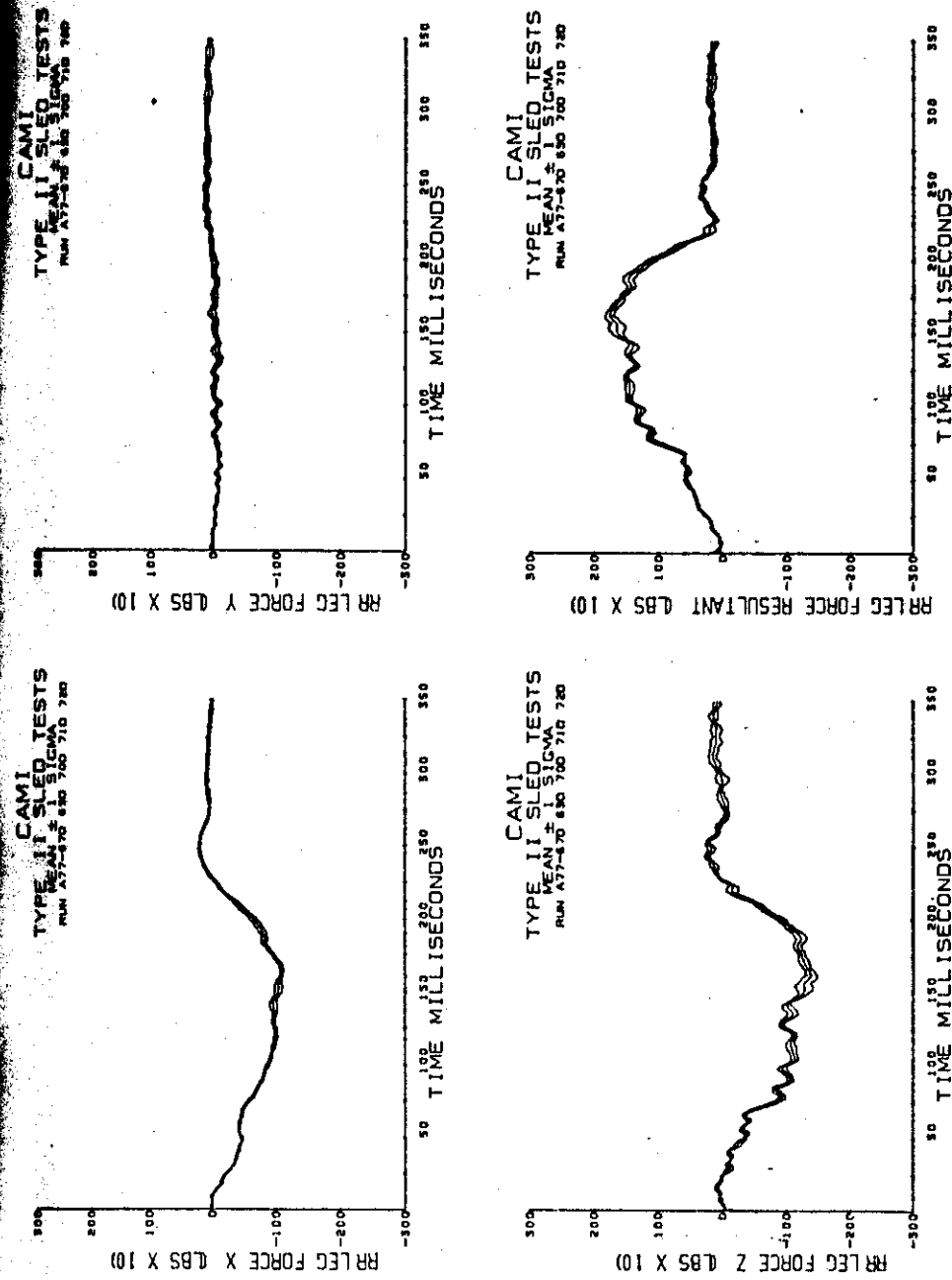


Figure A-1 (continued). Right rear seat leg loads.

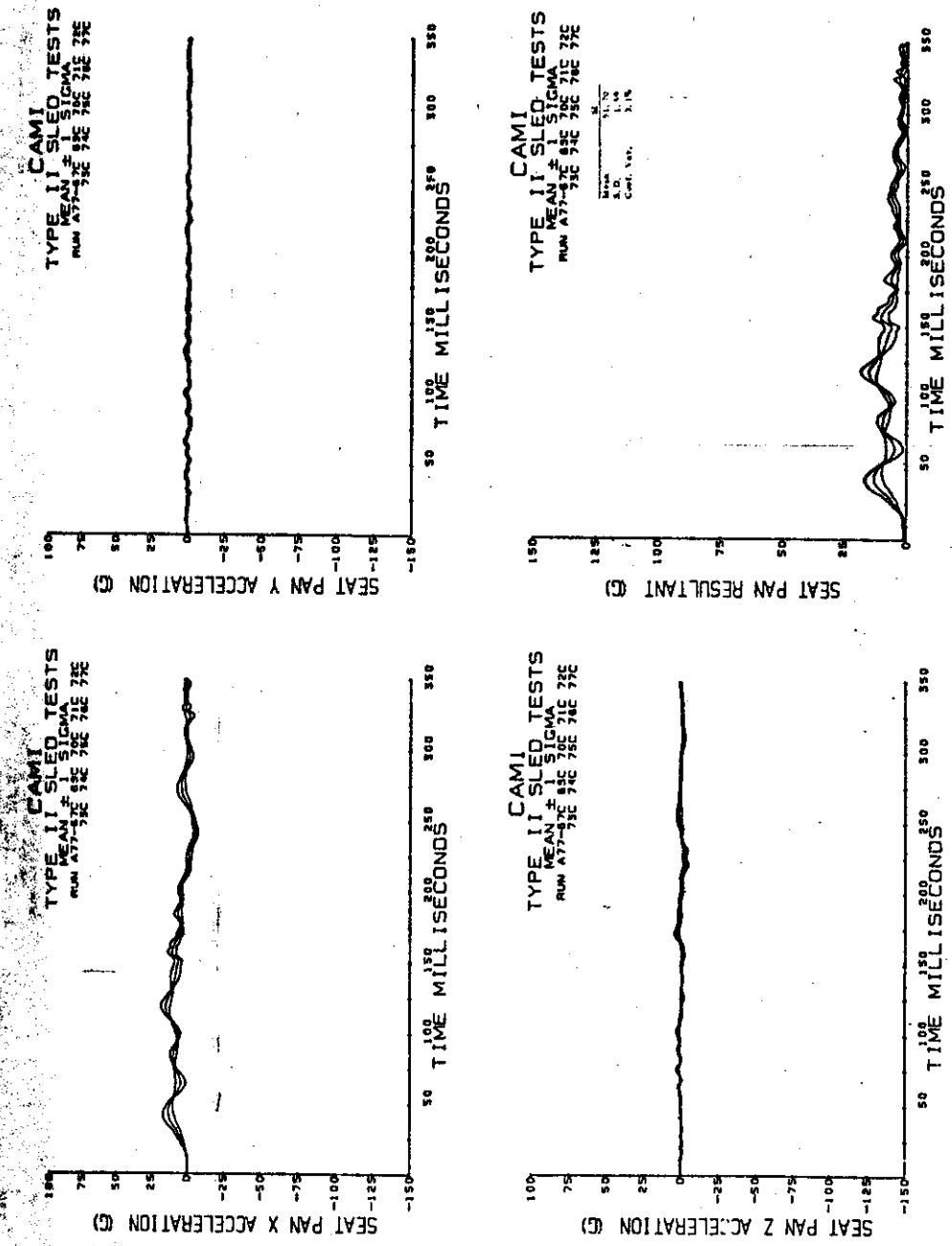
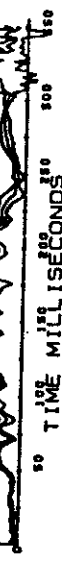
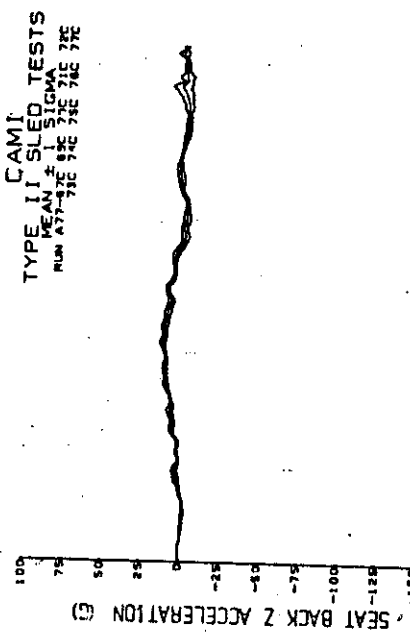
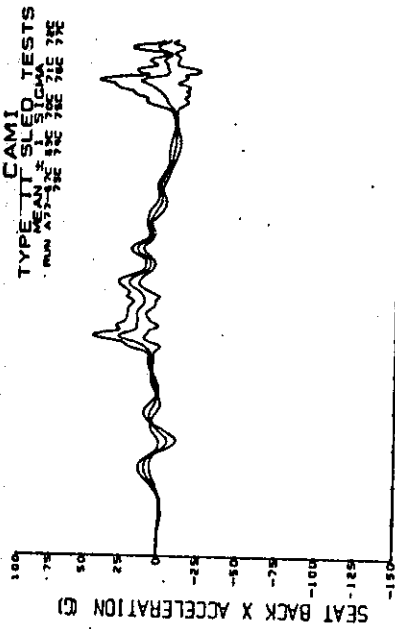


Figure A-1 (continued). Seat pan acceleration.



Mean 24.17  
S.D. 26.4  
Corr. Corr.

Figure A-1 (continued).  
Seat back  
acceleration.

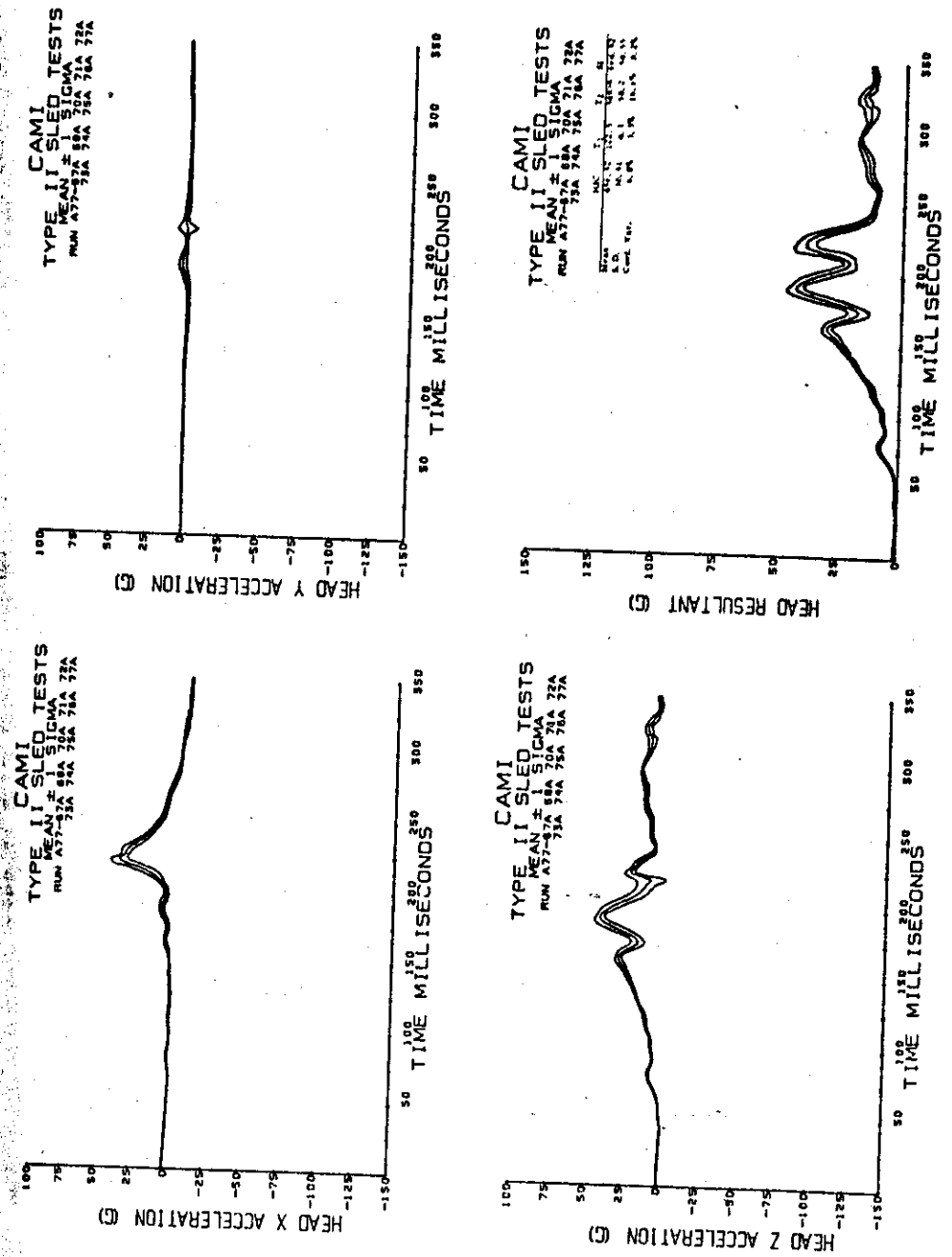


Figure A-1 (continued). Head acceleration.

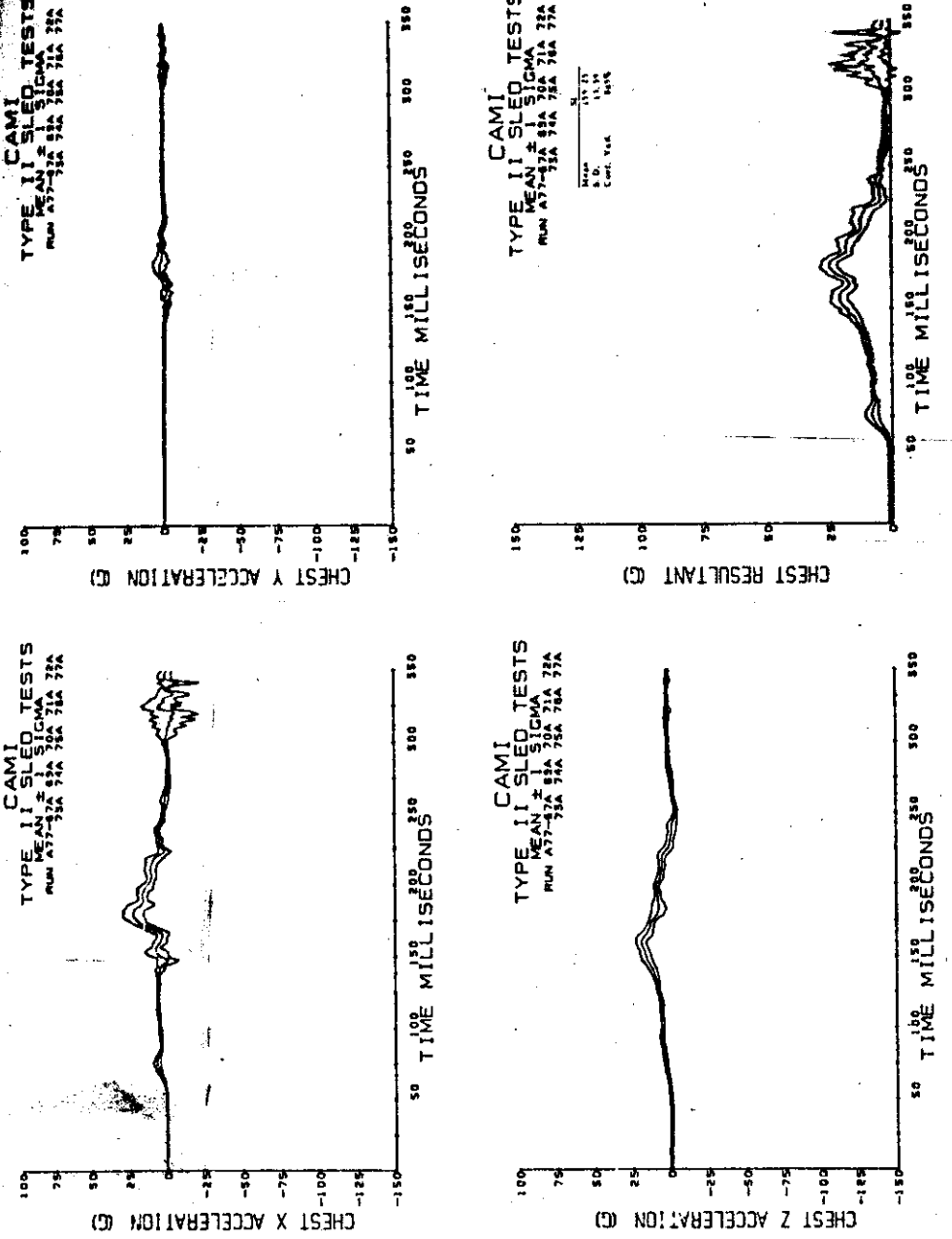


Figure A-1 (continued).  
Chest acceleration.

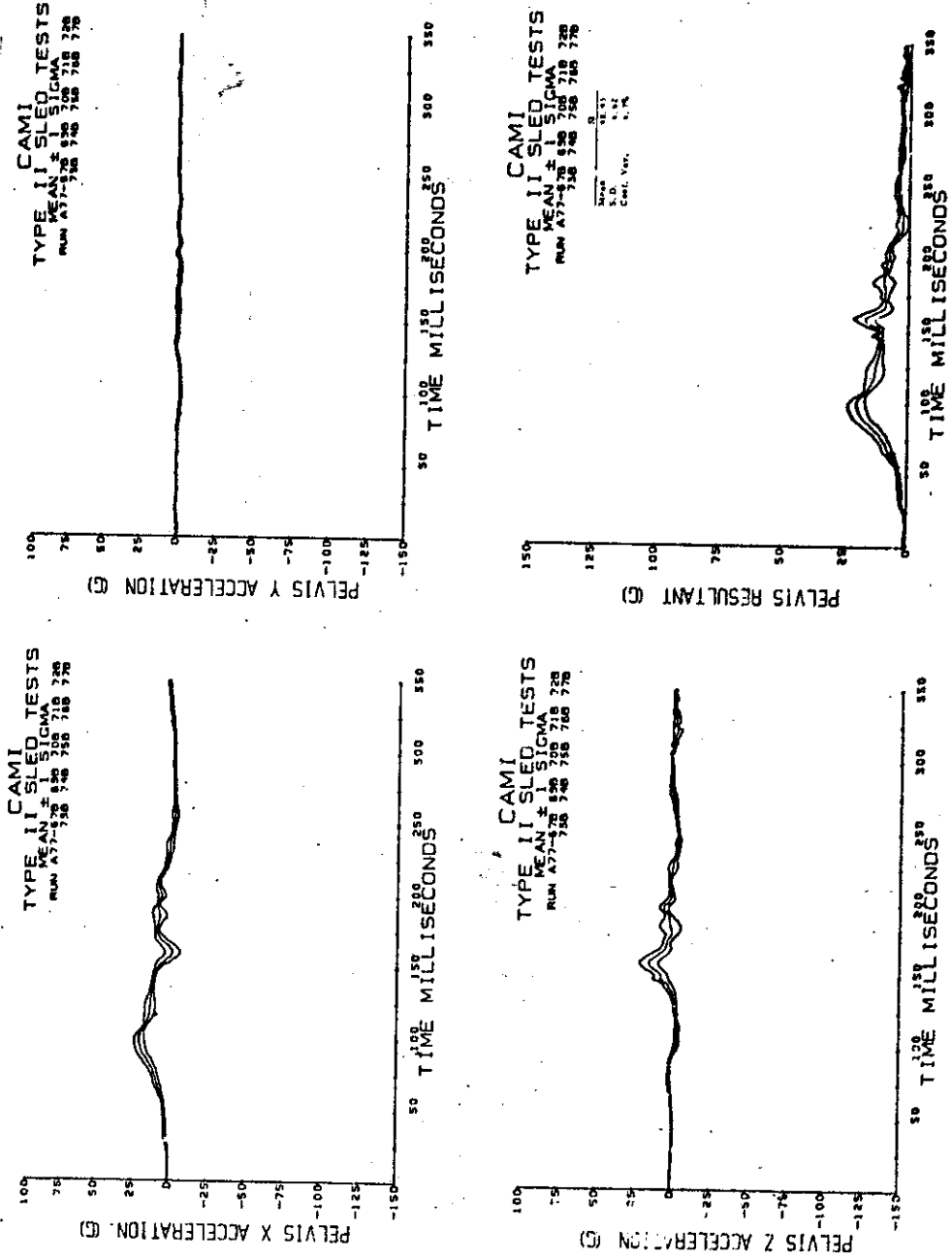


Figure A-1 (continued). Pelvis acceleration.

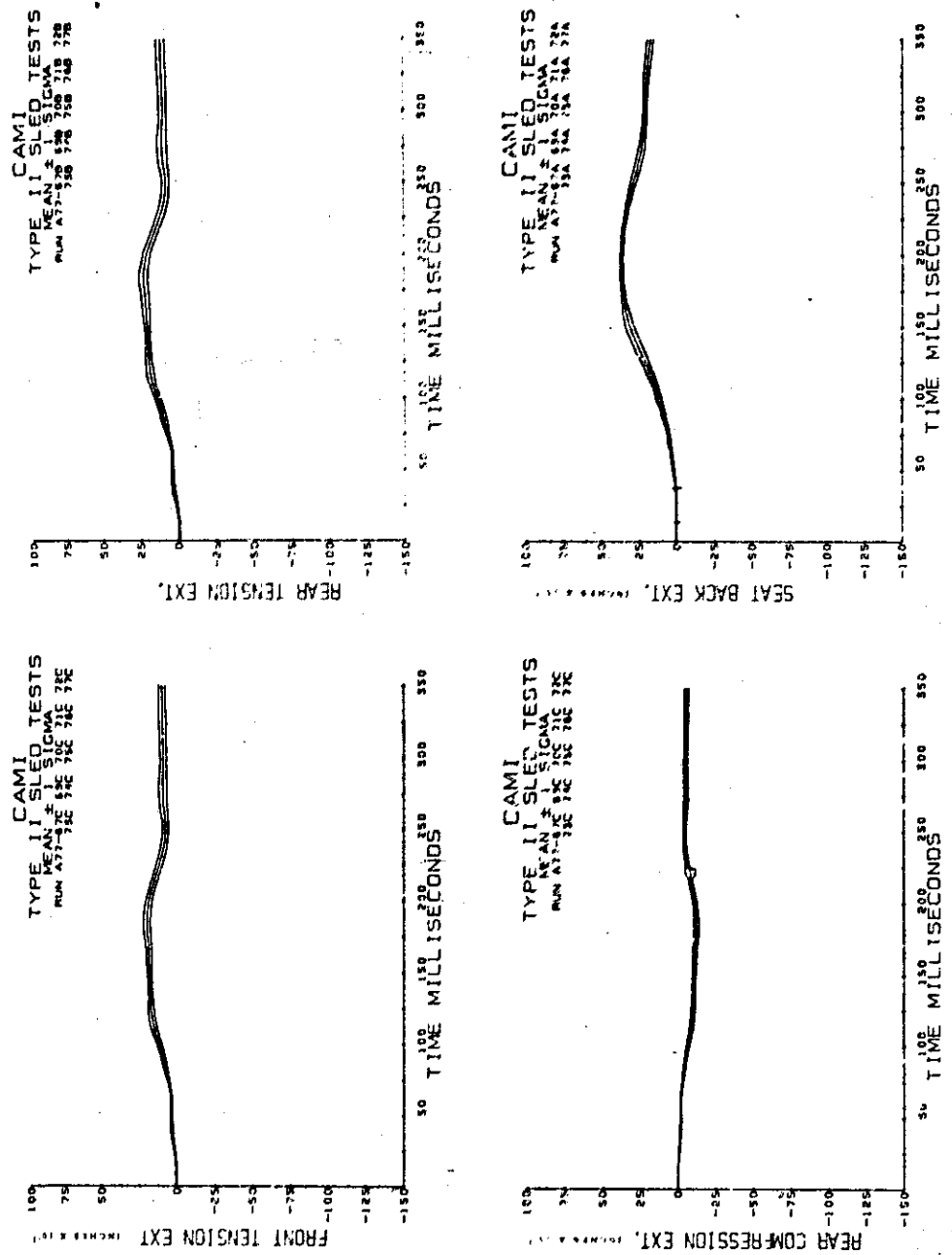


Figure A-1 (continued). Seat extensometer data.

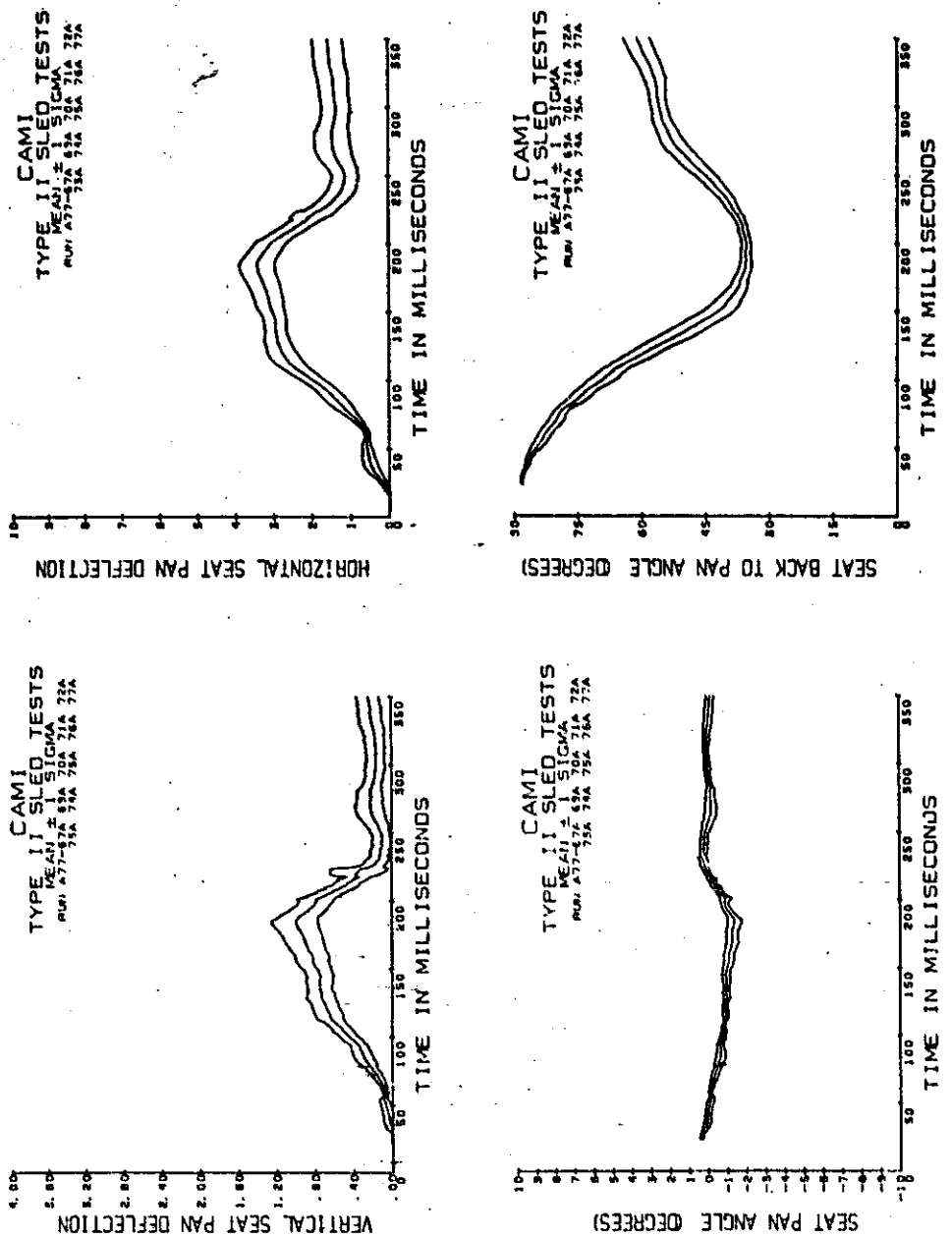


Figure A-1 (continued). Deflection data.

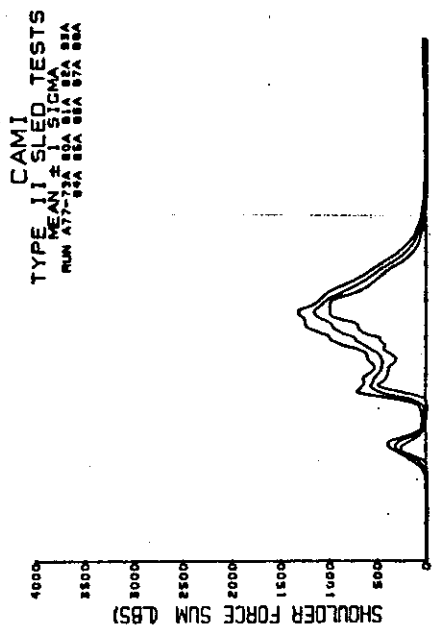
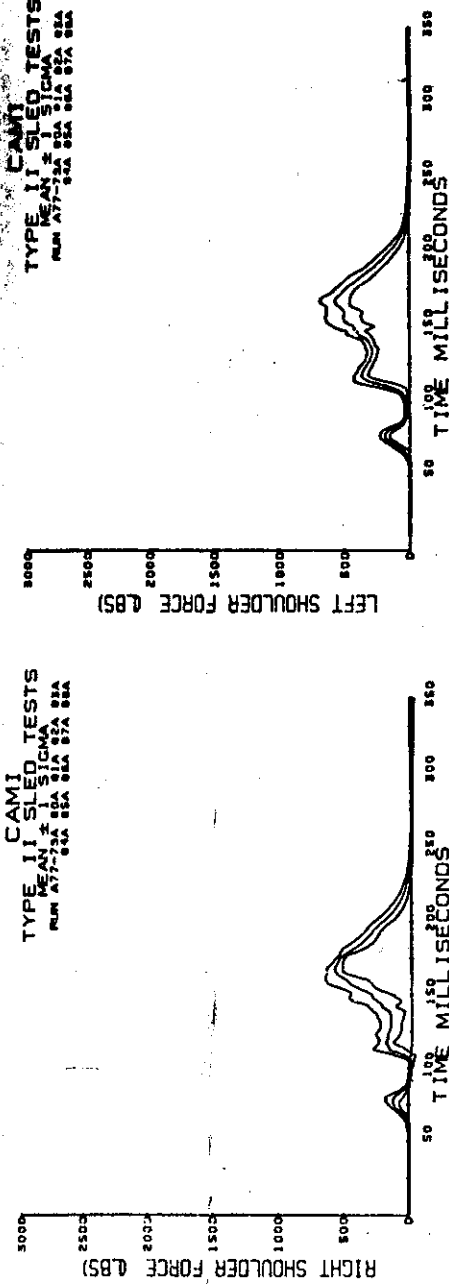


Figure A-2 (continued). Shoulder belt loads.

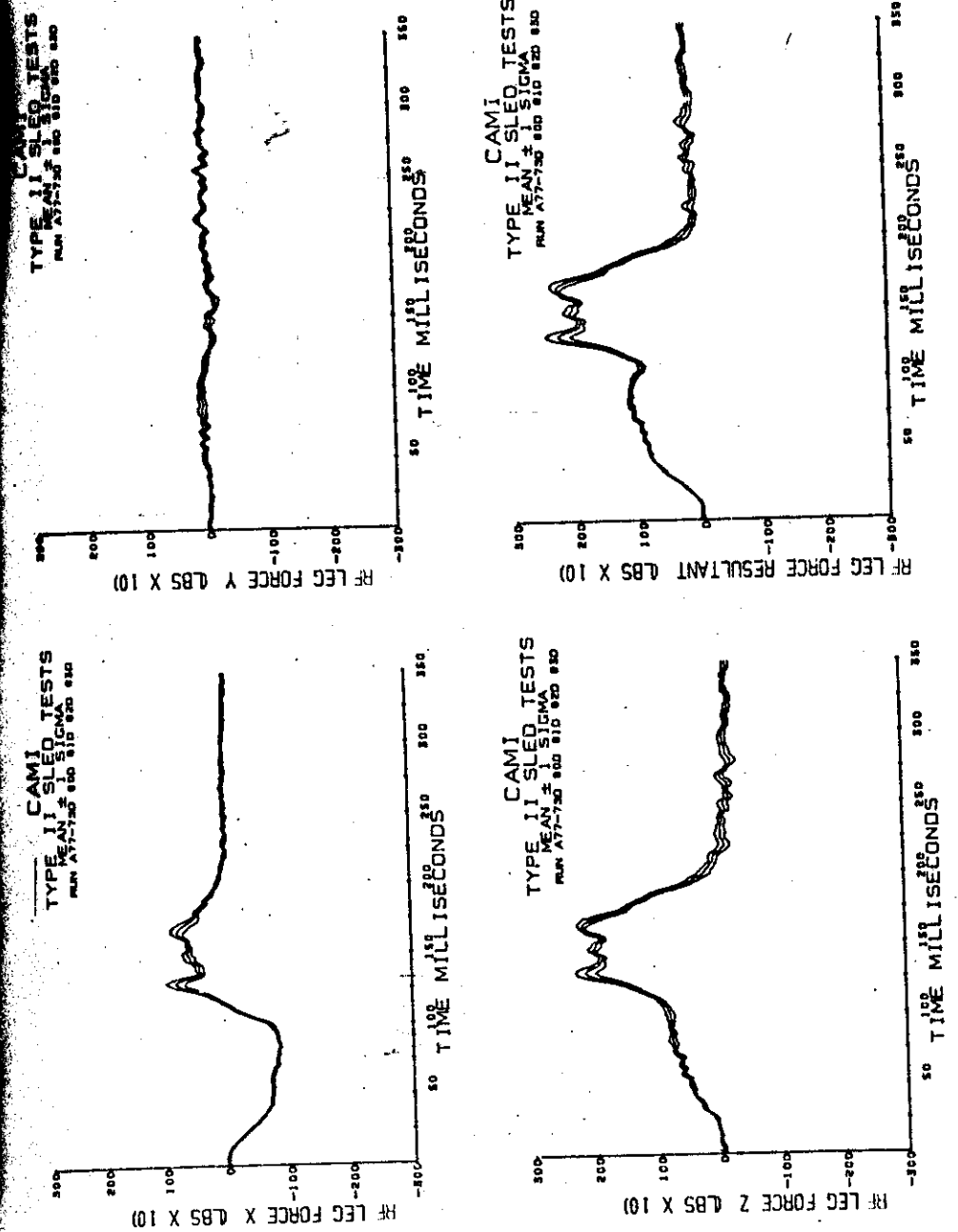


Figure A-2 (continued). Right front seat leg loads.

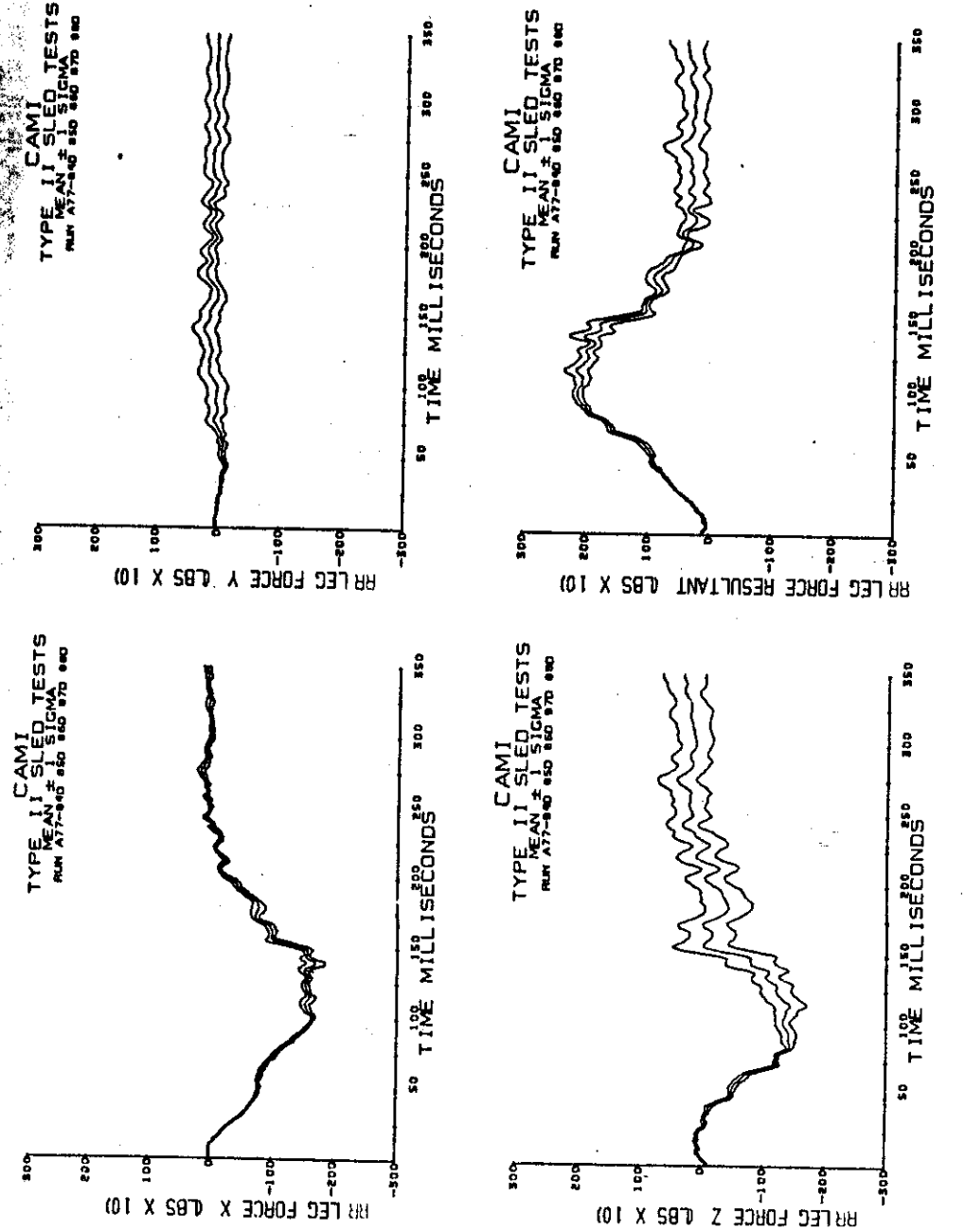


Figure A-2 (continued). Right rear seat leg loads.

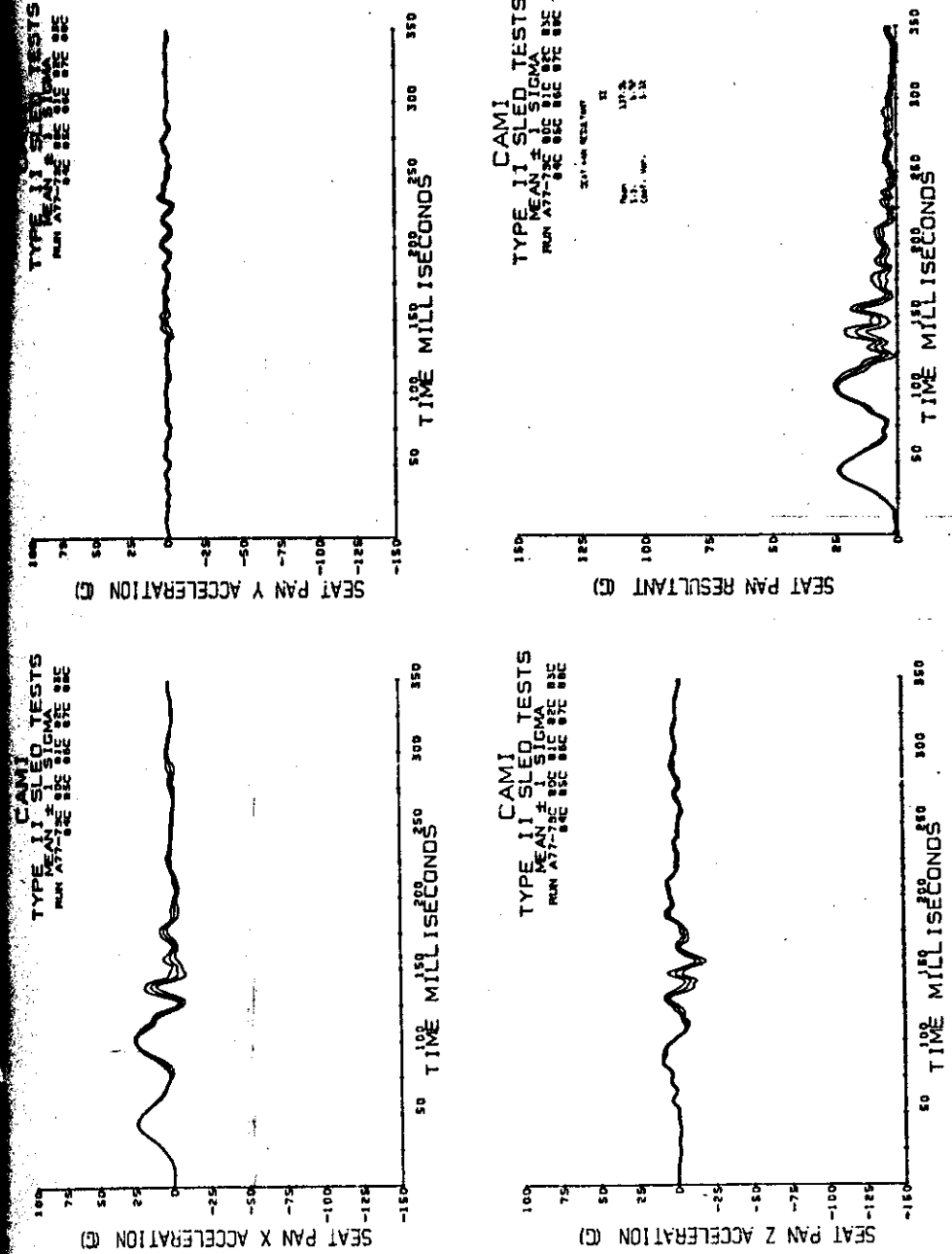


Figure A-2 (continued).  
Seat pan  
acceleration.

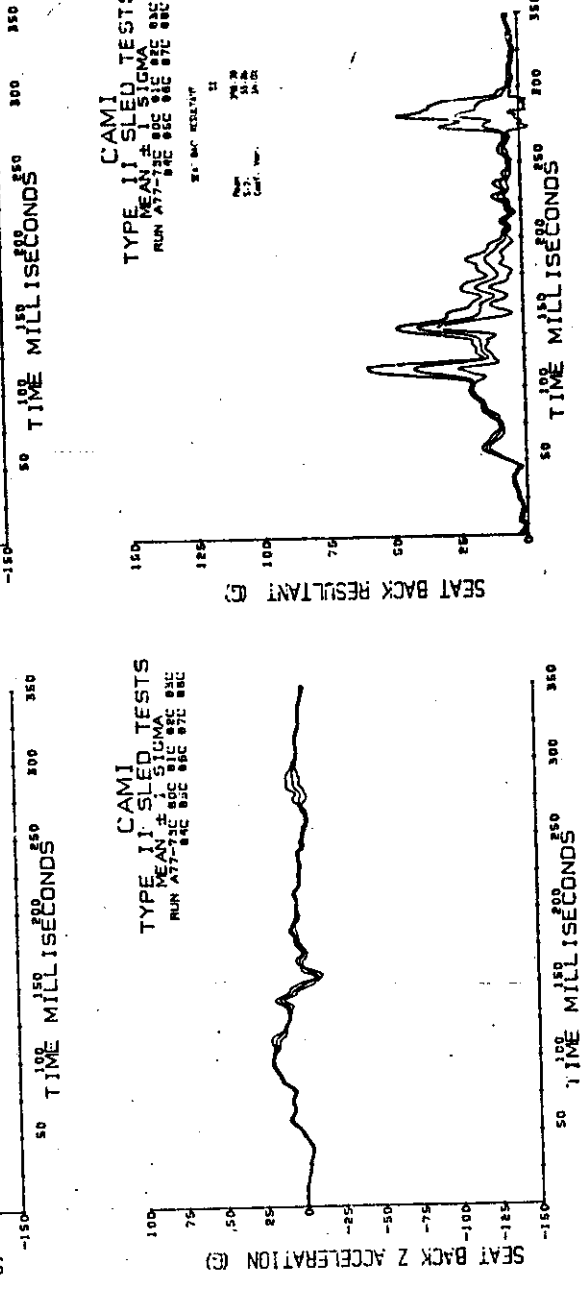
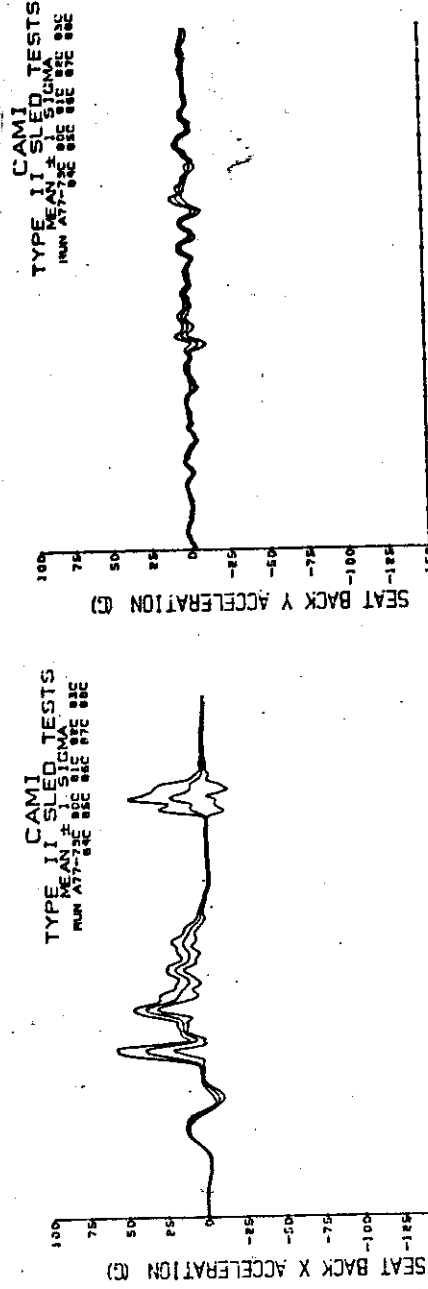


Figure A-2 (continued). Seat back acceleration.

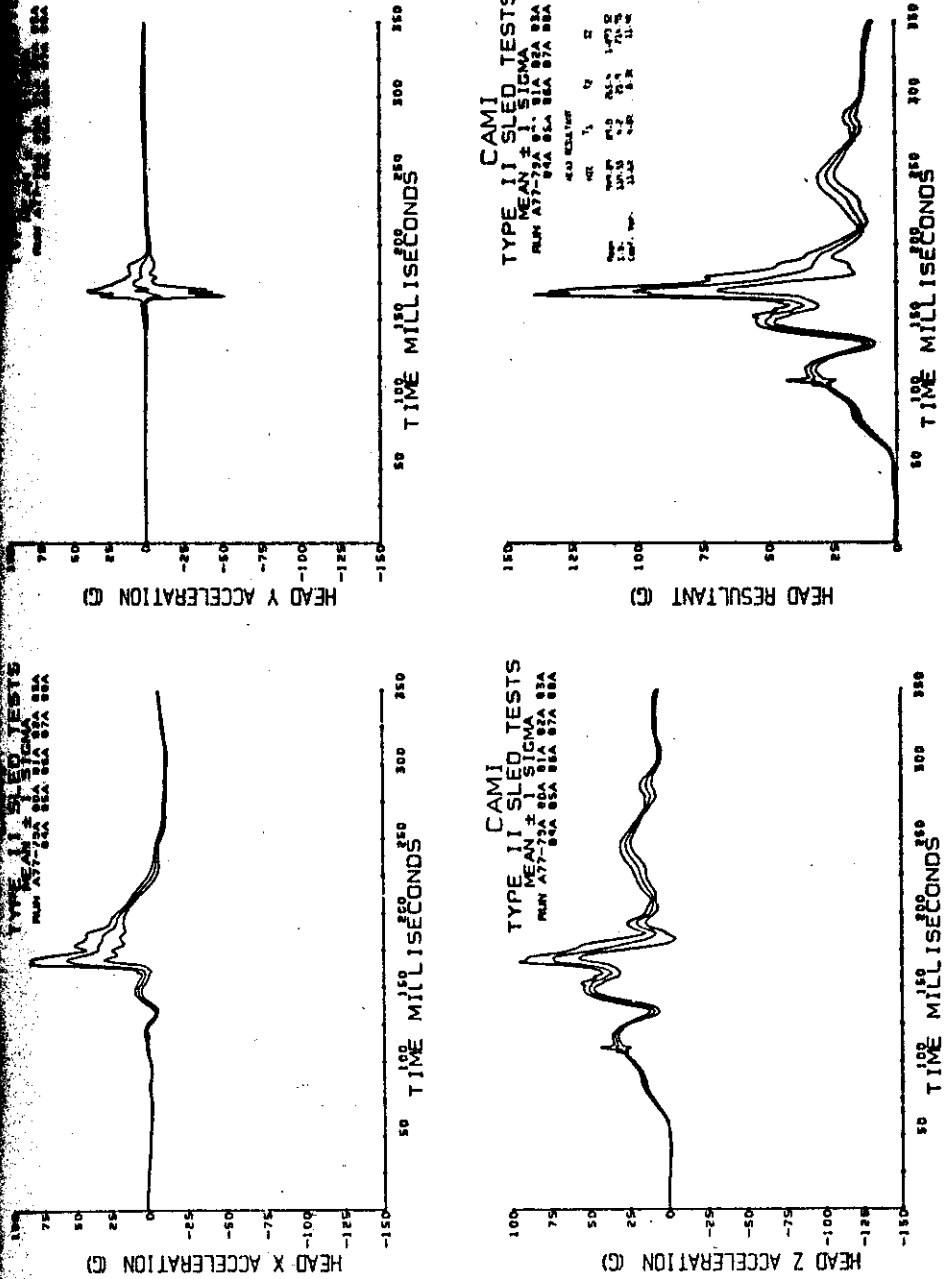


Figure A-2 (continued). Head acceleration.

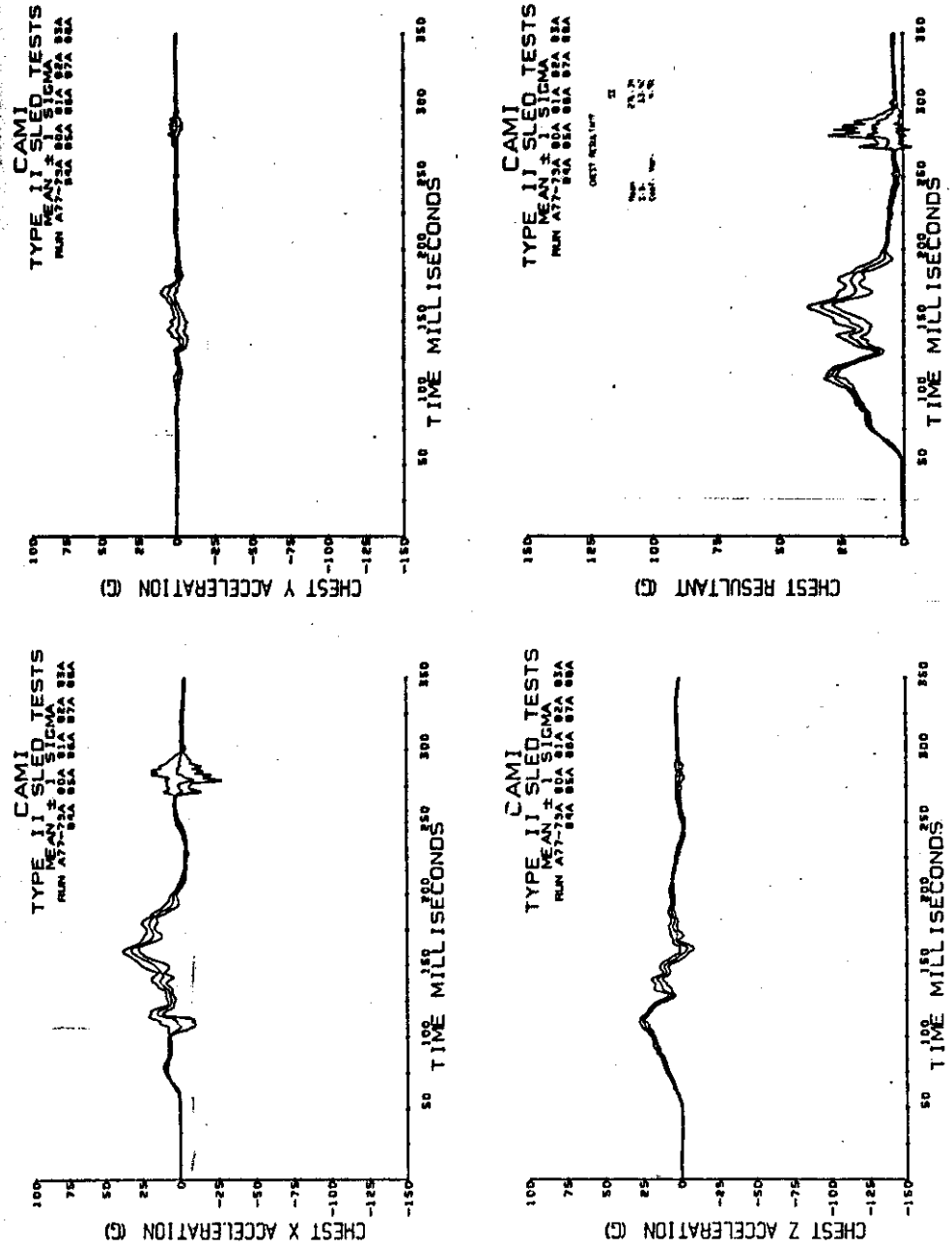


Figure A-2 (continued). Chest acceleration.

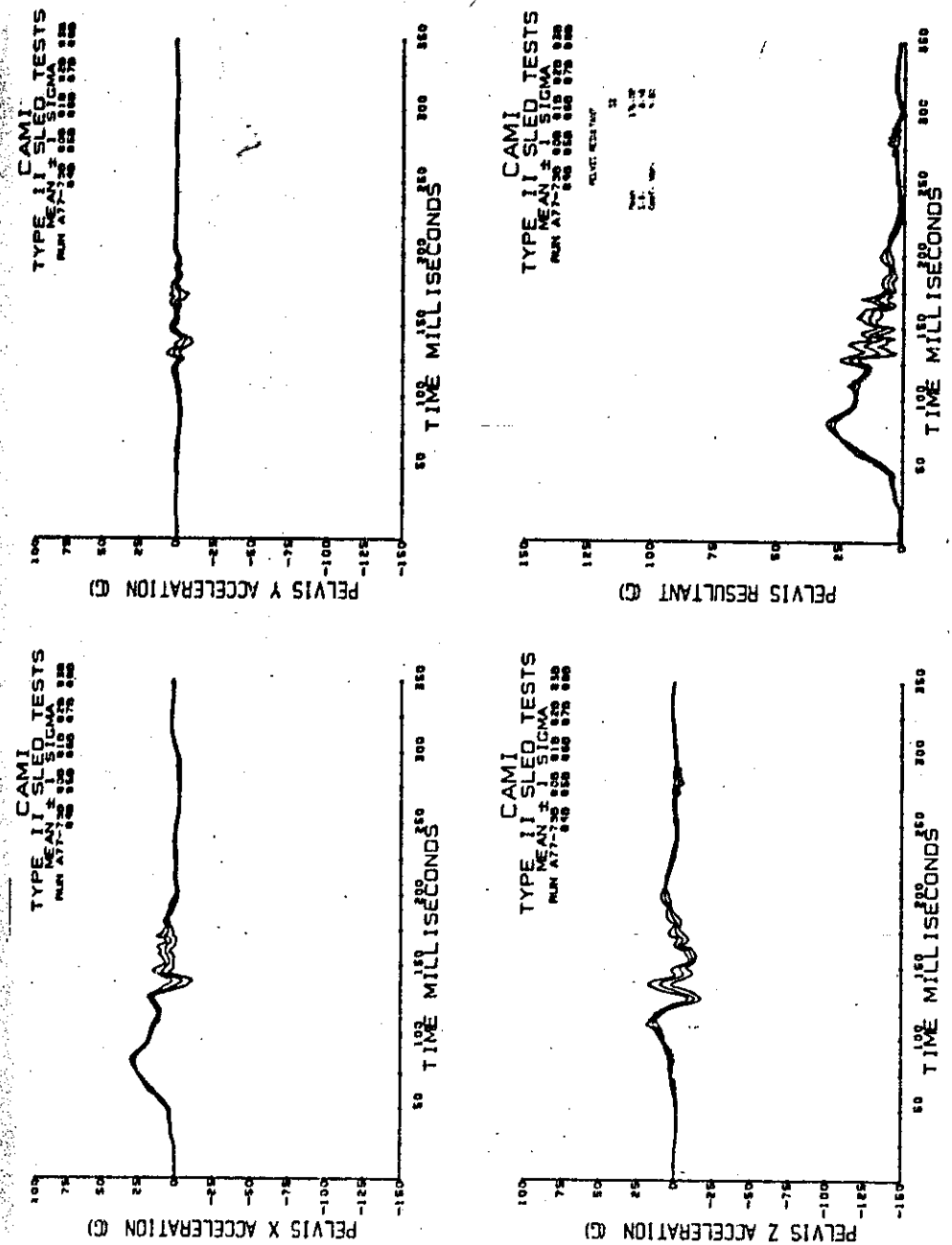


Figure A-2 (continued). Pelvis acceleration.

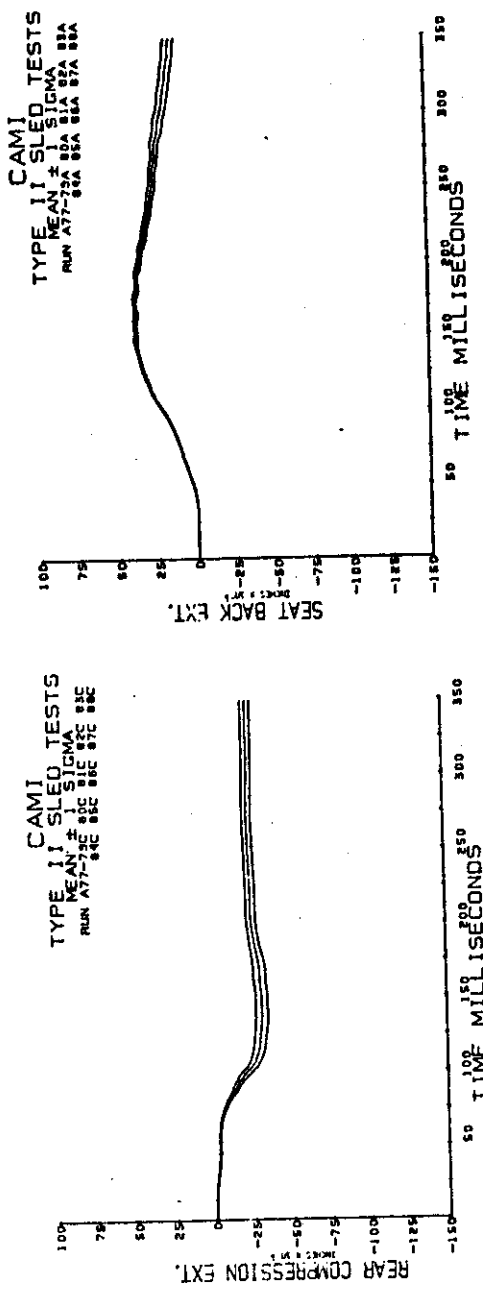
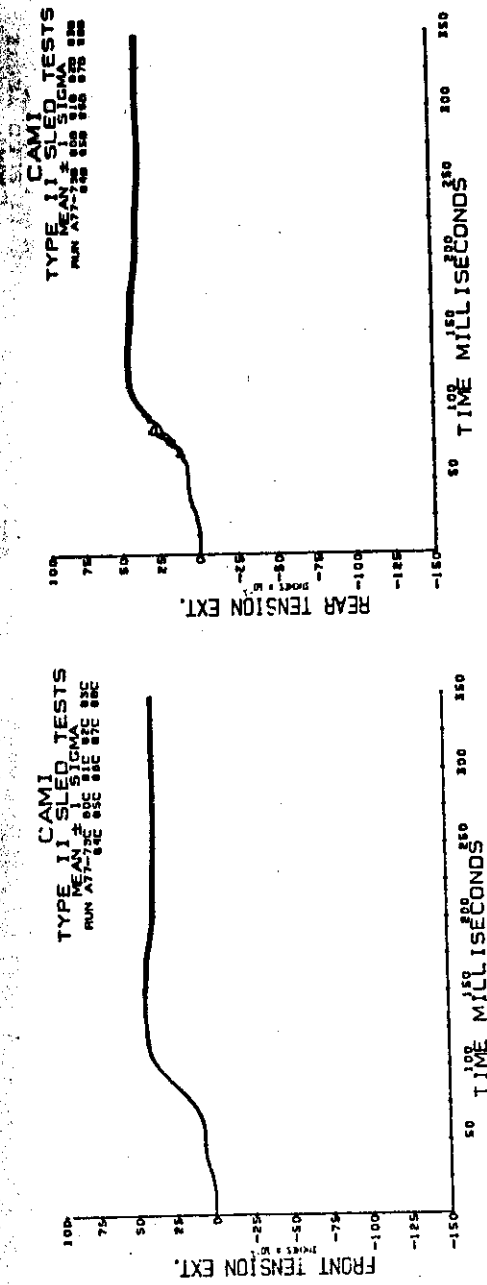


Figure A-2 (continued). Seat extensometer data.

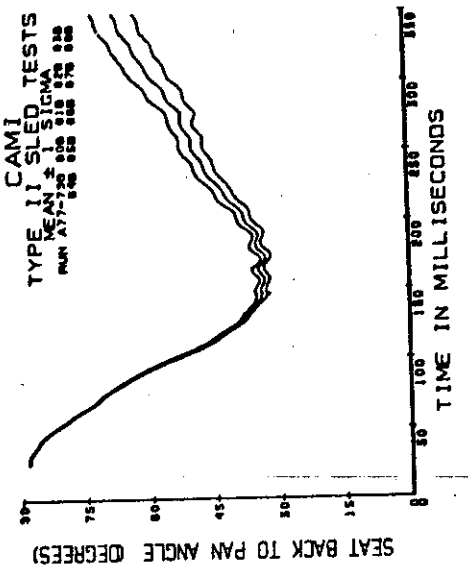
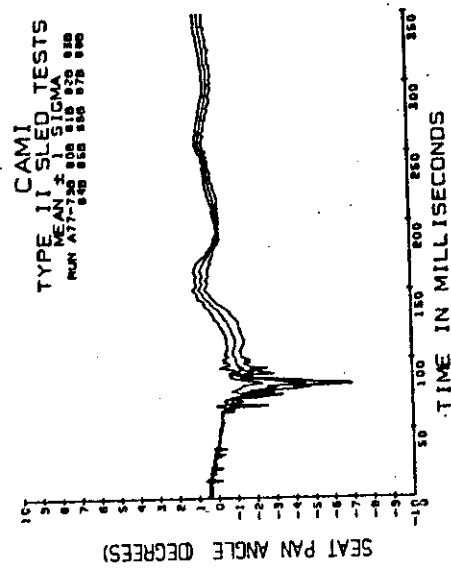
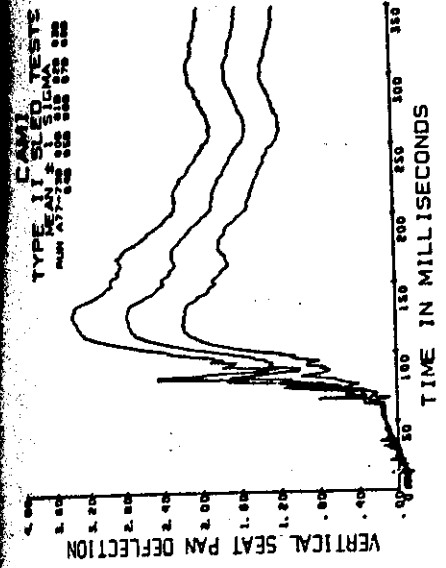
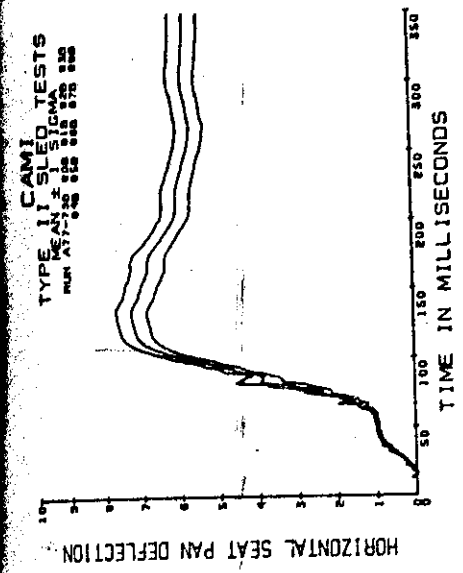


Figure A-2 (continued). Deflection data.

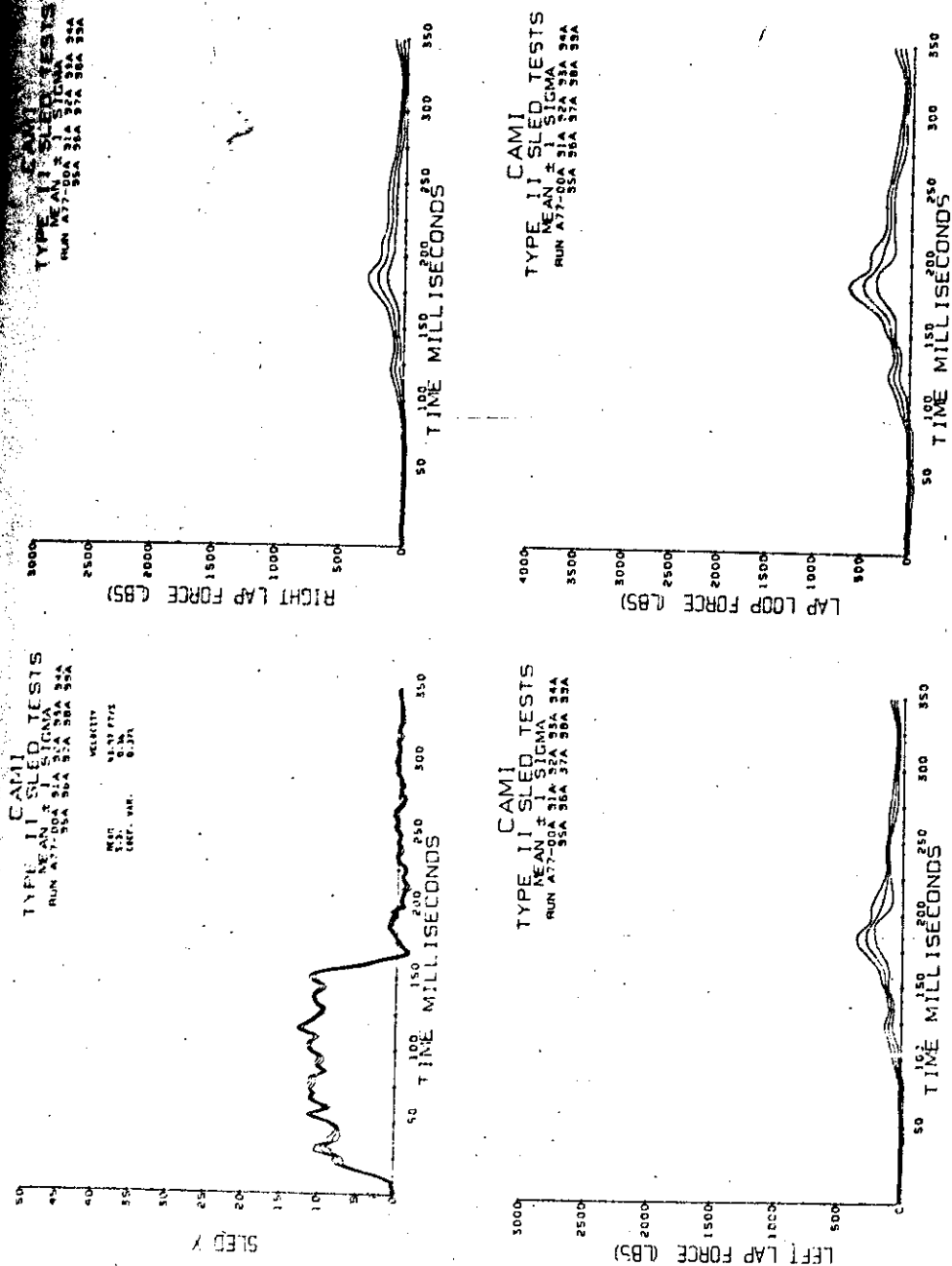


Figure A-3. Combined loading, low-deceleration tests.  
Sled deceleration and lapbelt loads.

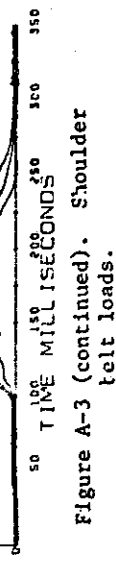
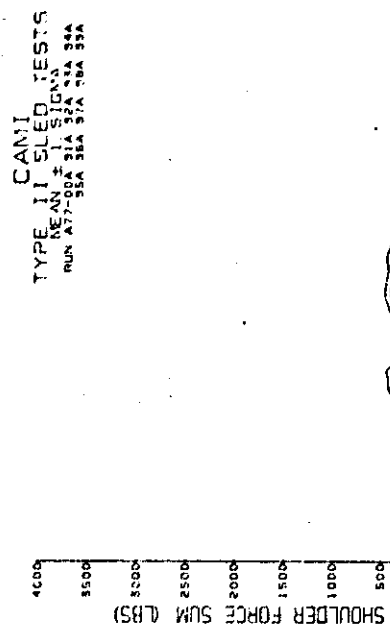
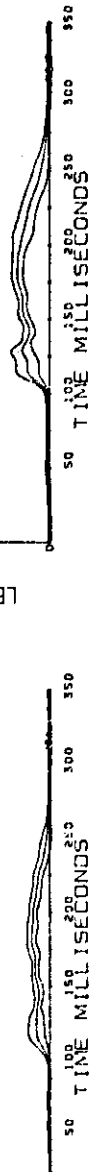
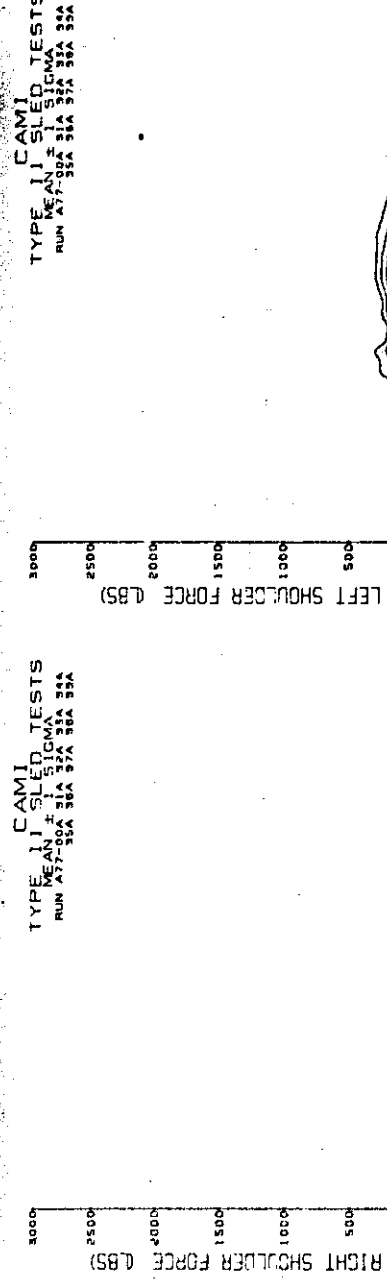


Figure A-3 (continued). Shoulder  
telt loads.

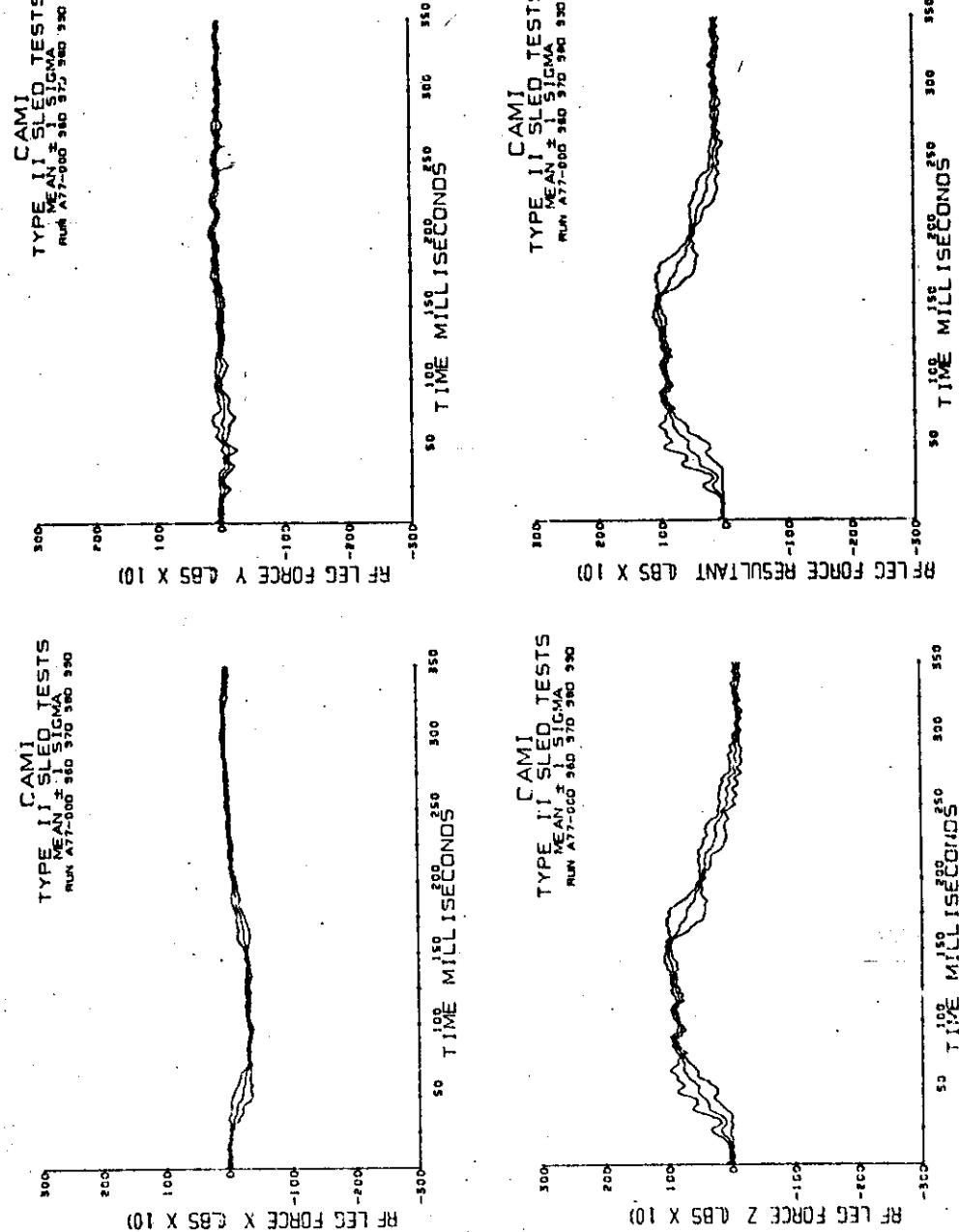


Figure A-3 (continued). Right front seat leg loads.

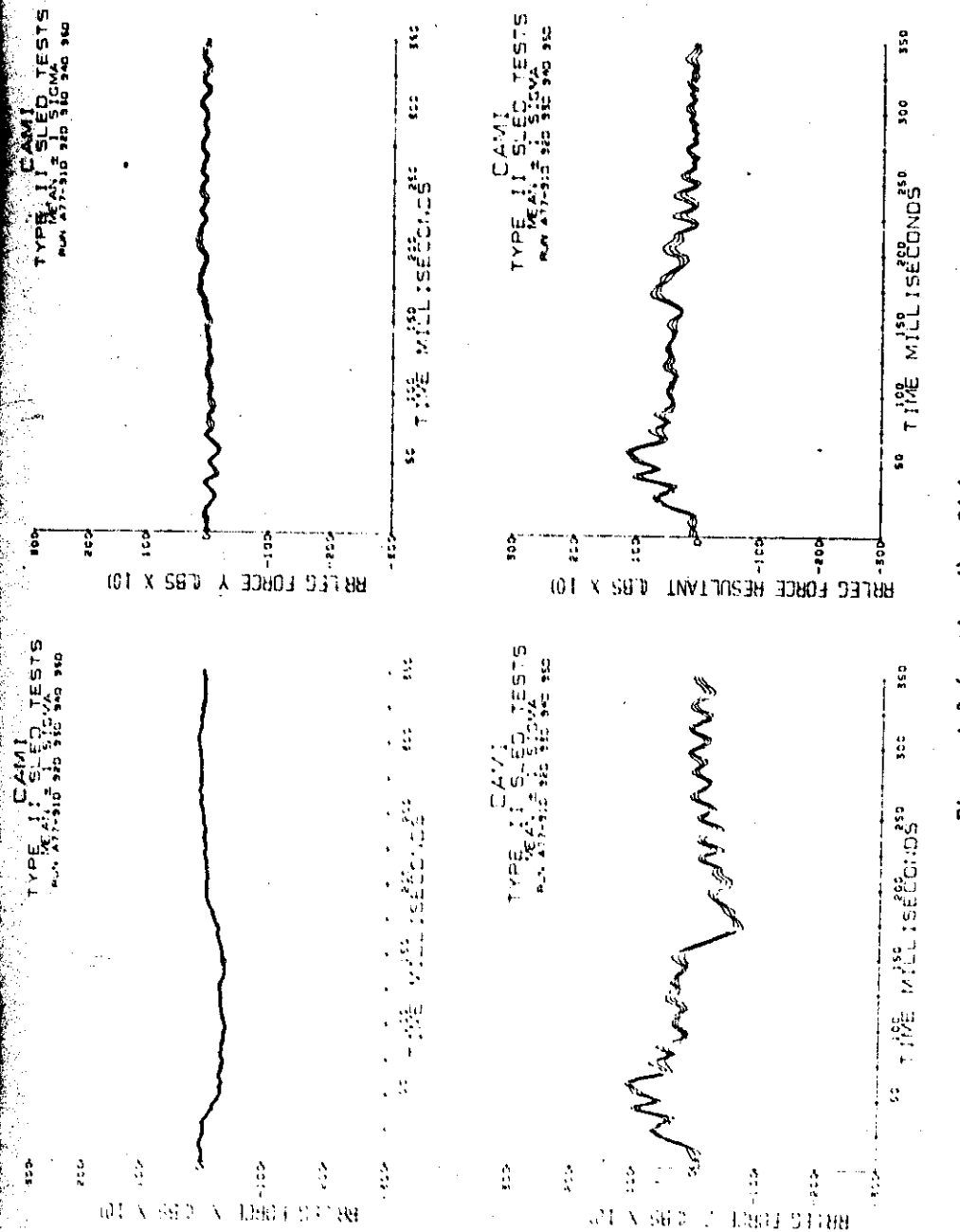


Figure A-3 (continued). Right rear seat leg loads.

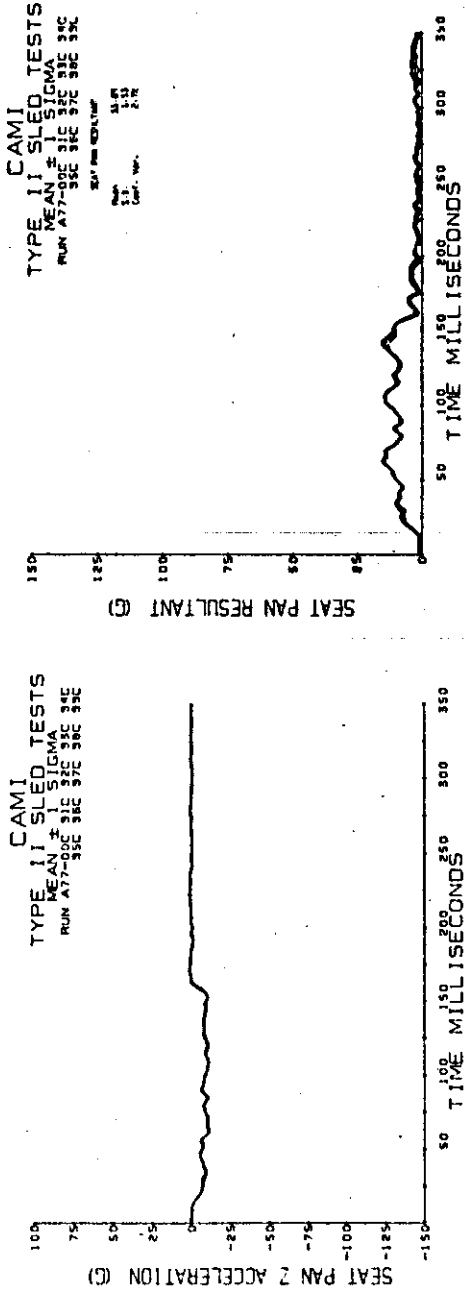
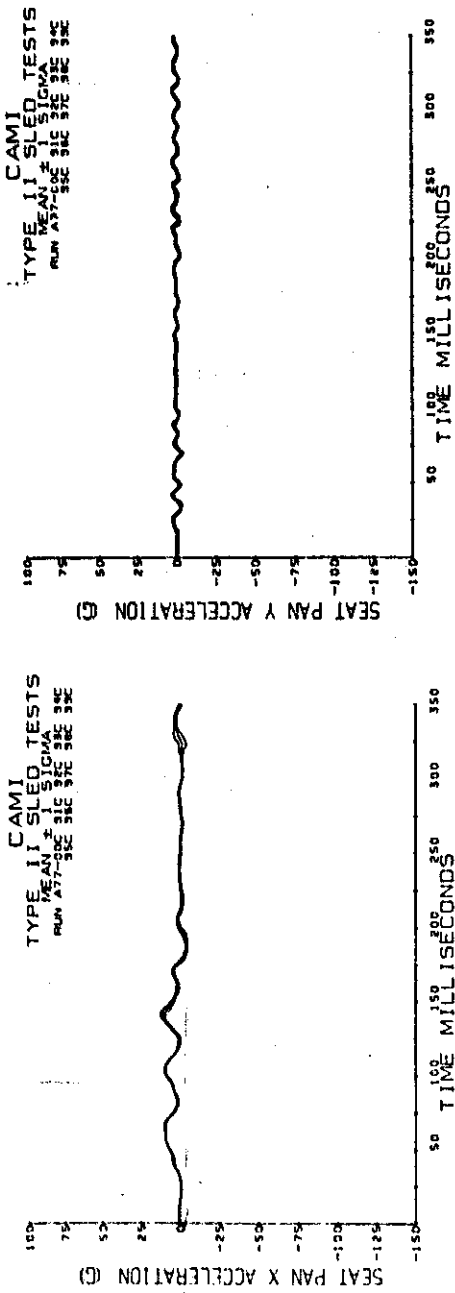


Figure A-3 (continued).  
Seat pan acceleration.

Figure A-3 (continued).  
Seat pan

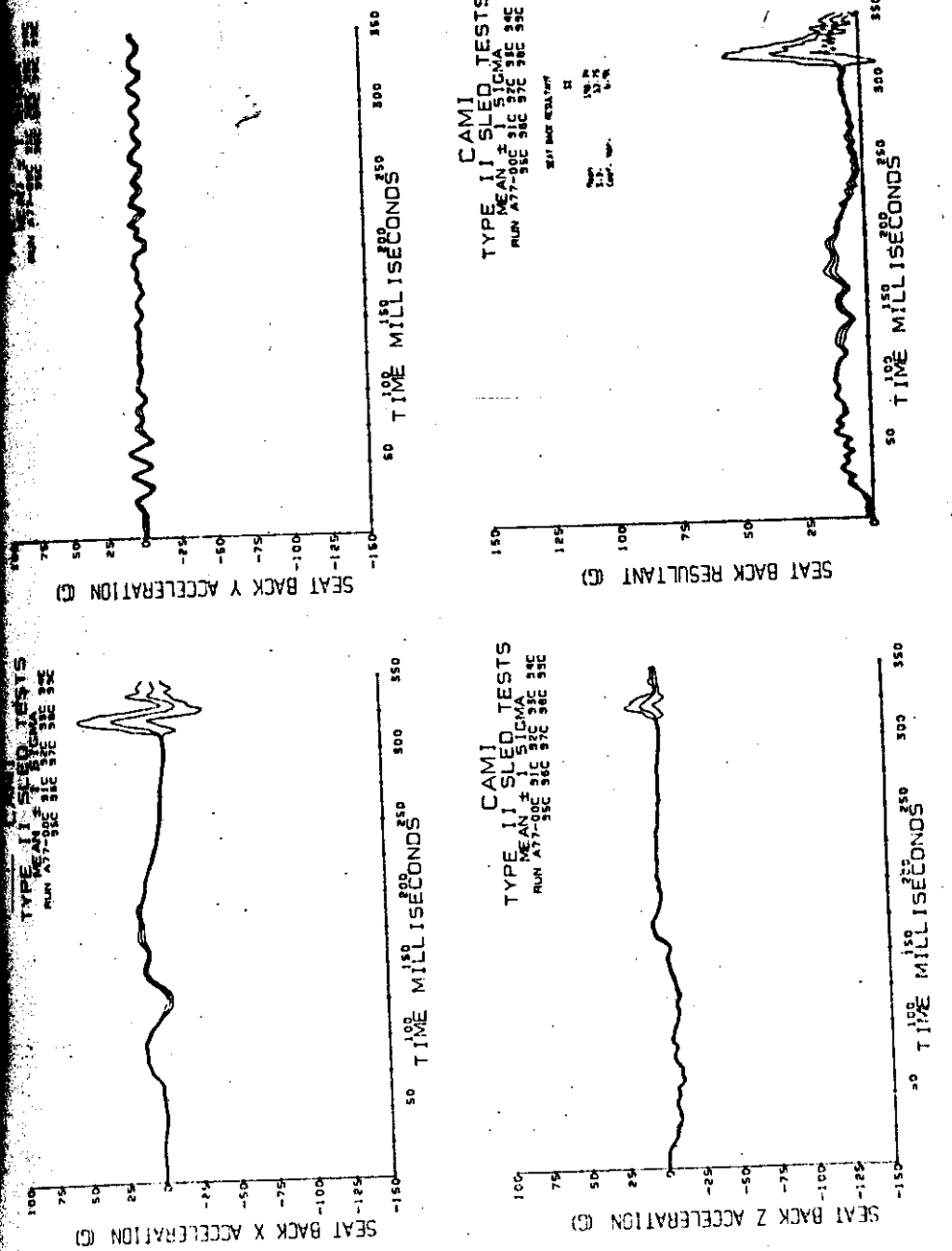
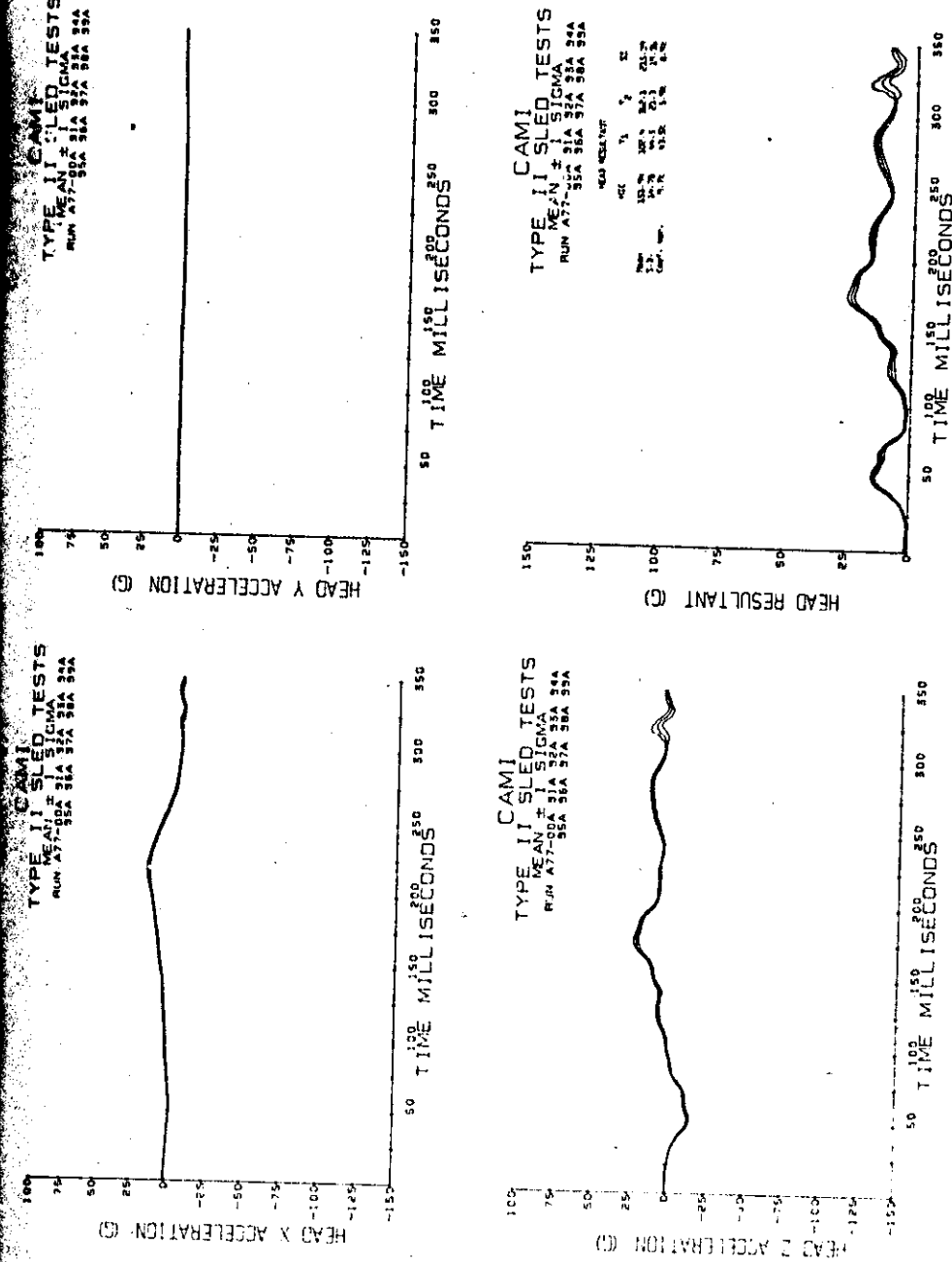
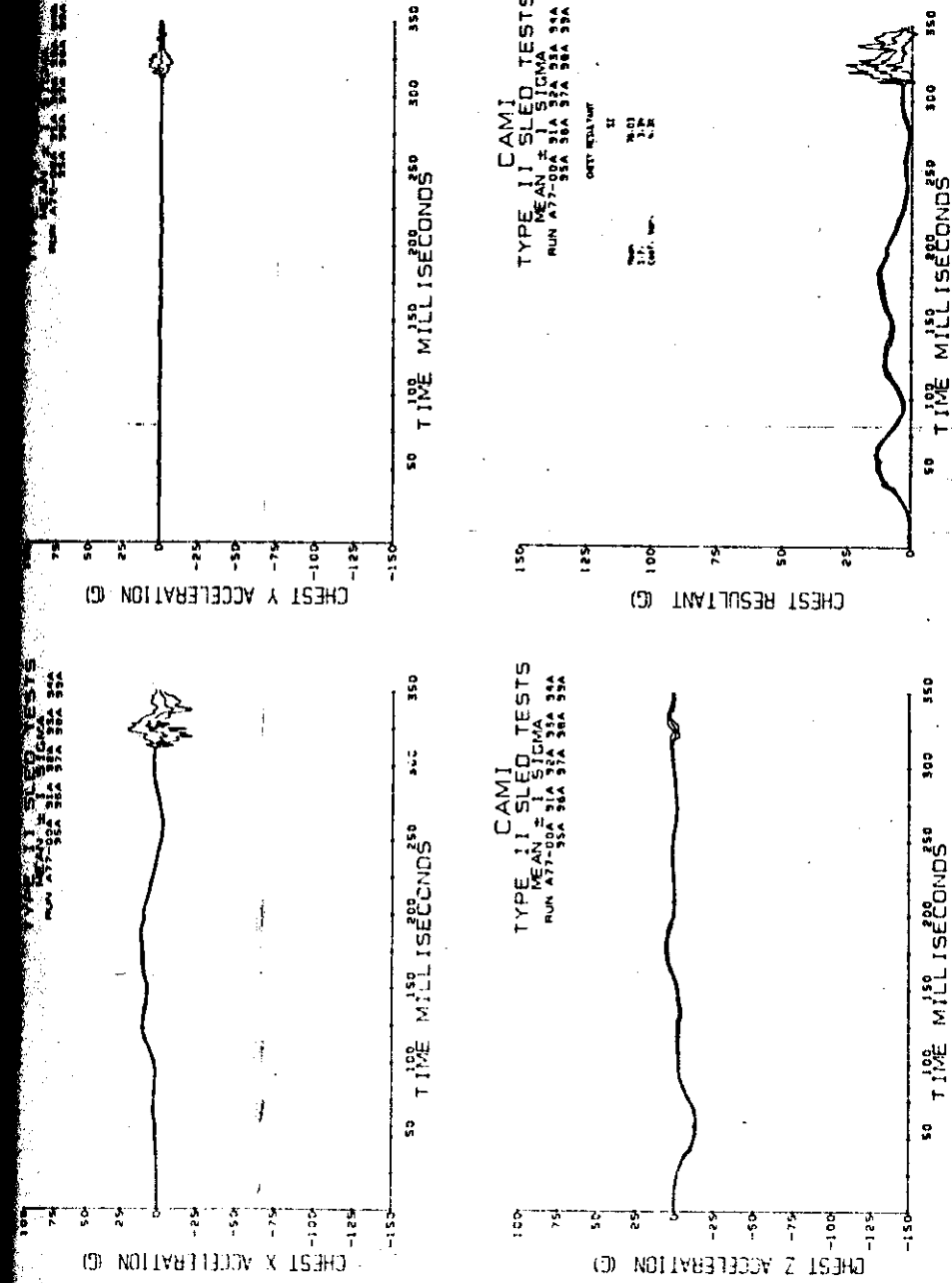


Figure A-3 (continued). Seat back acceleration.



**Figure A-3** (continued). Head acceleration.



42

Figure A-3 (continued). Chest acceleration.

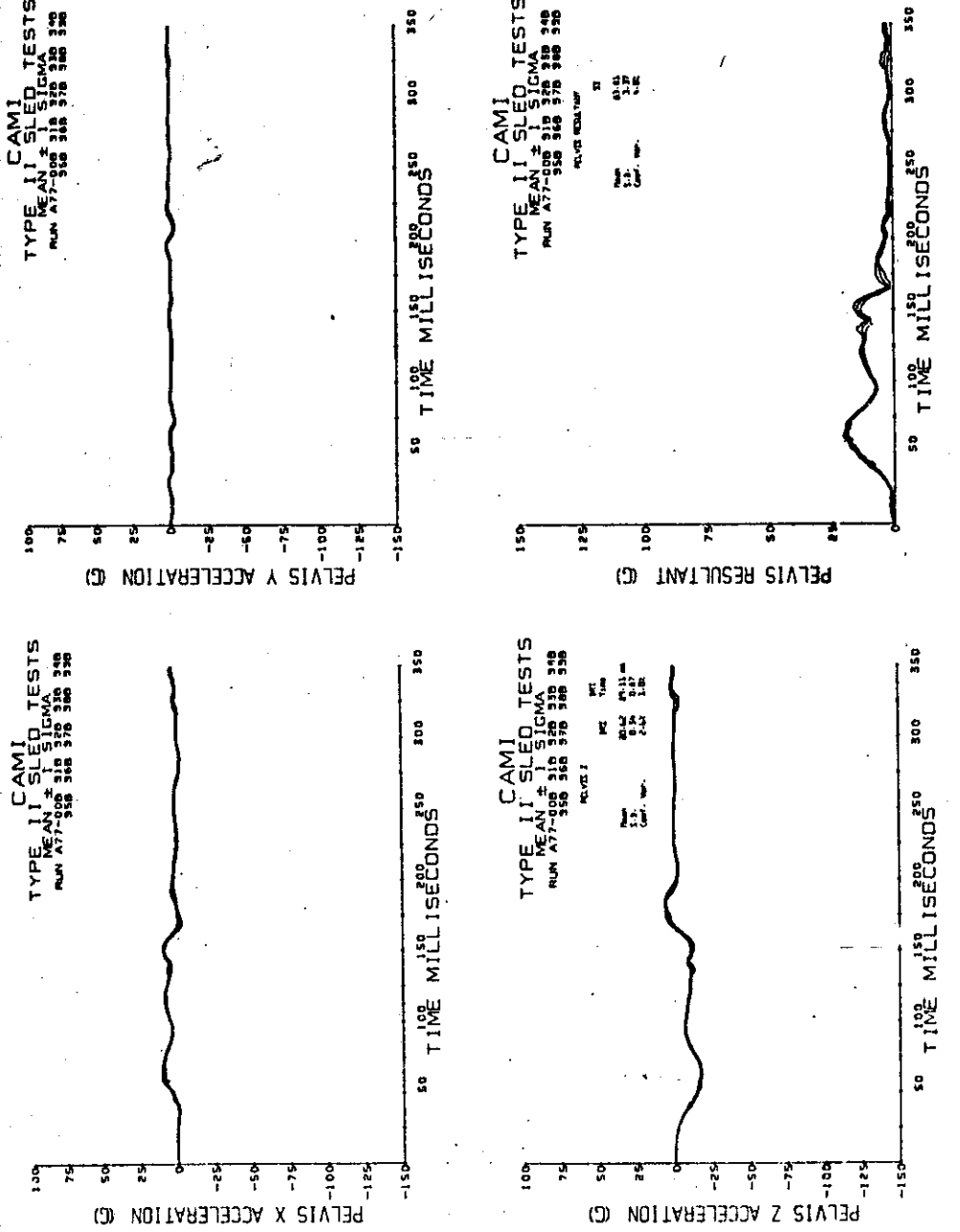


Figure A-3 (continued): Pelvis acceleration.

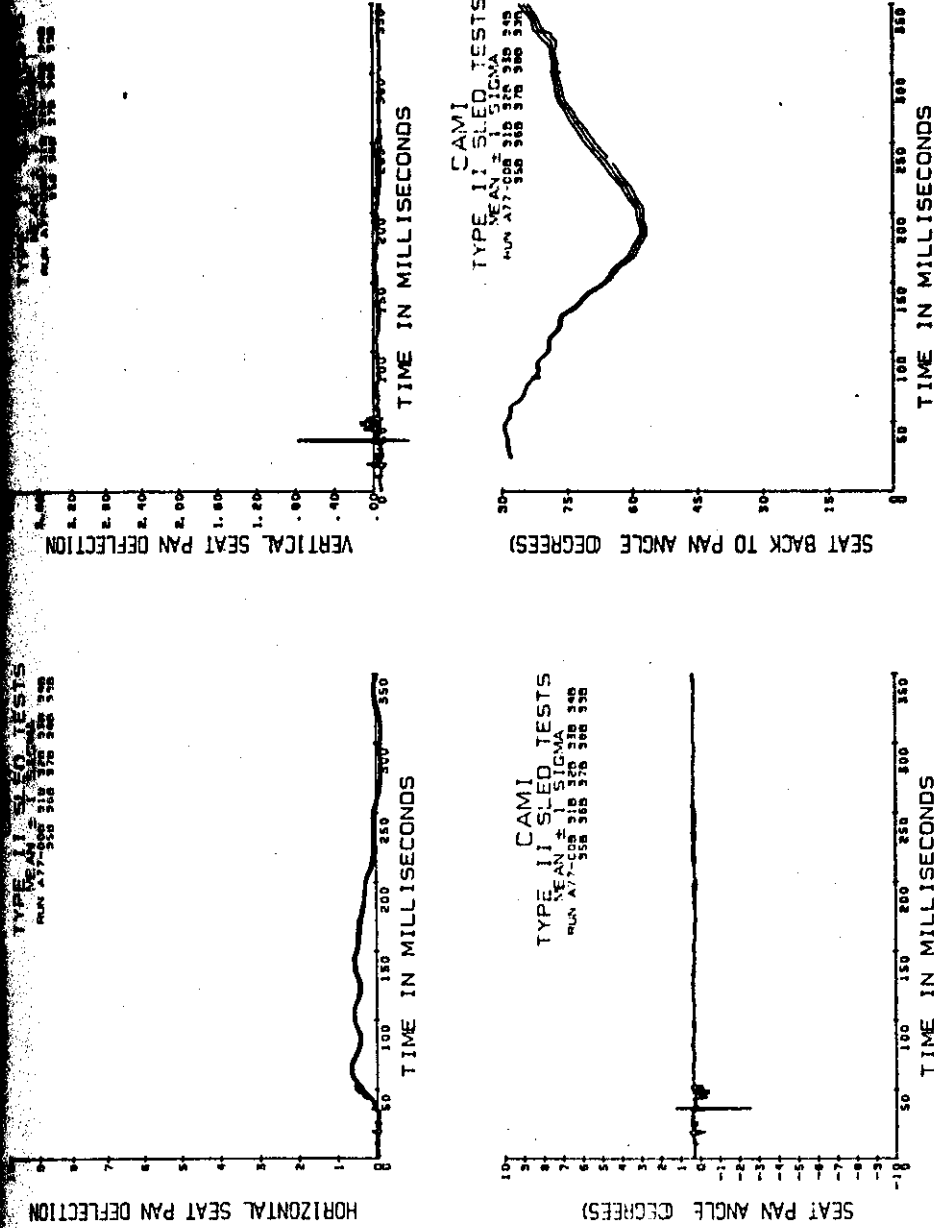


Figure A-3 (continued).  
Seat extensometer data.

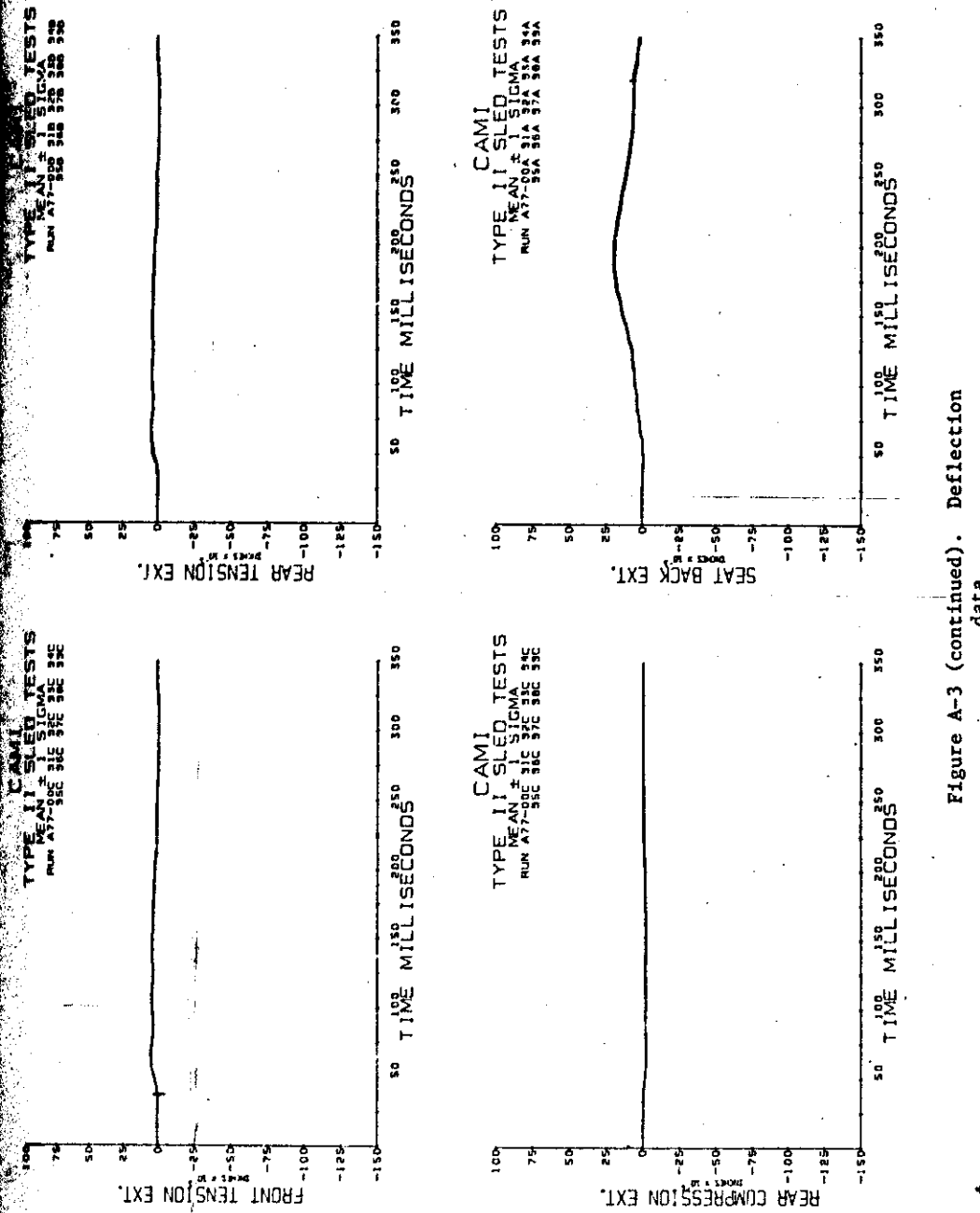


Figure A-3 (continued). Deflection data.

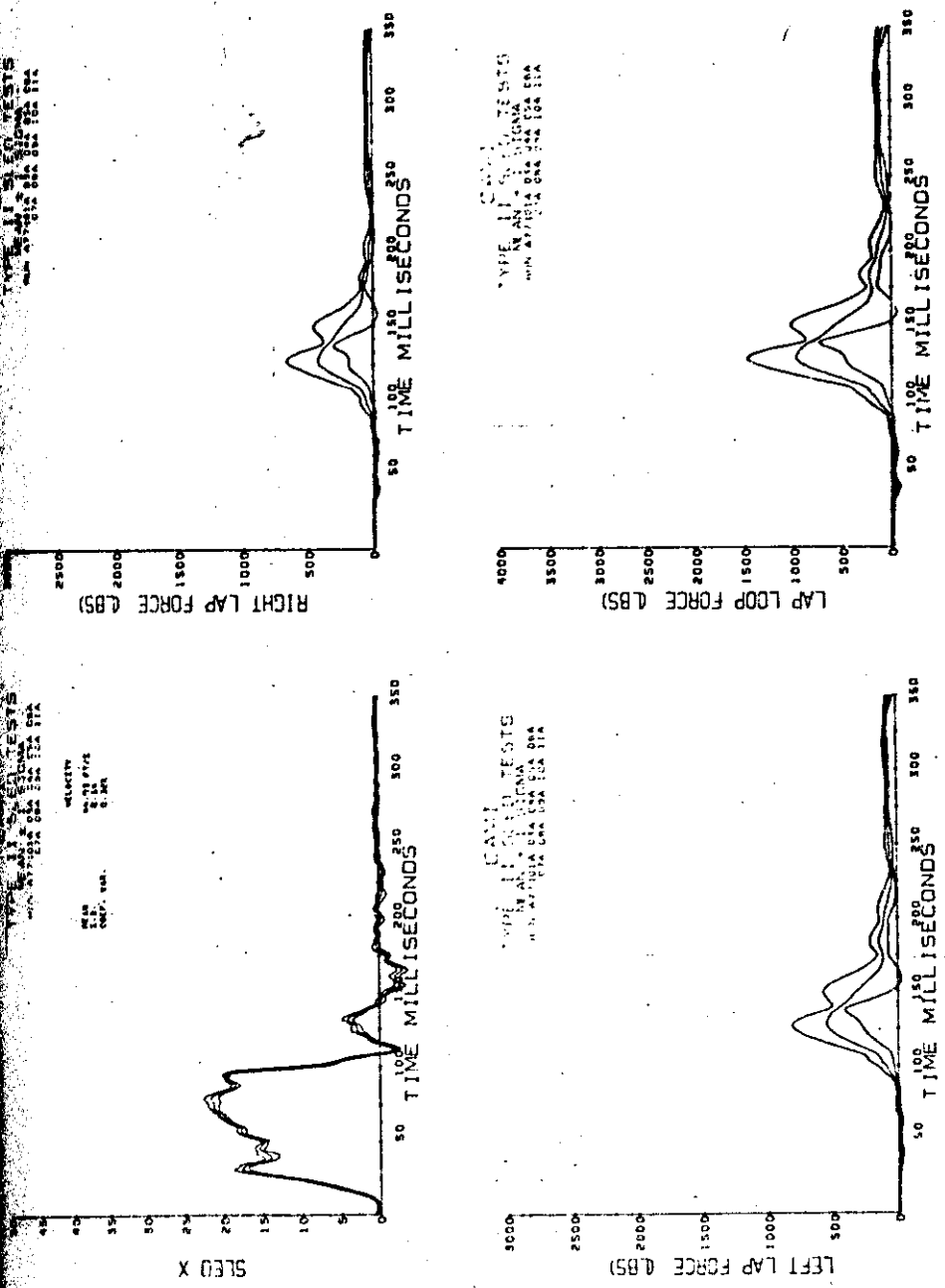


Figure A-4. Combined loading, higher  
deceleration tests.  
Sled deceleration and lapbelt loads.

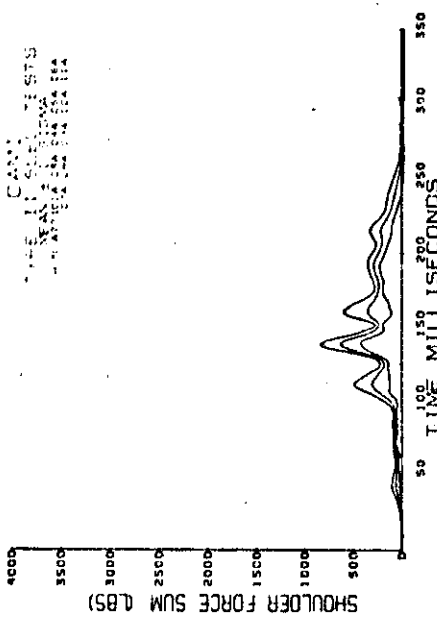
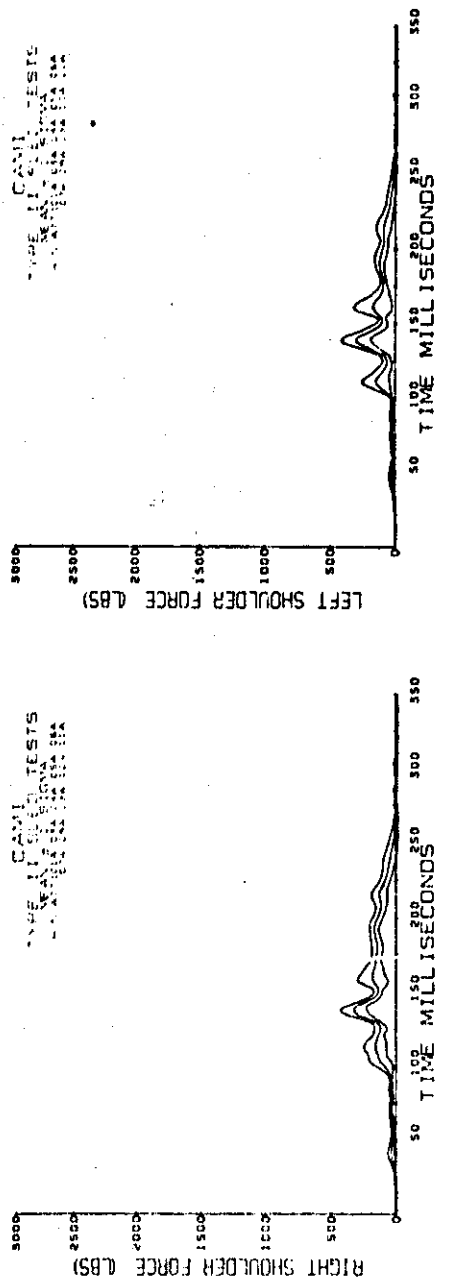


Figure A-4 (continued). Shoulder belt loads.

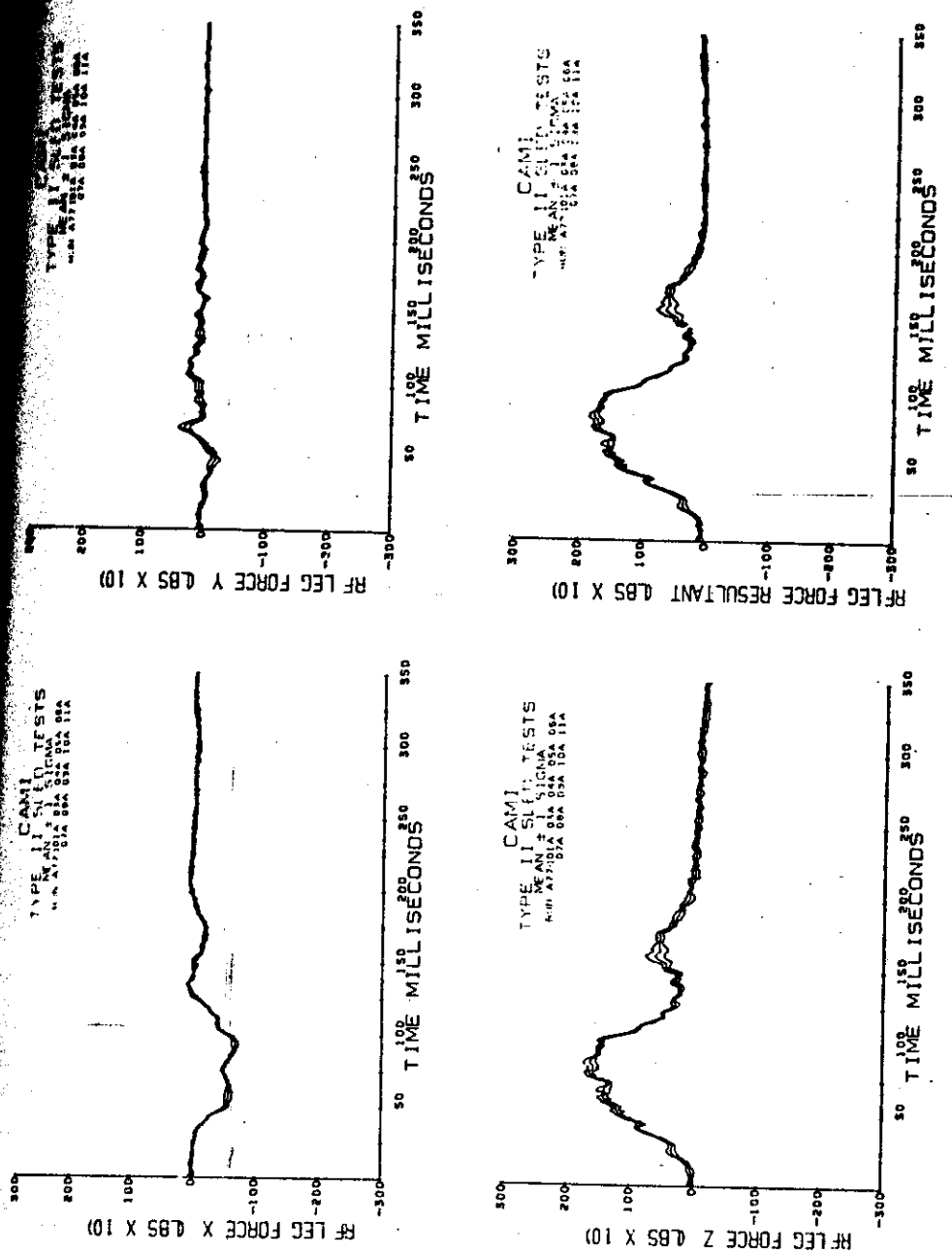


Figure A-4 (continued). Right front seat leg loads.

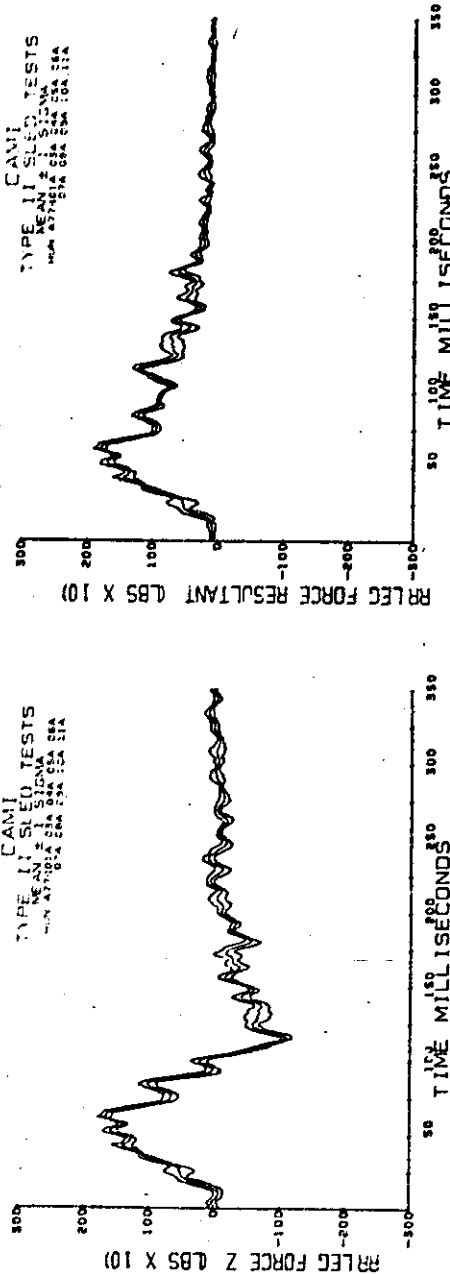
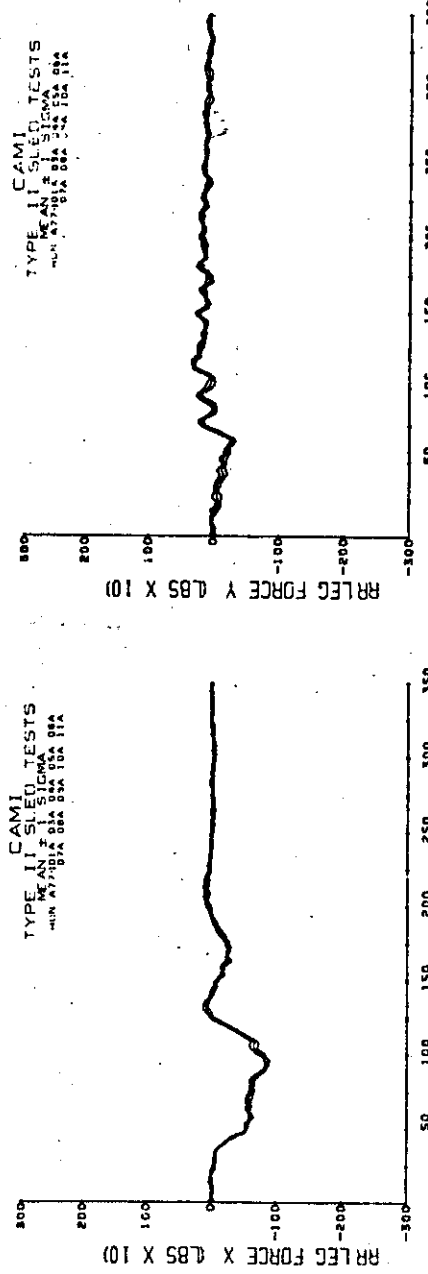


Figure A-4 (continued). Right rear seat leg loads.

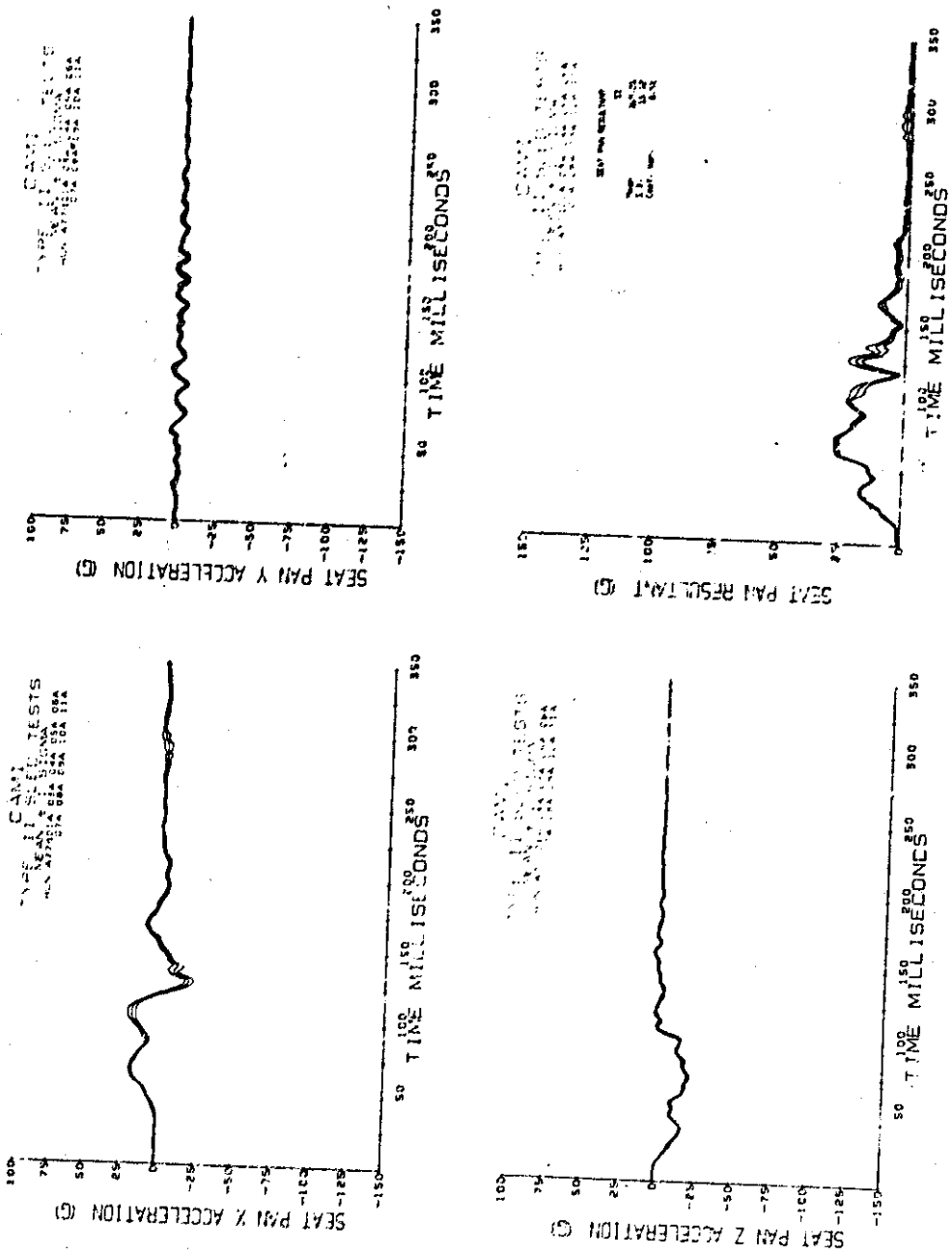


Figure A-4 (continued).  
a. Seat pan acceleration.

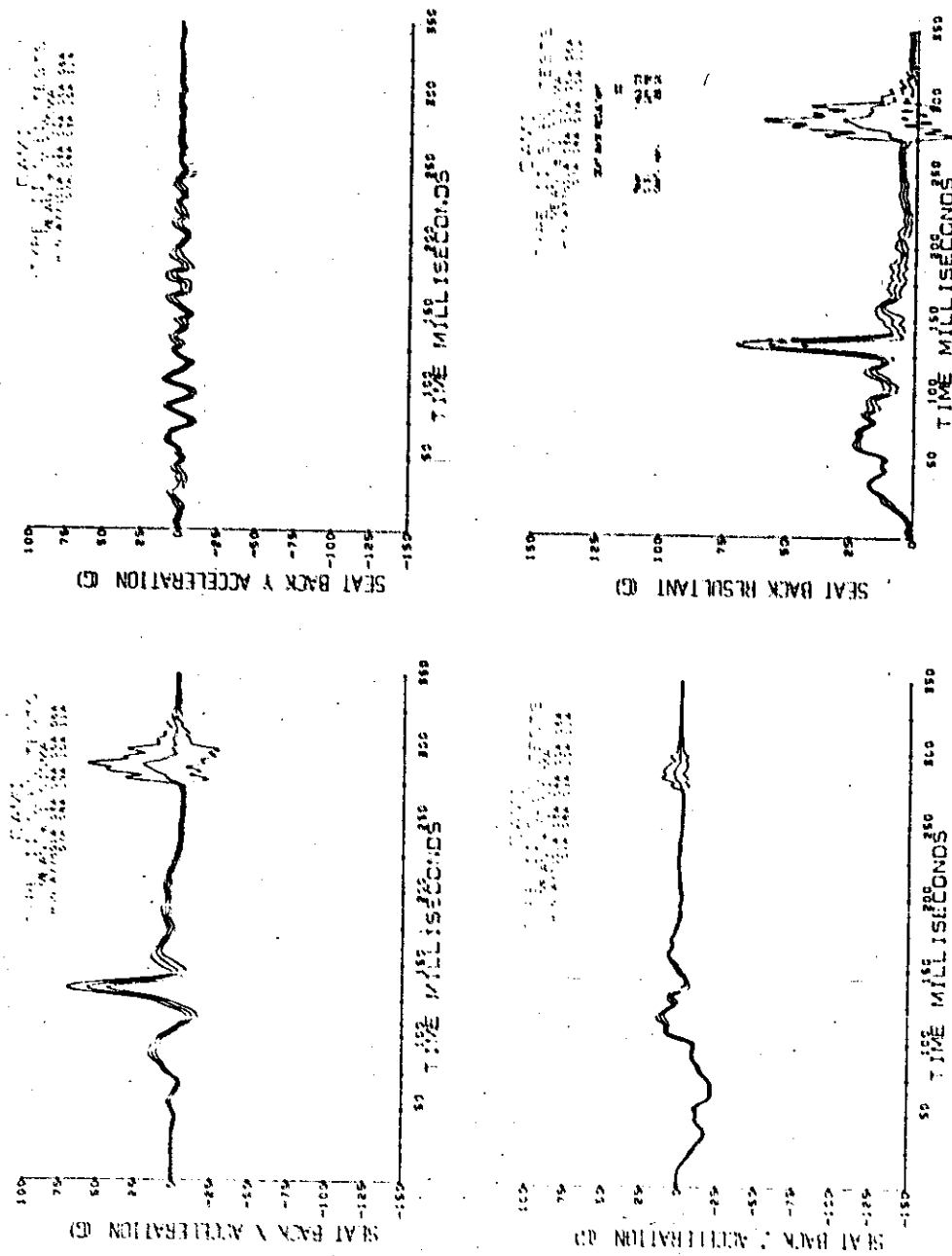


Figure A-4 (continued). Seat back acceleration.

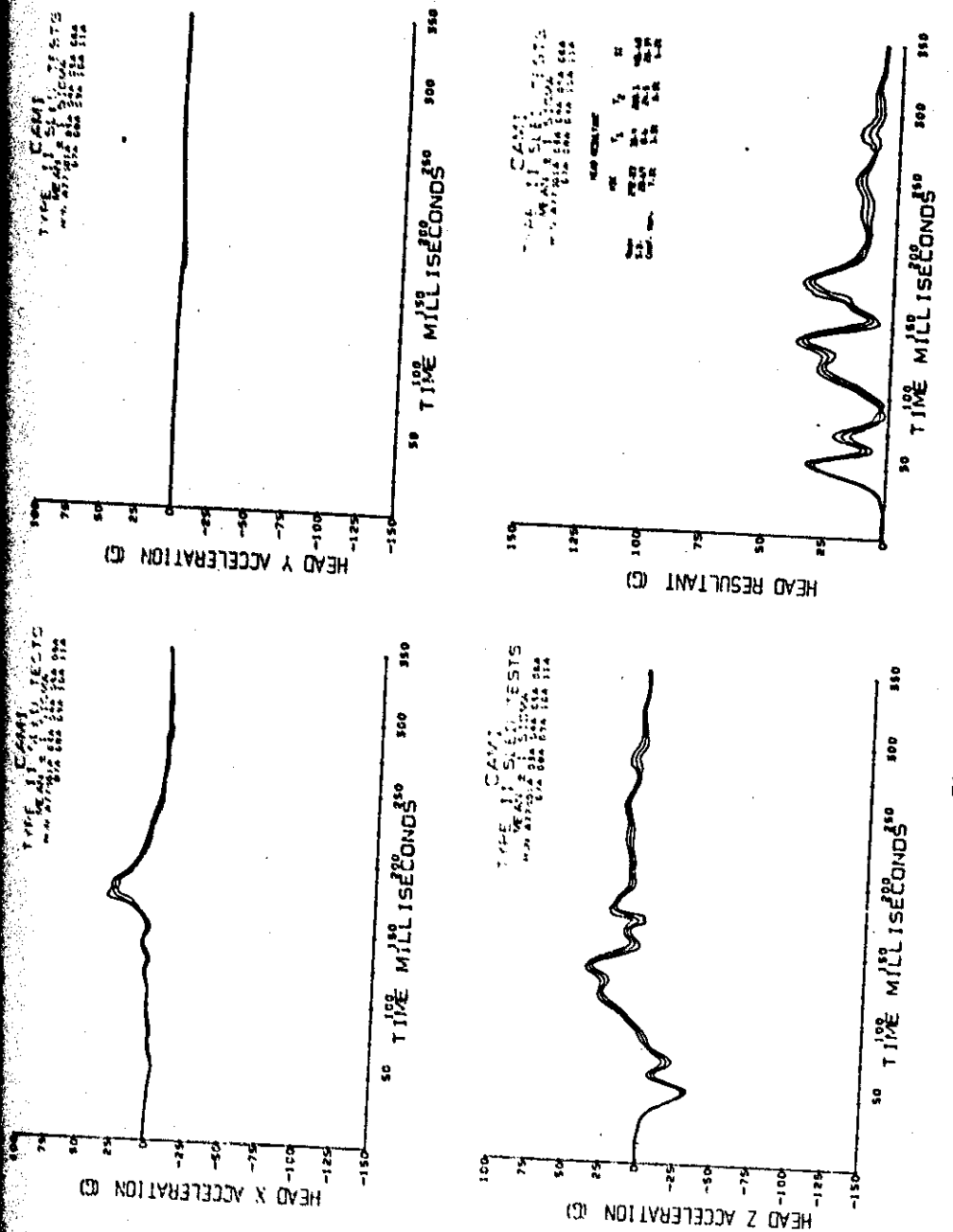


Figure A-4 (continued). Head acceleration.

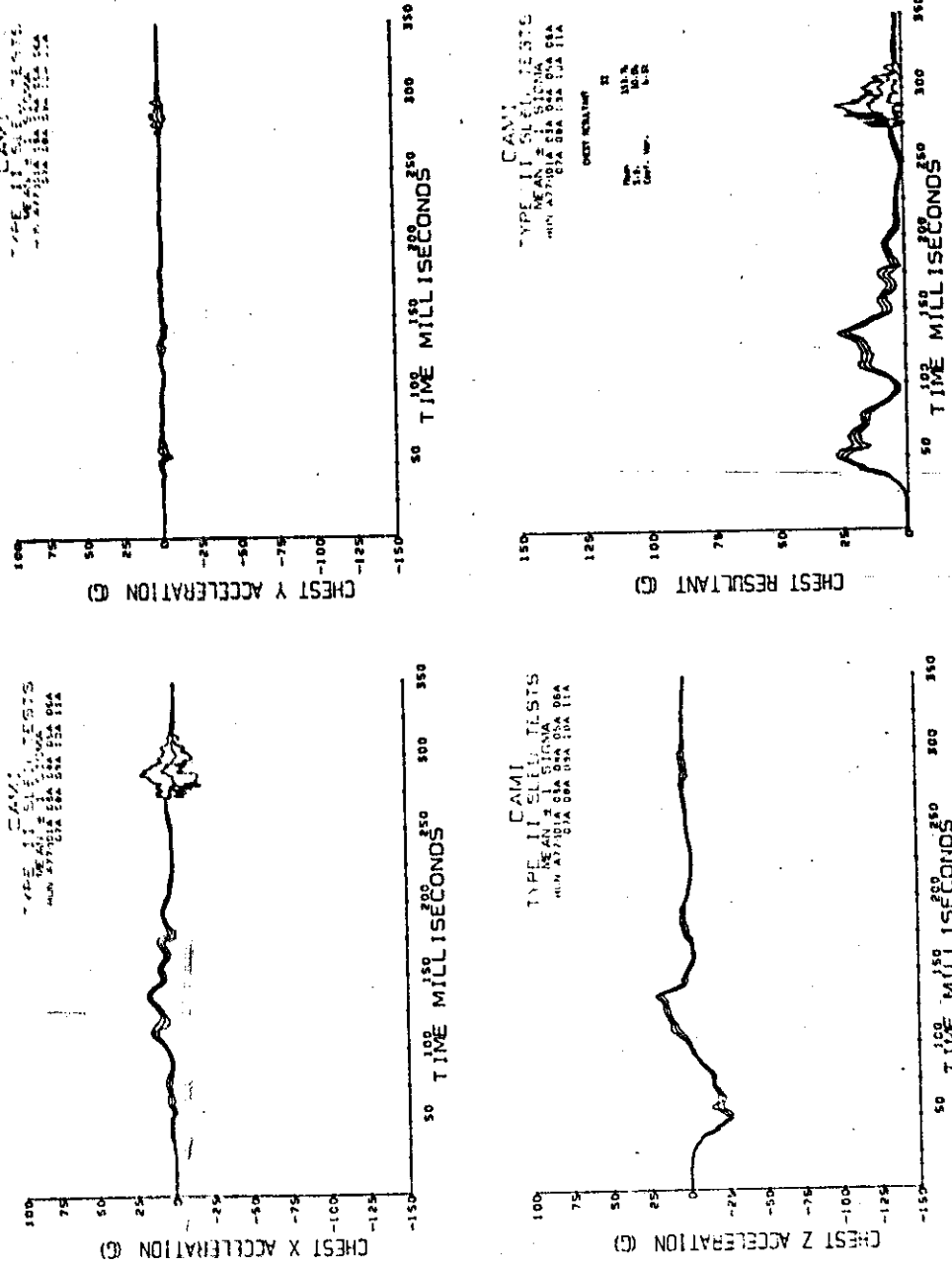


Figure A-4 (continued). Chest acceleration.

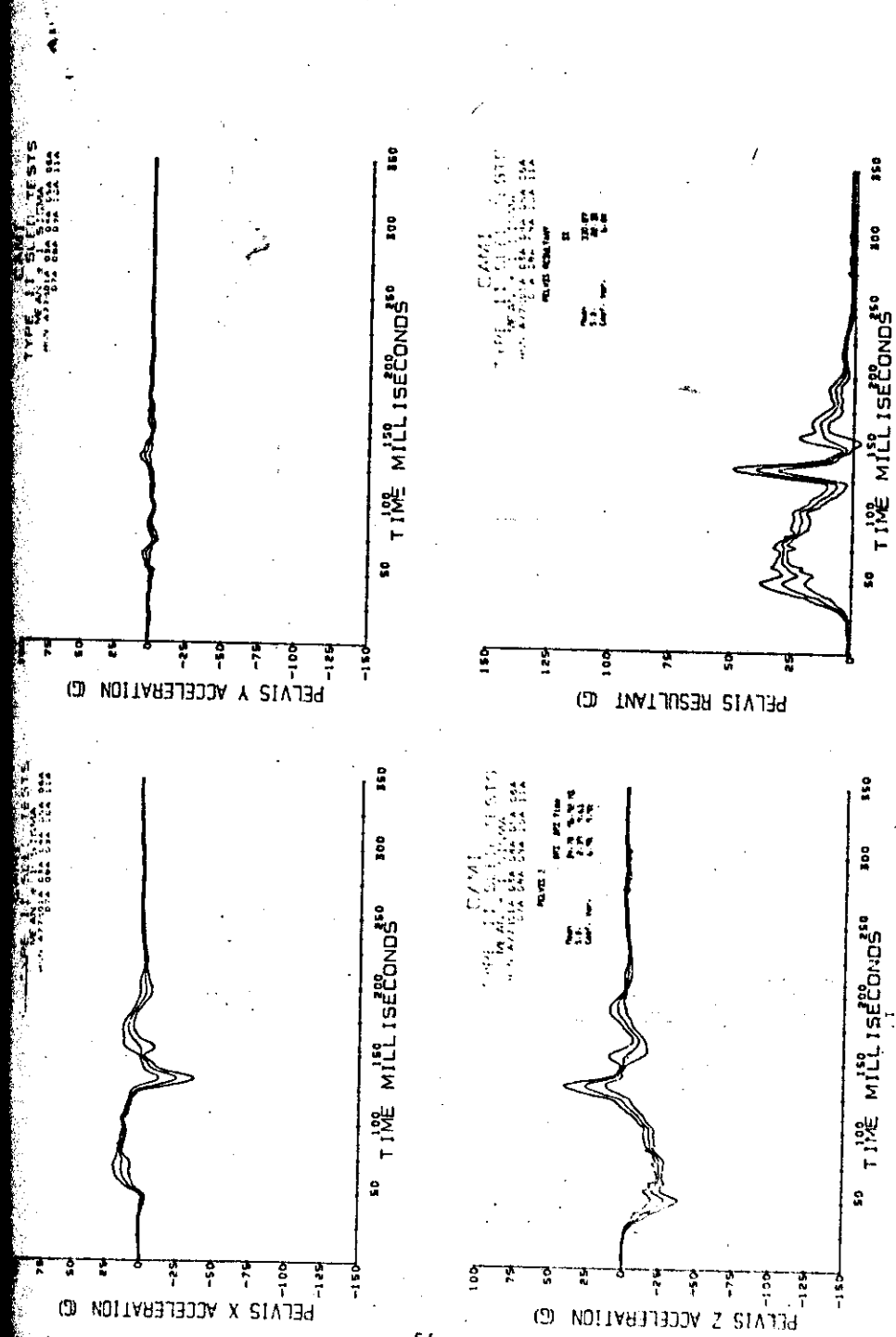


Figure A-4 (continued). Pelvis acceleration.

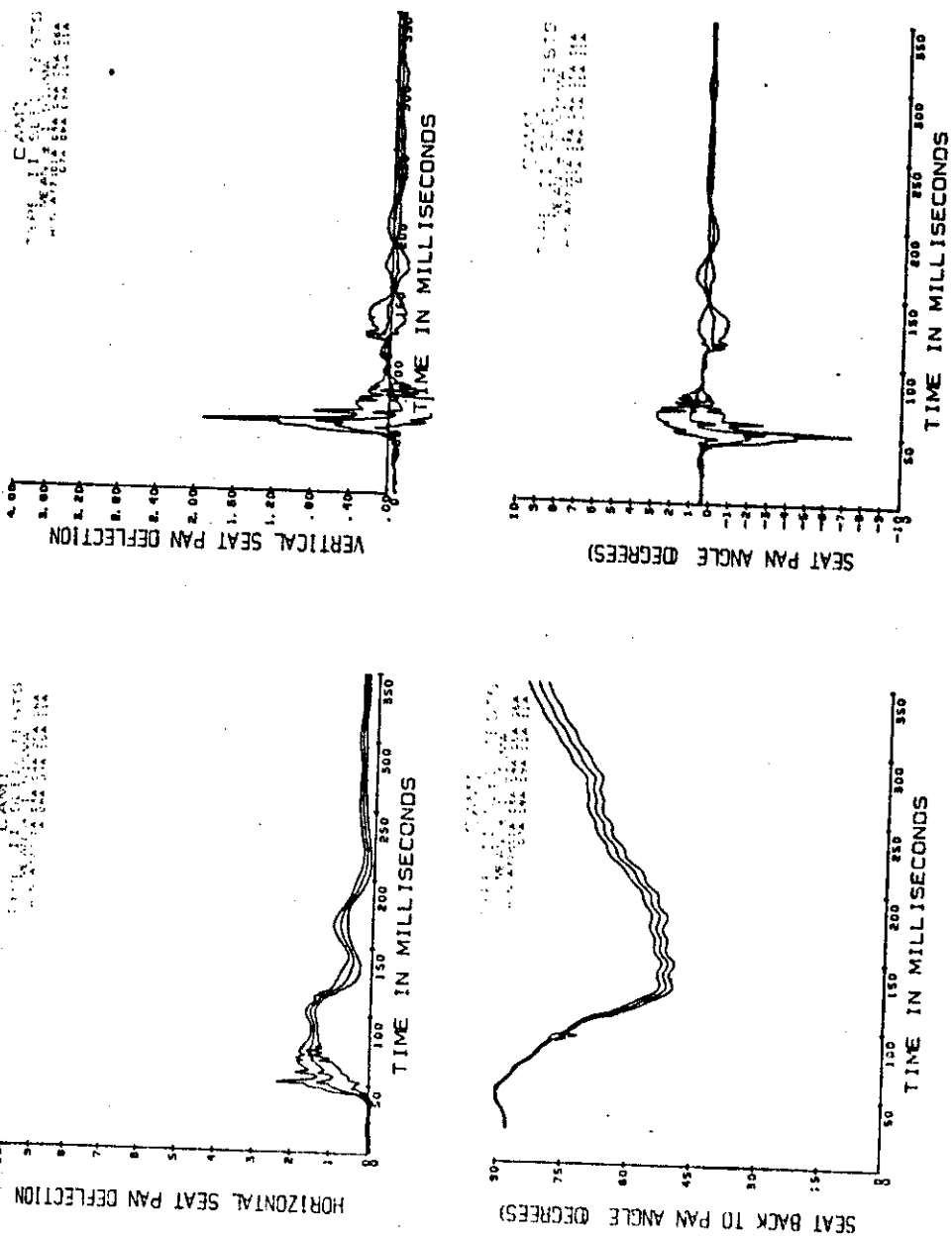


Figure A-4 (continued). Seat extensometer data.

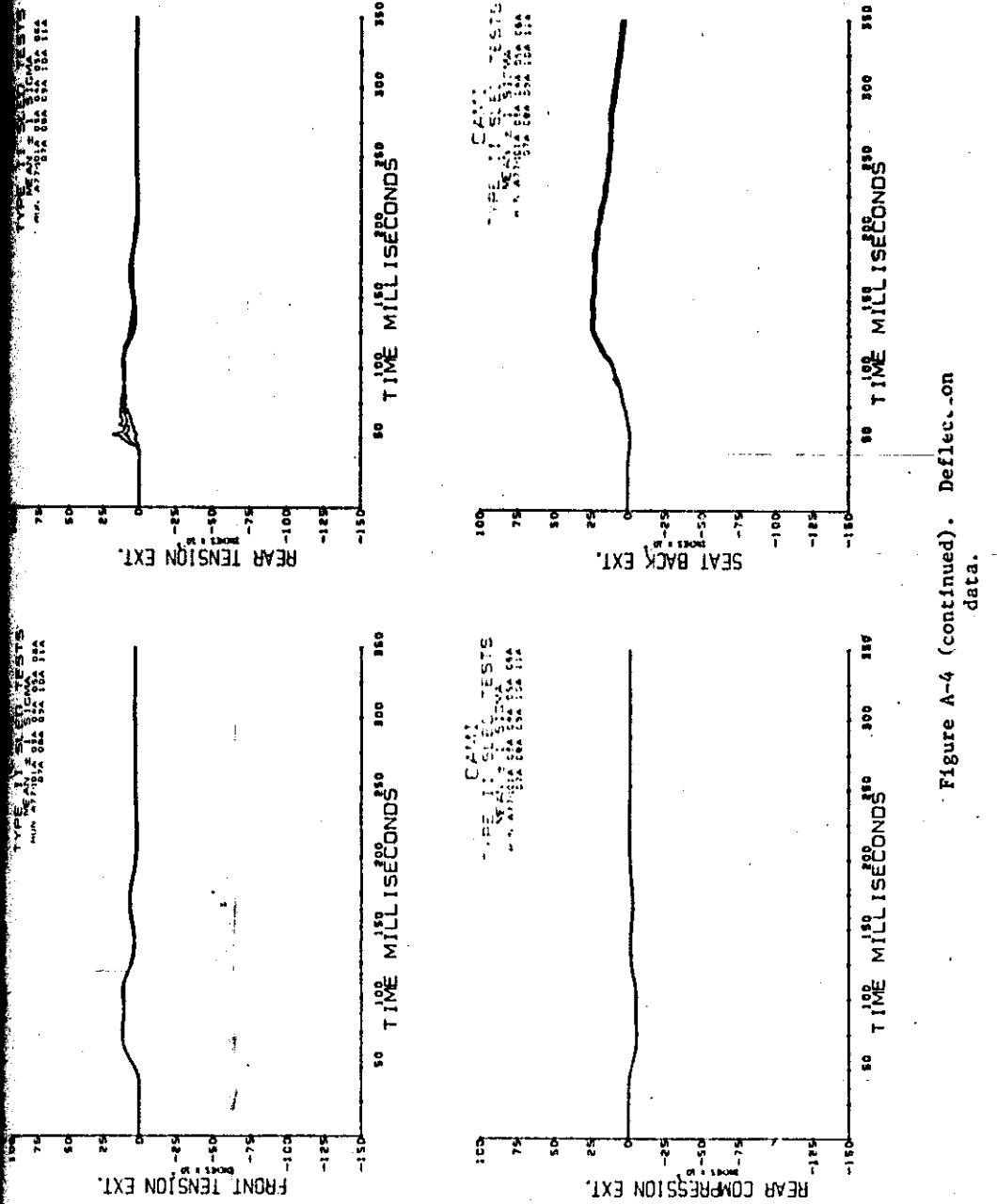


Figure A-4 (continued). Deflection data.

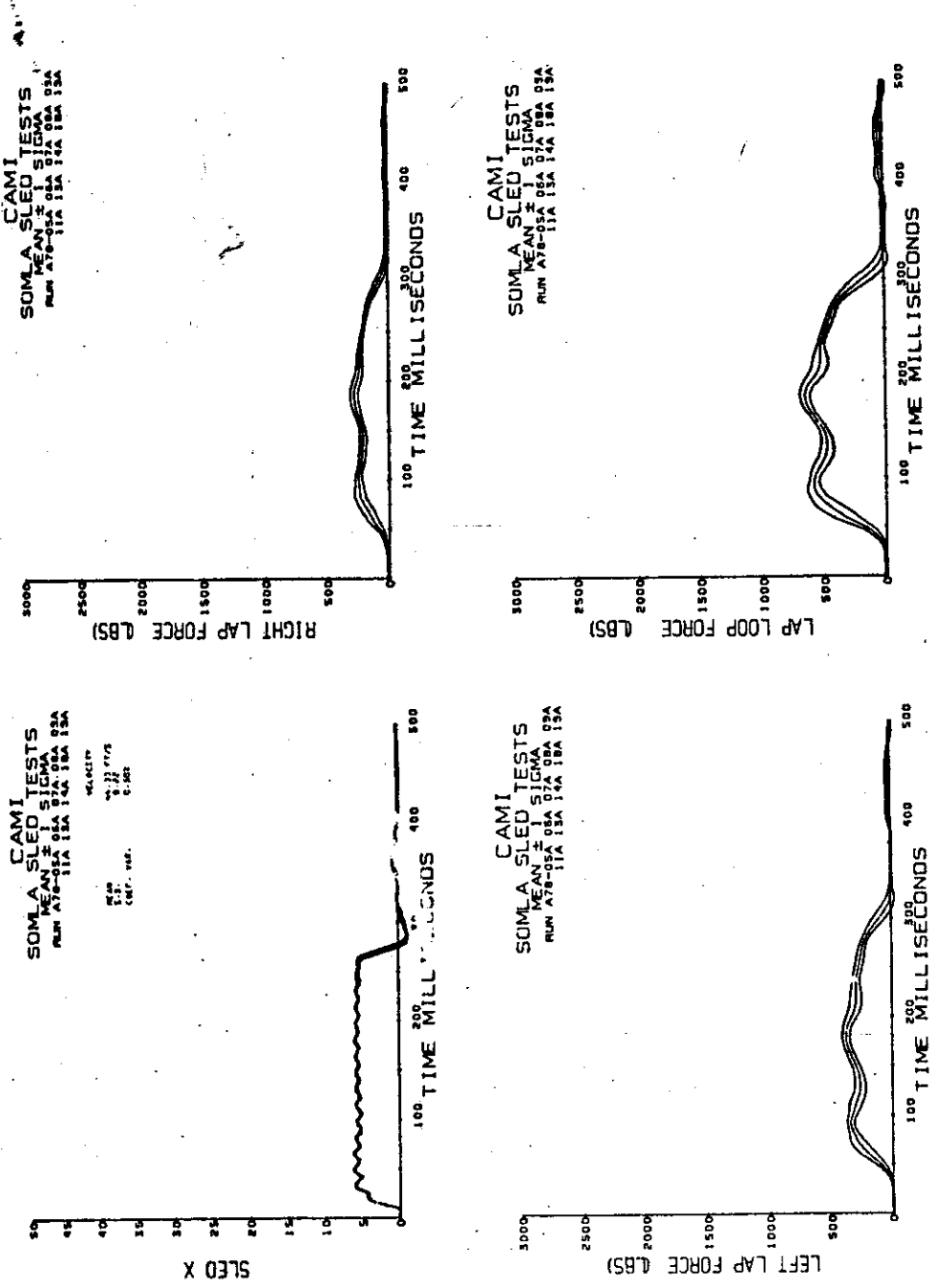


Figure A-5. Forward-facing, low-deceleration tests - simulated deceleration and lapbelt loads.

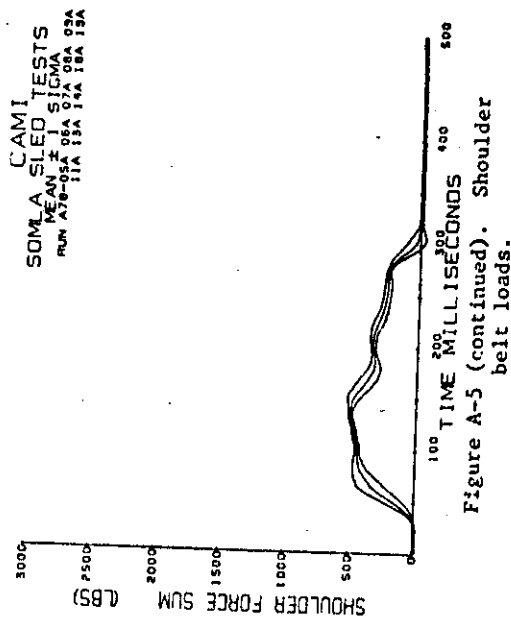
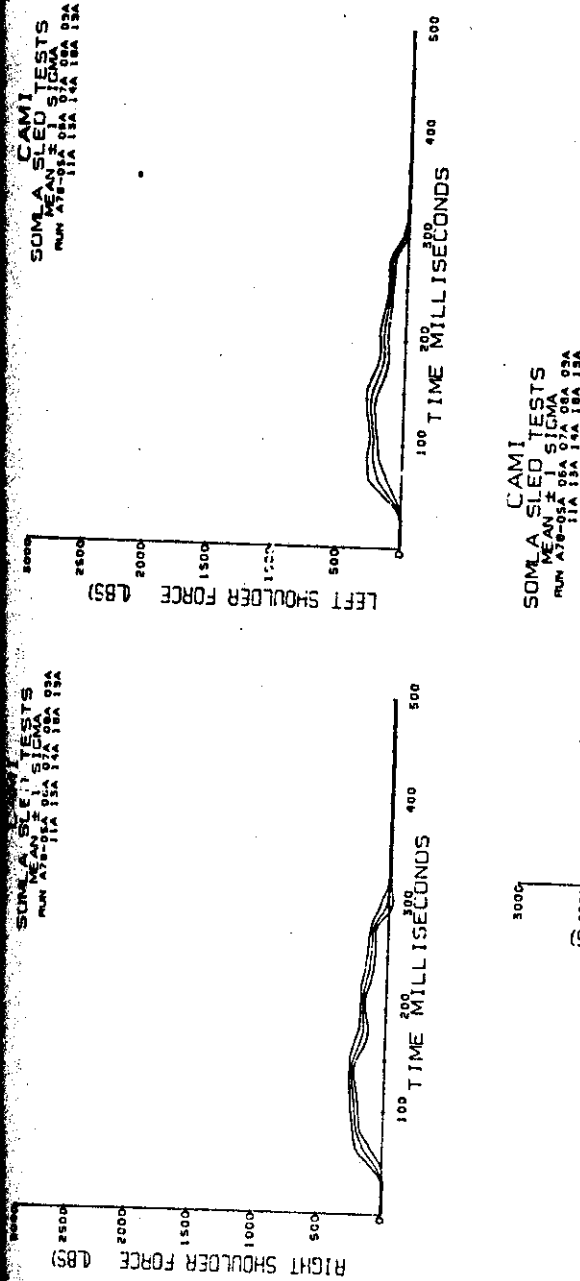


Figure A-5 (continued). Shoulder belt loads.

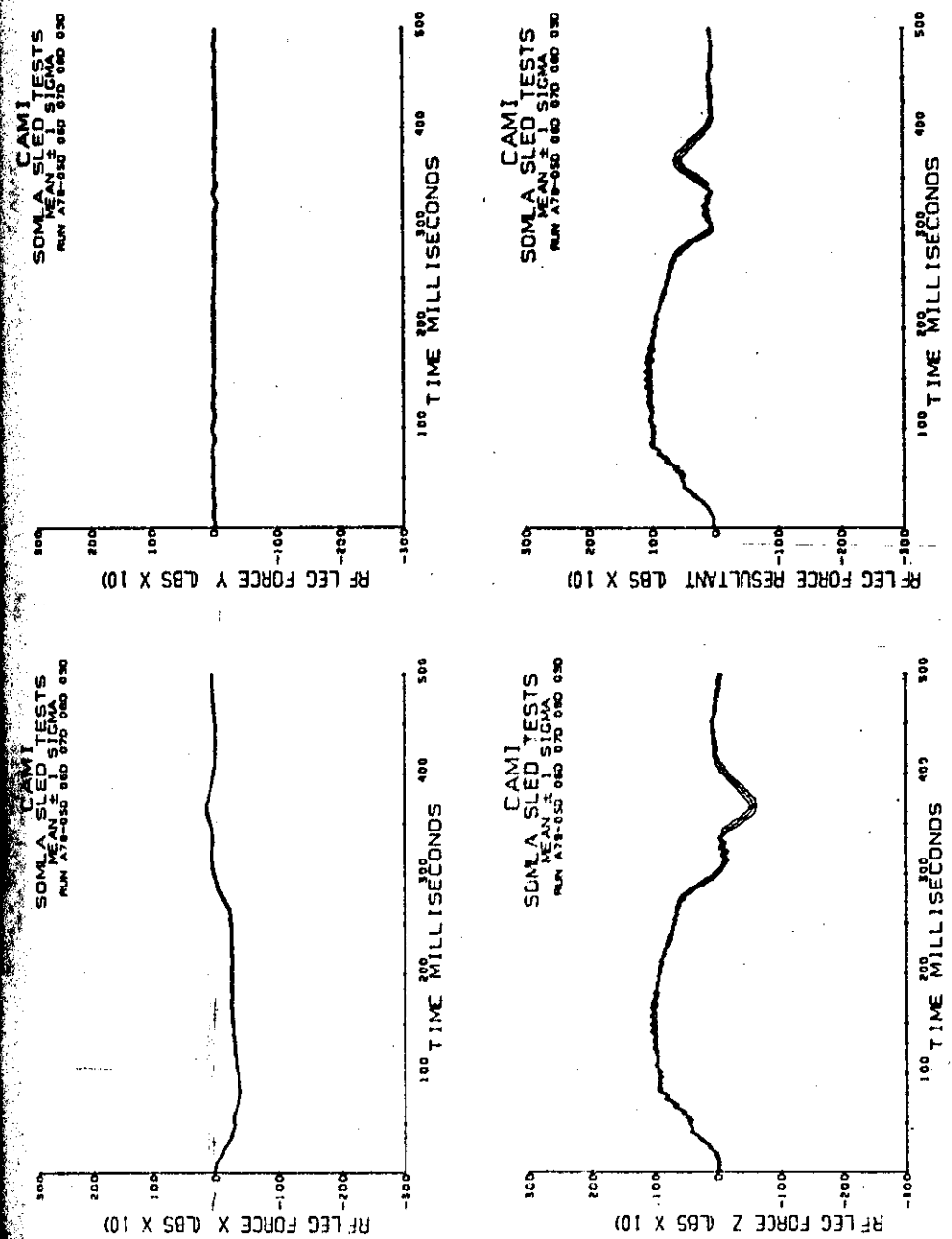


Figure A-5 (continued). Right front seat leg loads.

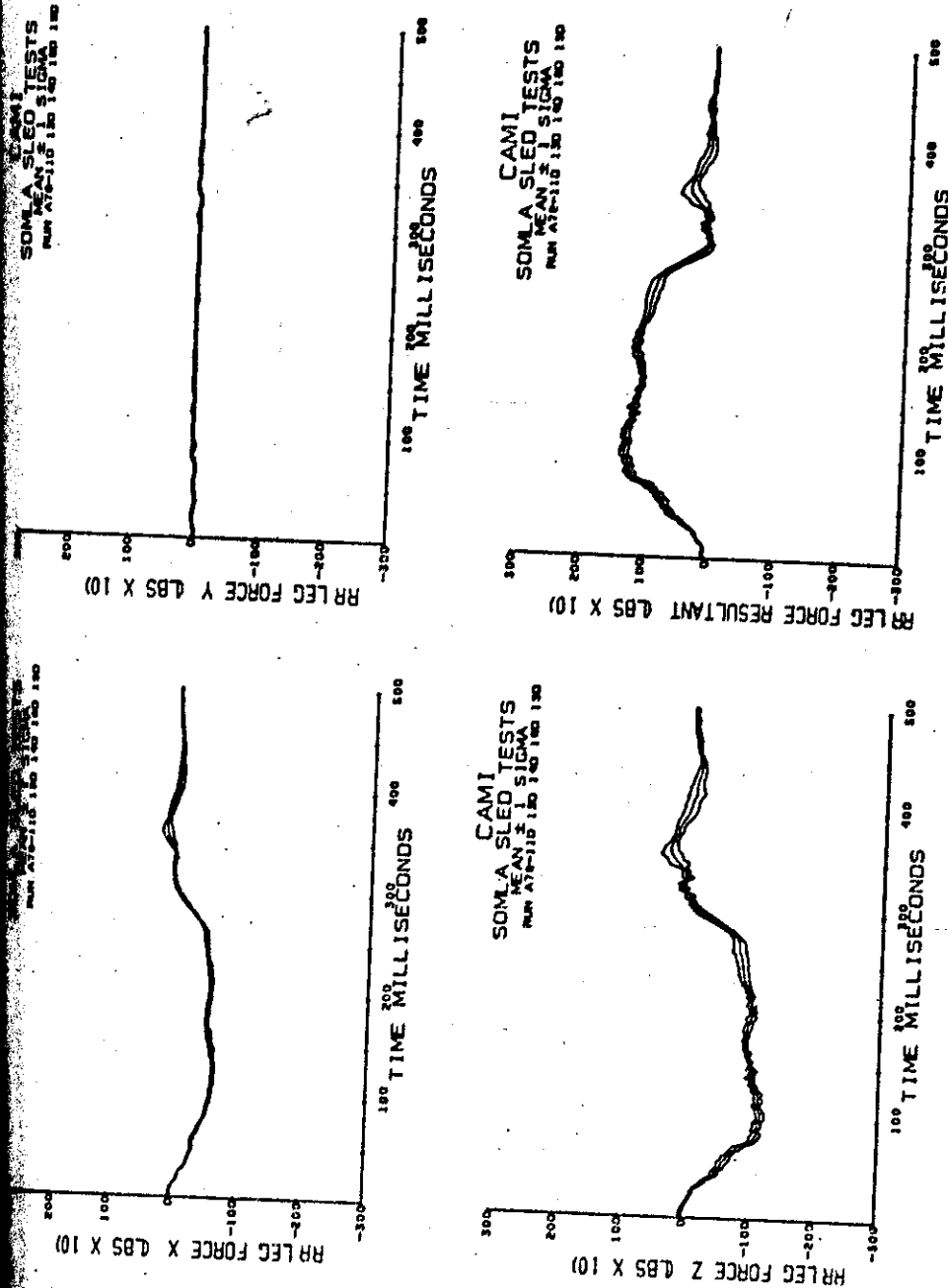


Figure A-5 (continued). Right rear seat leg loads.

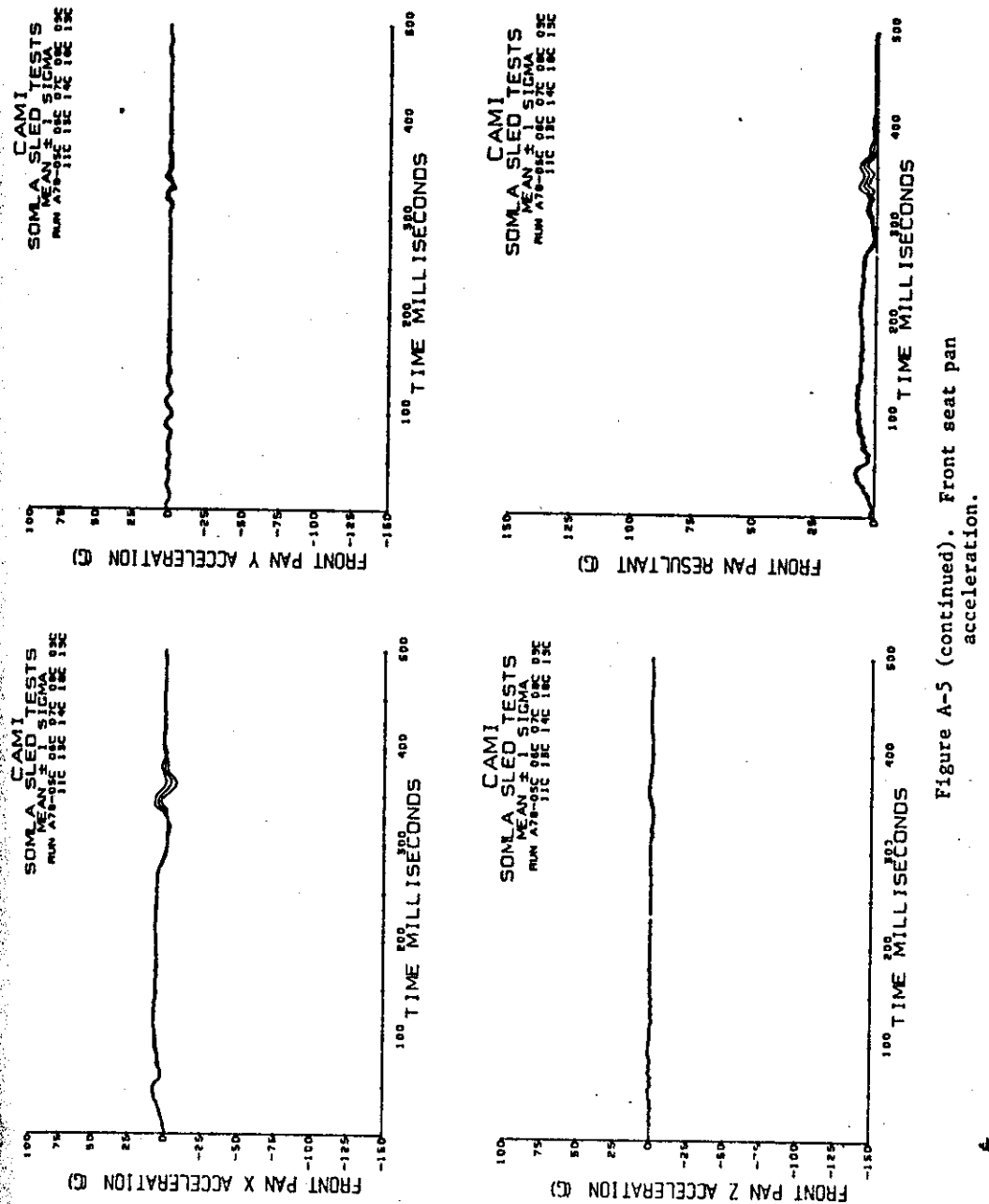


Figure A-5 (continued). Front seat pan acceleration.

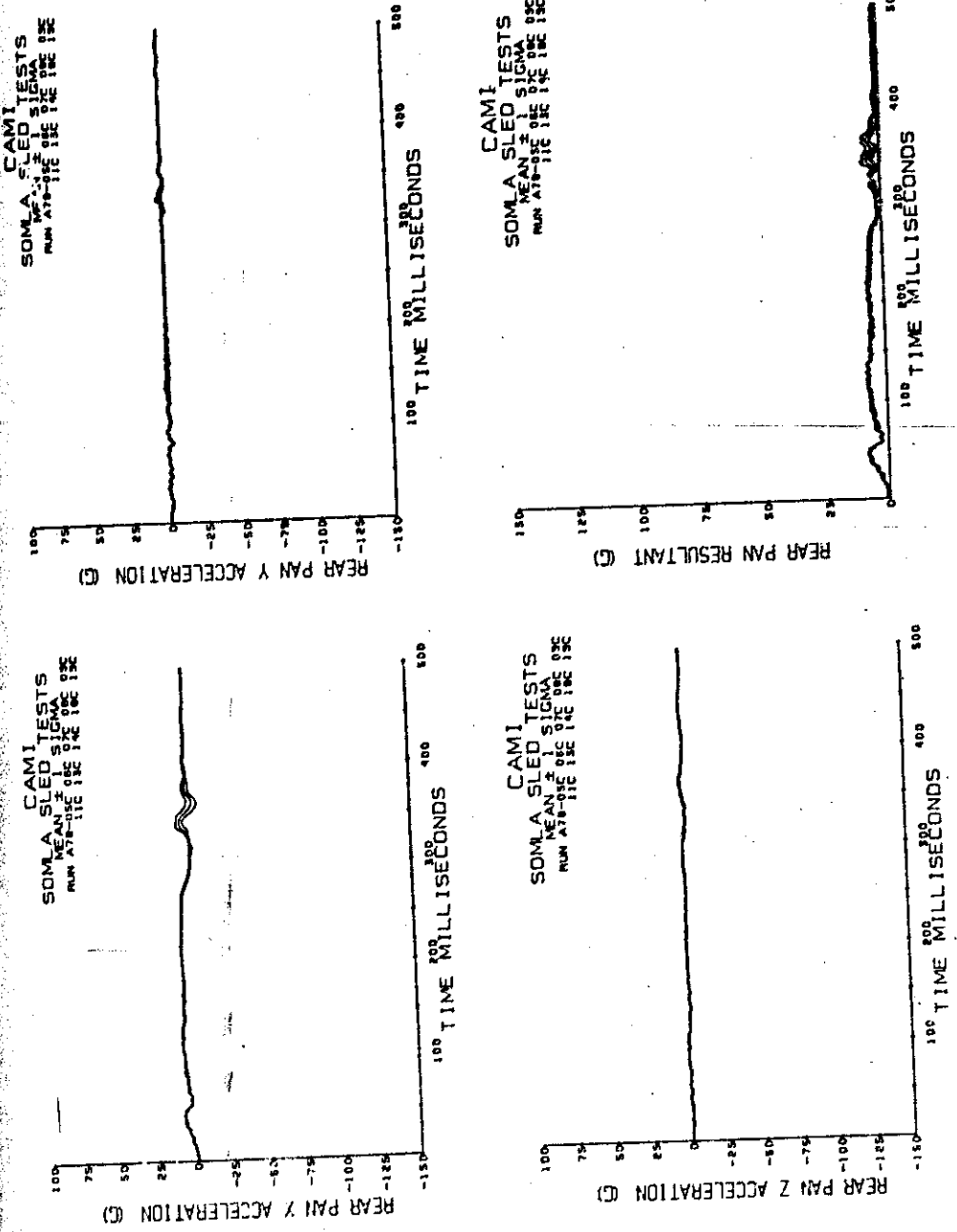


Figure A-5 (continued). Rear seat pan acceleration.

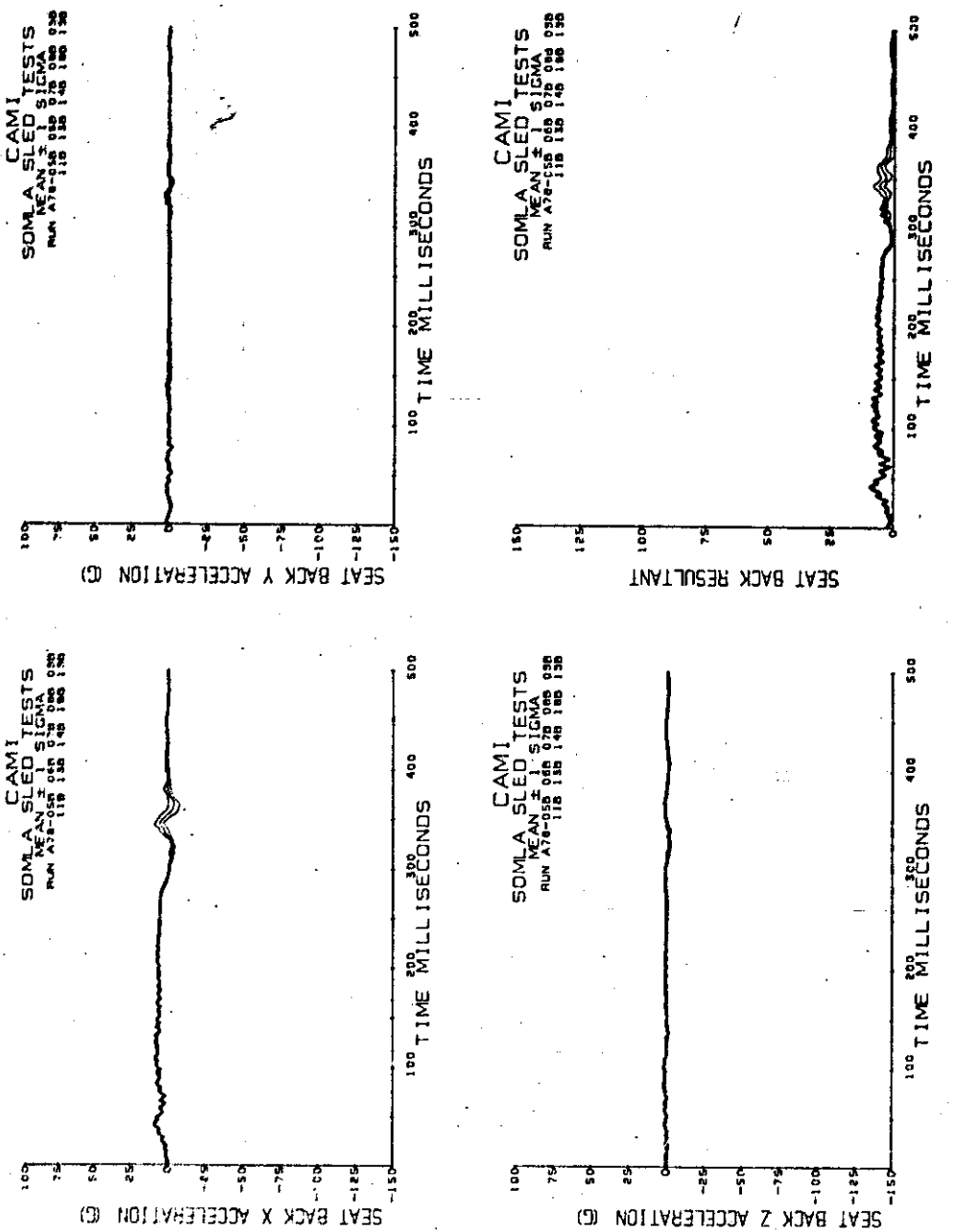


Figure A-5 (continued). Seat back acceleration.

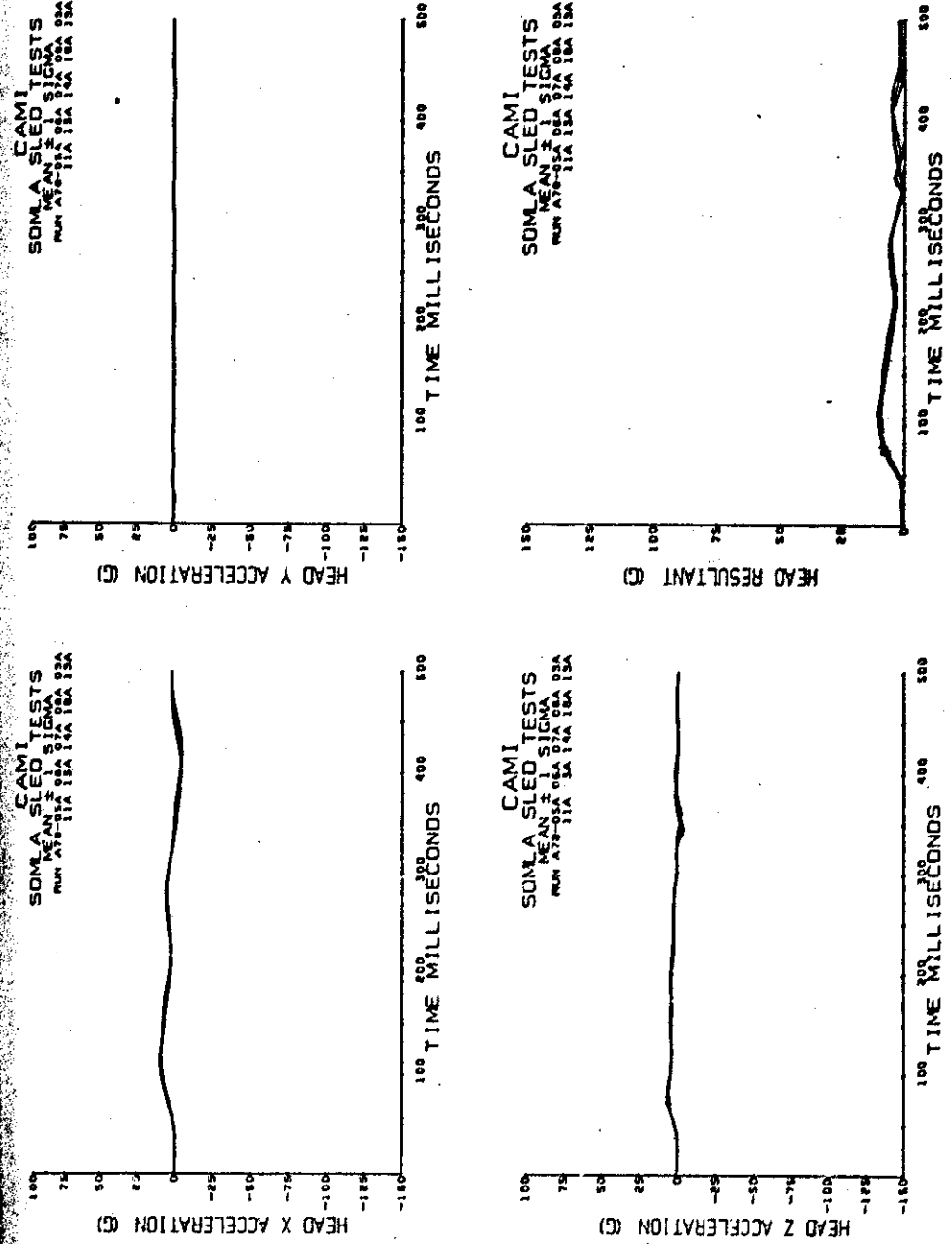


Figure A-5 (continued). Head acceleration.

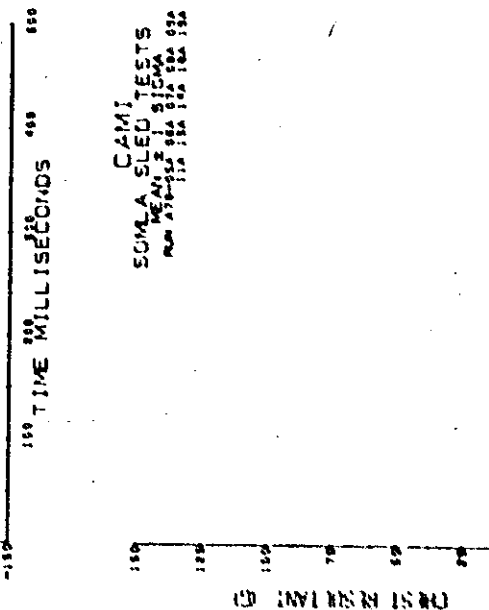
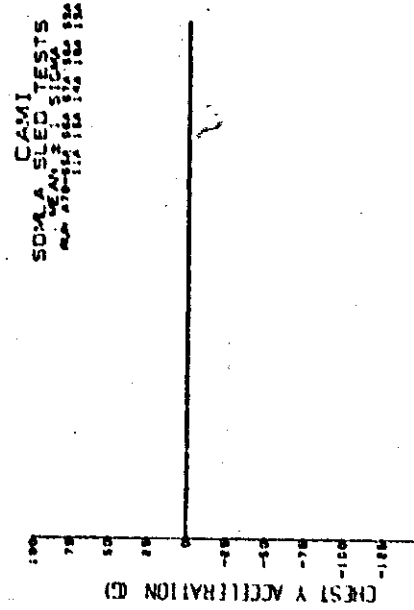
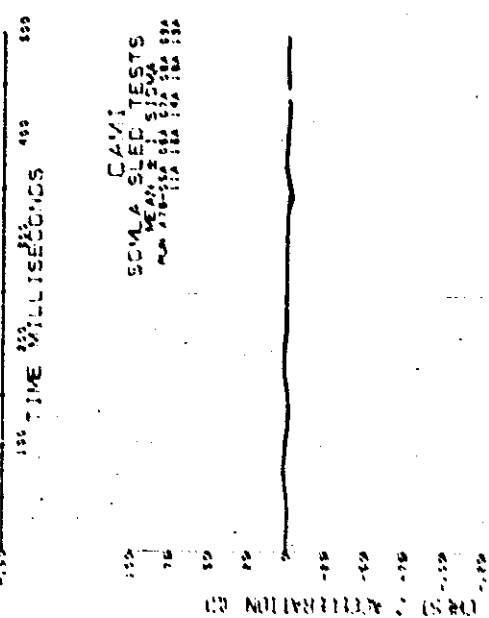
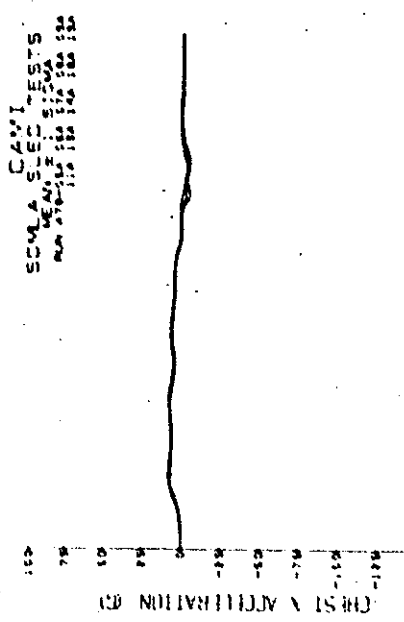


Figure 4-5. Quest X Acceleration Test Results.

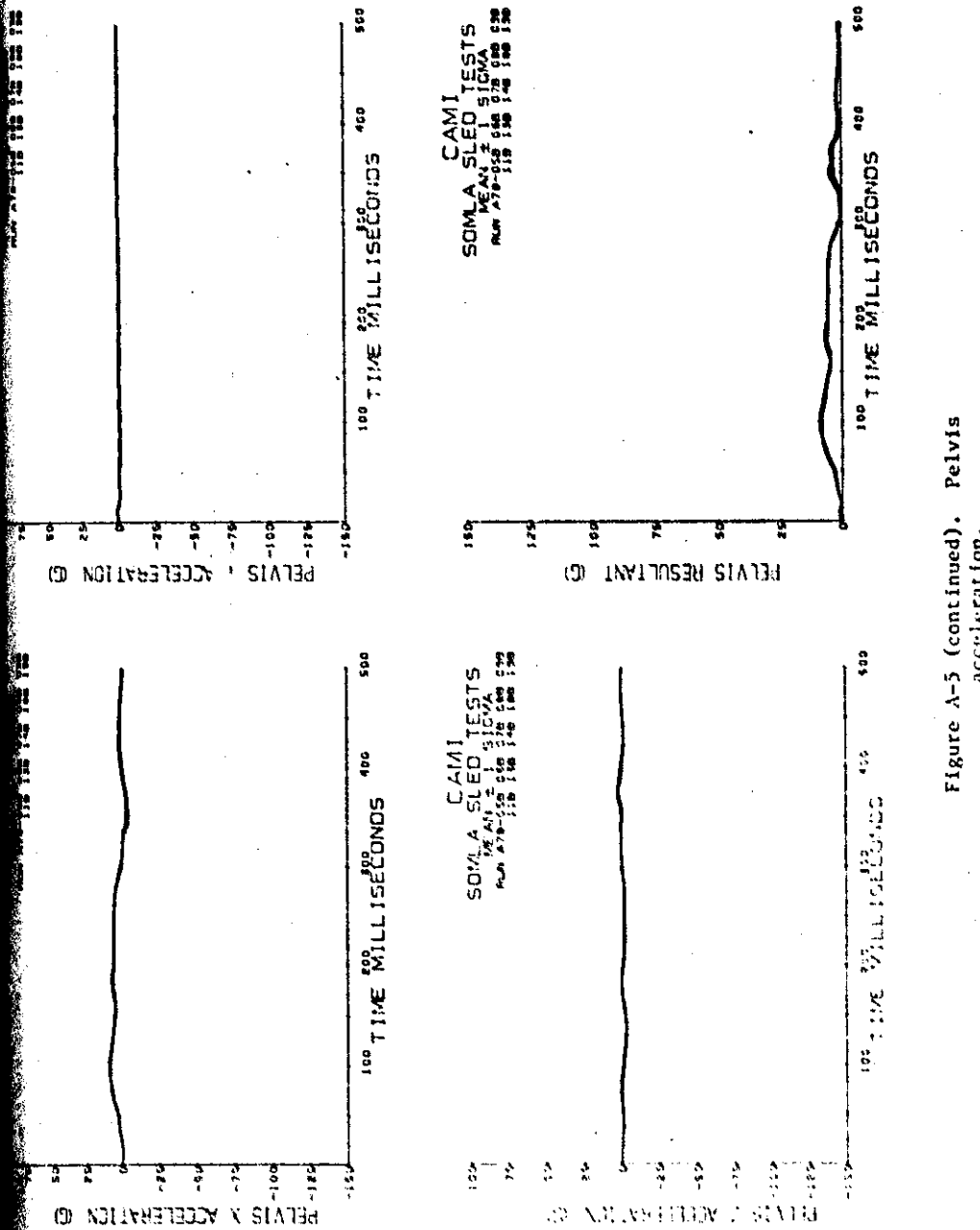


Figure A-5 (continued). Pelvis acceleration.

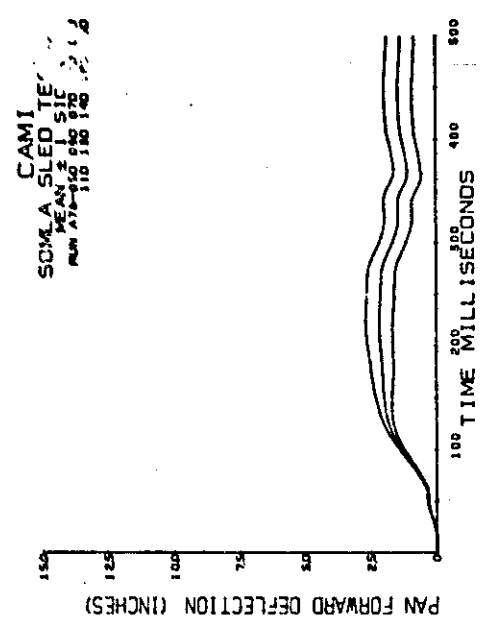


Figure A-5 (continued). Deflection data.

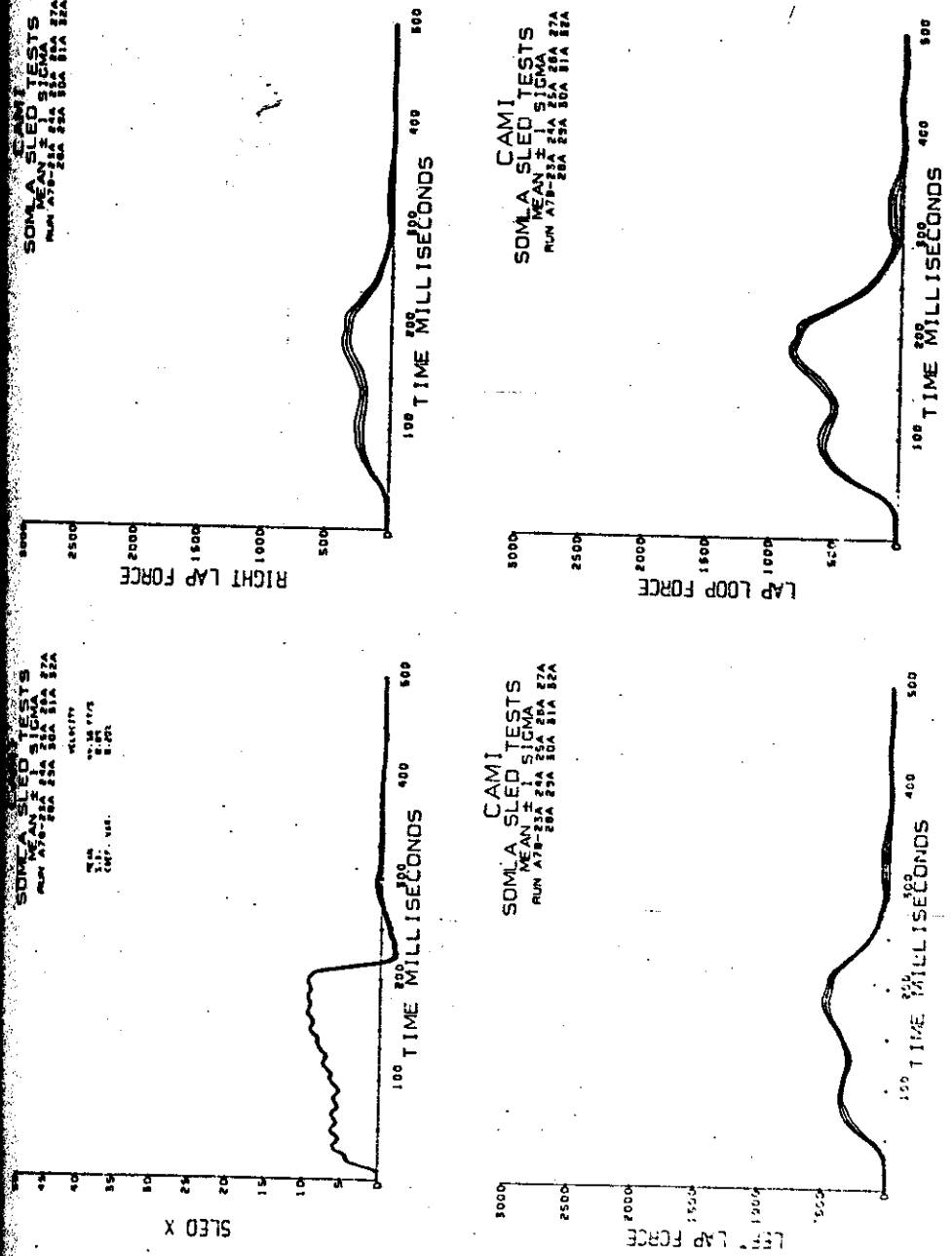


Figure A-6. Forward-facing, higher deceleration tests.  
Sled deceleration and lapbelt loads.

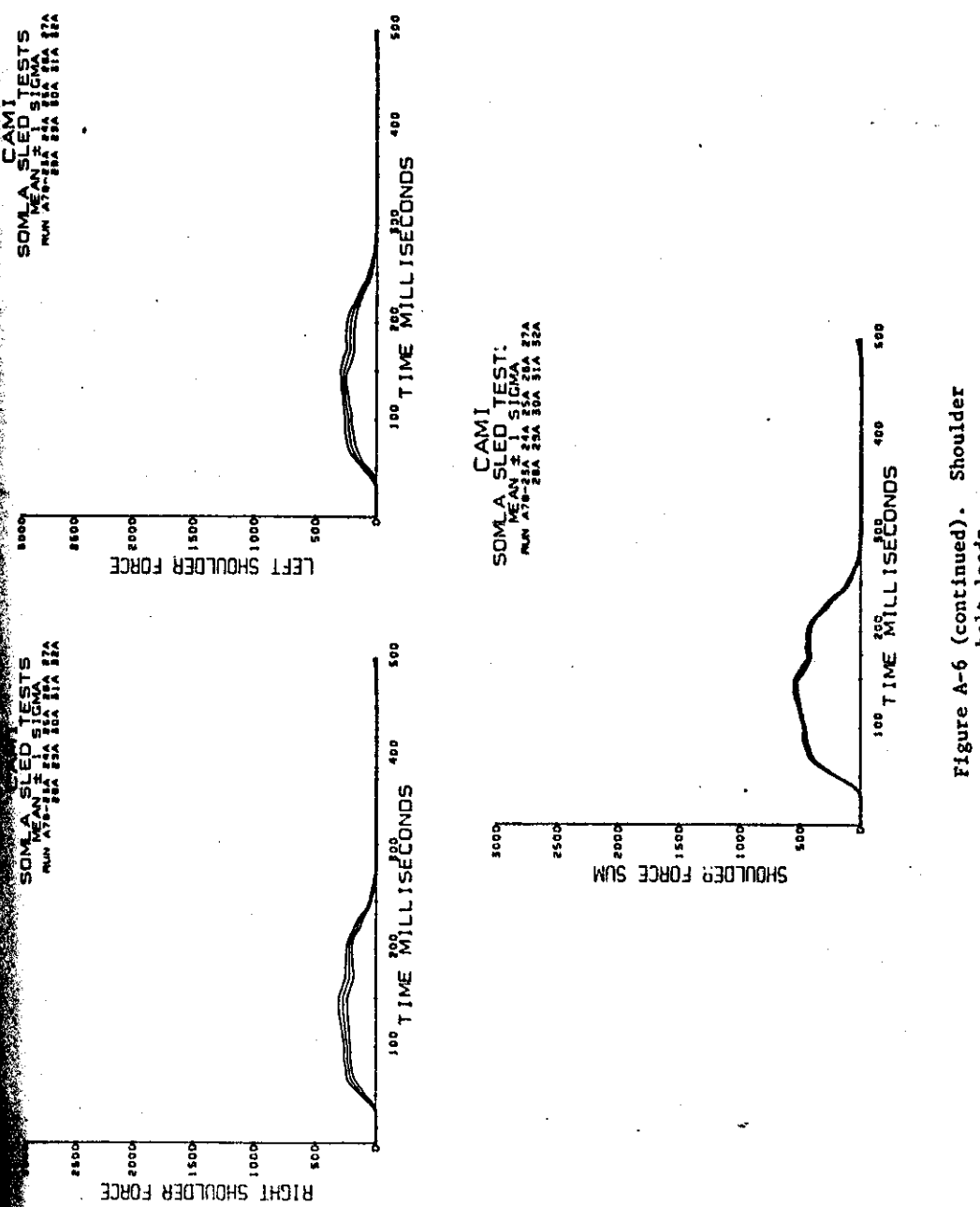


Figure A-6 (continued). Shoulder belt loads.

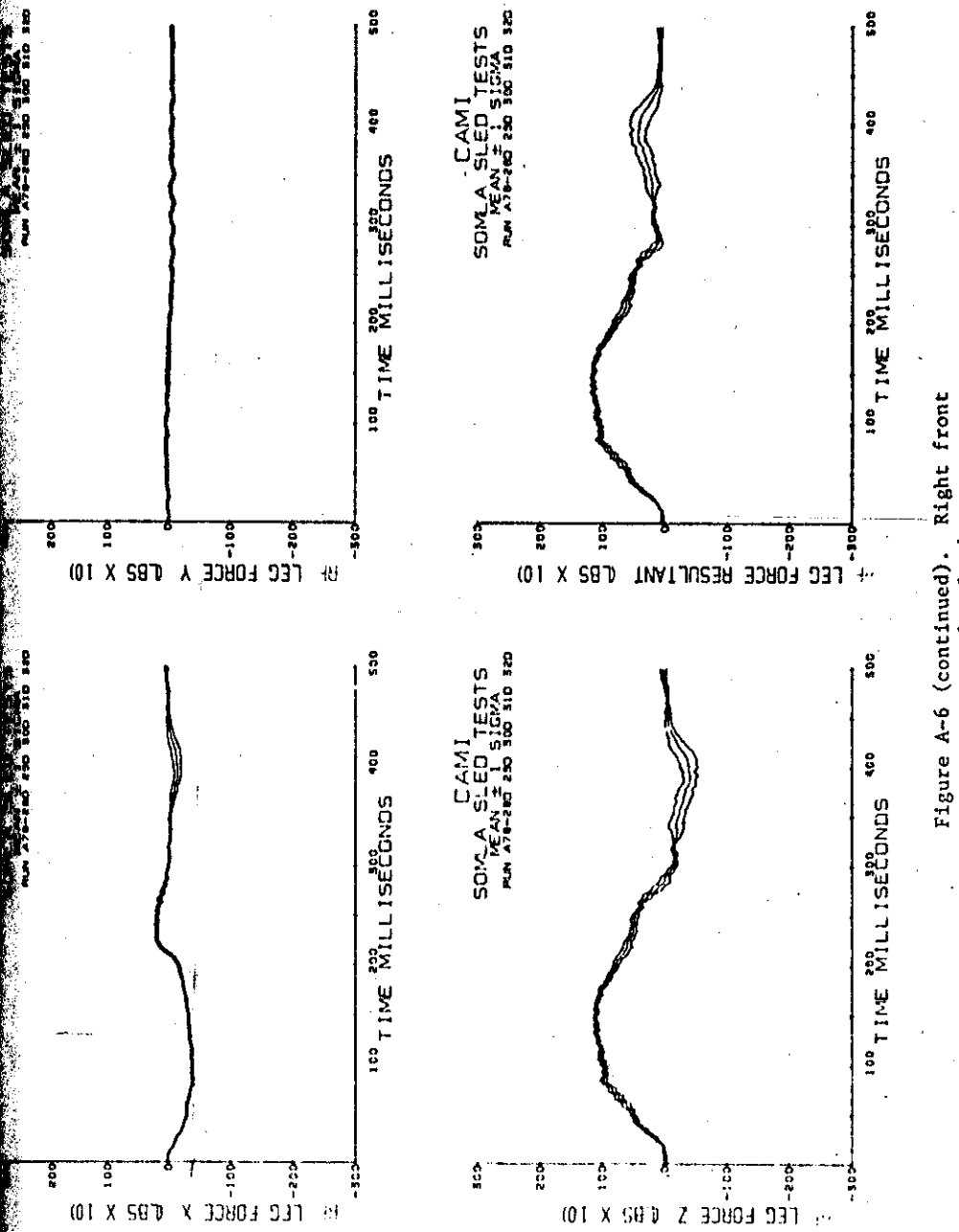


Figure A-6 (continued). Right front seat leg loads.

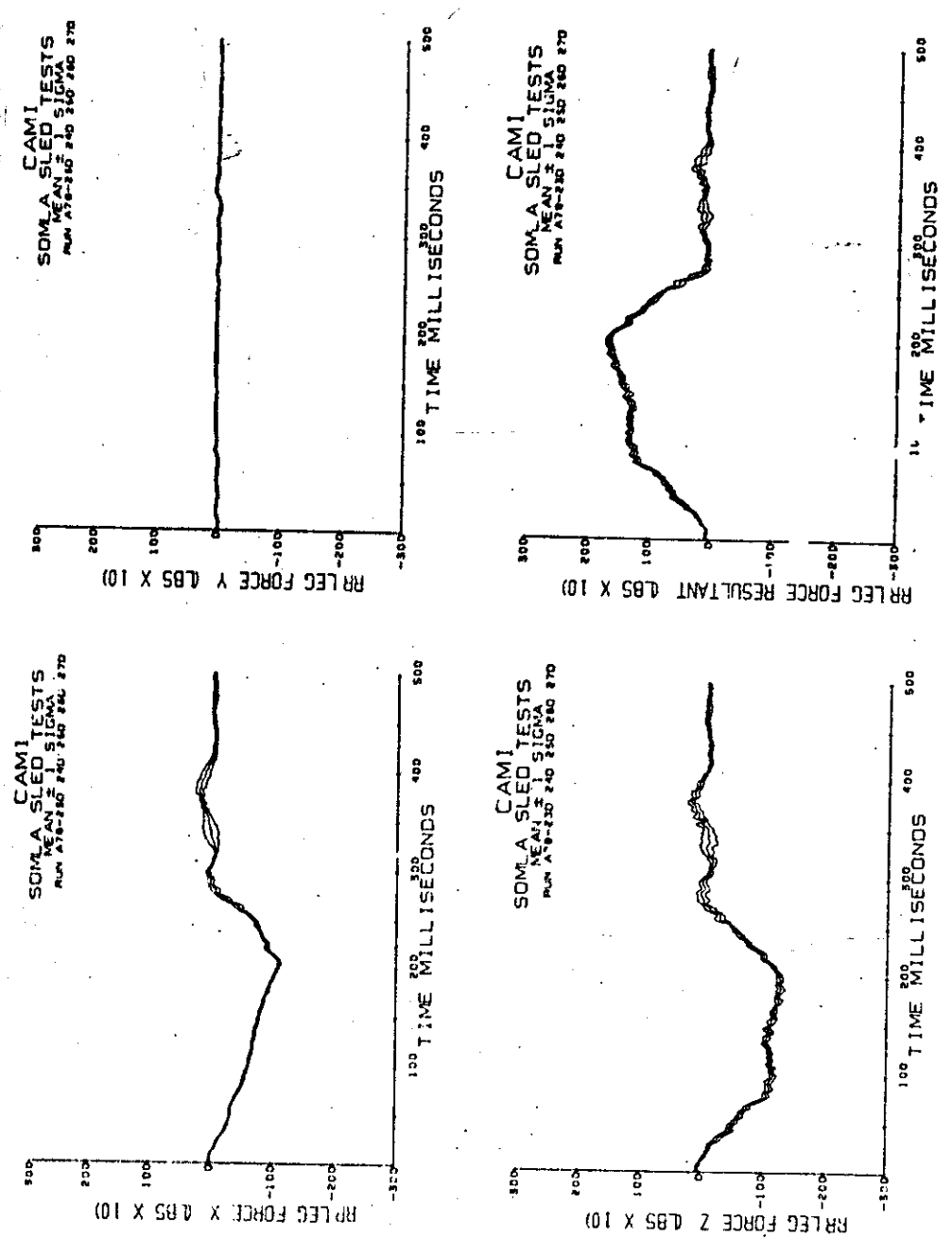


Figure A-6 (continued). Right rear seat leg loads.

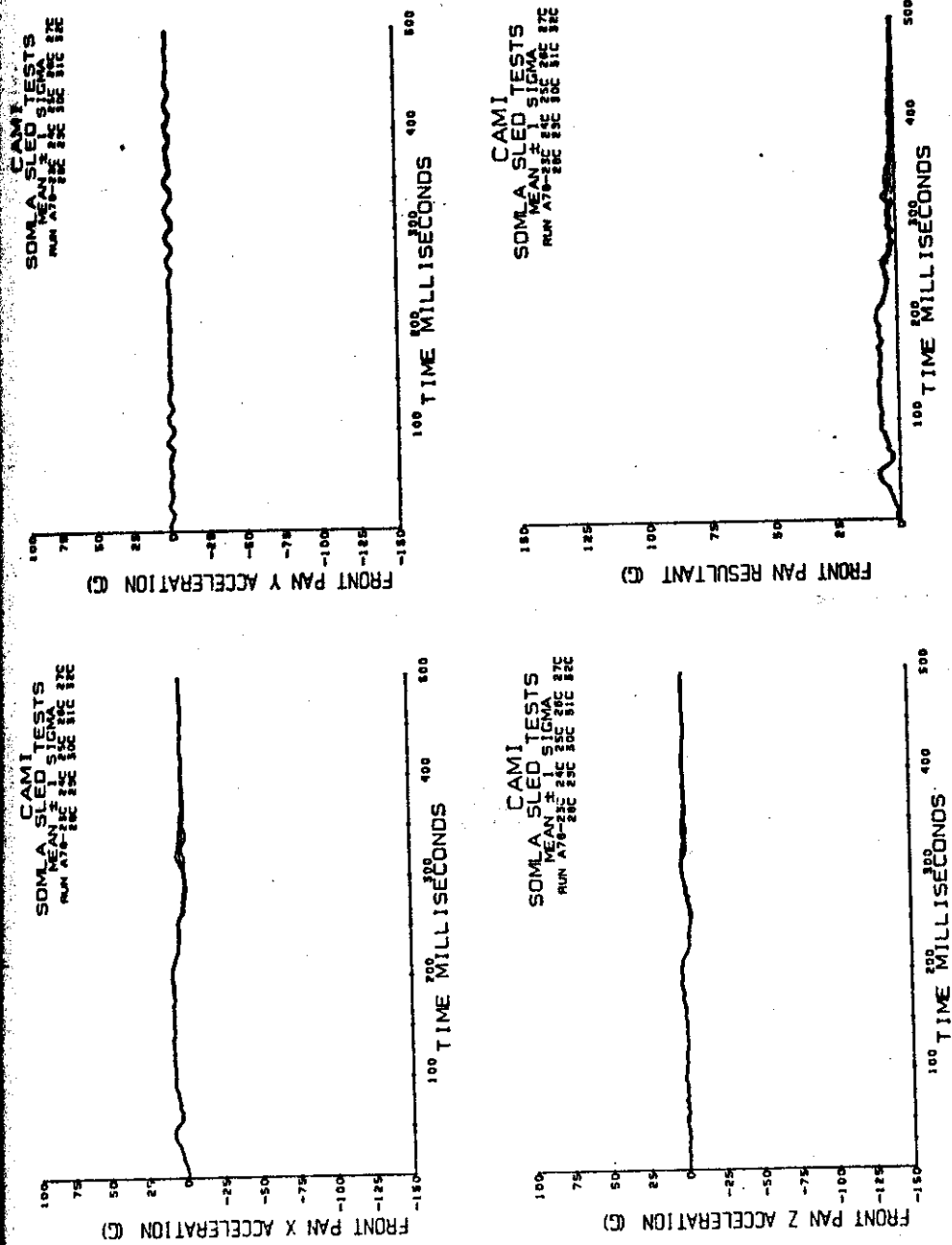


Figure A-6 (continued). Front seat pan acceleration.

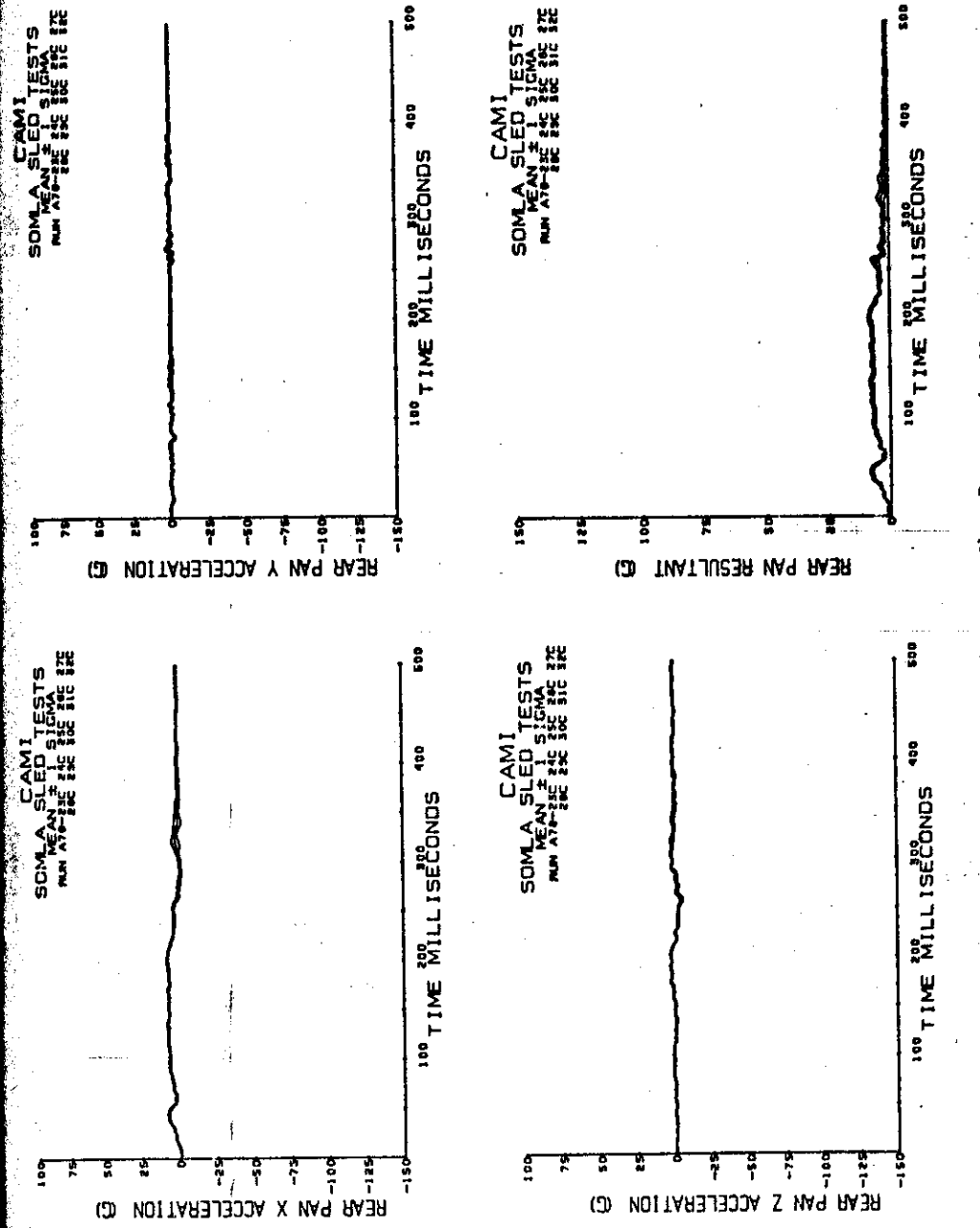


Figure A-6 (continued). Rear seat pan acceleration.

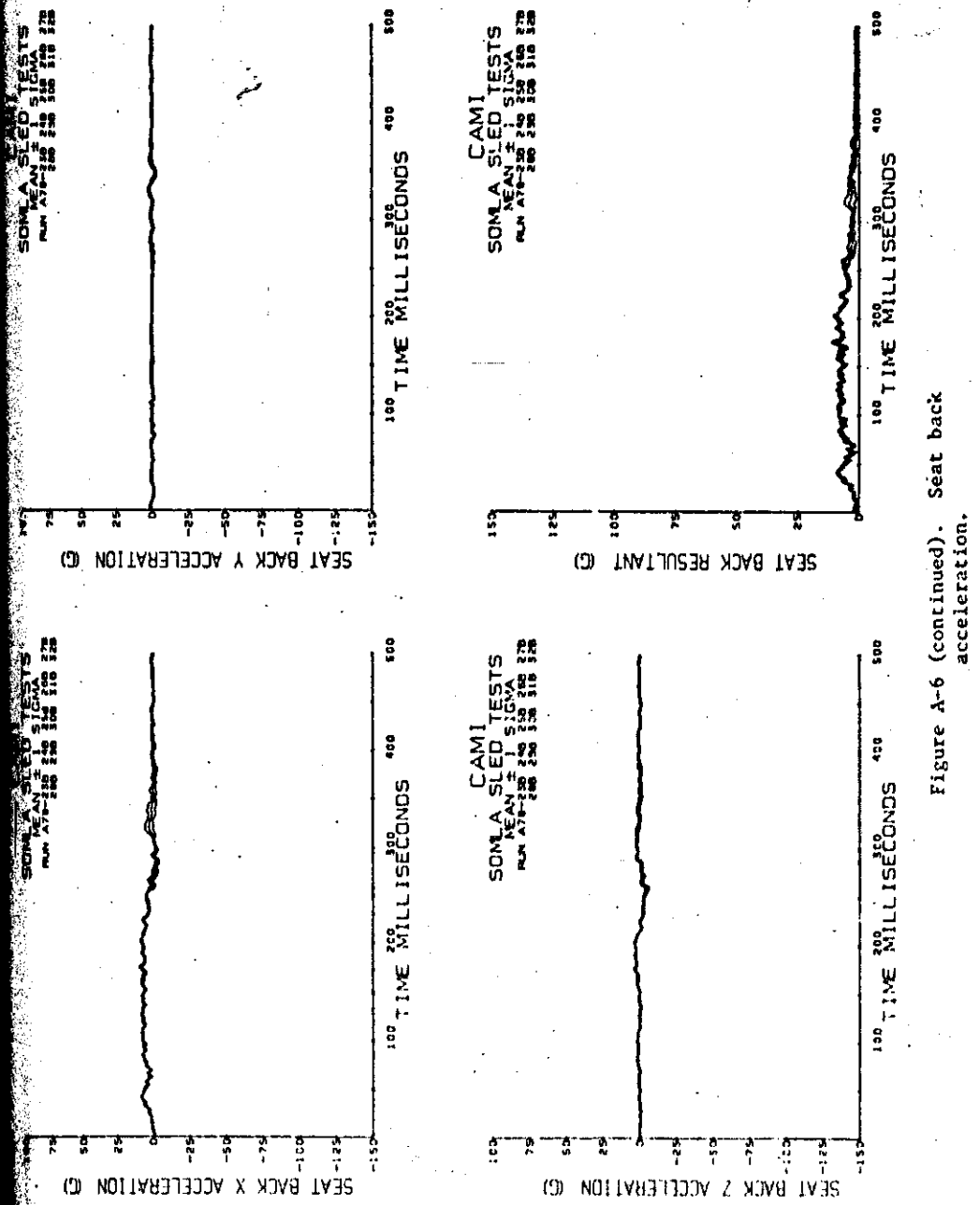


Figure A-6 (continued). Seat back acceleration.

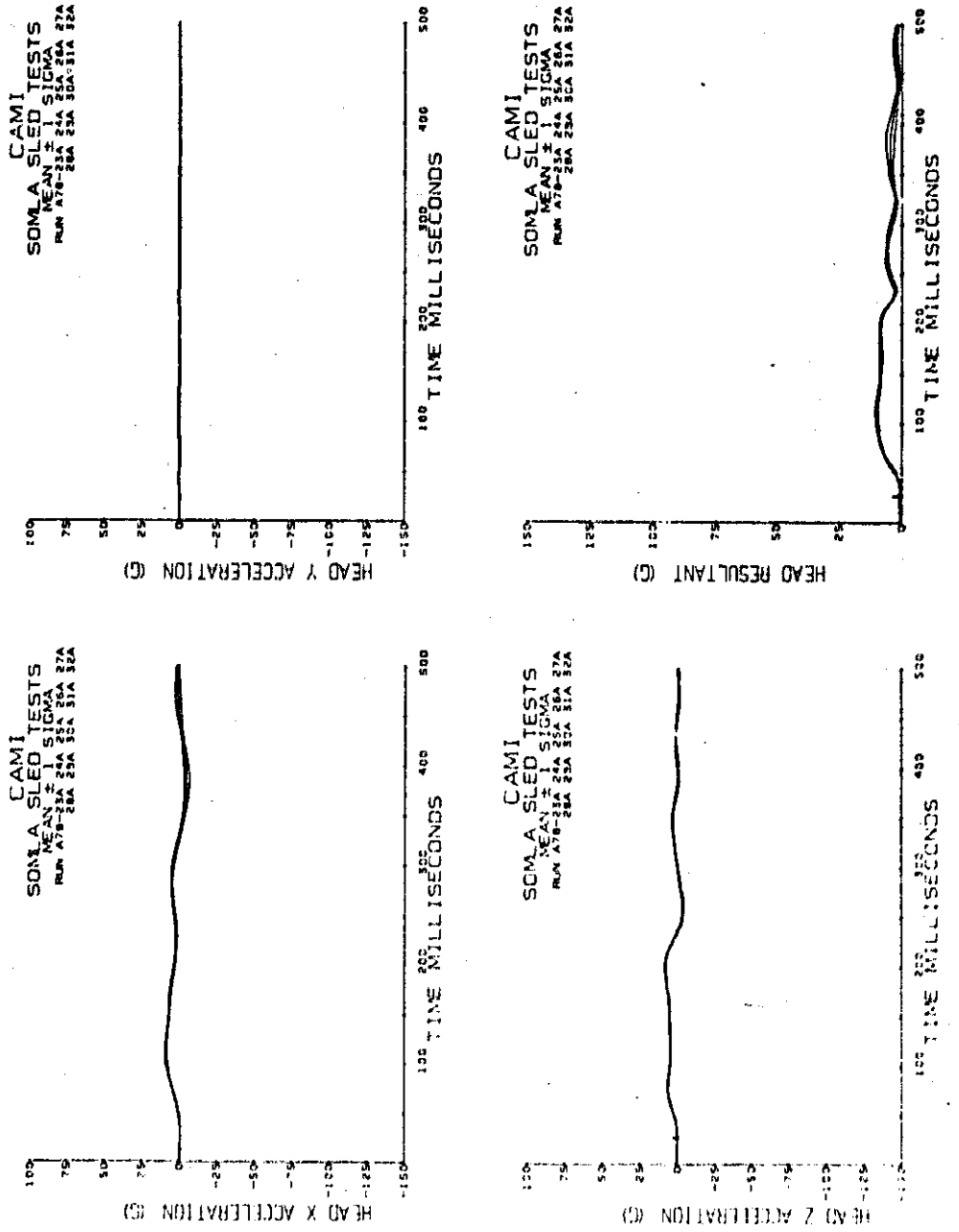


Figure A-6 (continued). Head acceleration.

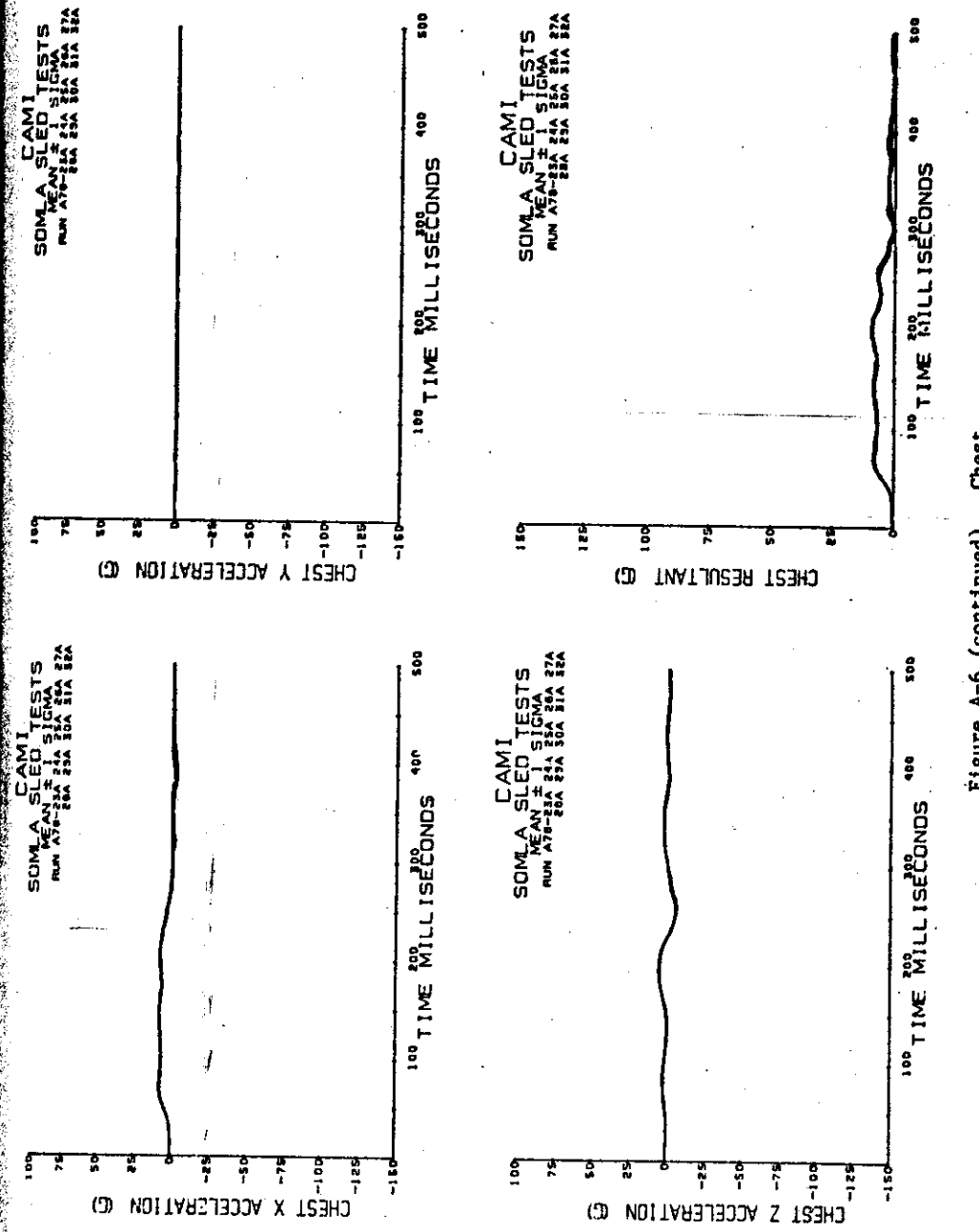


Figure A-6 (continued). Chest acceleration.

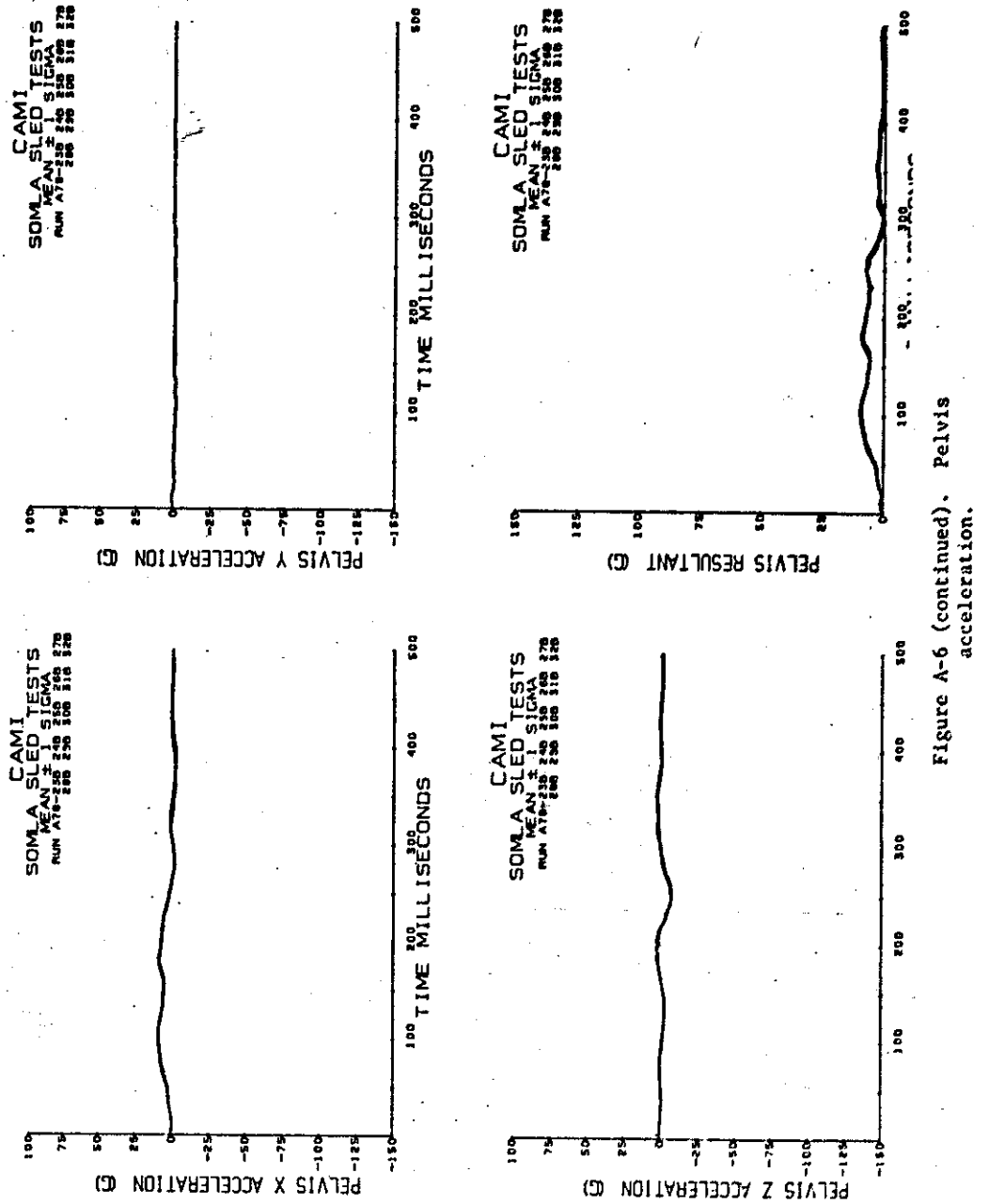


Figure A-6 (continued). Pelvis acceleration.

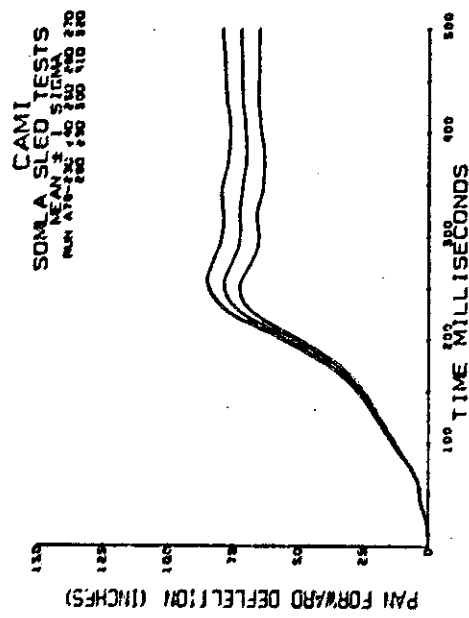


Figure A-6 (continued). Deflection data.

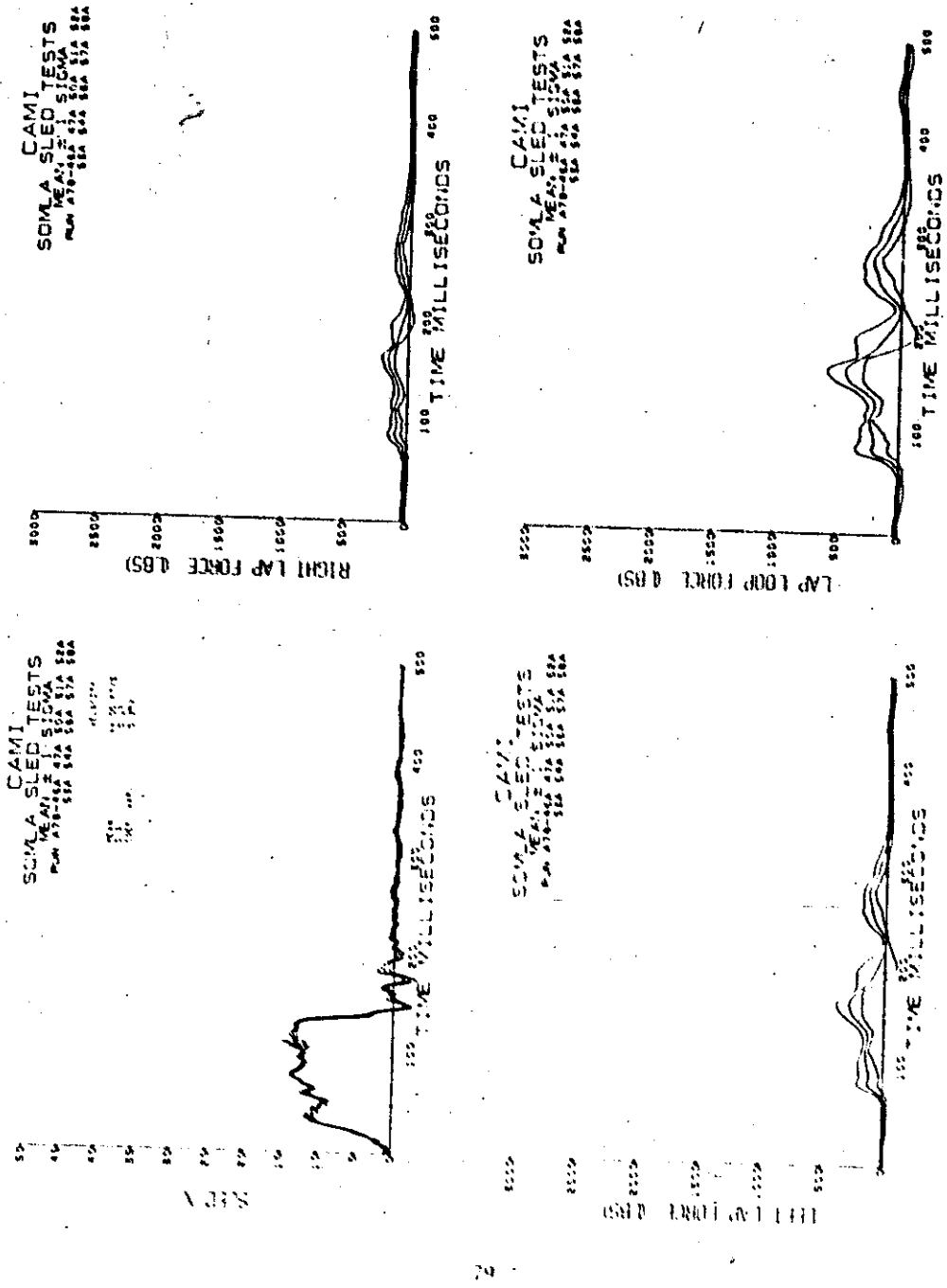
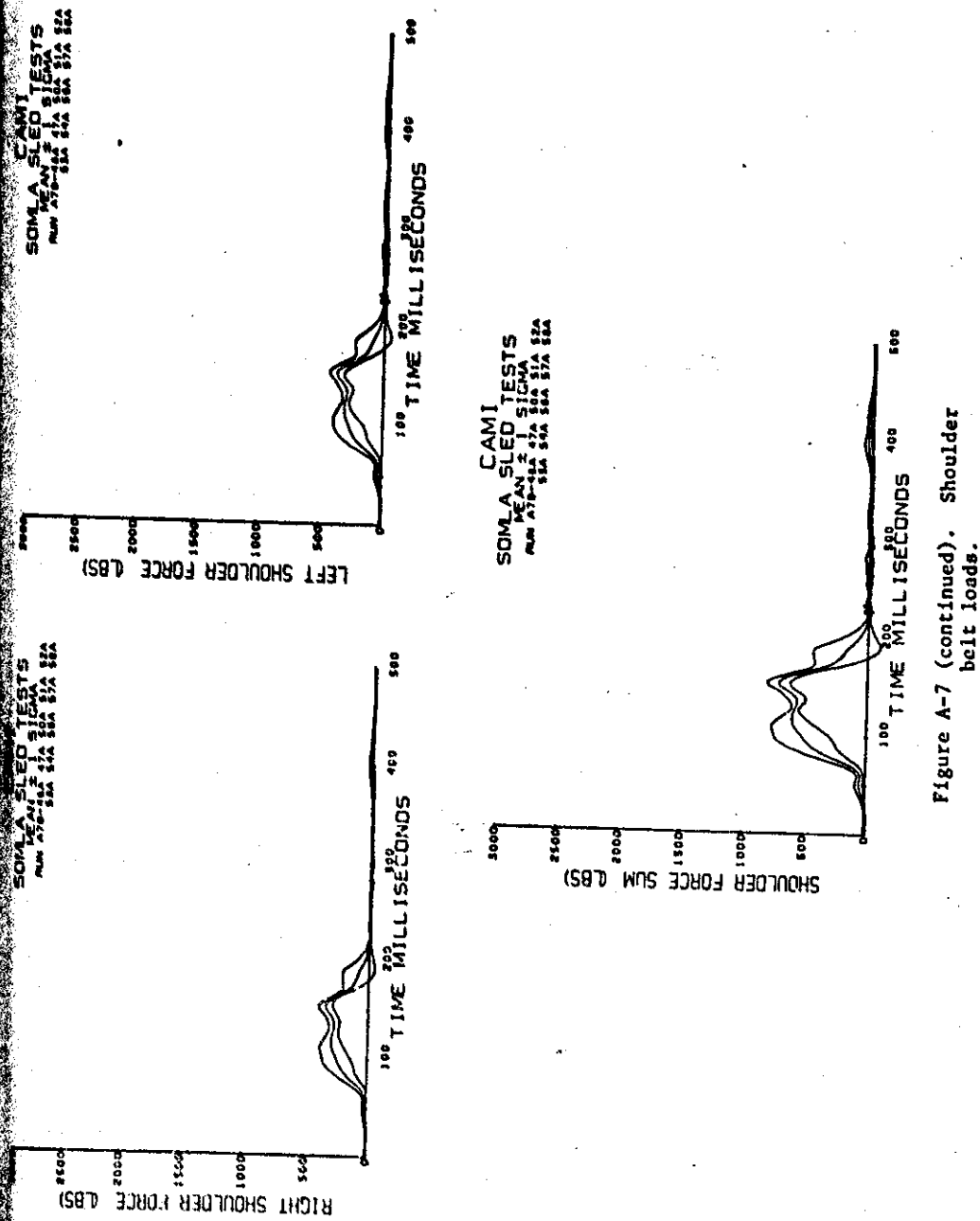


Figure A-7. Combined loading, low-deceleration tests.  
Sled deceleration and lapbelt loads.



**Figure A-7** (continued). Shoulder belt loads.

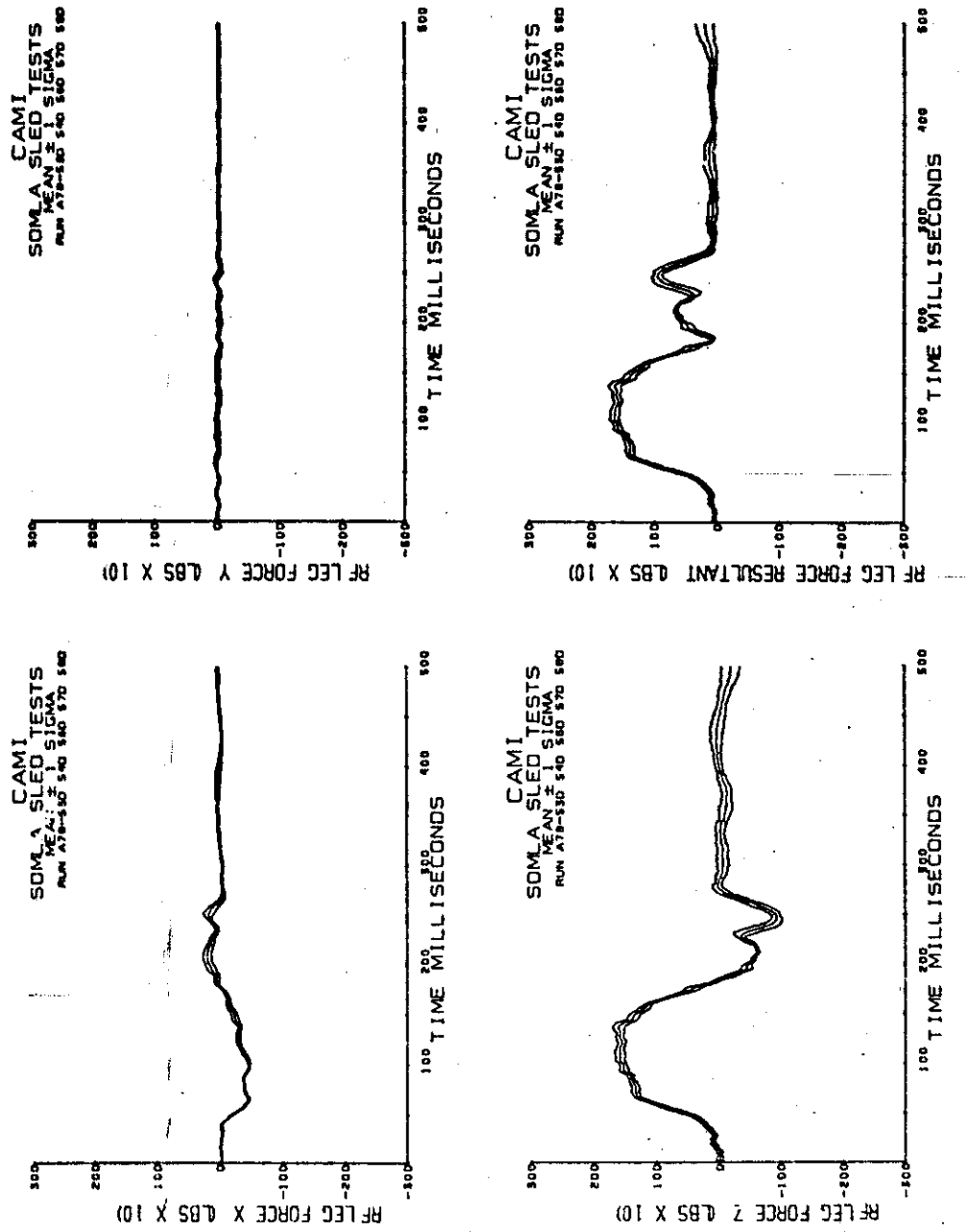


Figure A-7 (continued). Right front seat leg loads.

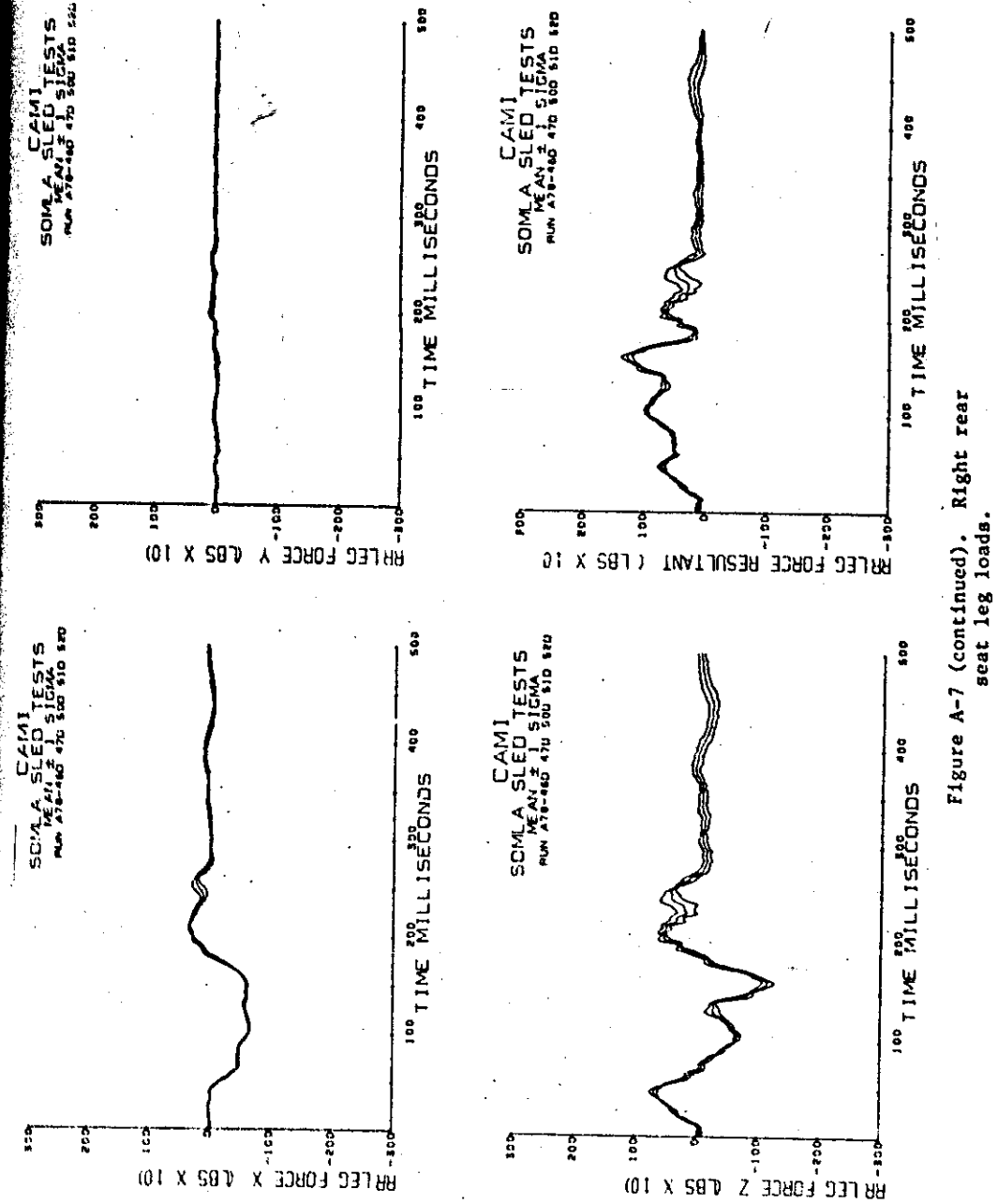


Figure A-7 (continued). Right rear seat leg loads.

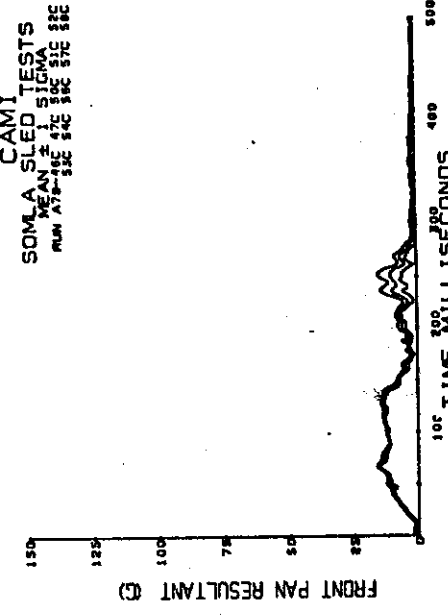
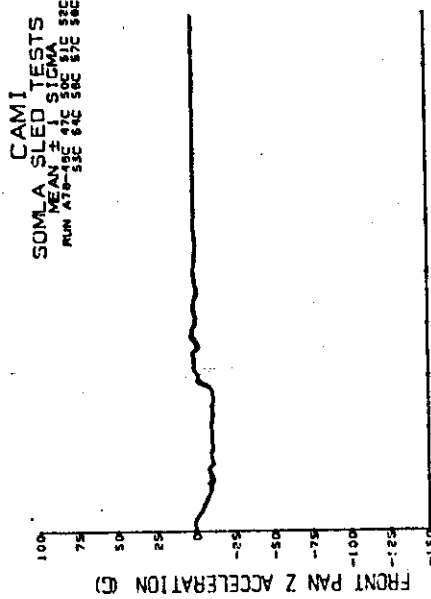
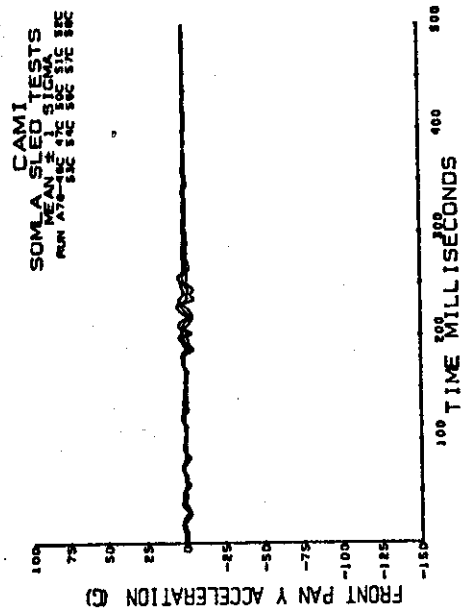
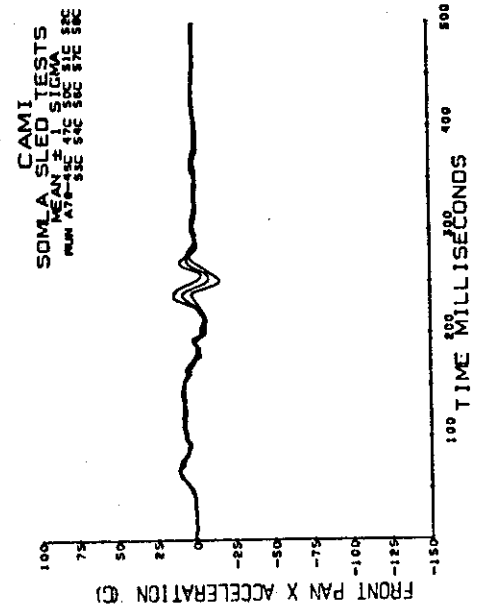
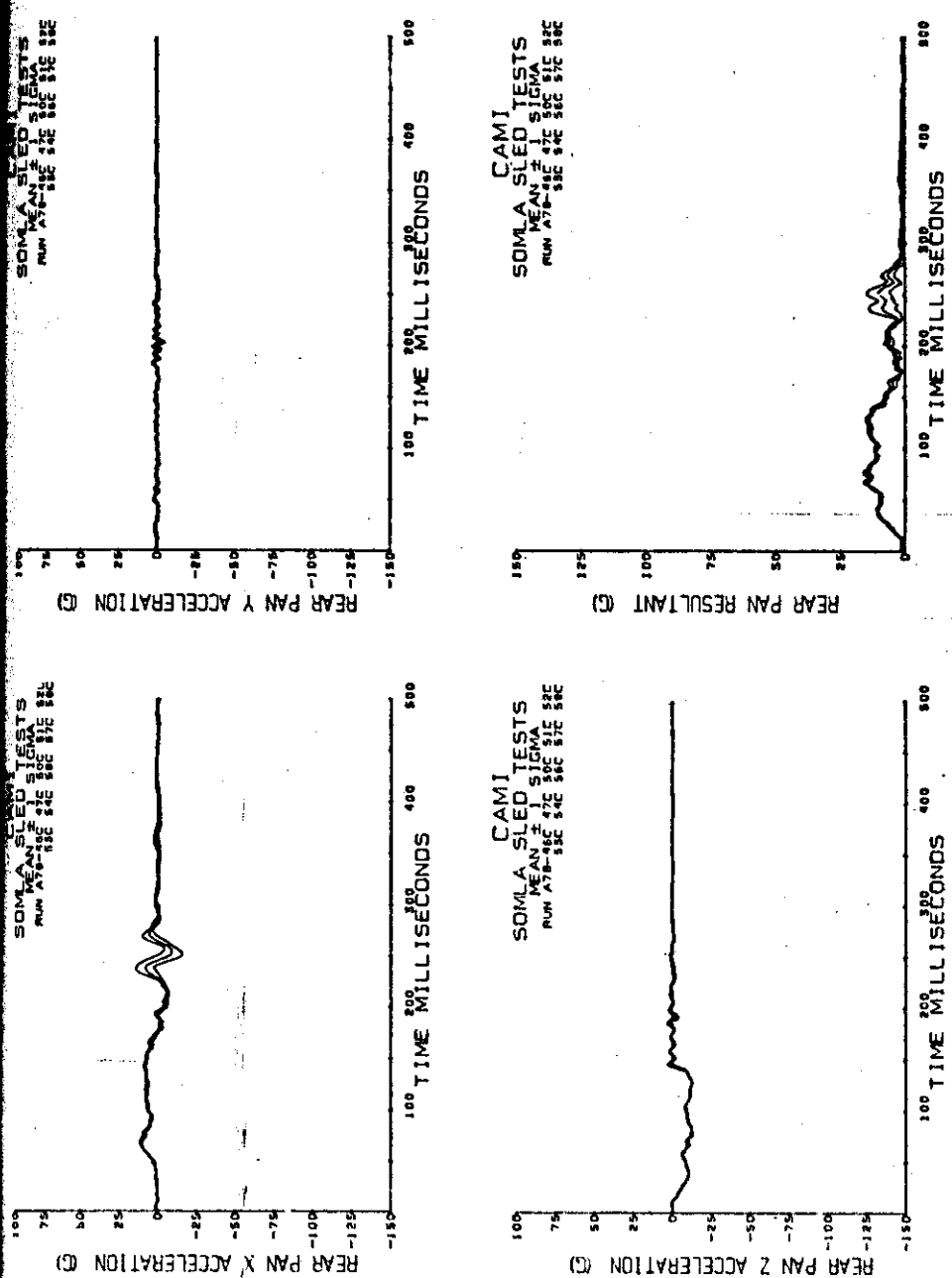


Figure A-7 (continued). Front seat pan acceleration.



**Figure A-7** (continued). Rear seat pan acceleration.

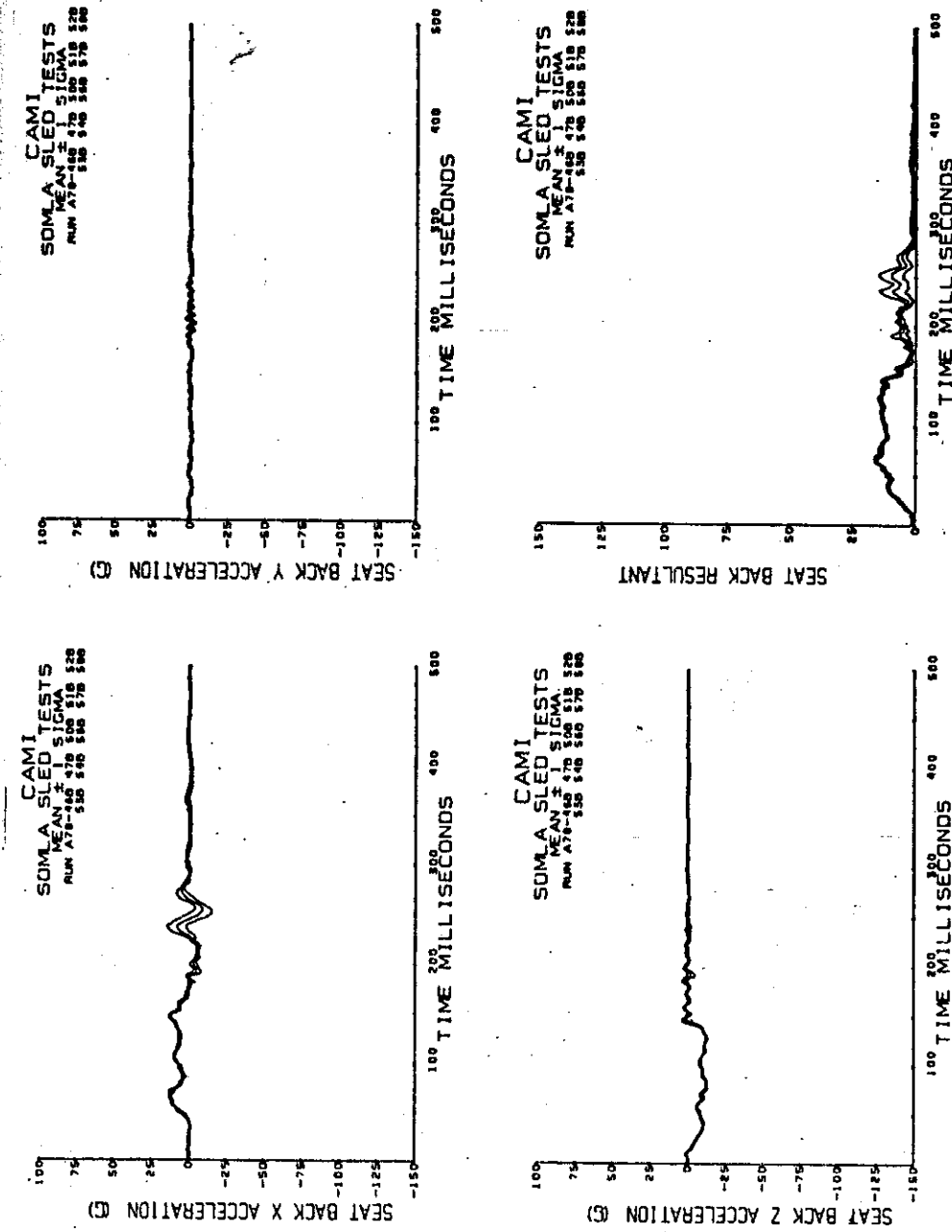


Figure A-7 (continued). Seat back acceleration.

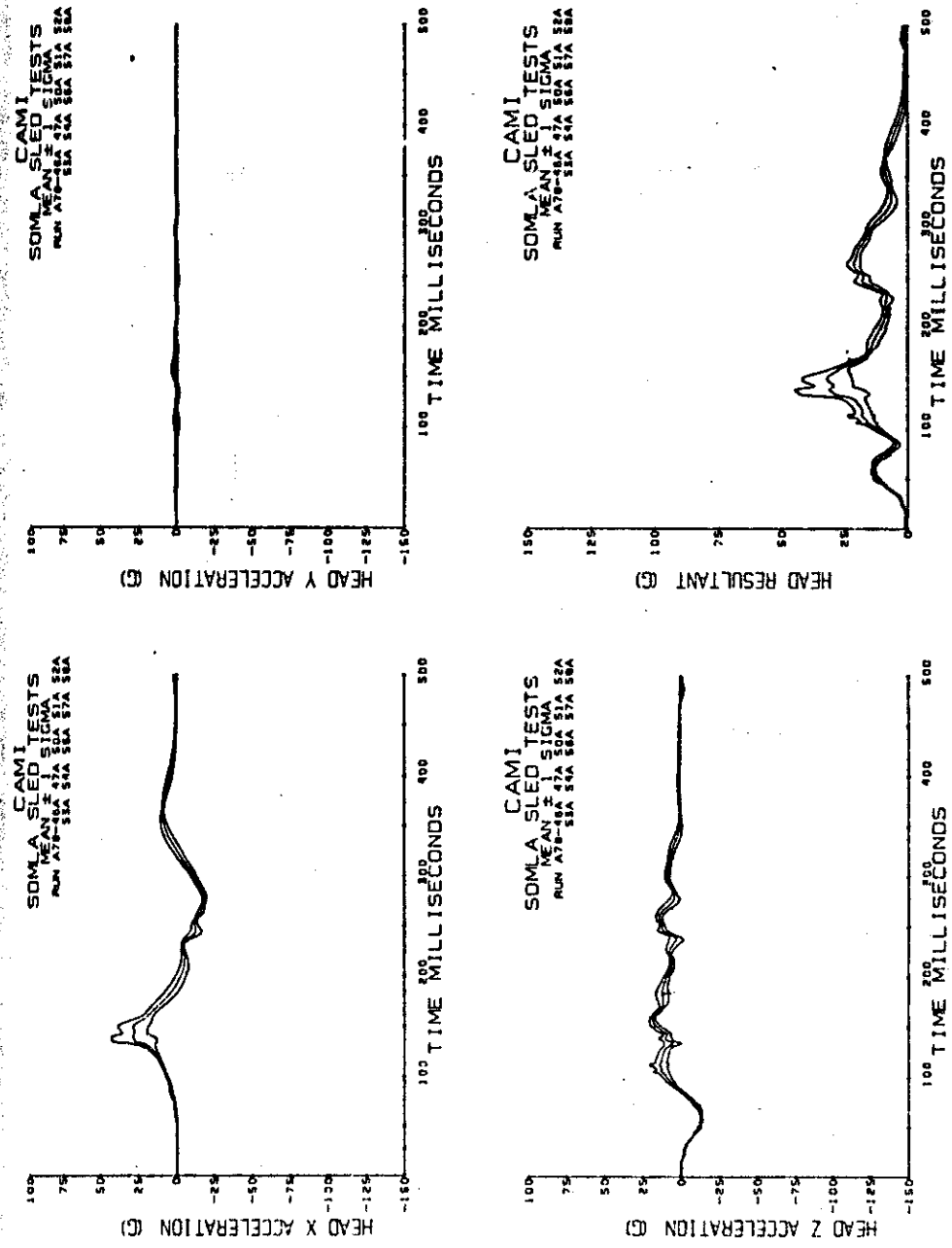
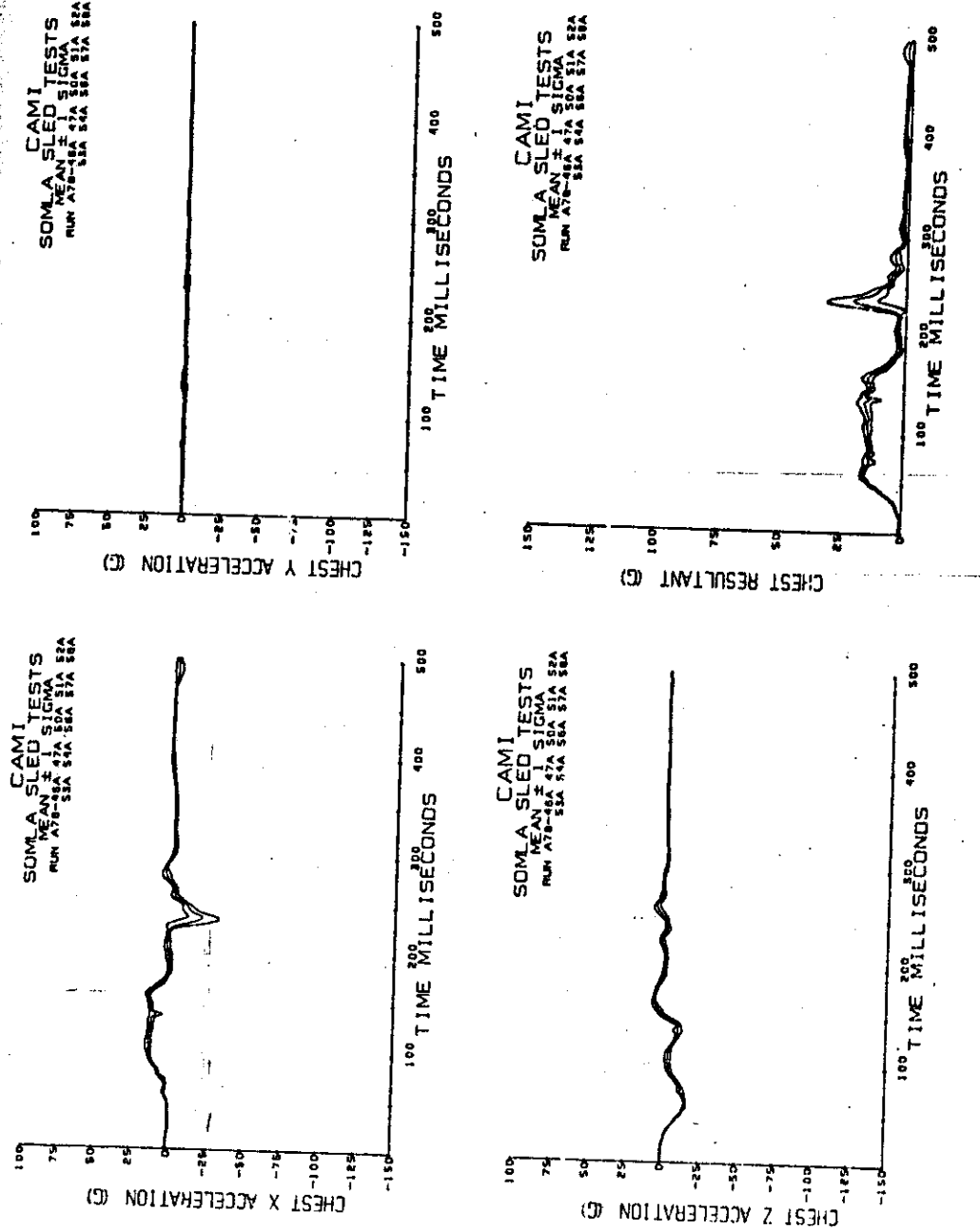


Figure A-7 (continued). Head acceleration.



**Figure A-7** (continued). Chest acceleration.

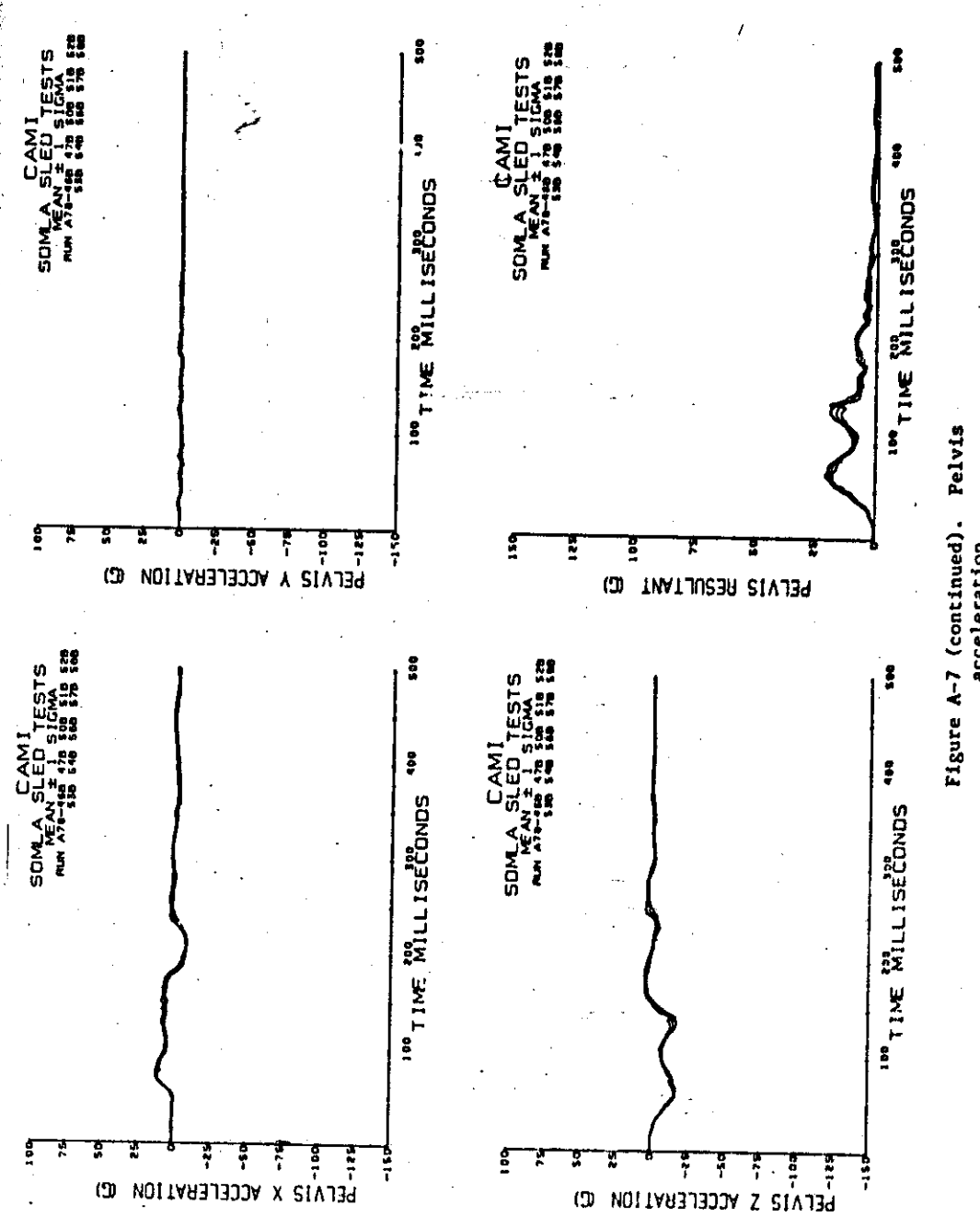


Figure A-7 (continued). Pelvis acceleration.

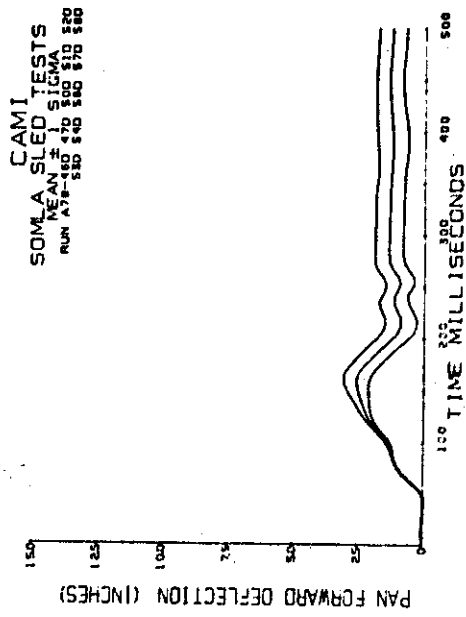


Figure A-7 (continued). Deflection data.

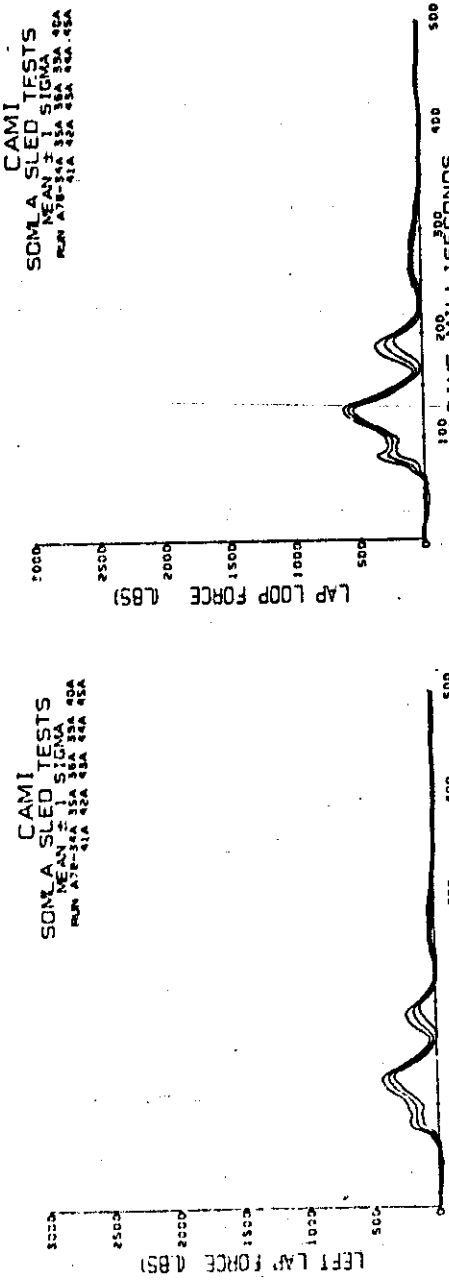
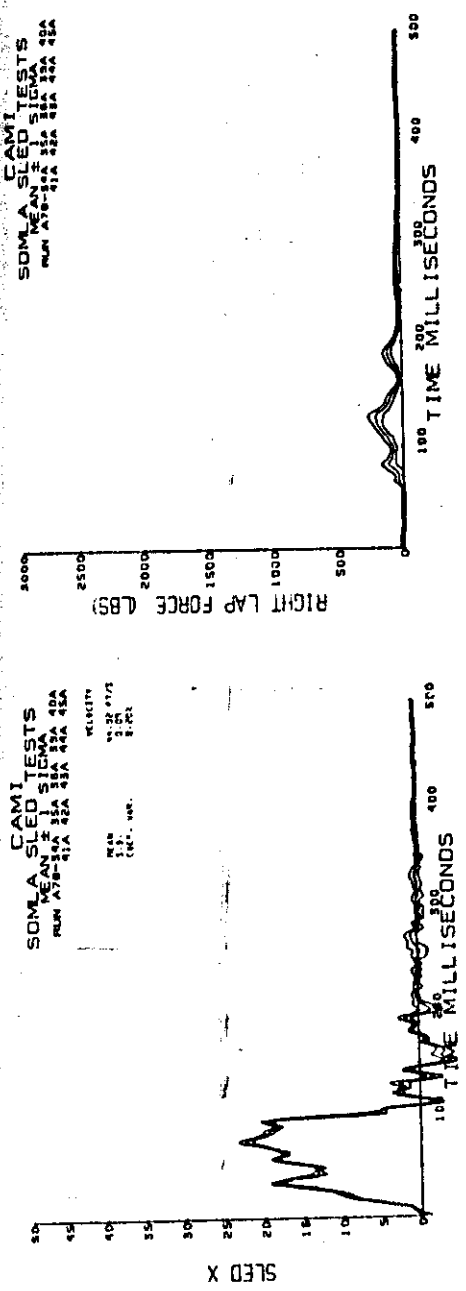


Figure A-8. Combined loading higher deceleration tests.  
Sled deceleration and lapbelt loads.

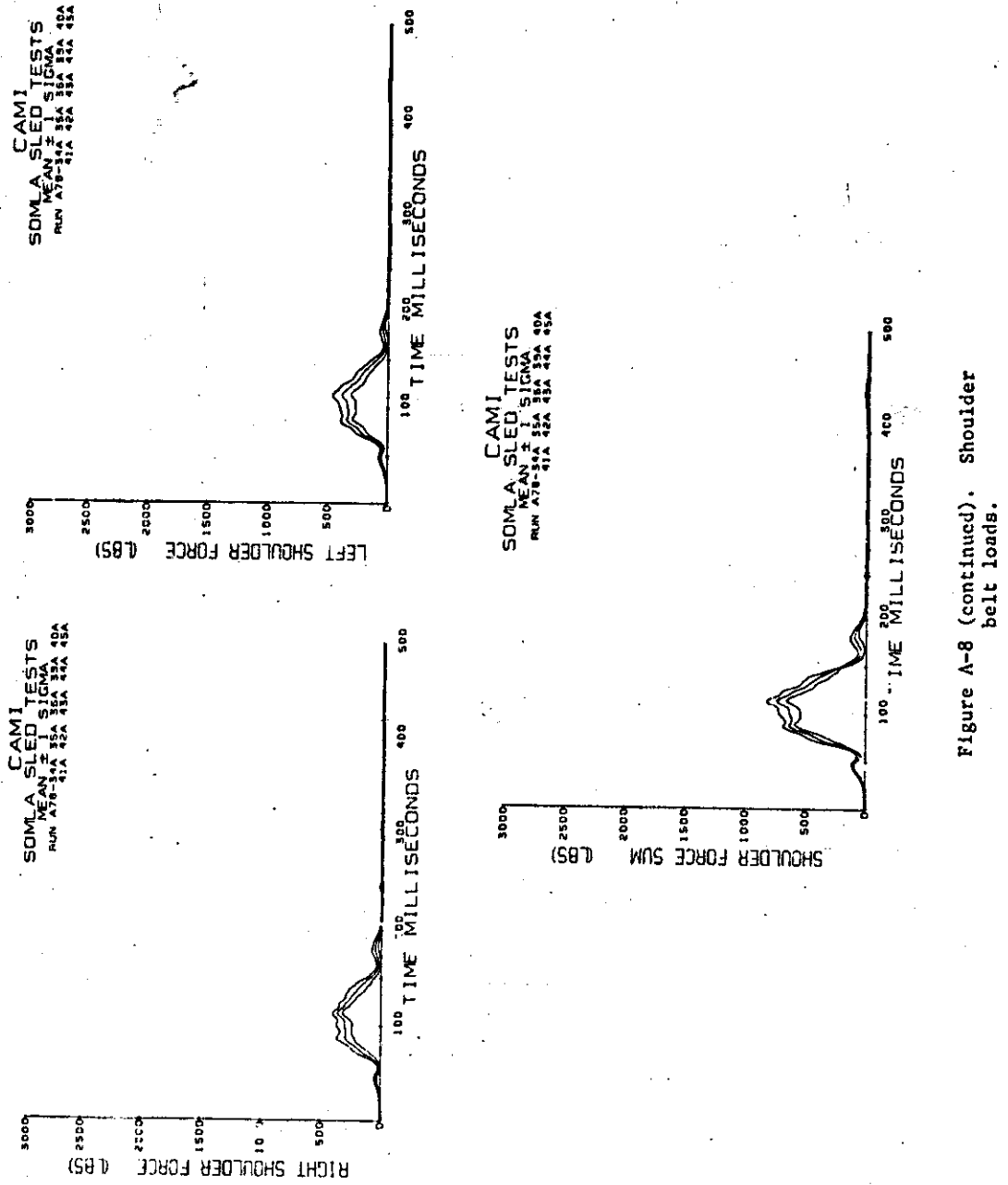


Figure A-8 (continued). Shoulder belt loads.

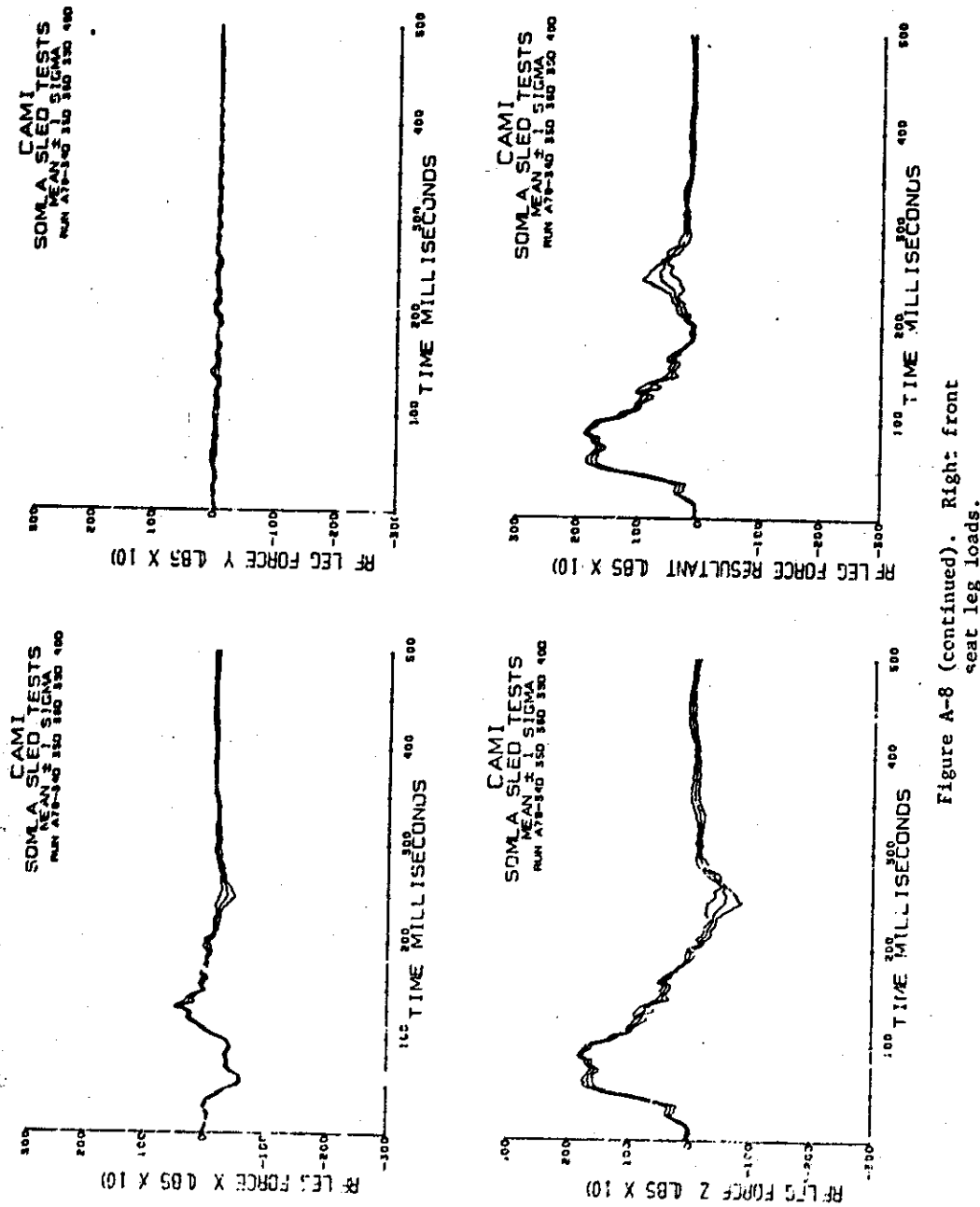
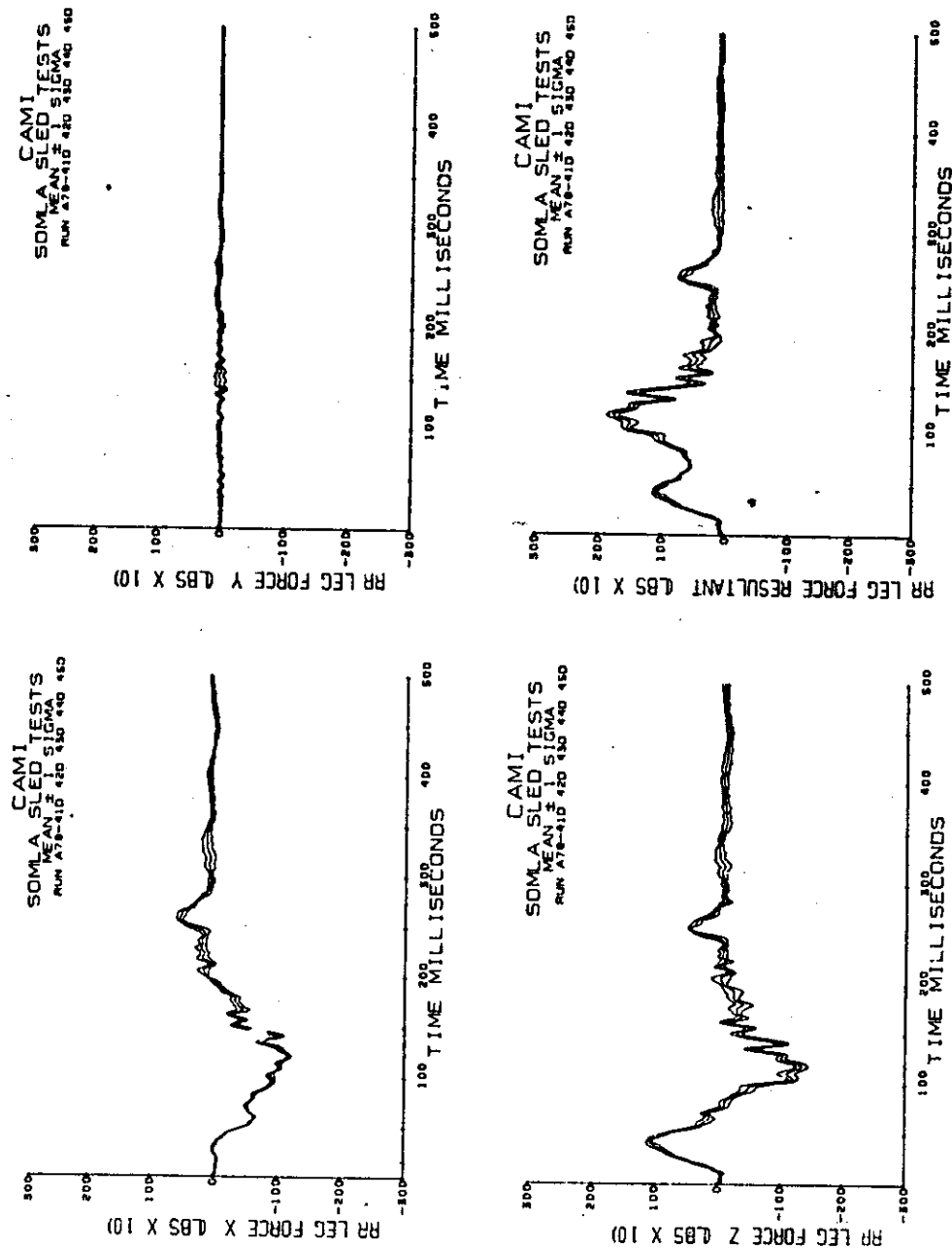


Figure A-8 (continued). Right: front seat leg loads.



297-957 0 - 79 - 7

Figure A-8 (continued). Right rear seat leg loads.

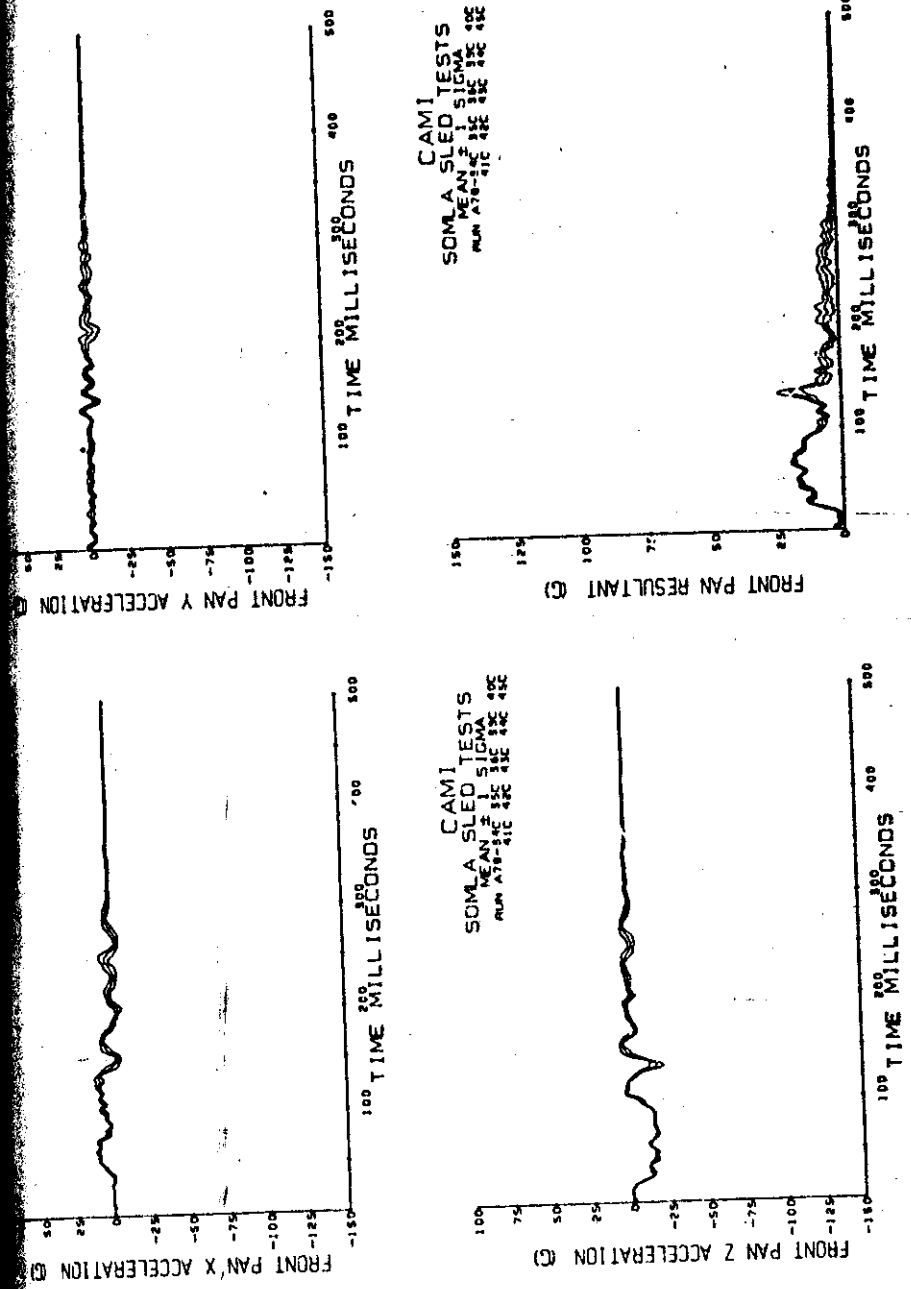


Figure A-8 (continued). Front seat pan acceleration.

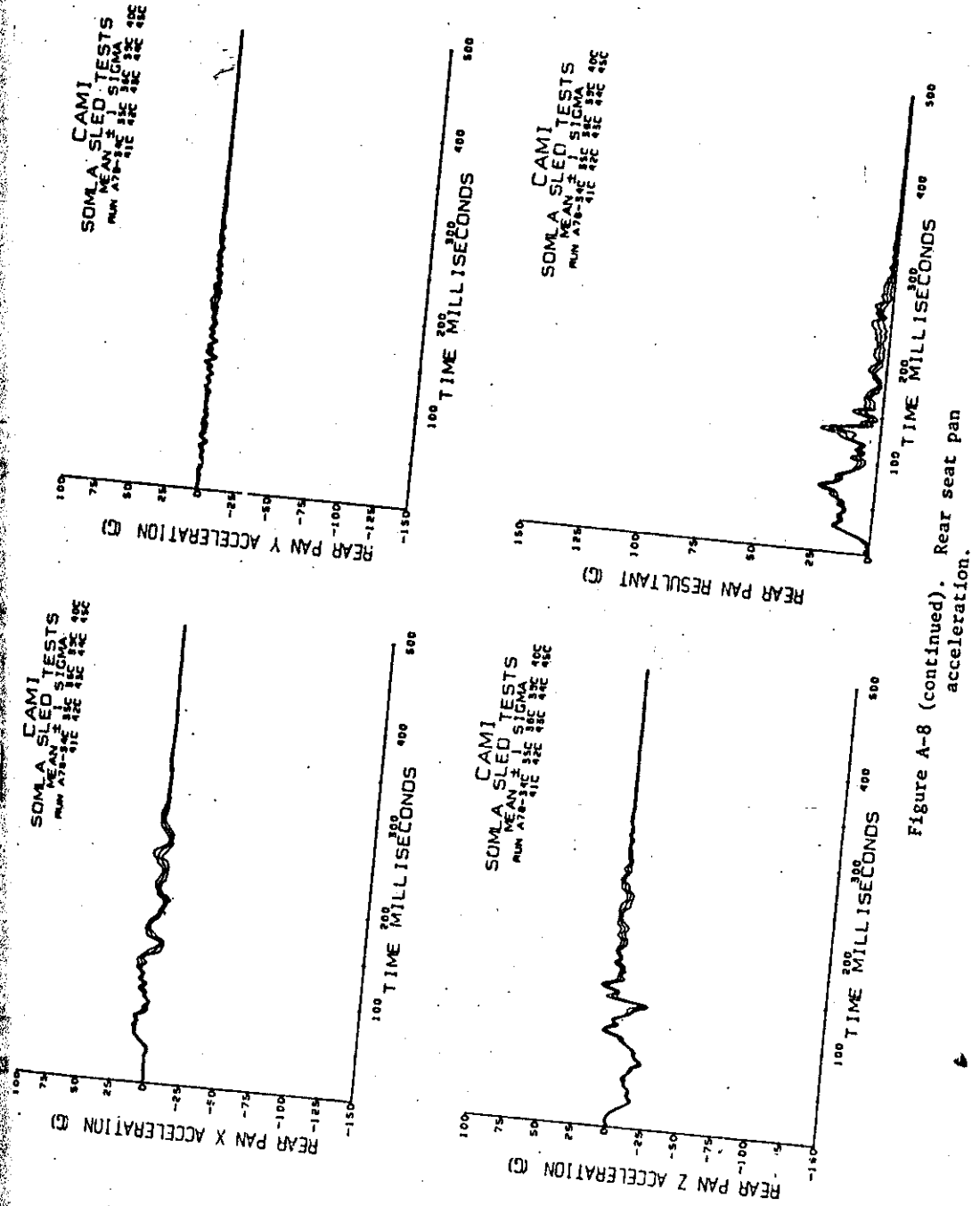


Figure A-8 (continued). Rear seat pan acceleration.

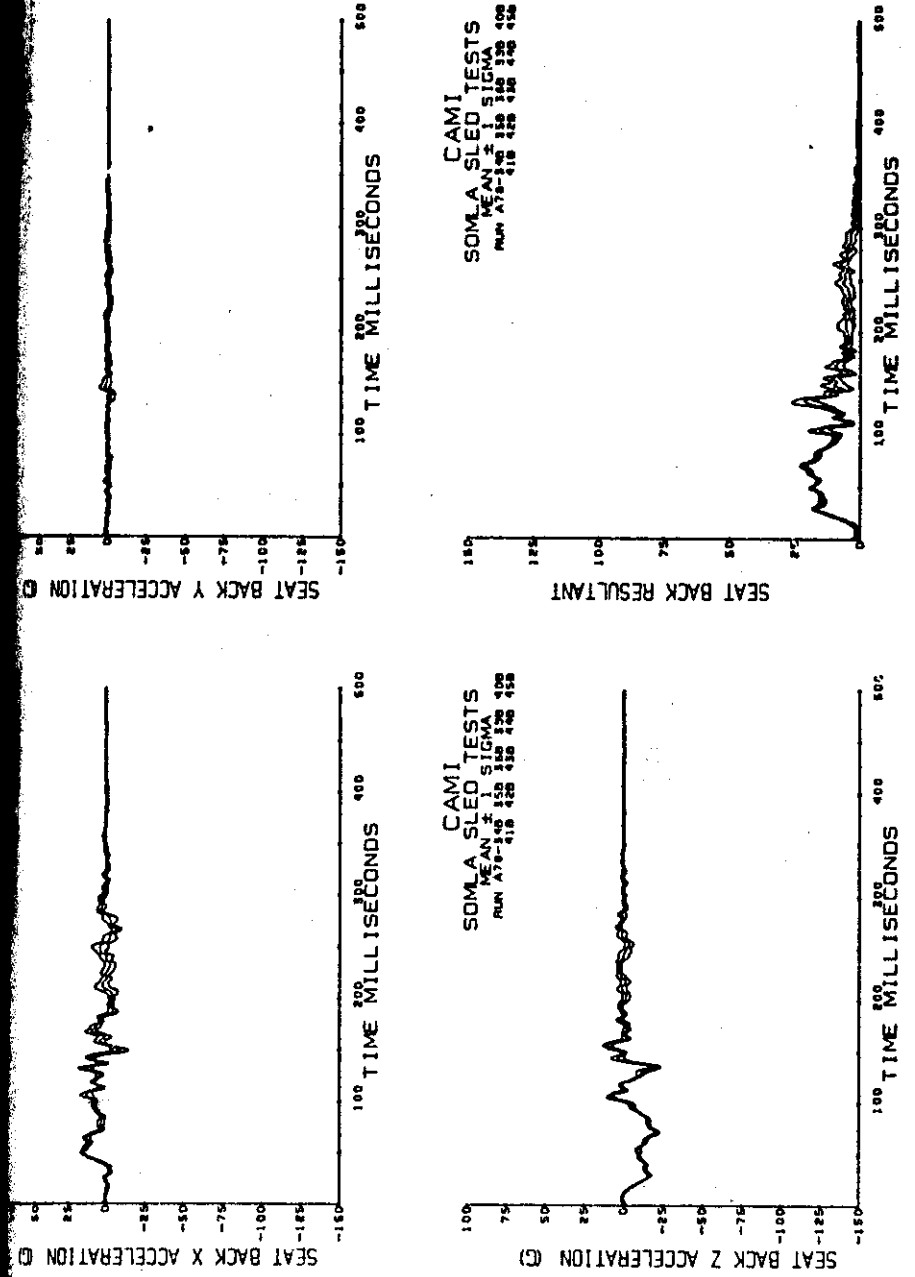


Figure A-8 (continued). Seat back acceleration.

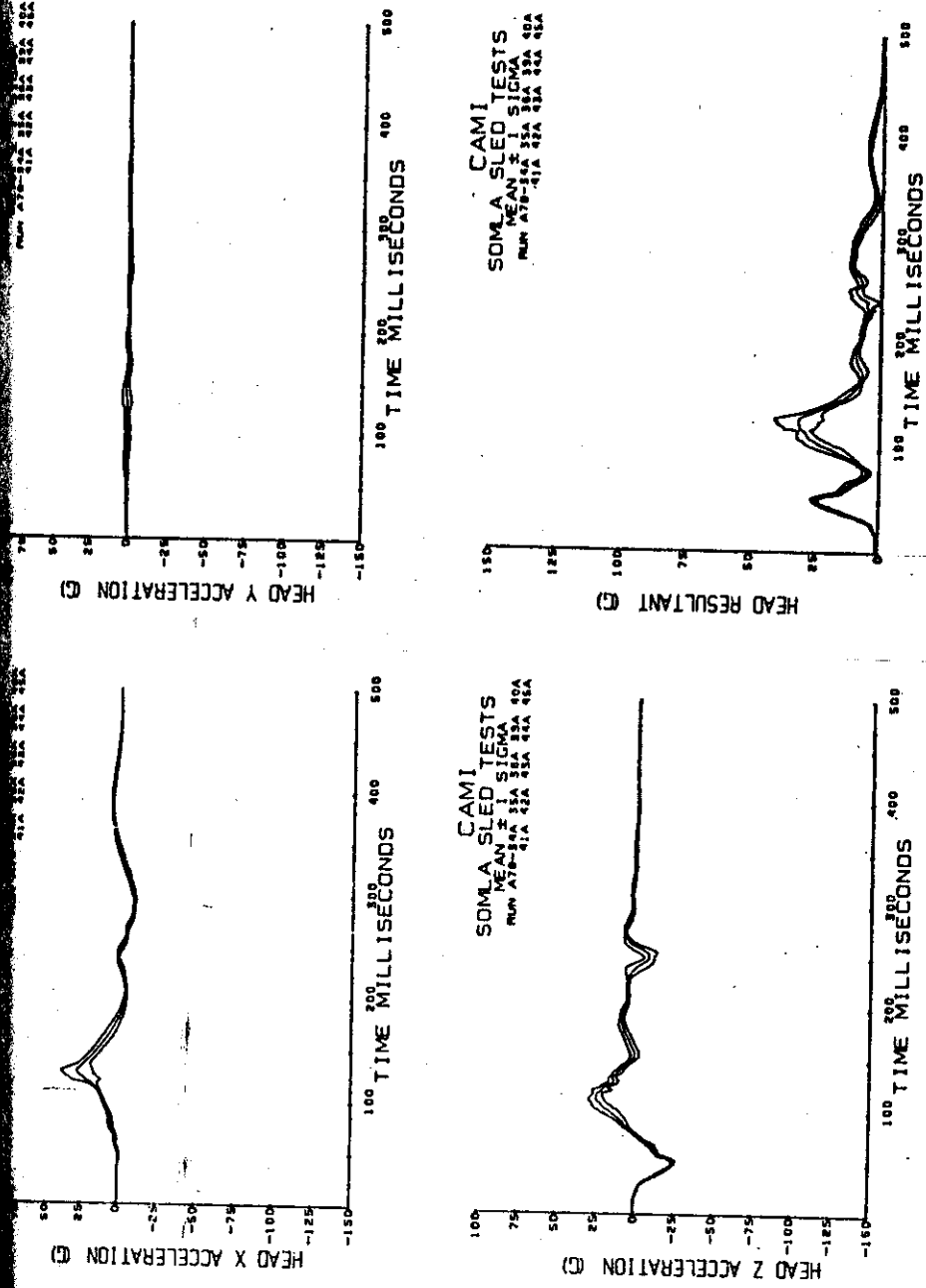


Figure A-8 (continued). Head acceleration.

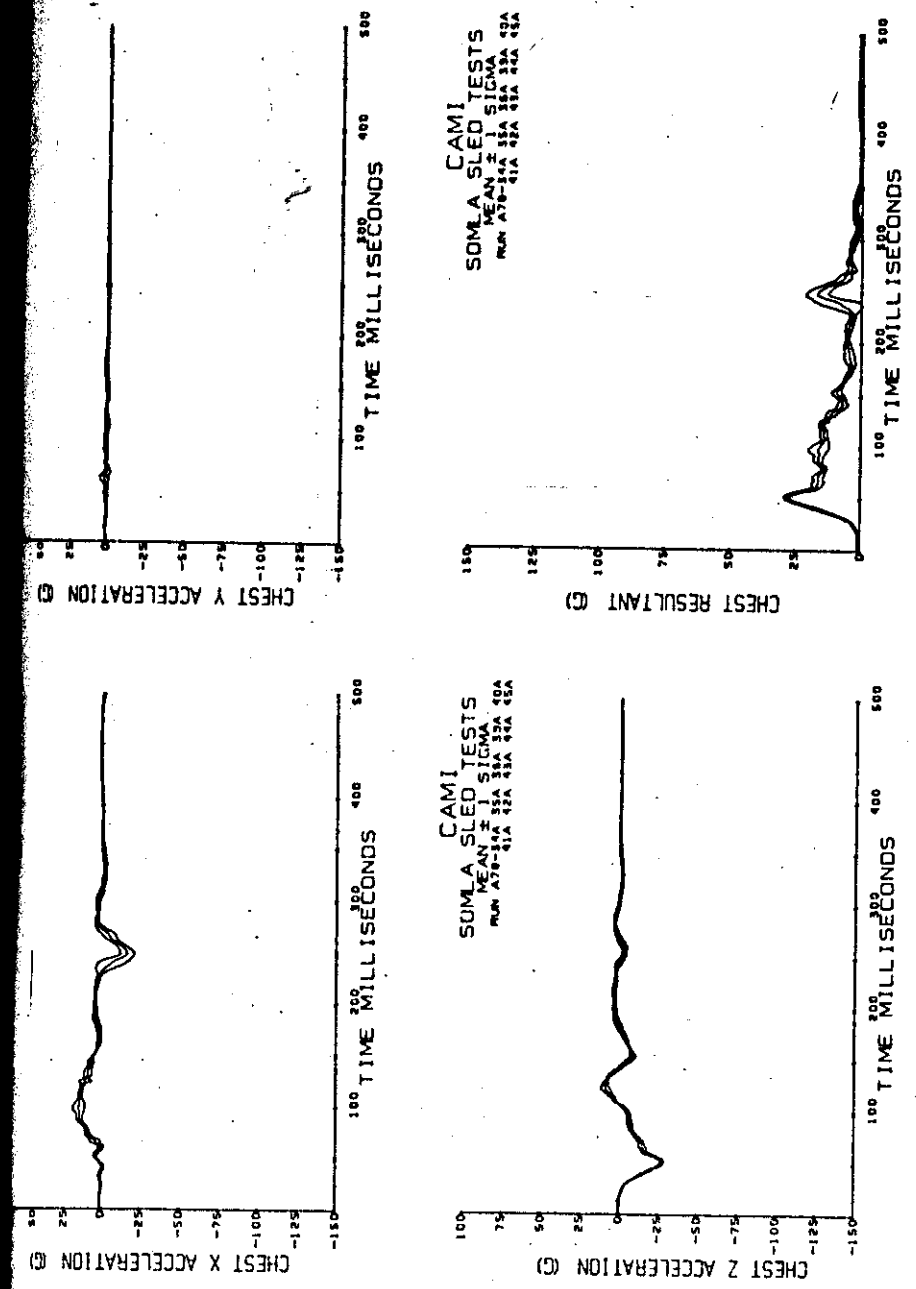


Figure A-8 (continued). Chest acceleration.

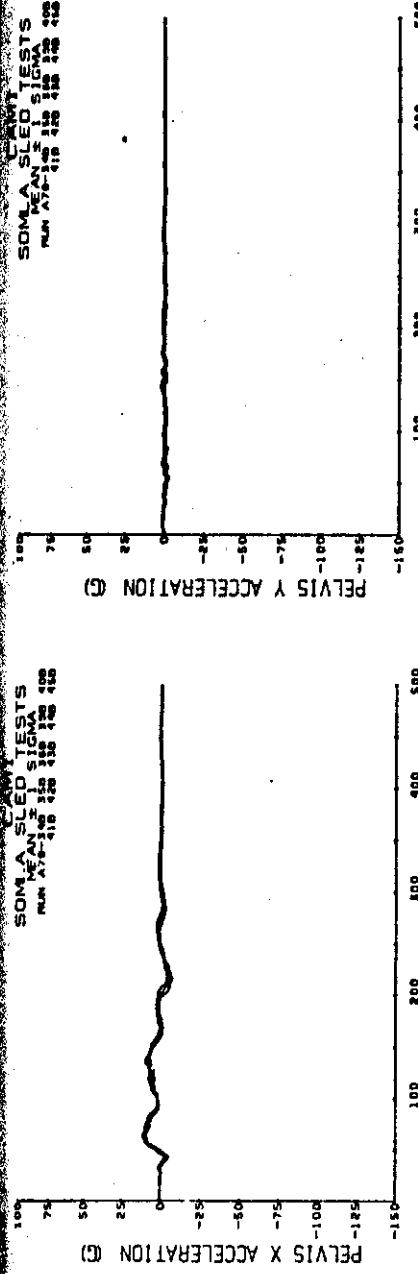


Figure A-8 (continued). Pelvis acceleration.

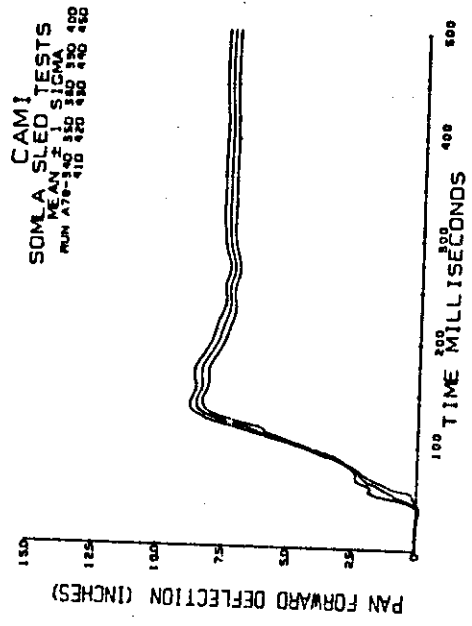


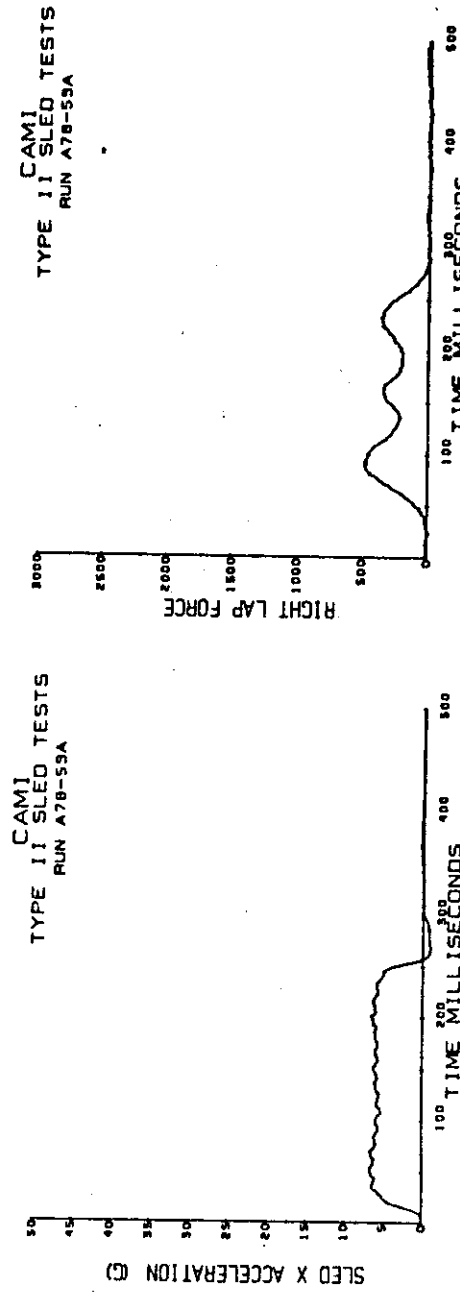
Figure A-8 (continued). Deflection data.

## APPENDIX B

### RESULTS OF DYNAMIC TESTS OF AN AFTERMARKET SHOULDER HARNESS

| <u>Figure No.</u>  |             | <u>page</u> |
|--|-------------|-------------|
| Tests 059, 060, and 061.<br>Front seatbelt short and attached to the seat frame.<br>Seatbelt loop length about 39 in with belt adjusted<br>snugly against dummy. |             |             |
| B-1  | 6-g tests.  | 102         |
| B-2  | 10-g tests. | 108         |
| B-3  | 14-g tests. | 114         |
| Tests 062 and 063.<br>Conditions same as for Tests 059-061<br>but with 70-in seatbelt loop length.   |             |             |
| B-4  | 10-g tests. | 120         |
| B-5  | 14-g tests. | 126         |
| Tests 064, 065 and 066.<br>Conditions same as for Tests 059-063<br>but with 76-in seatbelt loop length<br>(slack restraint system).                              |             |             |
| B-6  | 6-g tests.  | 132         |
| B-7  | 10-g tests. | 138         |
| B-8  | 14-g tests. | 144         |

RESULTS OF DYNAMIC TESTS OF AN AFTERMARKET SHOULDER HARNESS



102

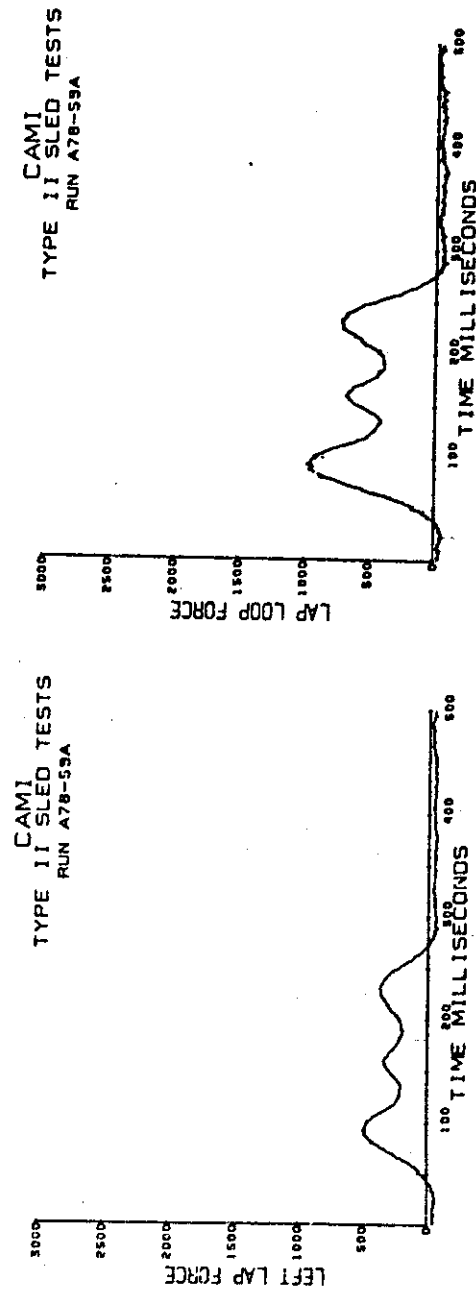


Figure B-1. 6-g tests.  
Sled deceleration and lapbelt loads.

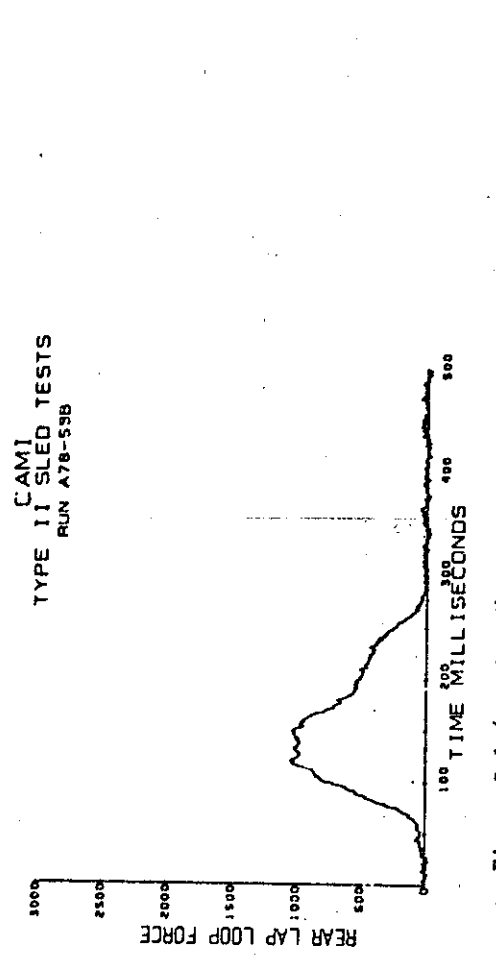
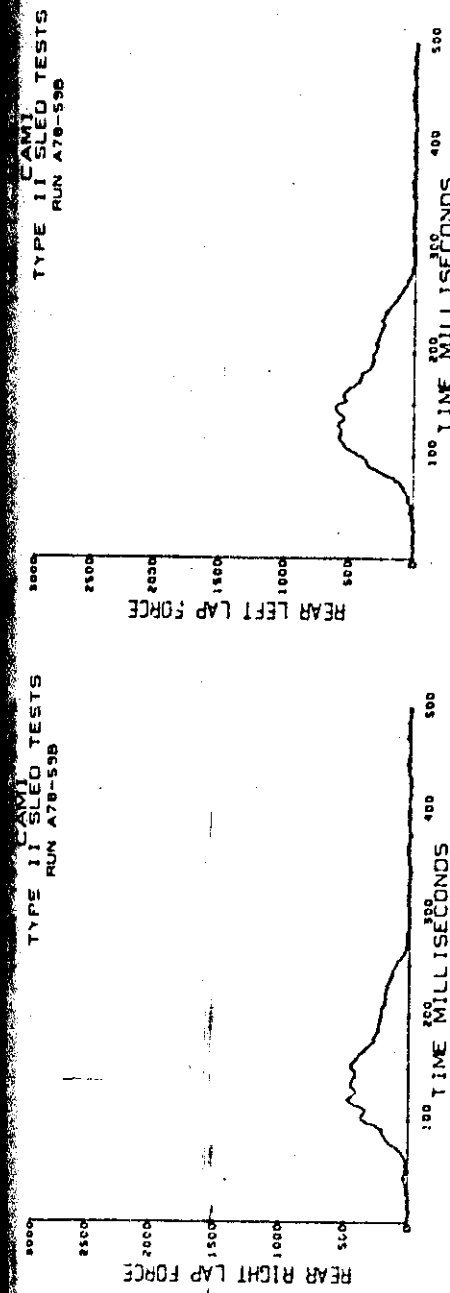
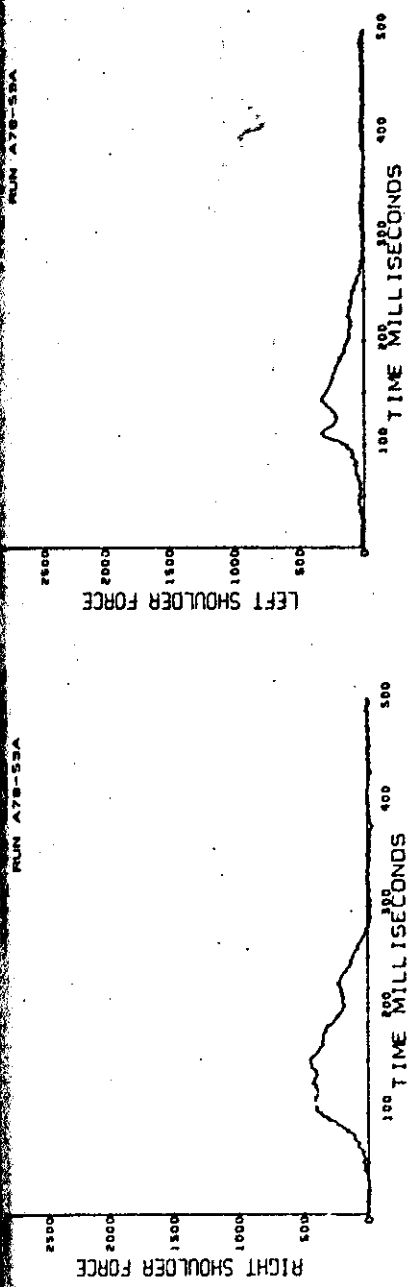


Figure B-1 (continued). Rear lapbelt loads.



CAMI  
TYPE II SLED TESTS  
RUN A78-59A

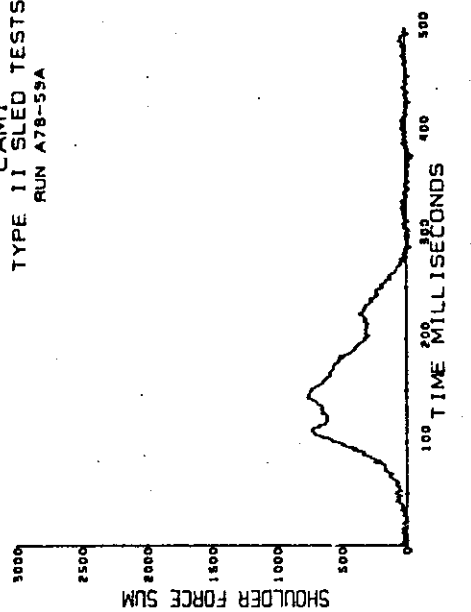


Figure B-1 (continued). Shoulder belt loads.

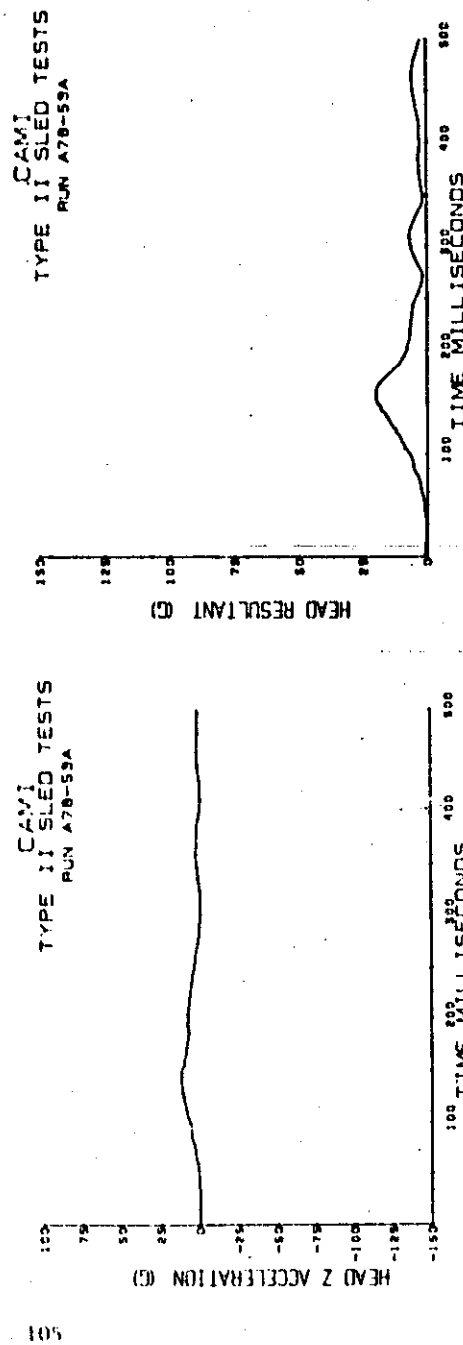
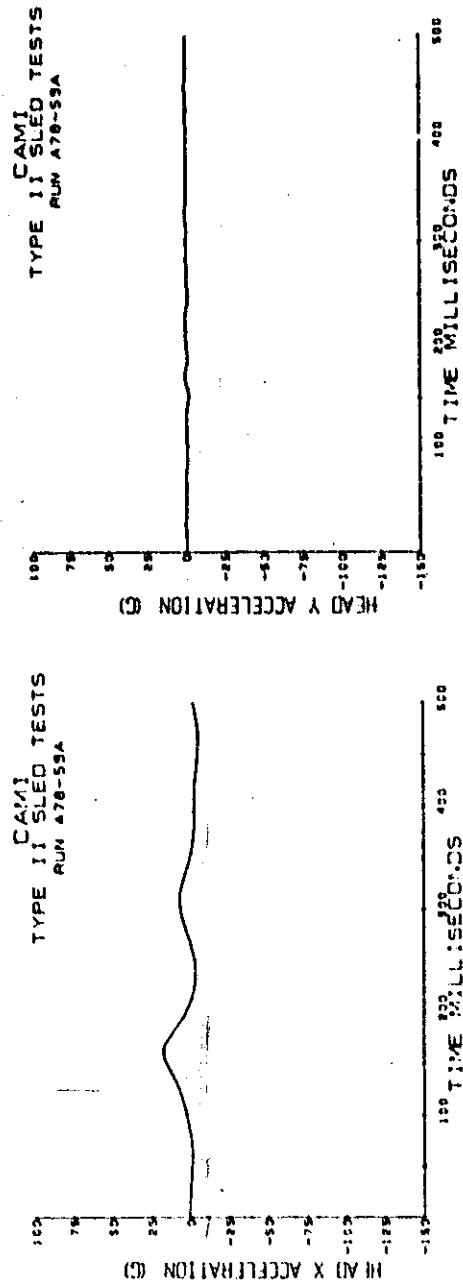


Figure B-1 (continued). Head acceleration.

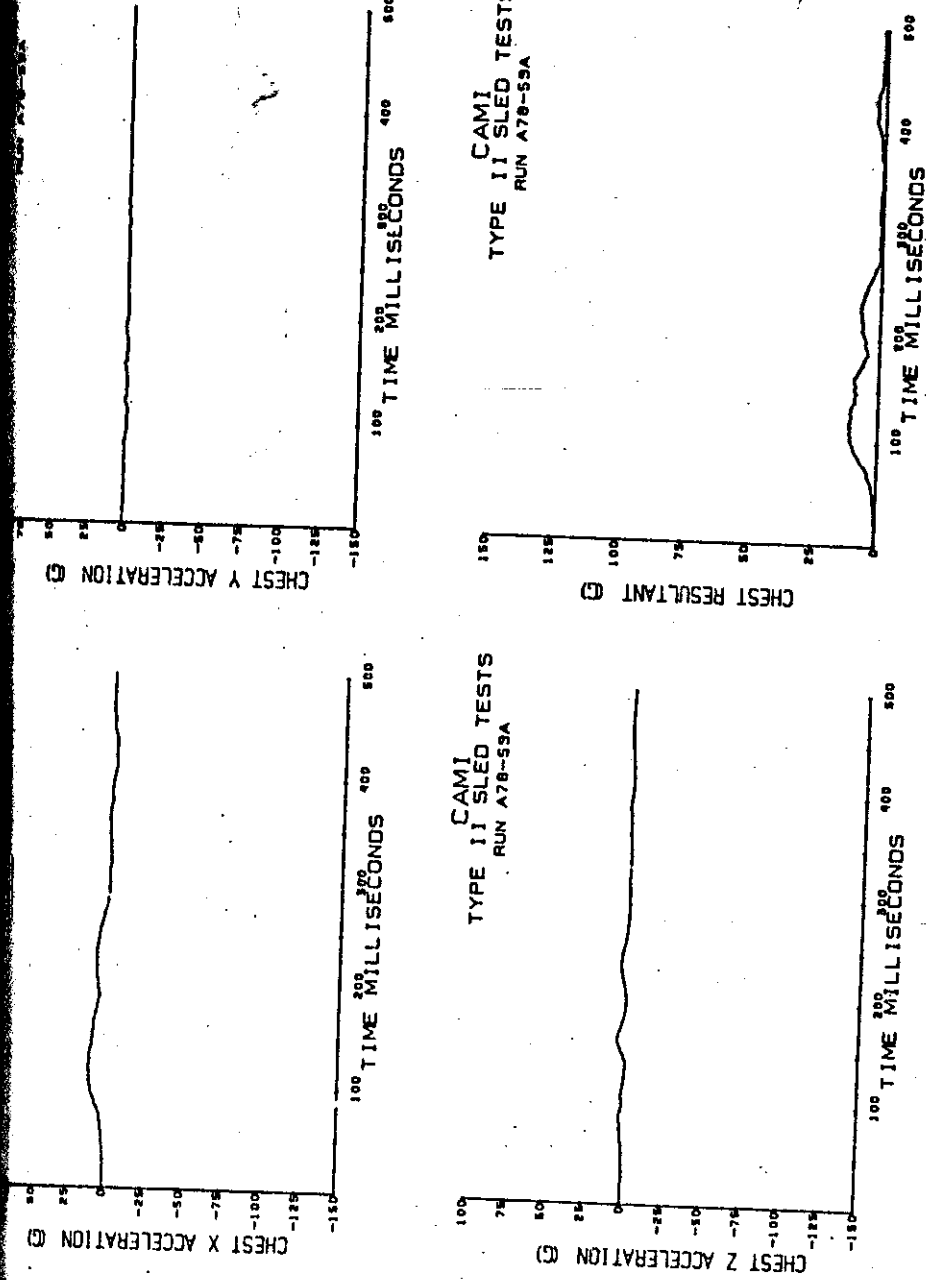


Figure B-1 (continued). Chest acceleration.

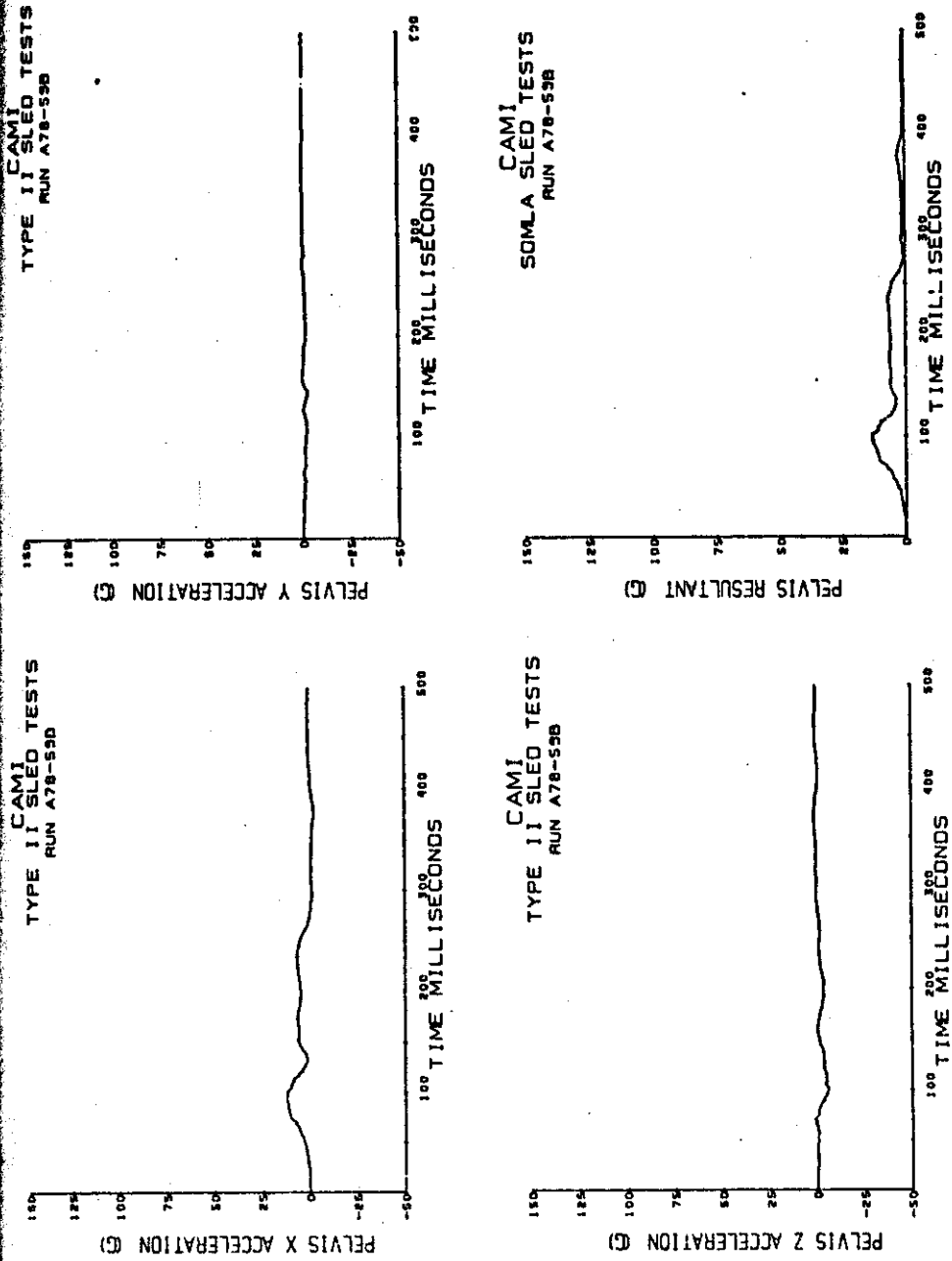


Figure B-1 (continued). Pelvis acceleration.

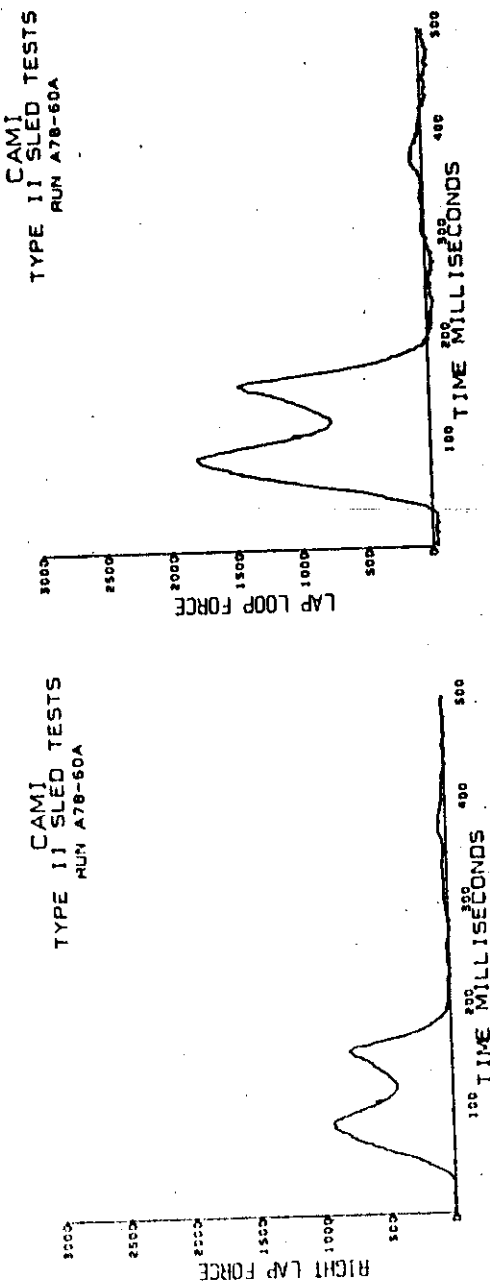
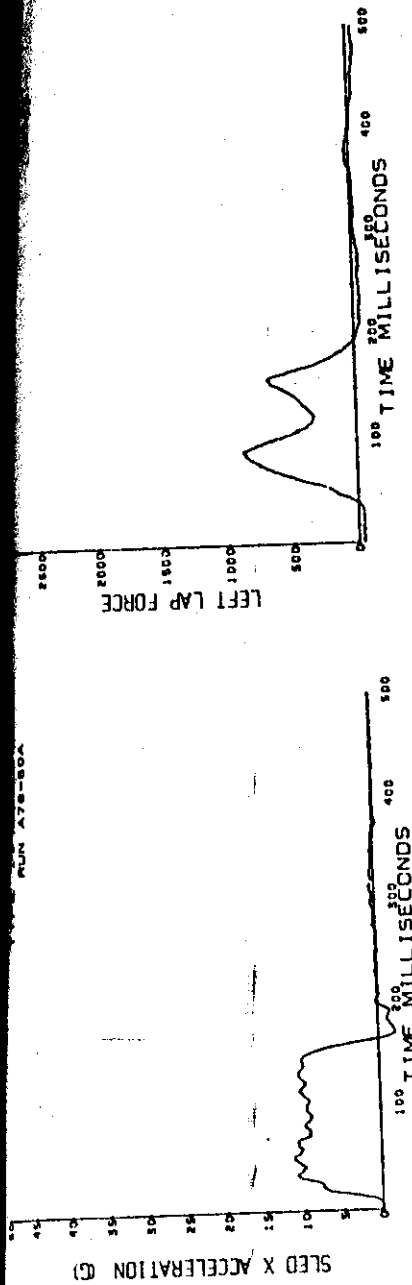


Figure B-2. 10-g tests.  
Sled acceleration and lapbelt forces.

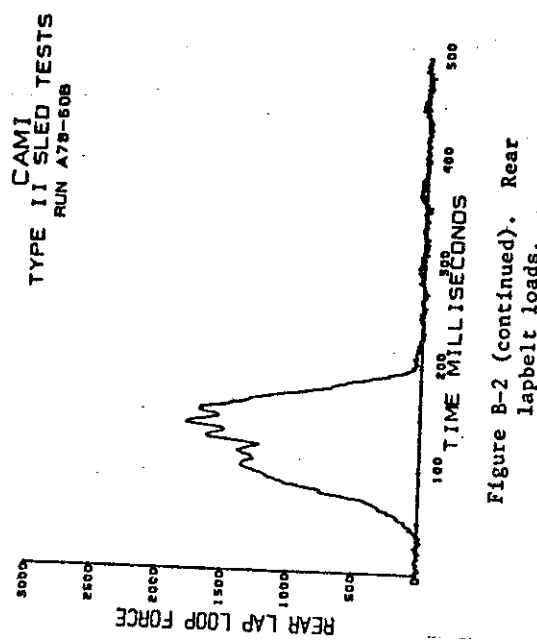
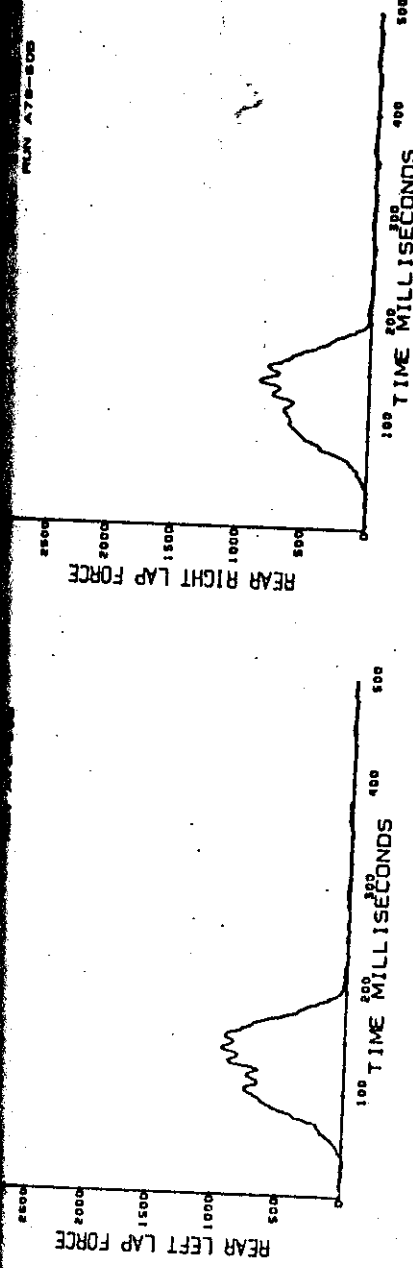
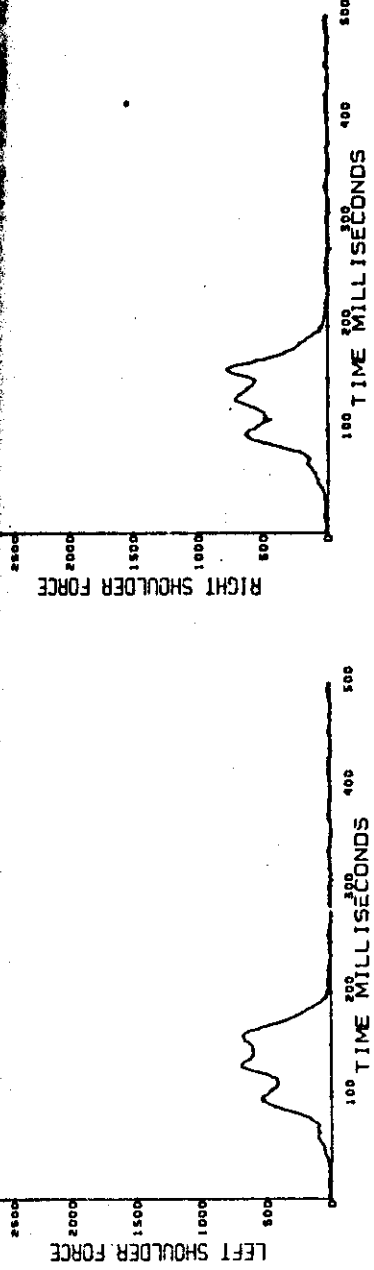


Figure B-2 (continued). Rear lapbelt loads.



CAMI  
TYPE II SLED TESTS  
RUN A78-60A

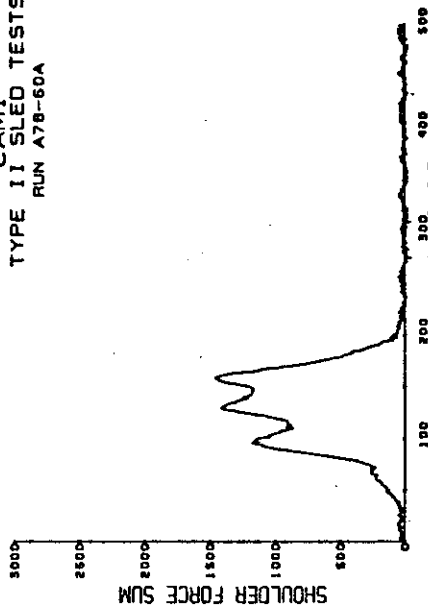


Figure B-2 (continued). Shoulder belt loads.

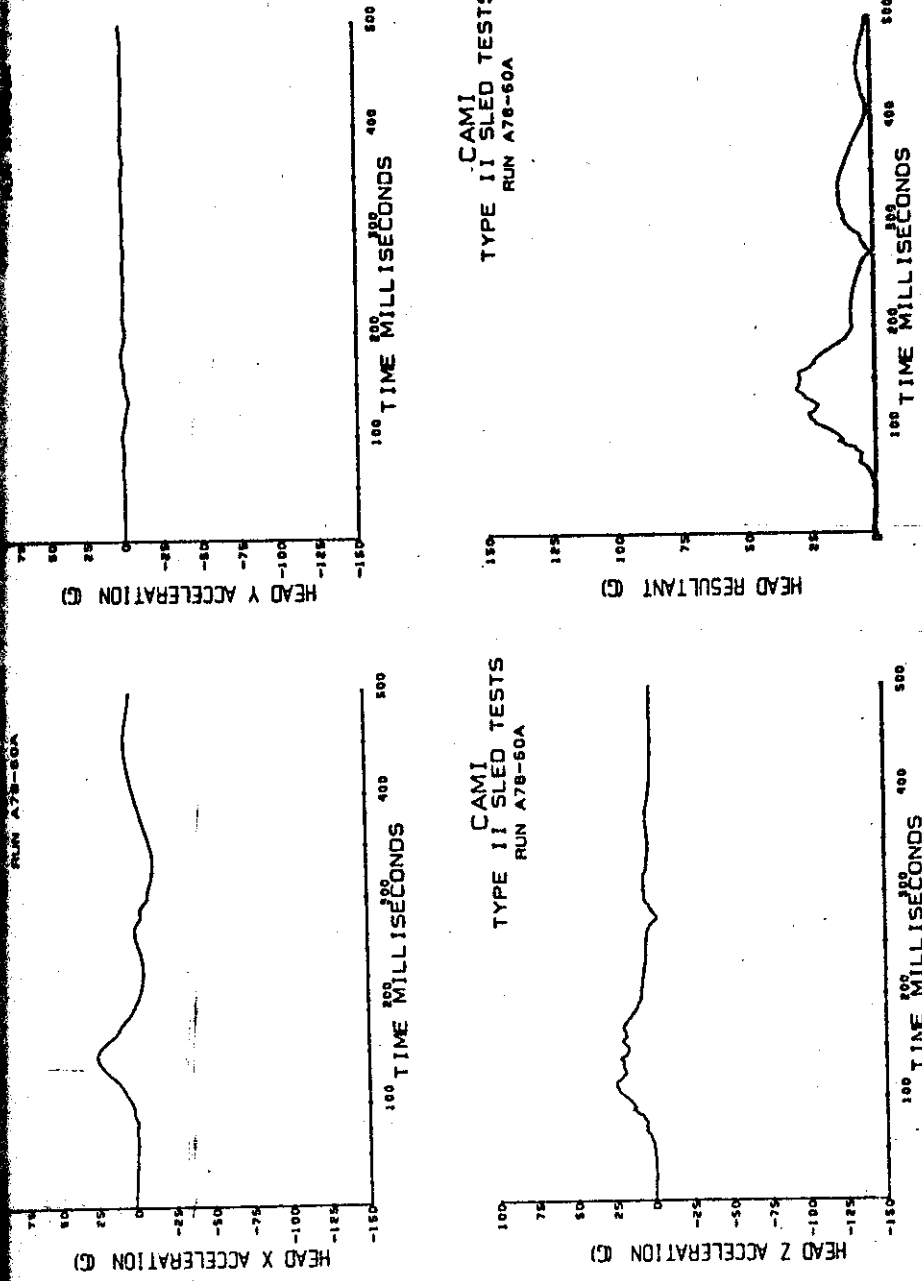


Figure B-2 (continued). Head acceleration.

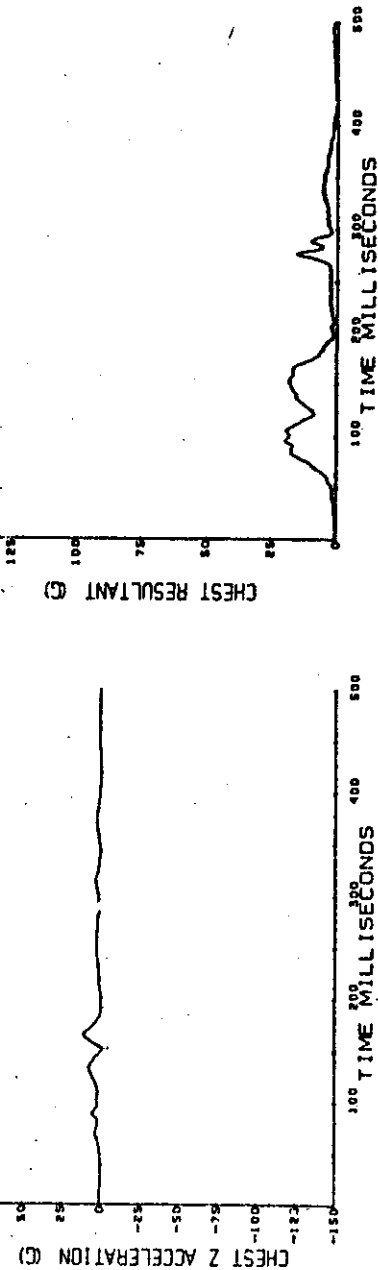
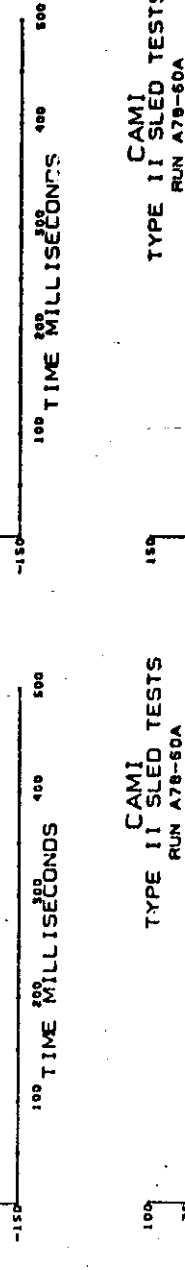
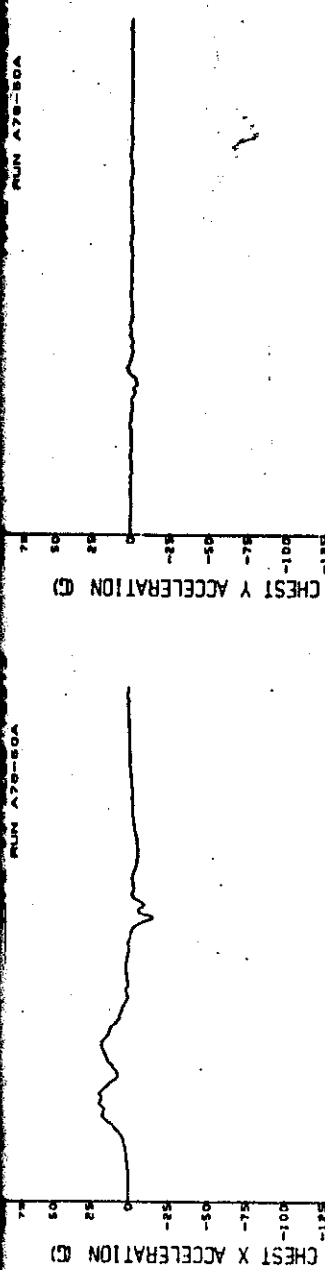


Figure B-2 (continued). Chest acceleration.

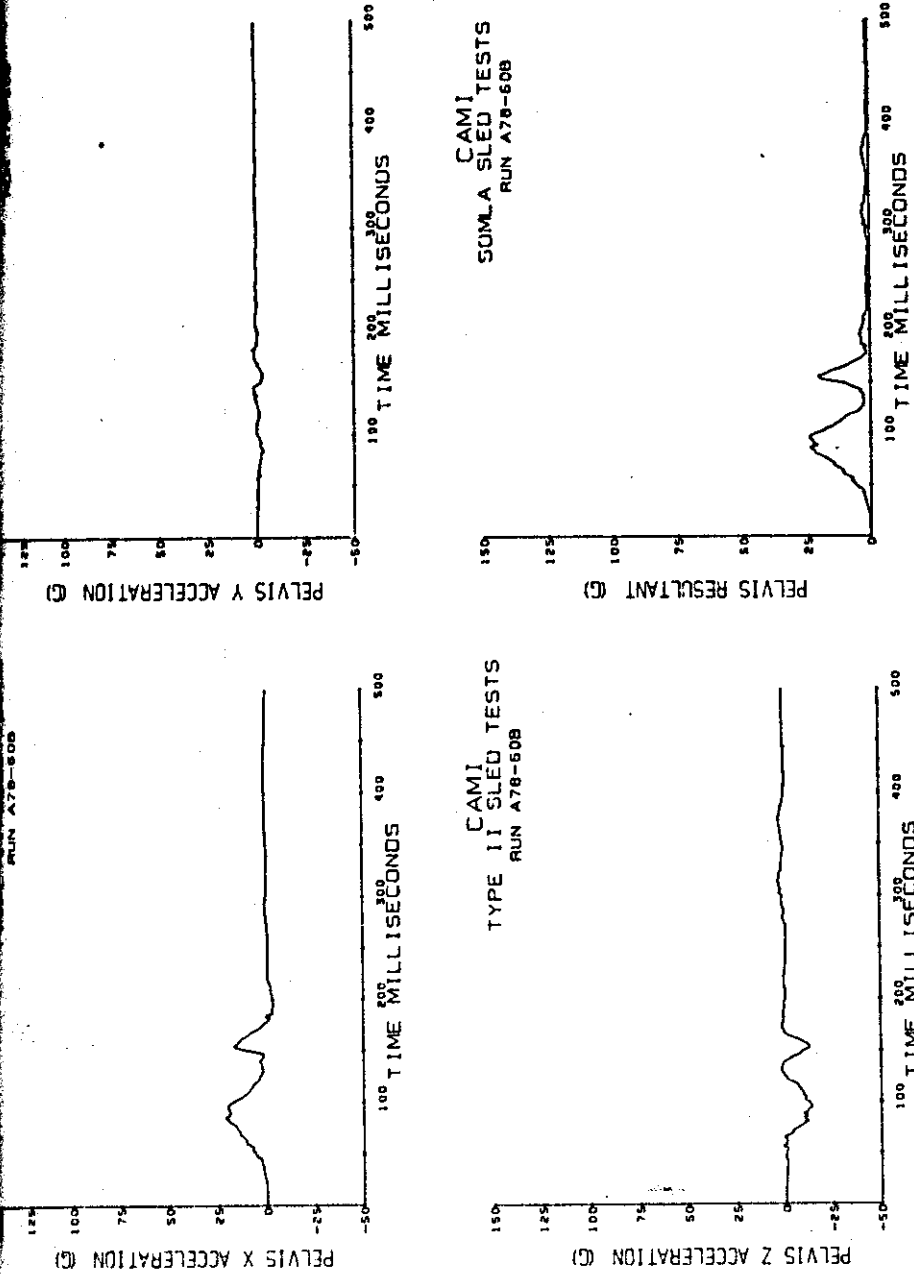


Figure B-2 (continued). Pelvis acceleration.

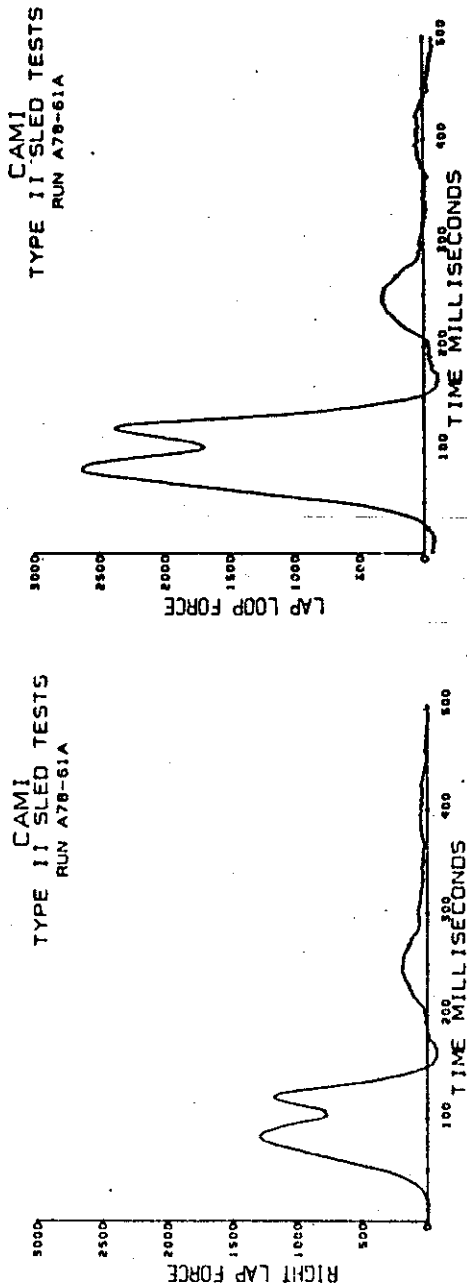
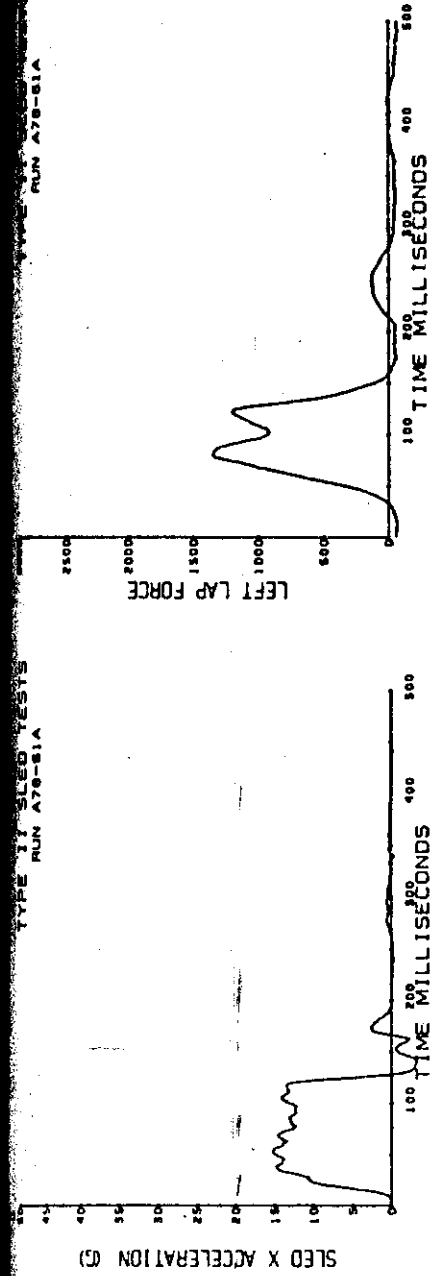


Figure B-3. 14-8 tests.  
Sled acceleration and lapbelt loads.

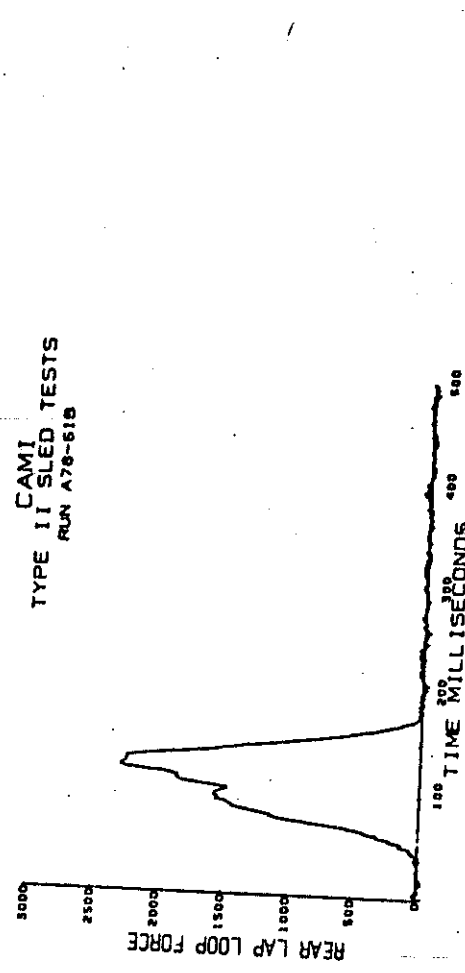
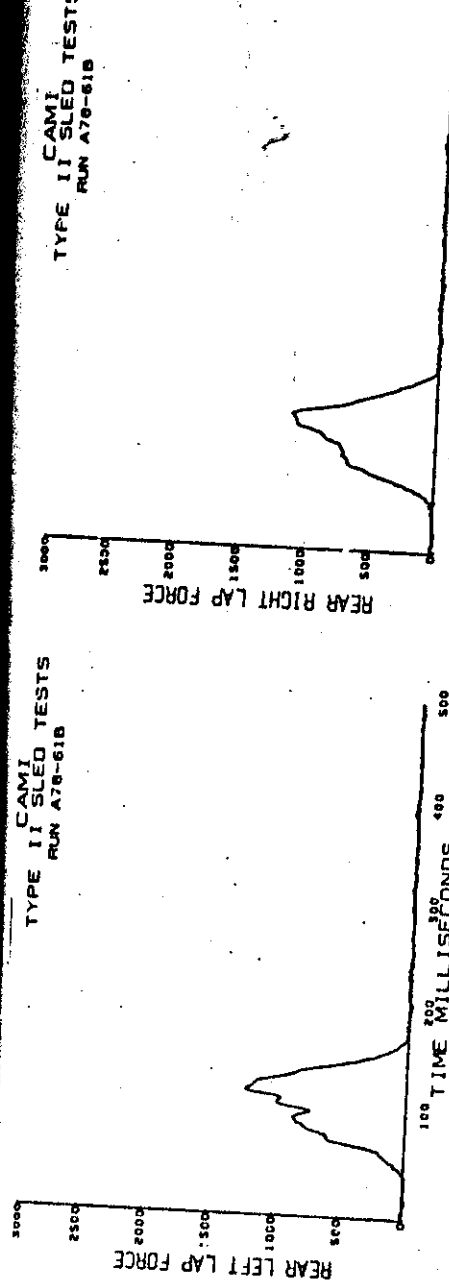
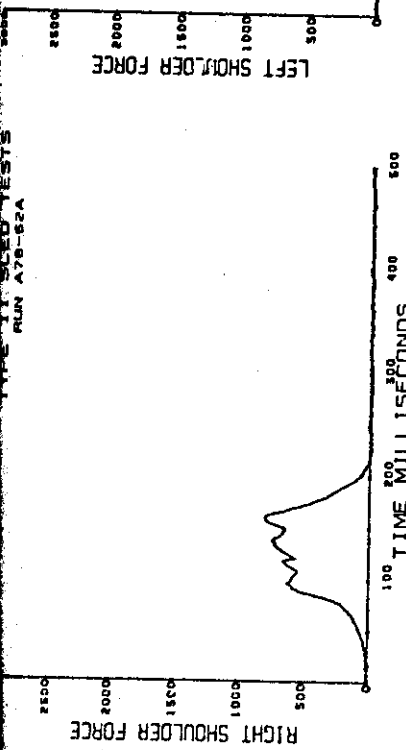
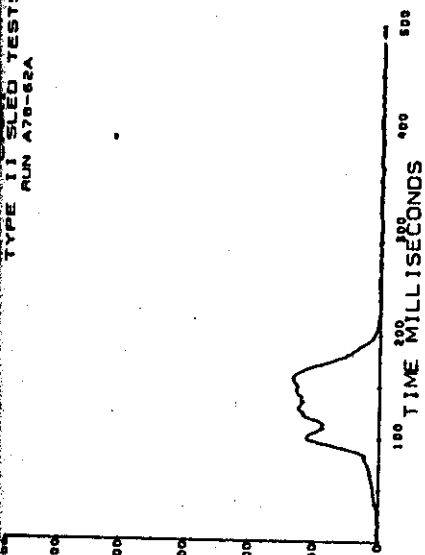


Figure B-3 (continued). Rear Lap belt loads.

TYPE II SLED TESTS  
RUN A78-62A



TYPE II SLED TESTS  
RUN A78-62A



TYPE II SLED TESTS  
RUN A78-62A

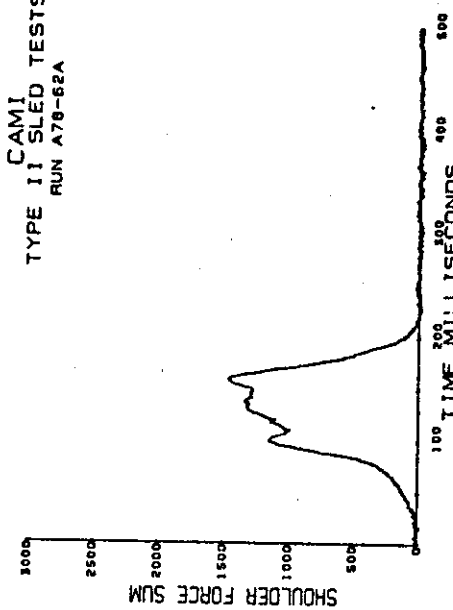


Figure B-3 (continued). Shoulder belt loads.

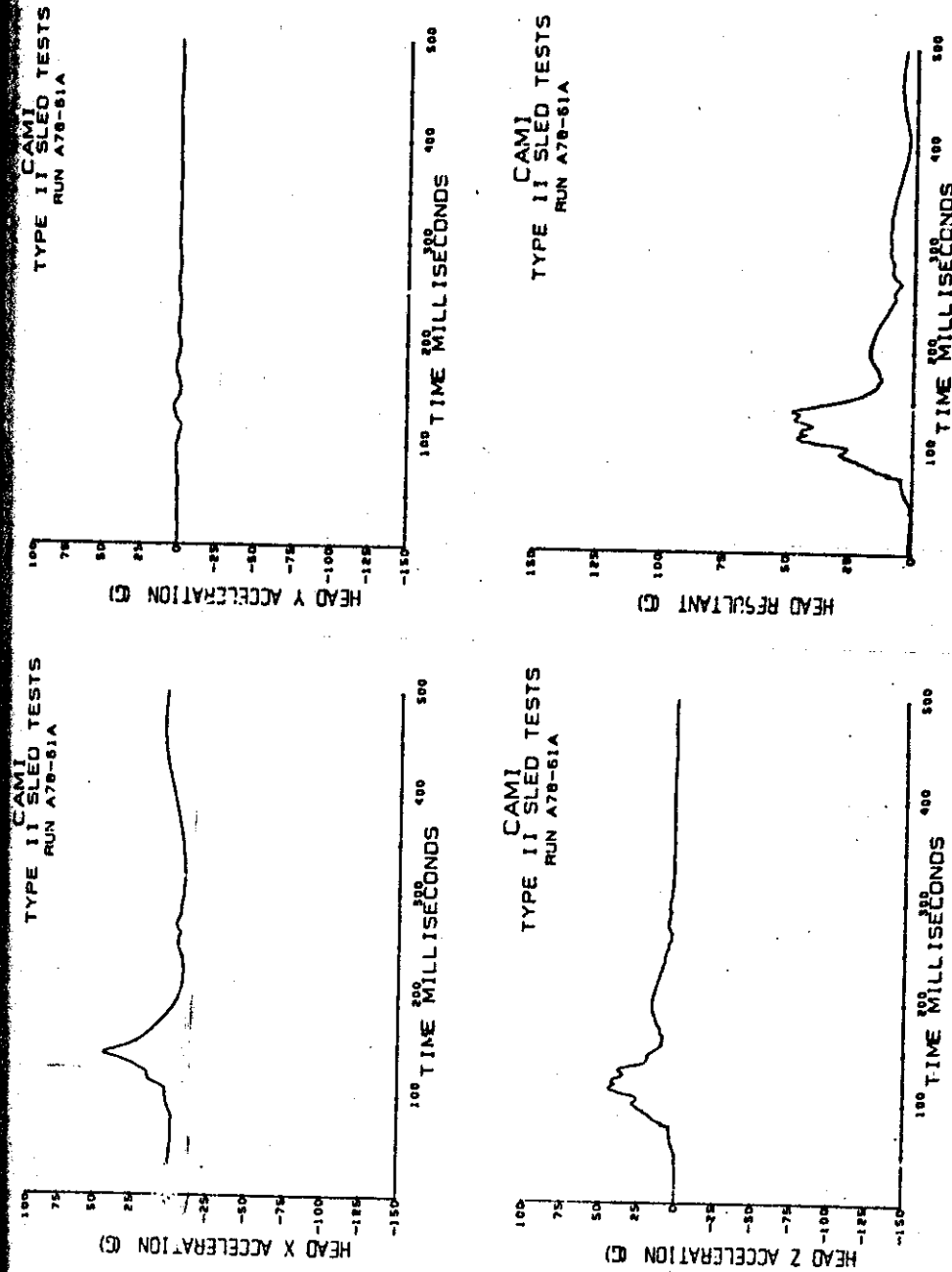


Figure B-3 (continued). Head acceleration.

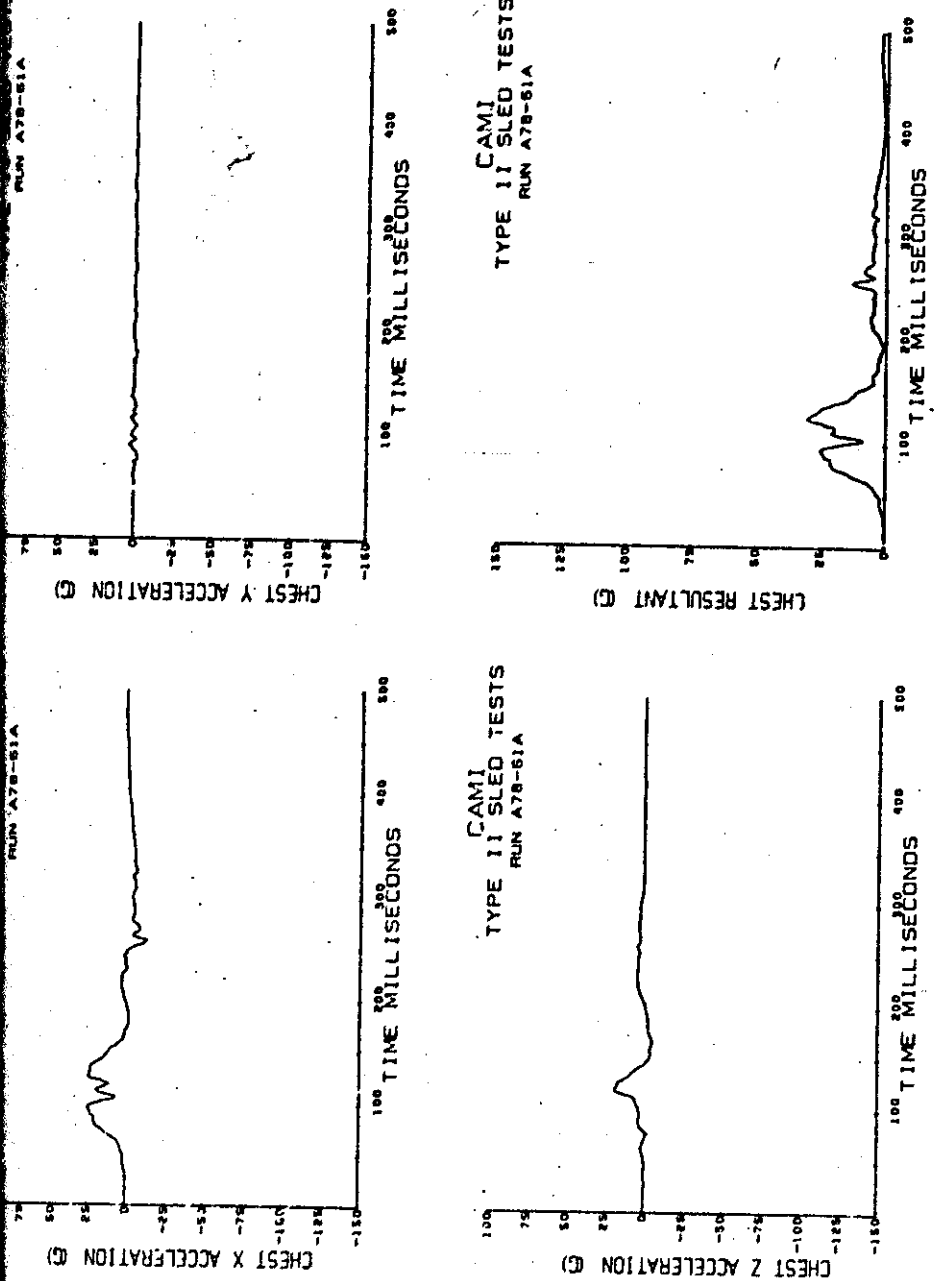


Figure B-3 (continued). Chest acceleration.

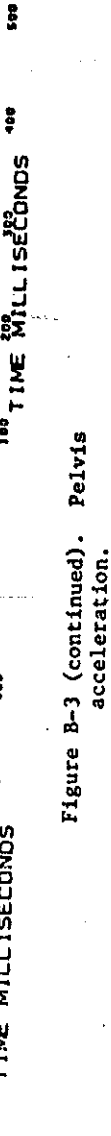
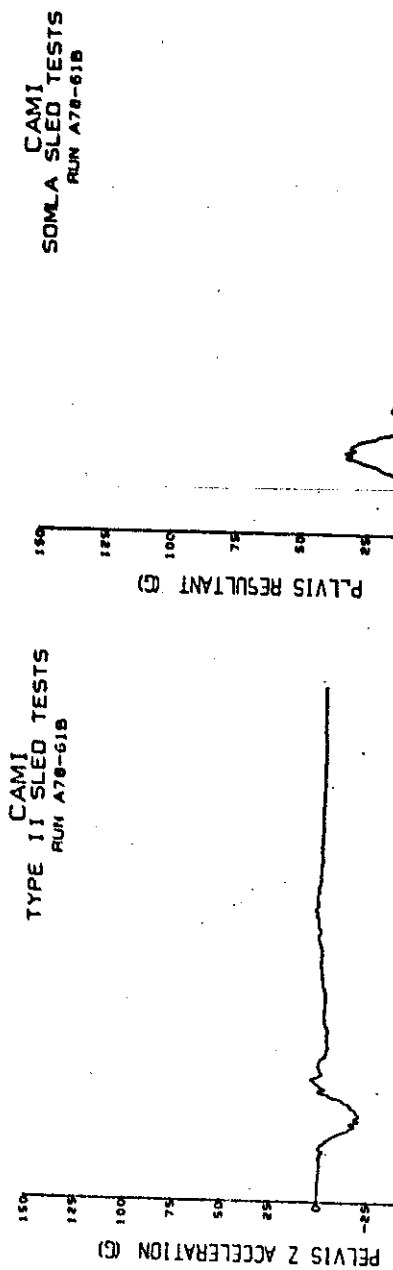
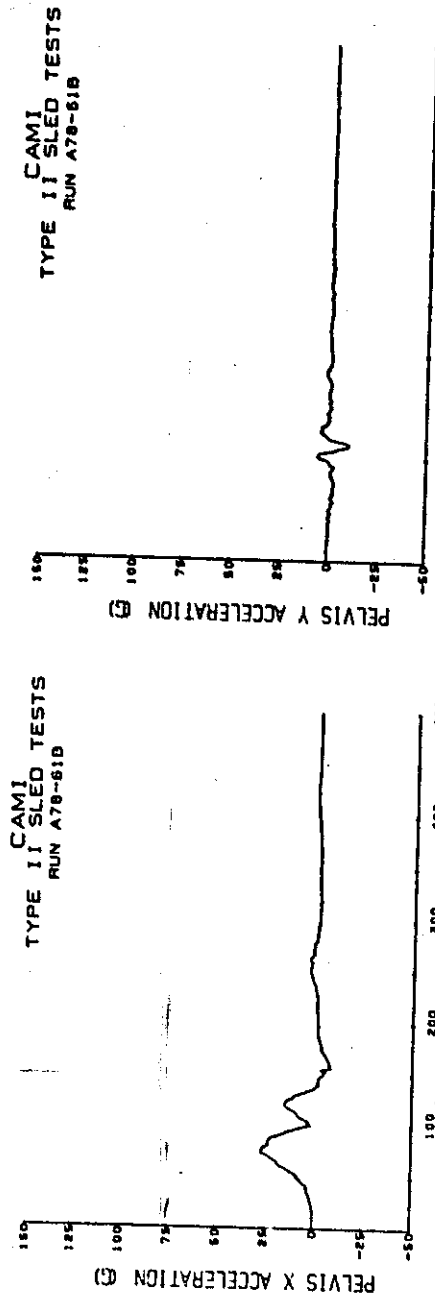


Figure B-3 (continued). Pelvis acceleration.

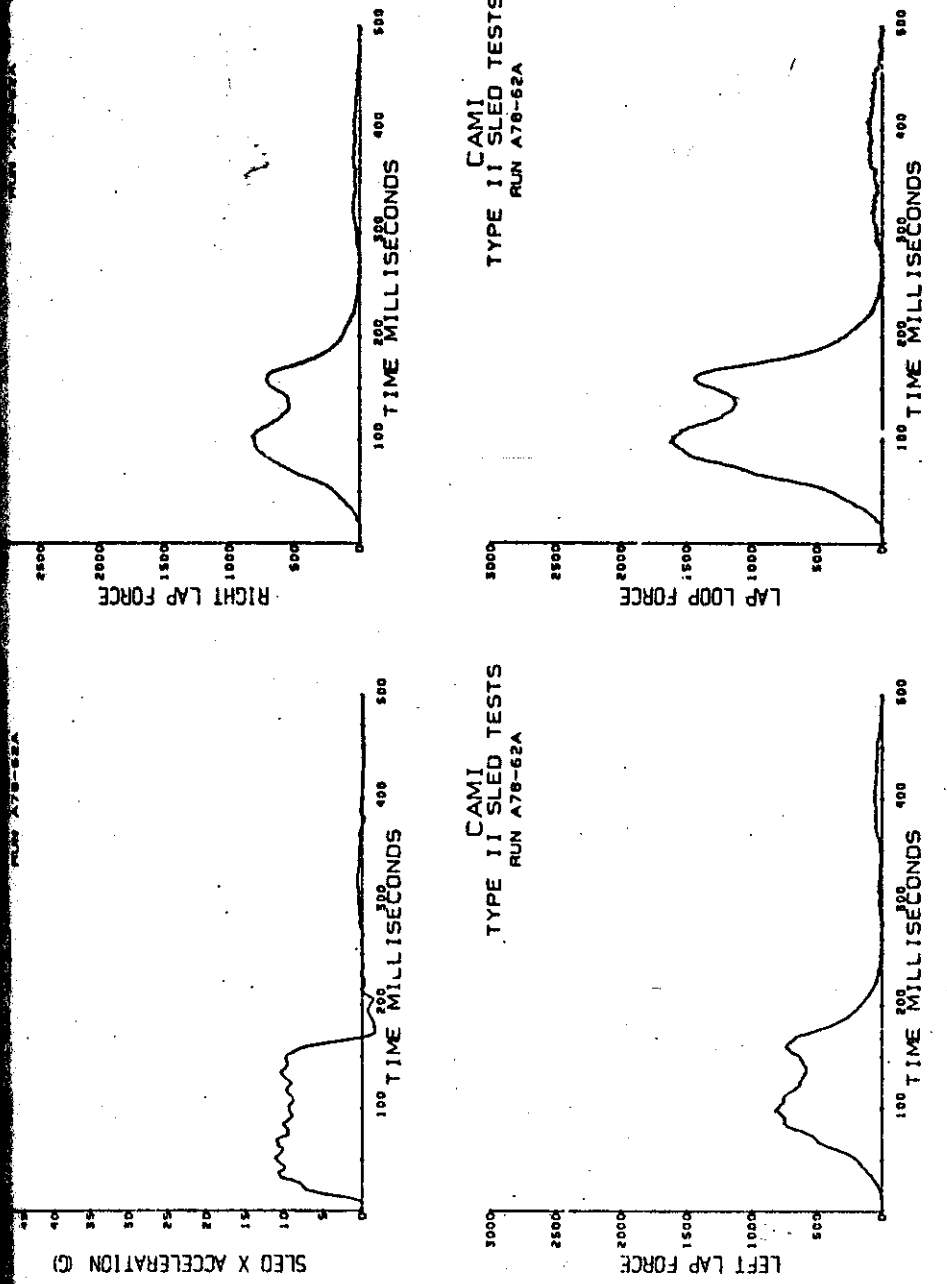
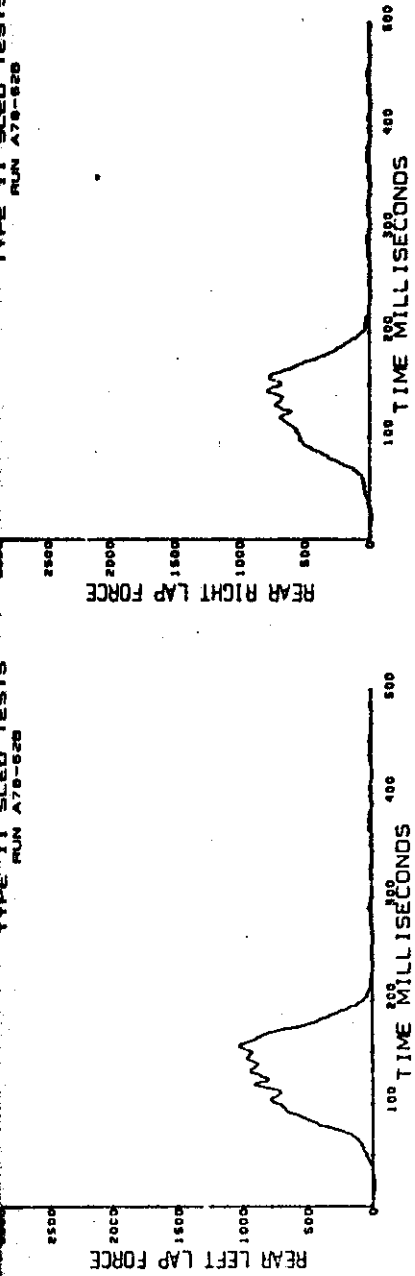


Figure B-4. 10-g tests.  
Sled acceleration and lapbelt loads.

TYPE II SLED TESTS  
RUN A78-628



TYPE II SLED TESTS  
RUN A78-628

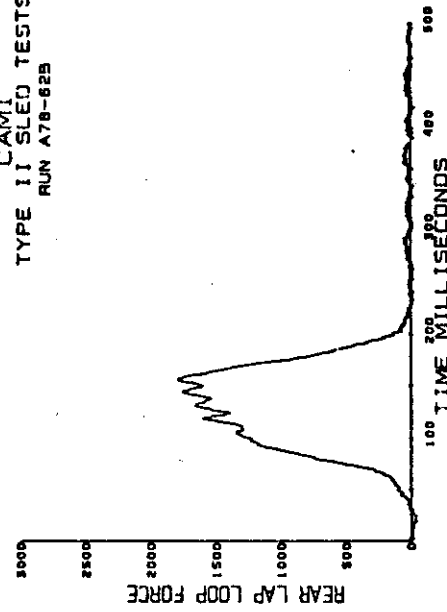
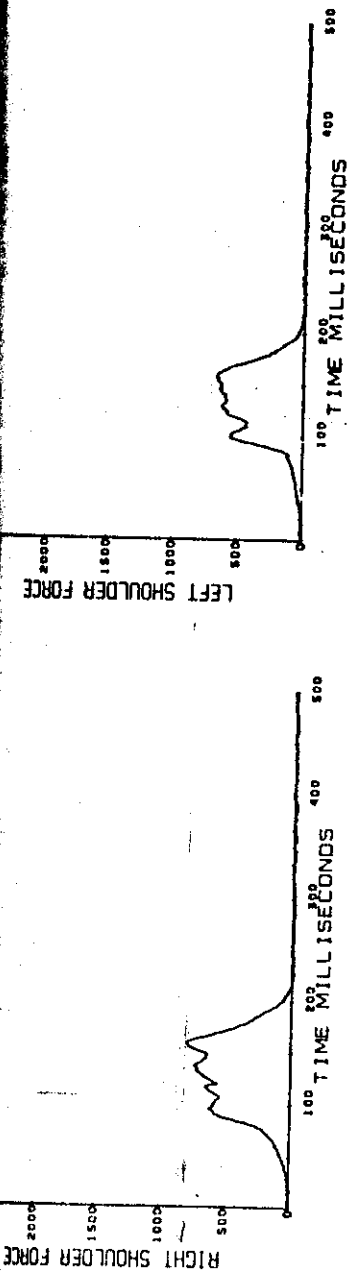


Figure B-4 (continued). Rear lap belt loads.



TYPE I CAMI  
RUN A78-62A

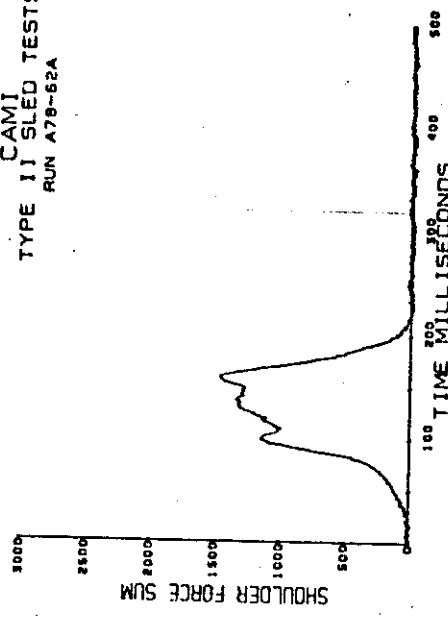


Figure B-4 (continued). Shoulder belt loads.

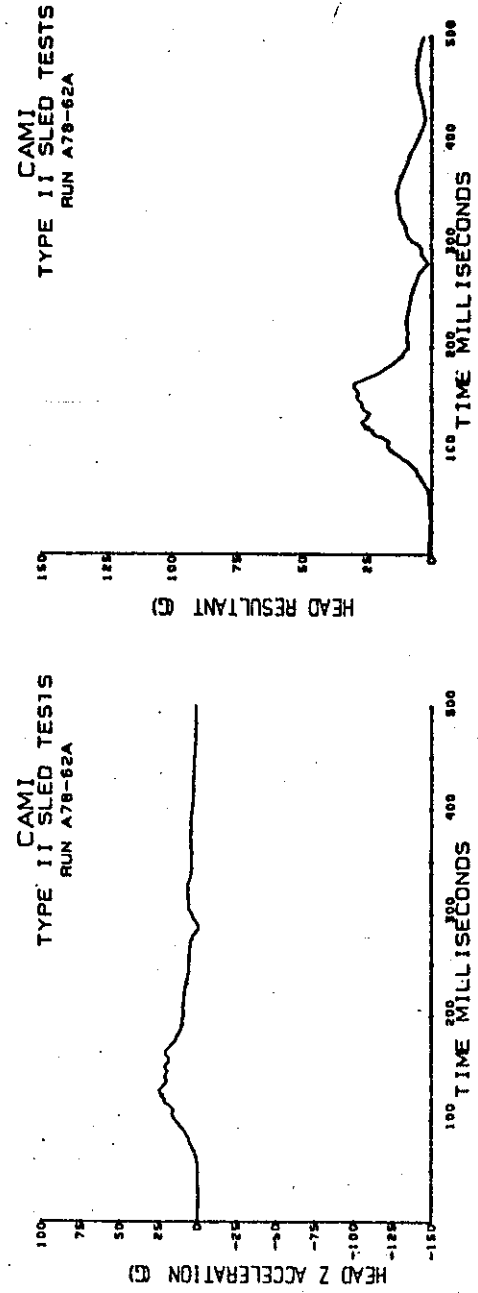
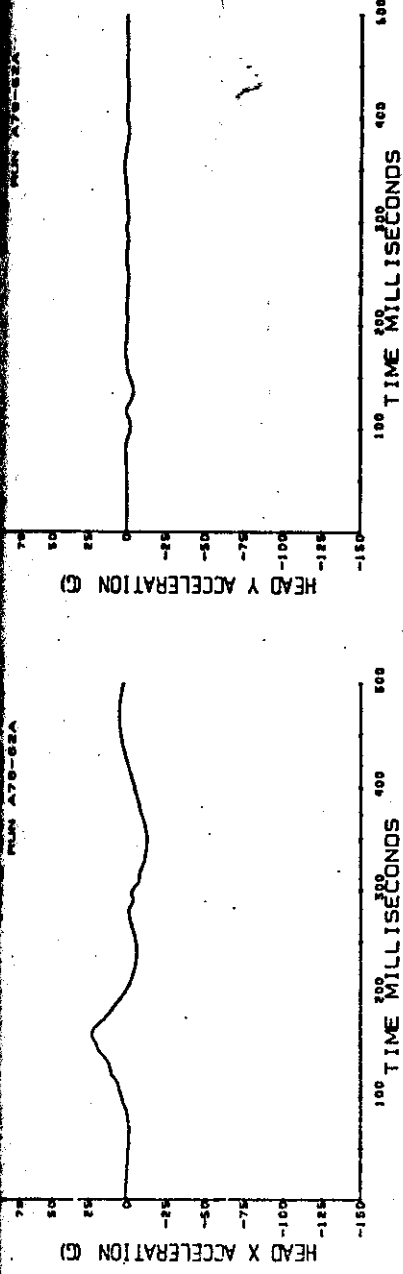


Figure B-4 (continued). Head acceleration.

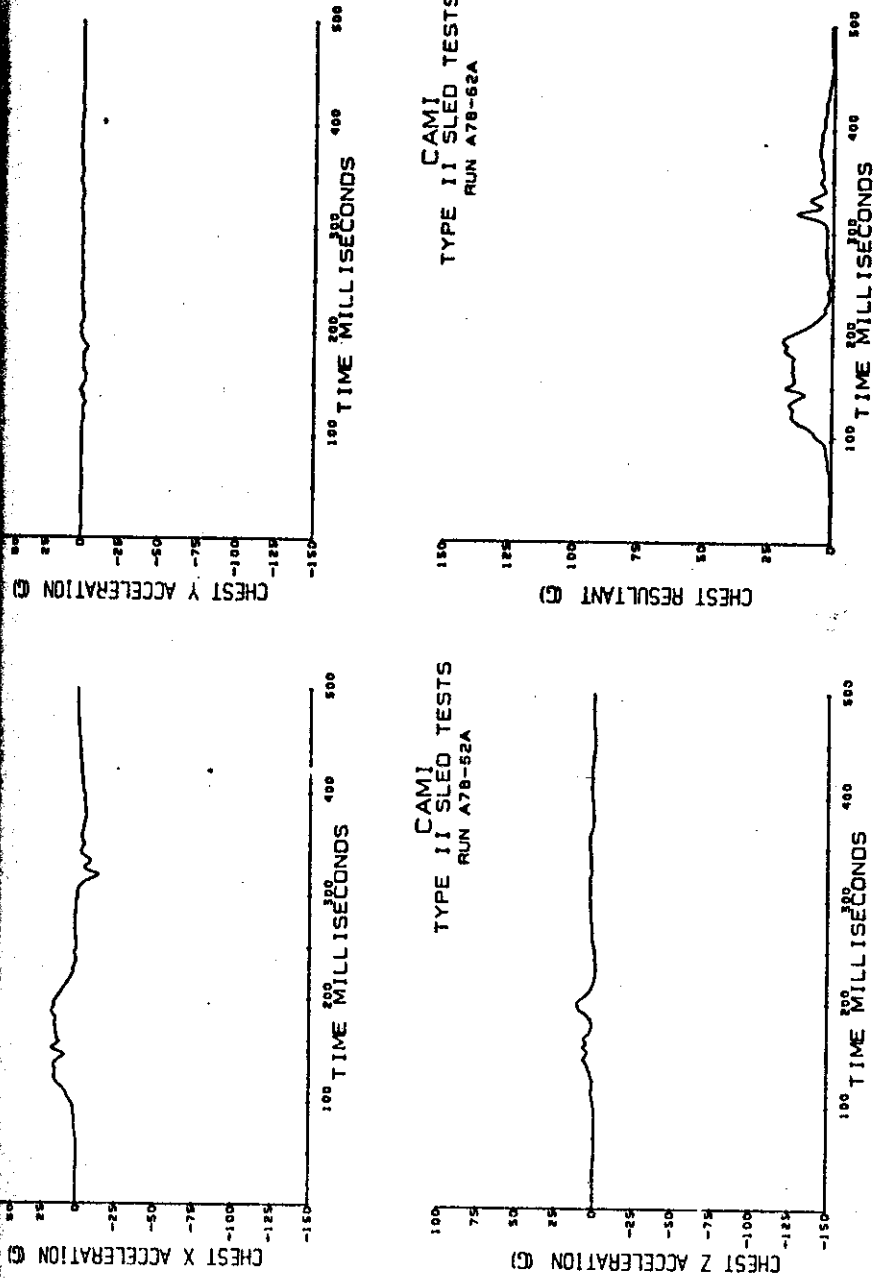


Figure B-4 (continued). Chest acceleration.

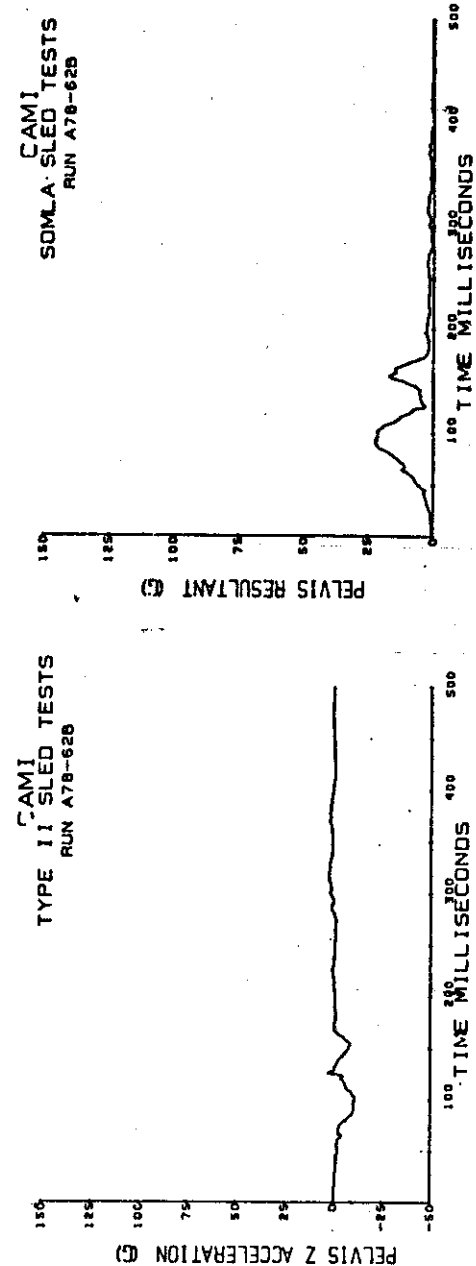
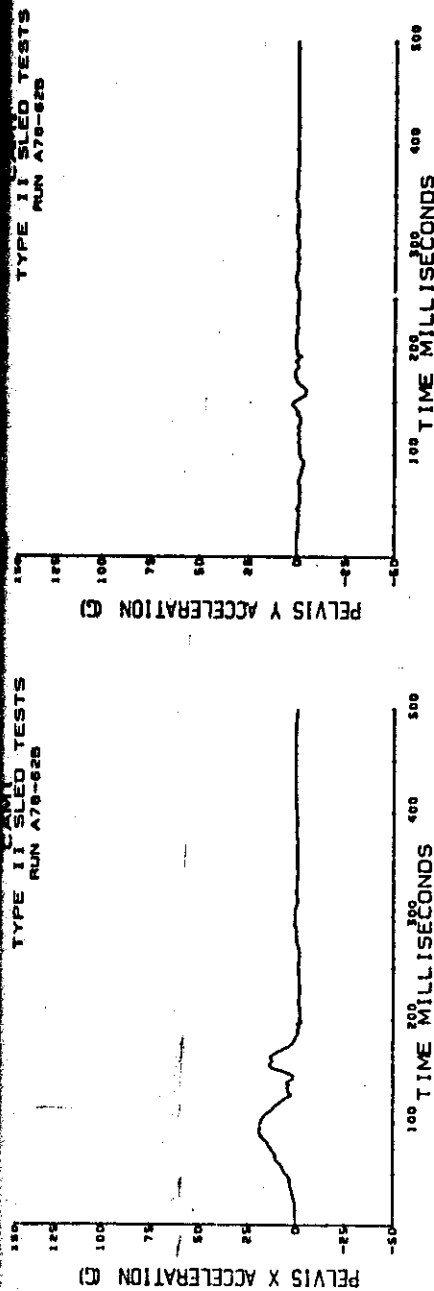


Figure E-4 (continued). Pelvis acceleration.

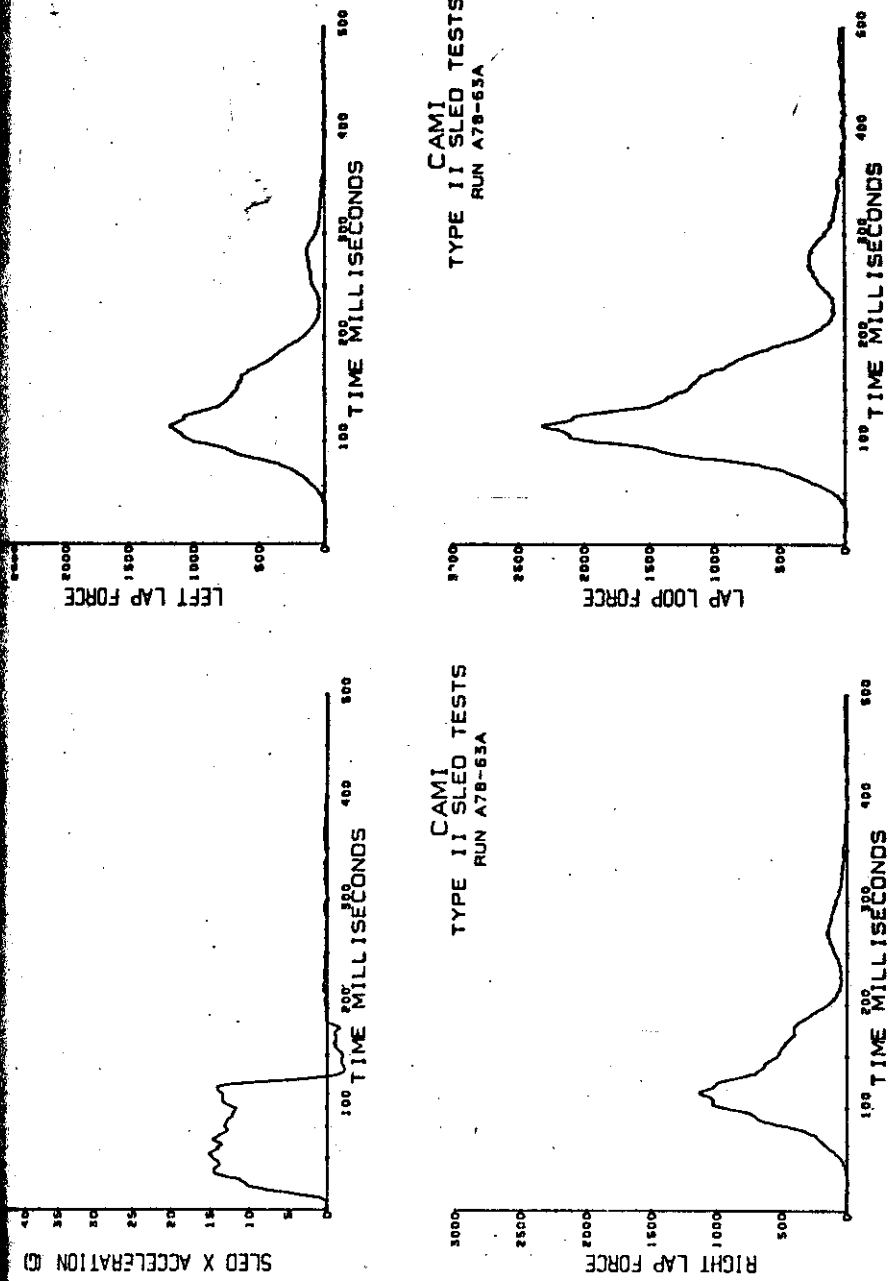


Figure B-5. 14-8 tests.  
Sled acceleration and lapbelt loads.

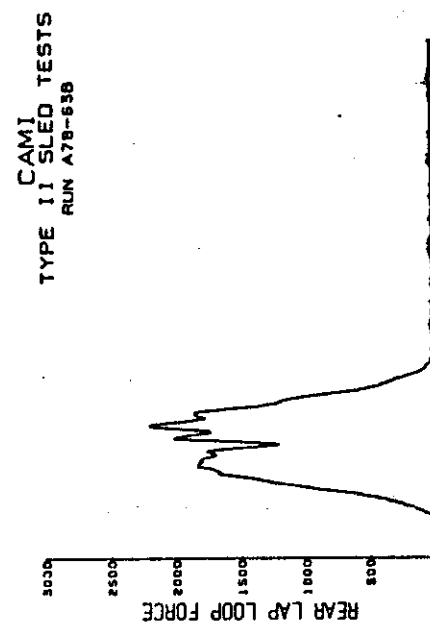
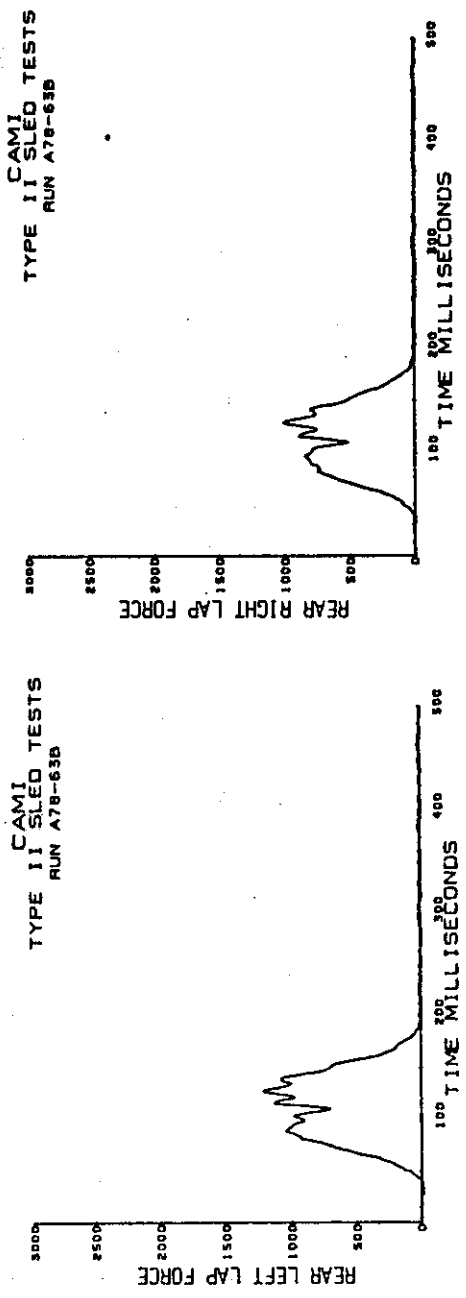


Figure B-5 (continued). Rear lap belt loads.

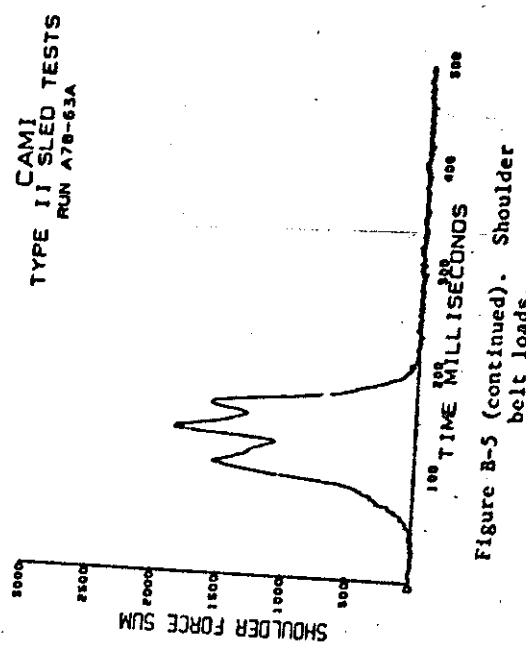
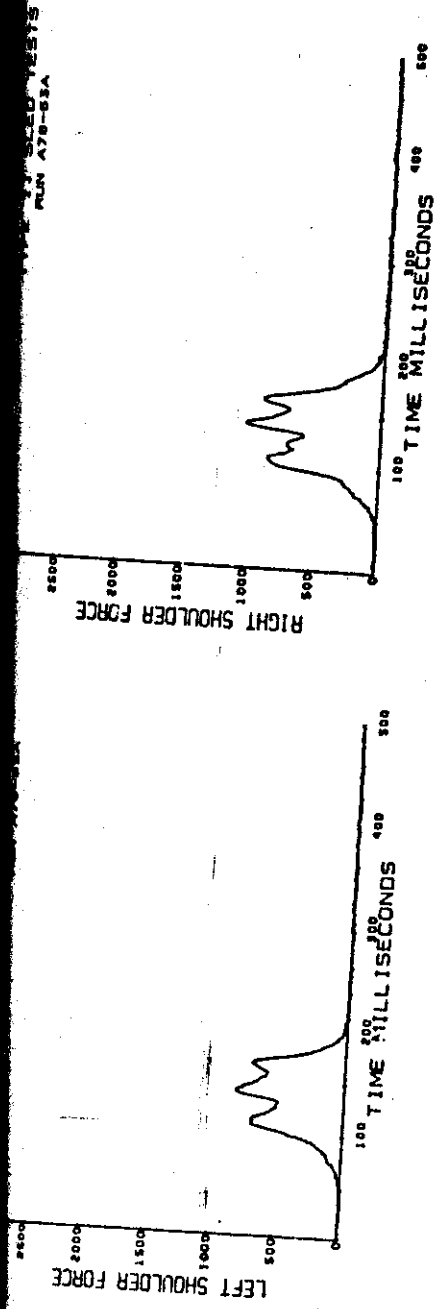
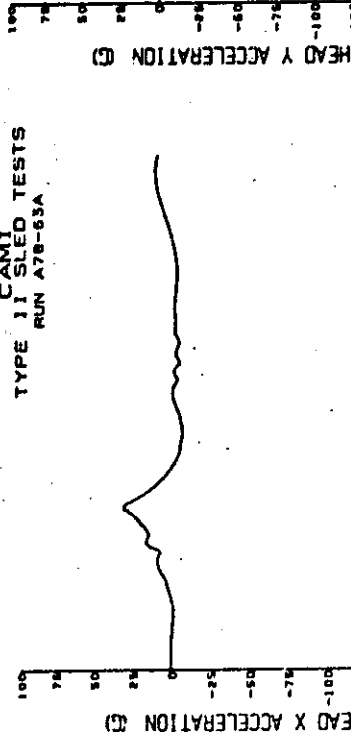
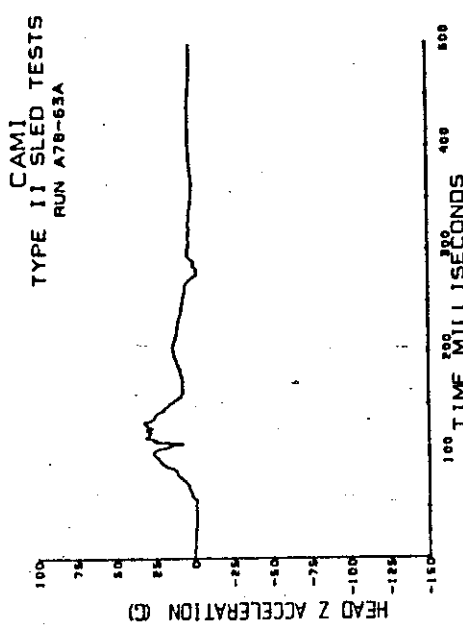


Figure B-5 (continued). Shoulder belt loads.

CAMI  
TYPE II SLED TESTS  
RUN A78-63A



CAMI  
TYPE II SLED TESTS  
RUN A78-63A



CAMI  
TYPE II SLED TESTS  
RUN A78-63A

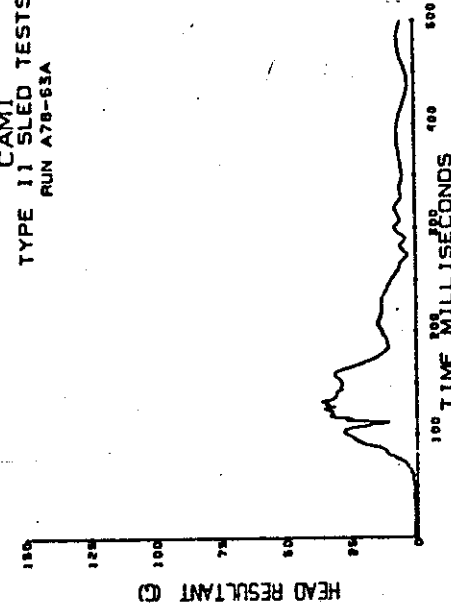


Figure B-5 (continued). Head acceleration.

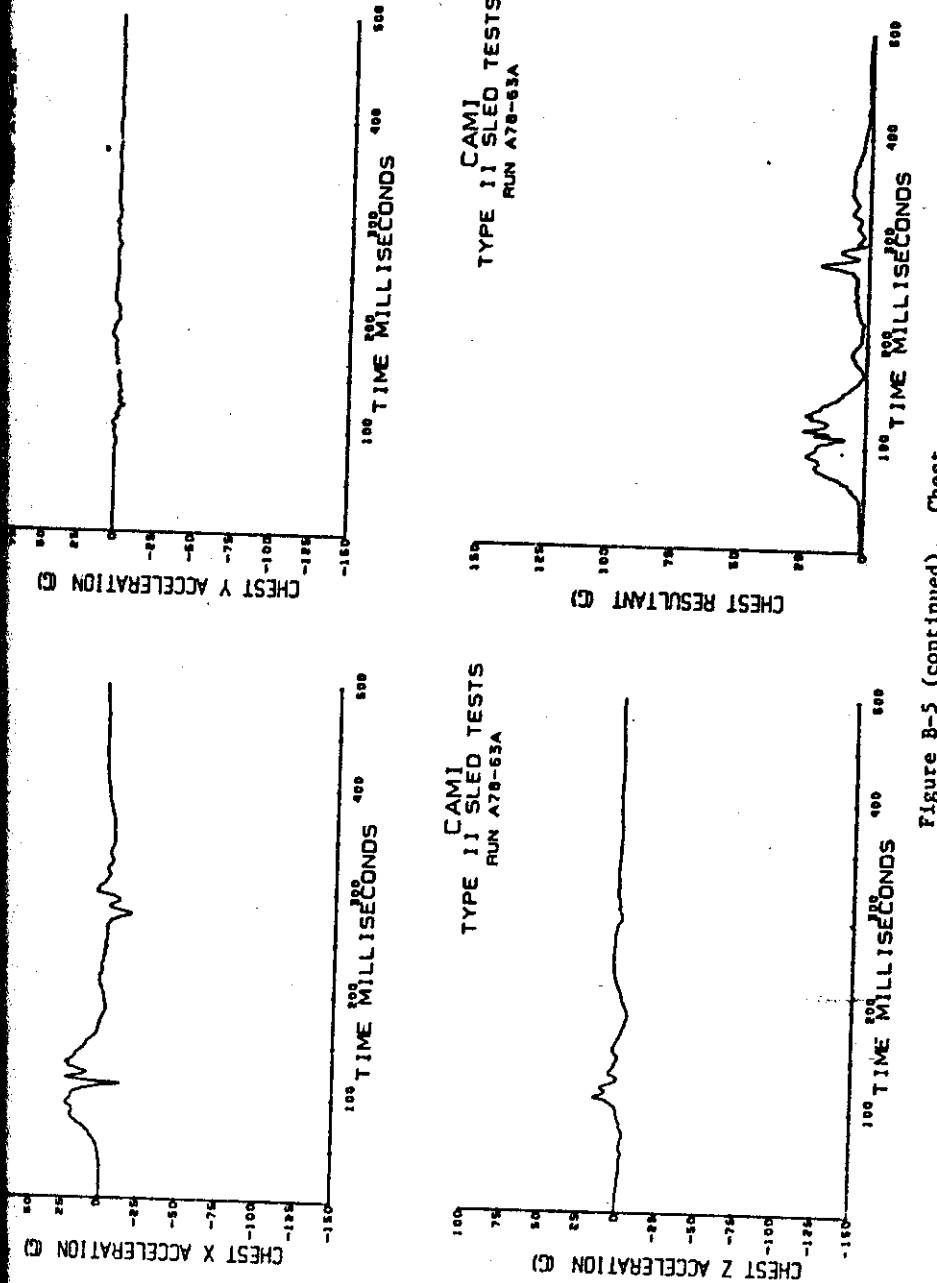


Figure B-5 (continued). Chest acceleration.

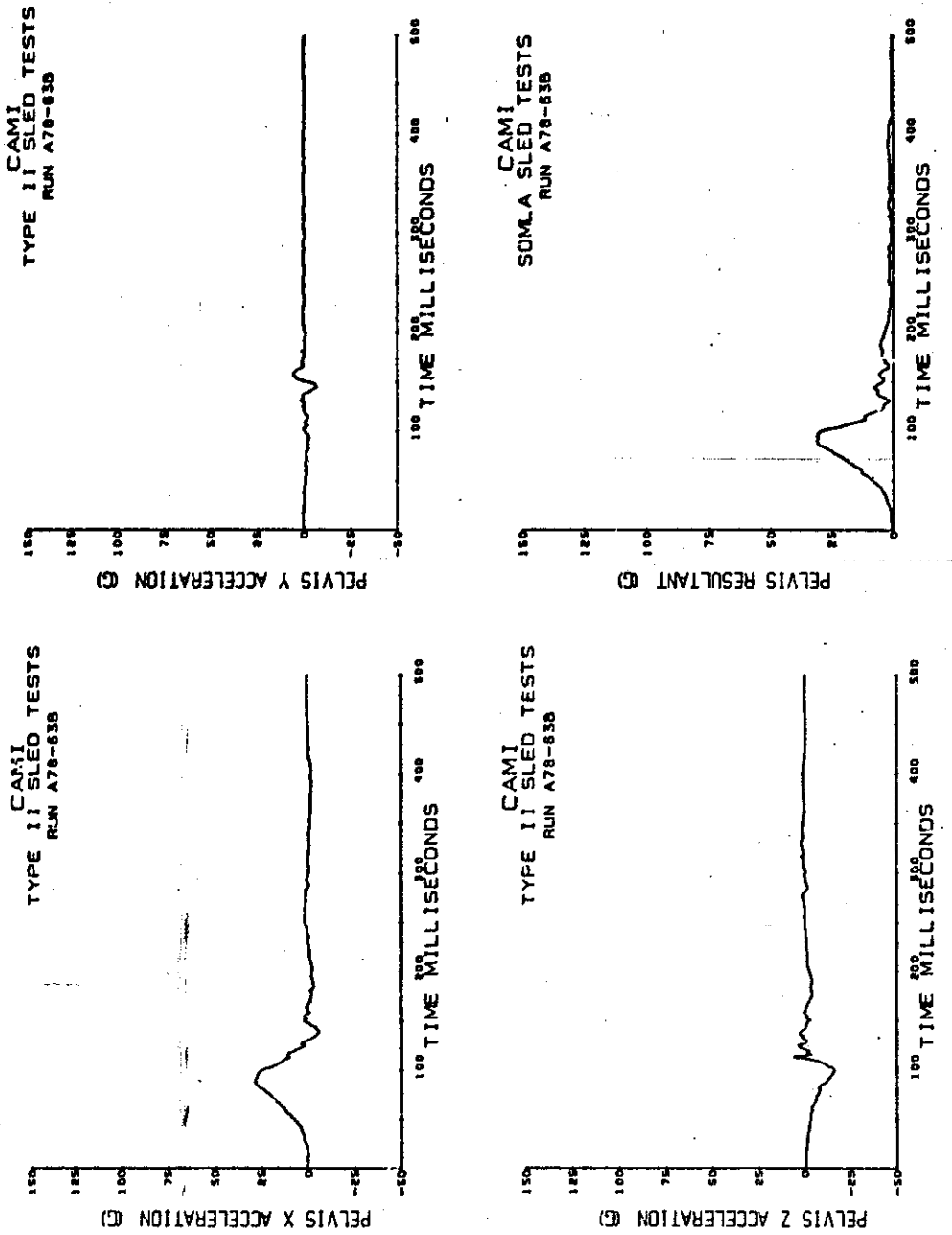


Figure B-5 (continued). Pelvis acceleration.

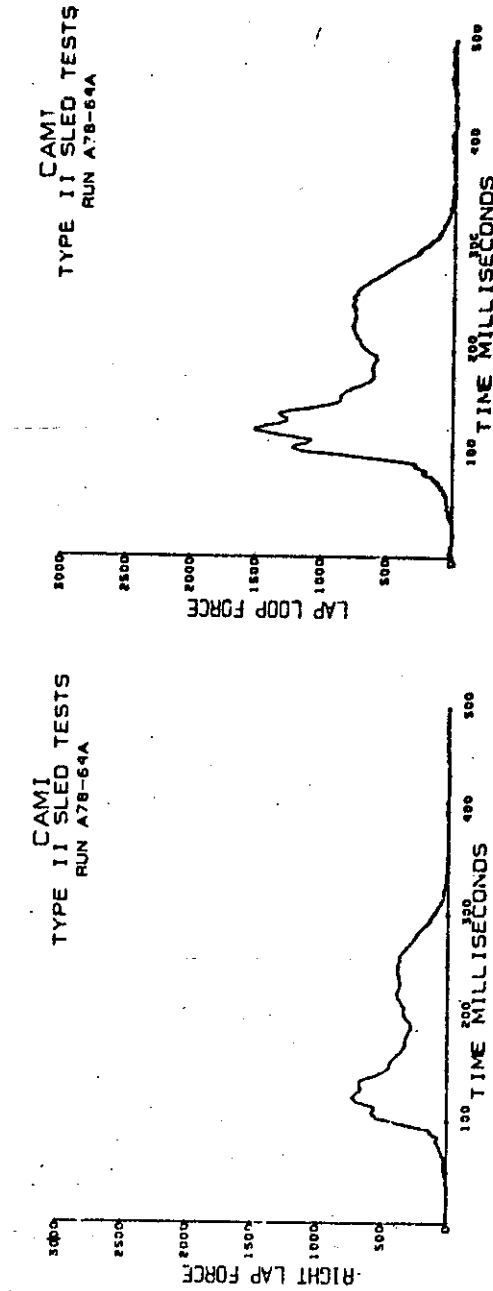
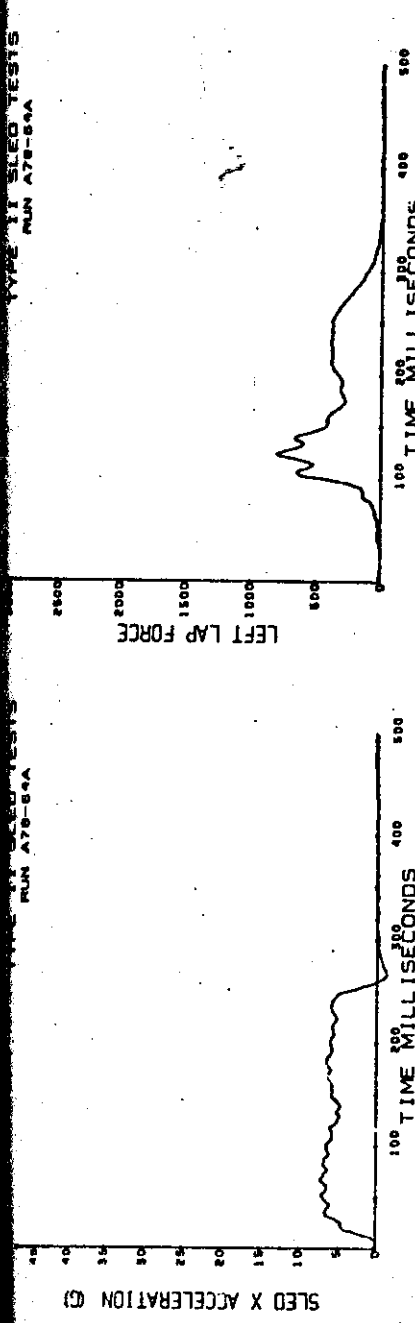


Figure B-6. 6-8 tests.  
Sled acceleration and lapbelt loads.

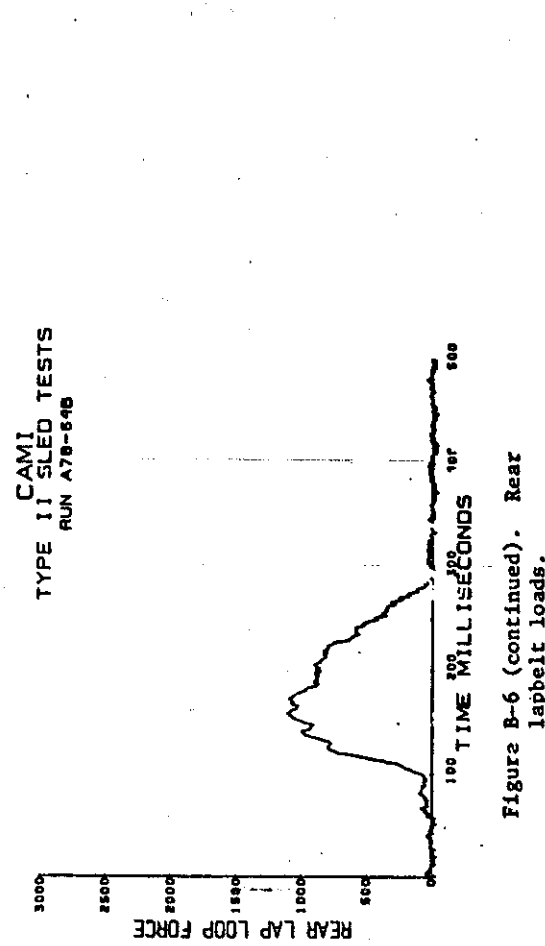
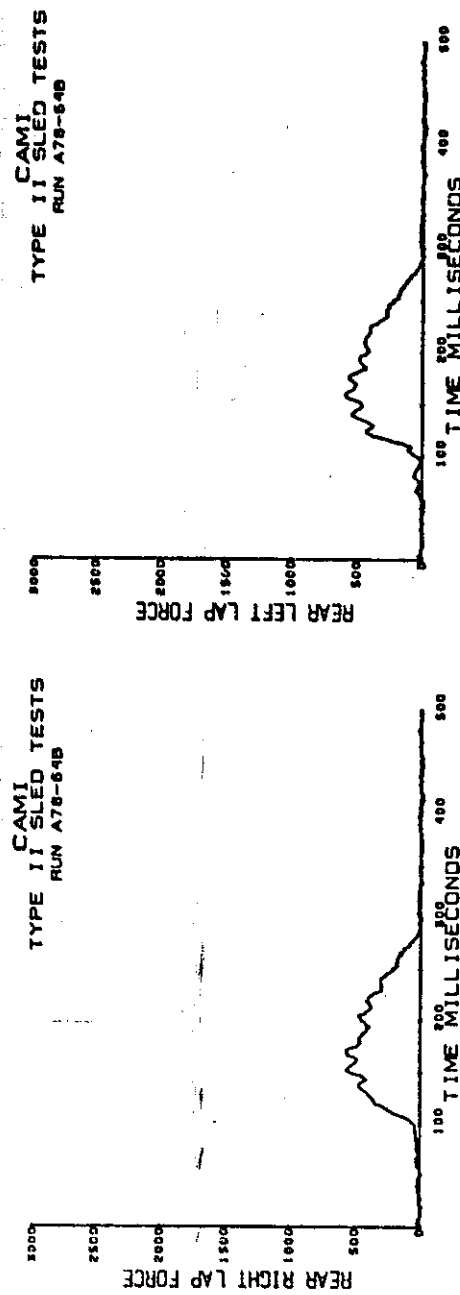


Figure B-6 (continued). Rear lap belt loads.

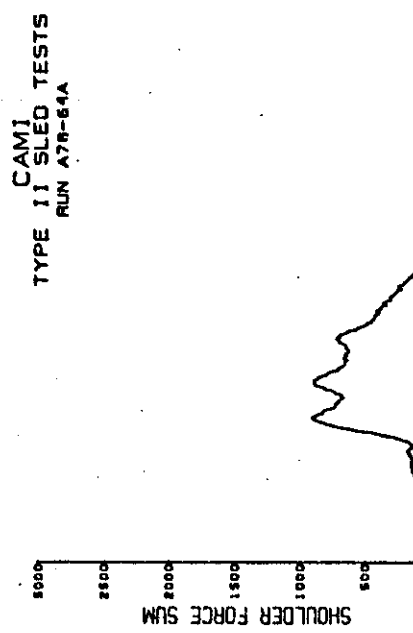
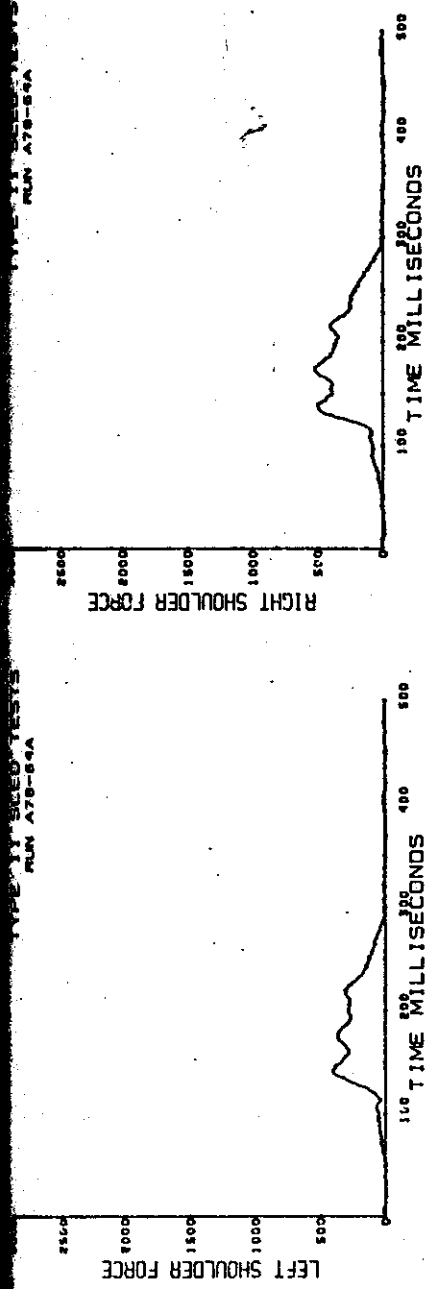


Figure B-6 (continued). - Shoulder belt loads.

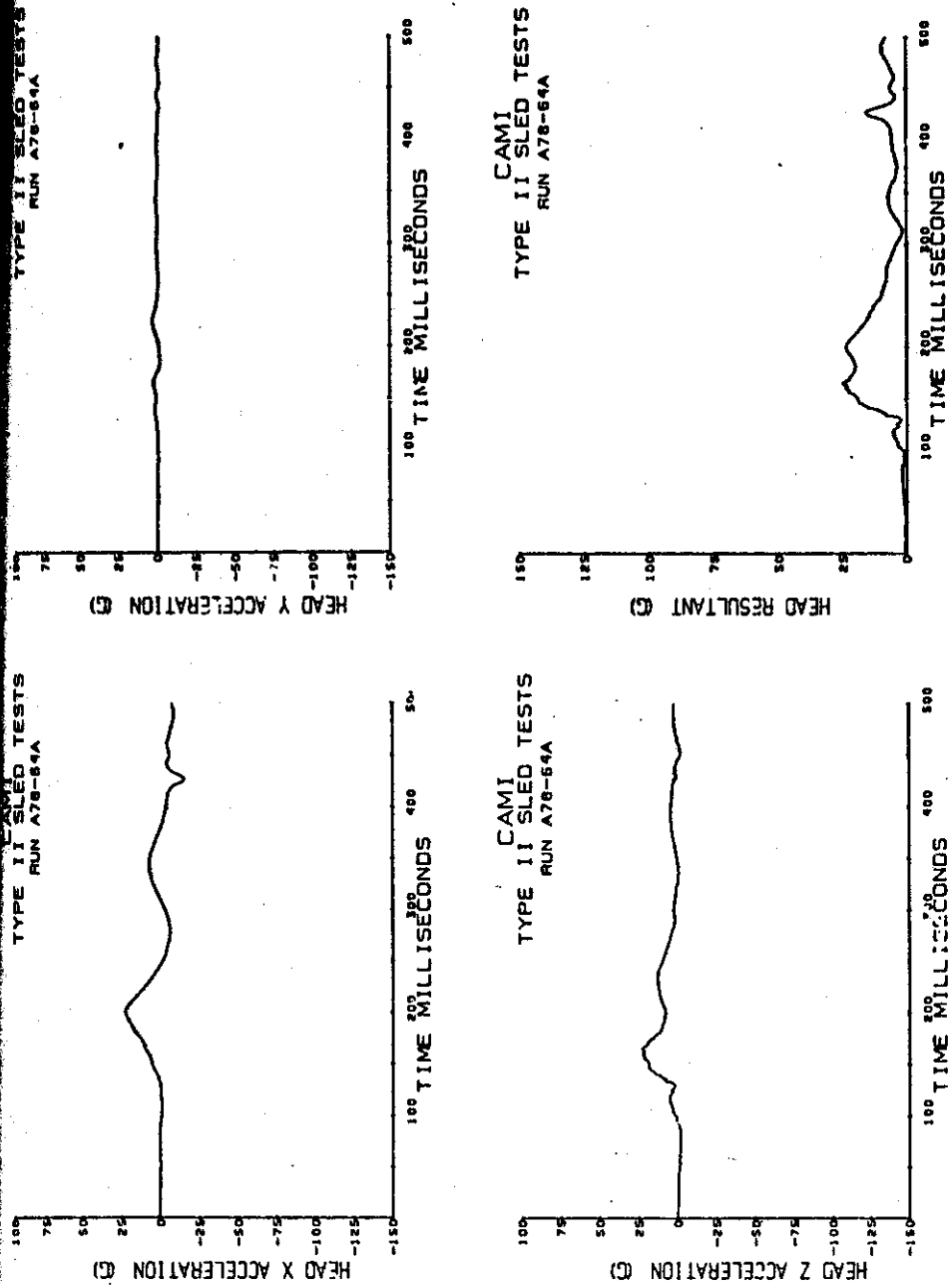
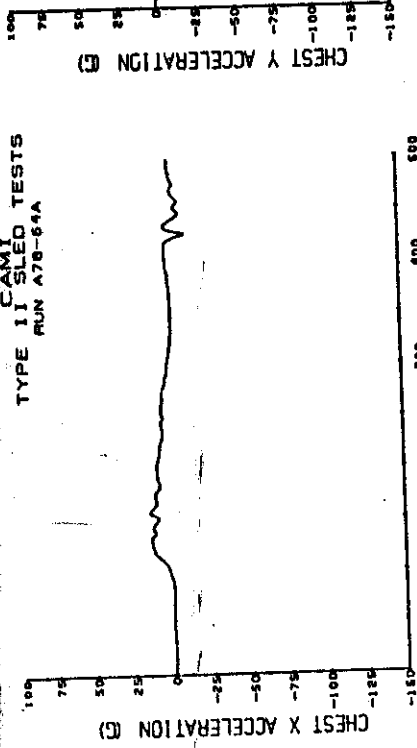
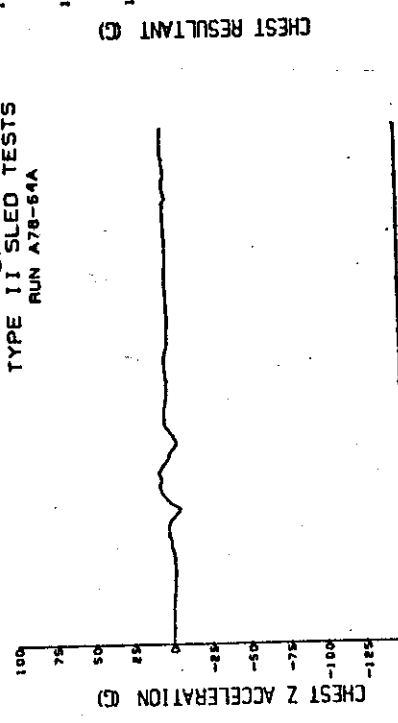


Figure B-6 (continued). Head acceleration.

TYPE II SLED TESTS  
RUN A78-64A



CAMI  
TYPE II SLED TESTS  
RUN A78-64A



CAMI  
TYPE II SLED TESTS  
RUN A78-64A



Figure B-6 (continued). Chest acceleration.

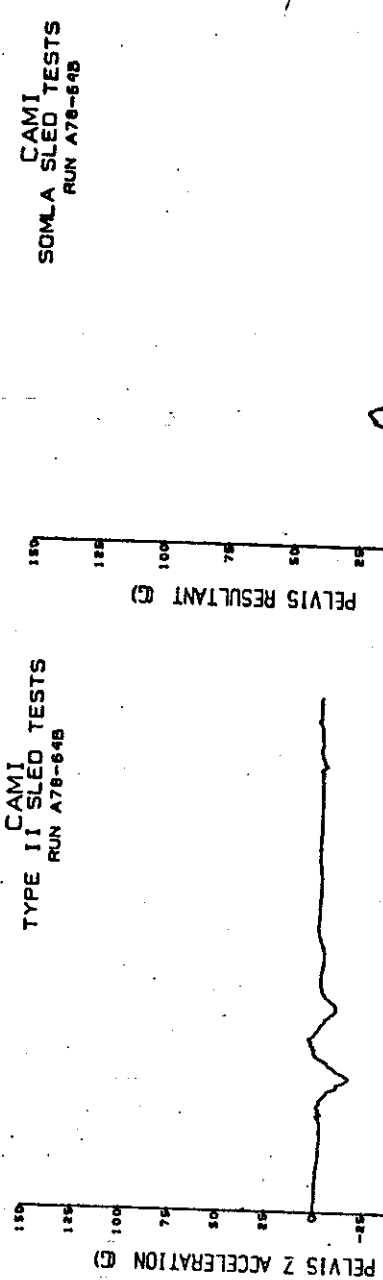
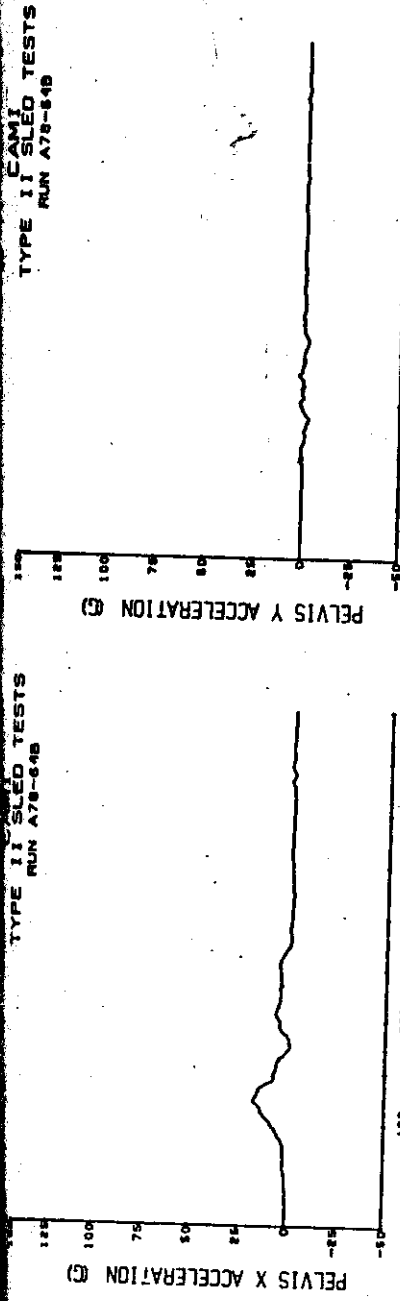


Figure B-6 (continued). Pelvis acceleration.

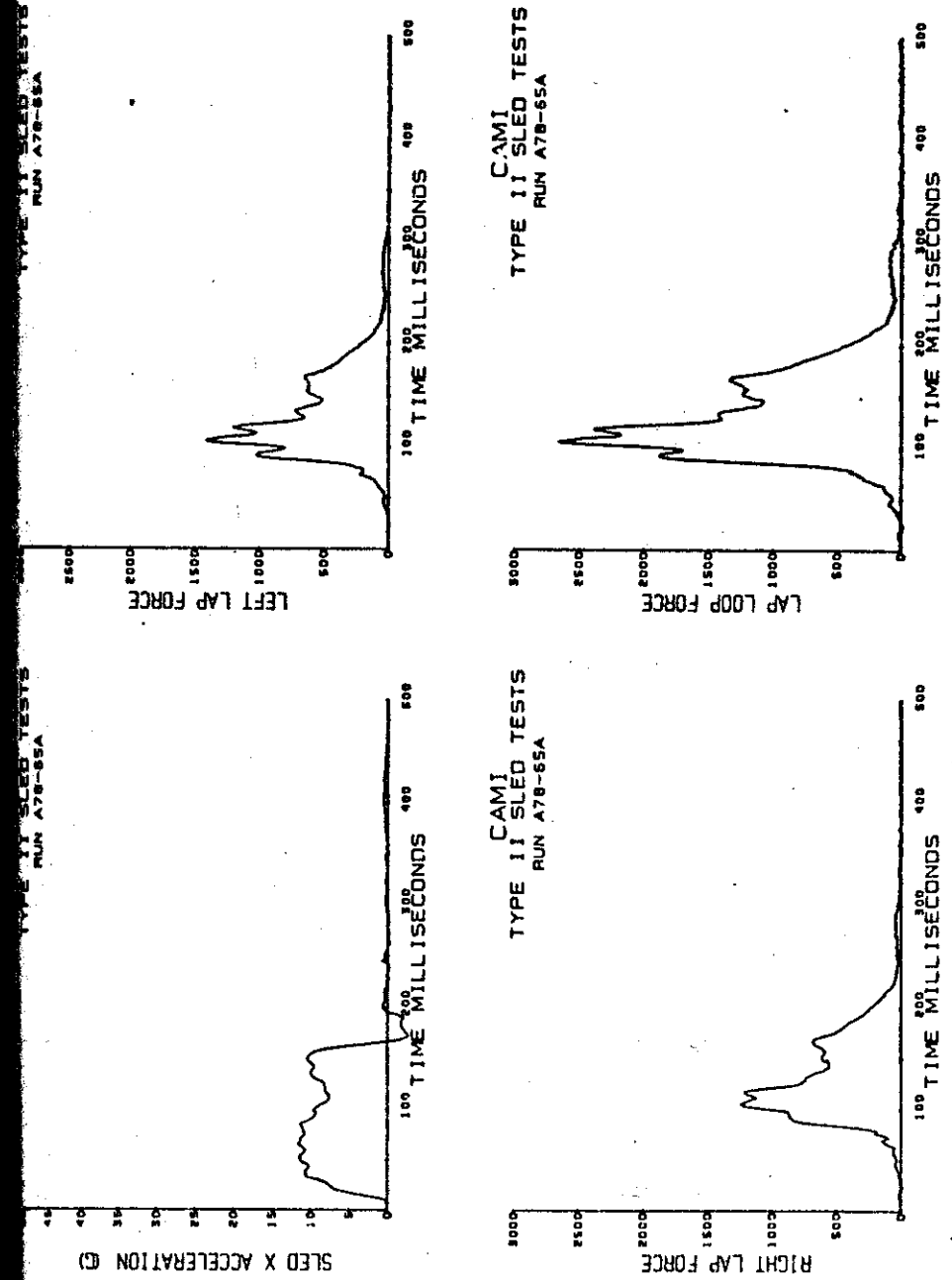


Figure B-7. 10-8 tests.  
Sled acceleration and lapbelt loads.

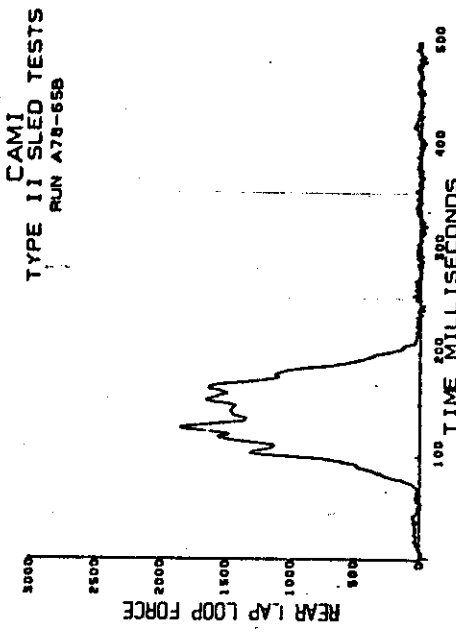
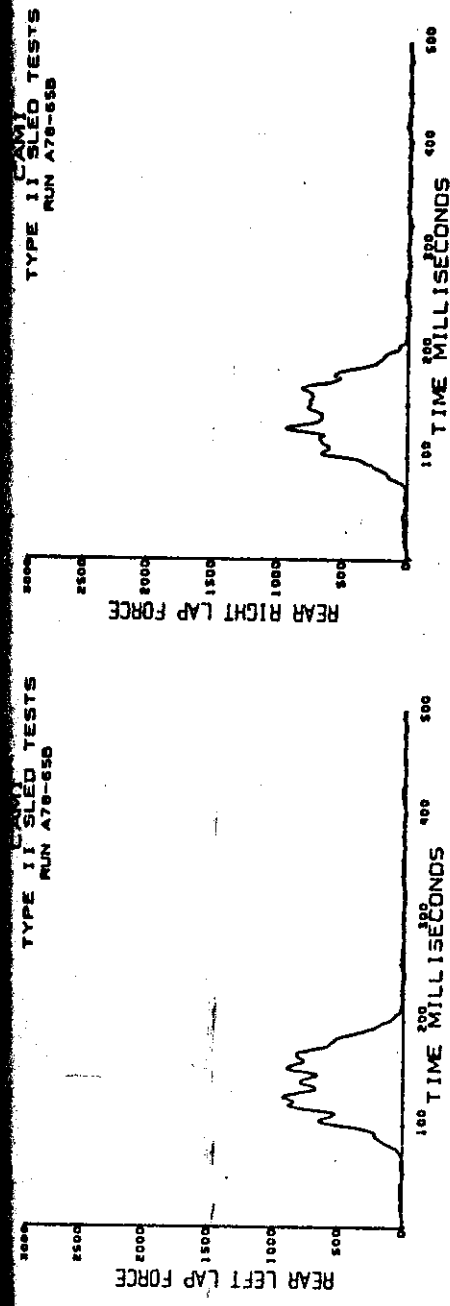


Figure B-7 (continued). Rear lapbelt loads.

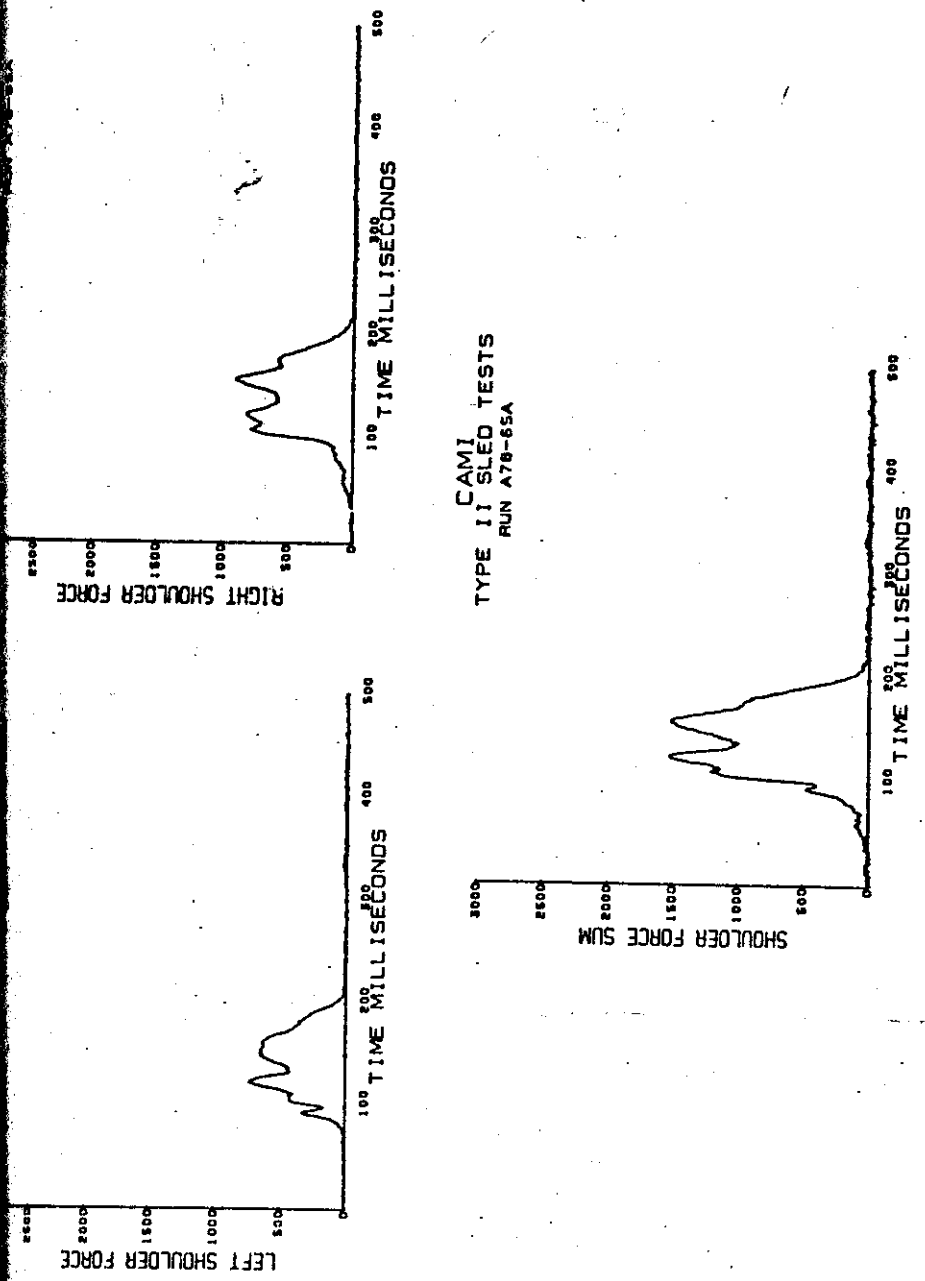


Figure B-7 (continued). Shoulder belt loads.

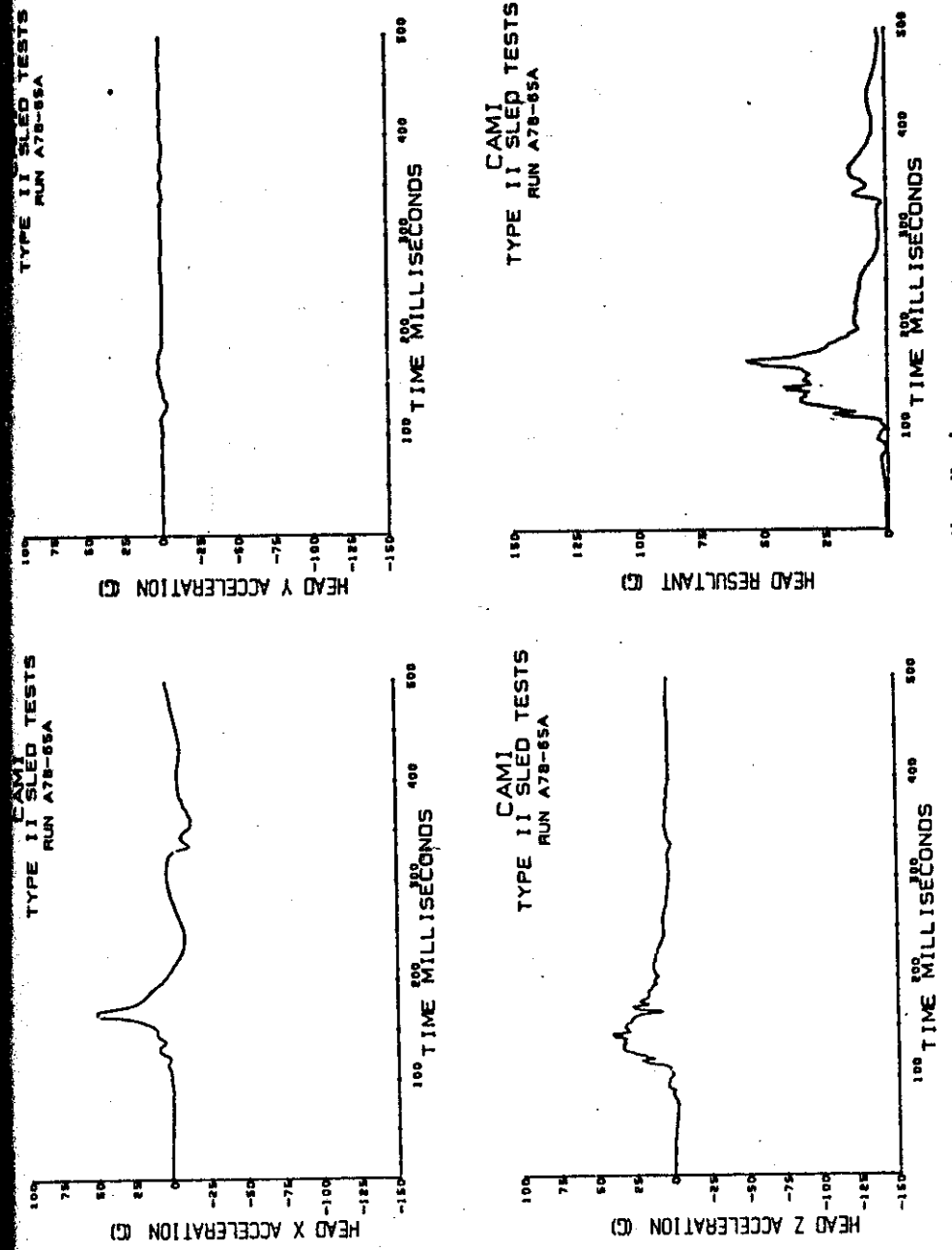


Figure B-7 (continued). Head acceleration.

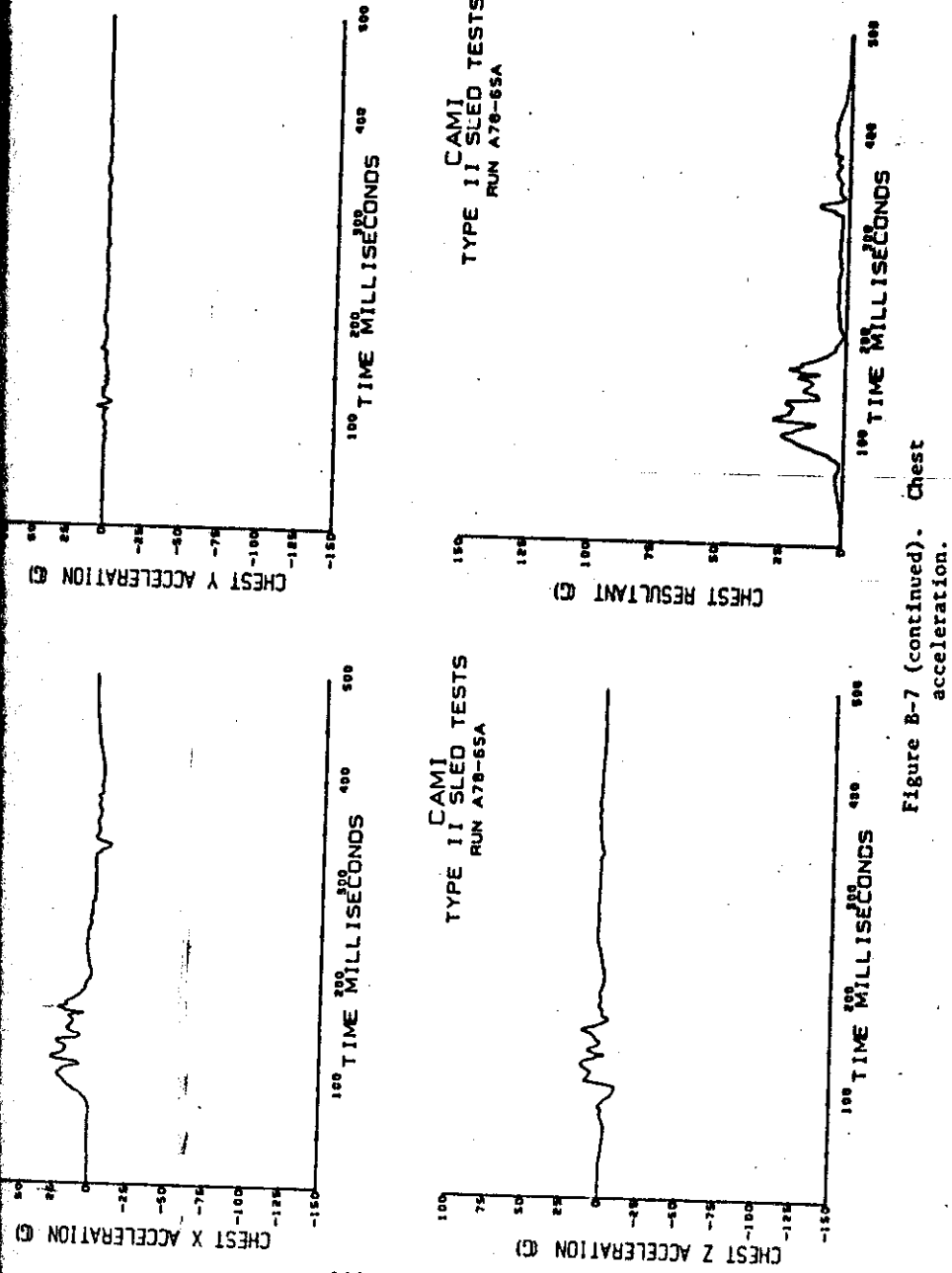


Figure B-7 (continued). Chest acceleration.

## TYPE I SLED TESTS

RUN A78-658

## PELVIS Y ACCELERATION (G)

## PELVIS X ACCELERATION (G)

## PELVIS Z ACCELERATION (G)

TIME 100 200 300 400 500 MILLISECONDS

TIME 100 200 300 400 500 MILLISECONDS

TIME 100 200 300 400 500 MILLISECONDS

CAMI  
SUMLA SLED TESTS  
RUN A78-658

## PELVIS RESULTANT (G)

## PELVIS RESULTANT (G)

TIME 100 200 300 400 500 MILLISECONDS

TIME 100 200 300 400 500 MILLISECONDS

TIME 100 200 300 400 500 MILLISECONDS

Figure B-7 (continued). Pelvis acceleration.

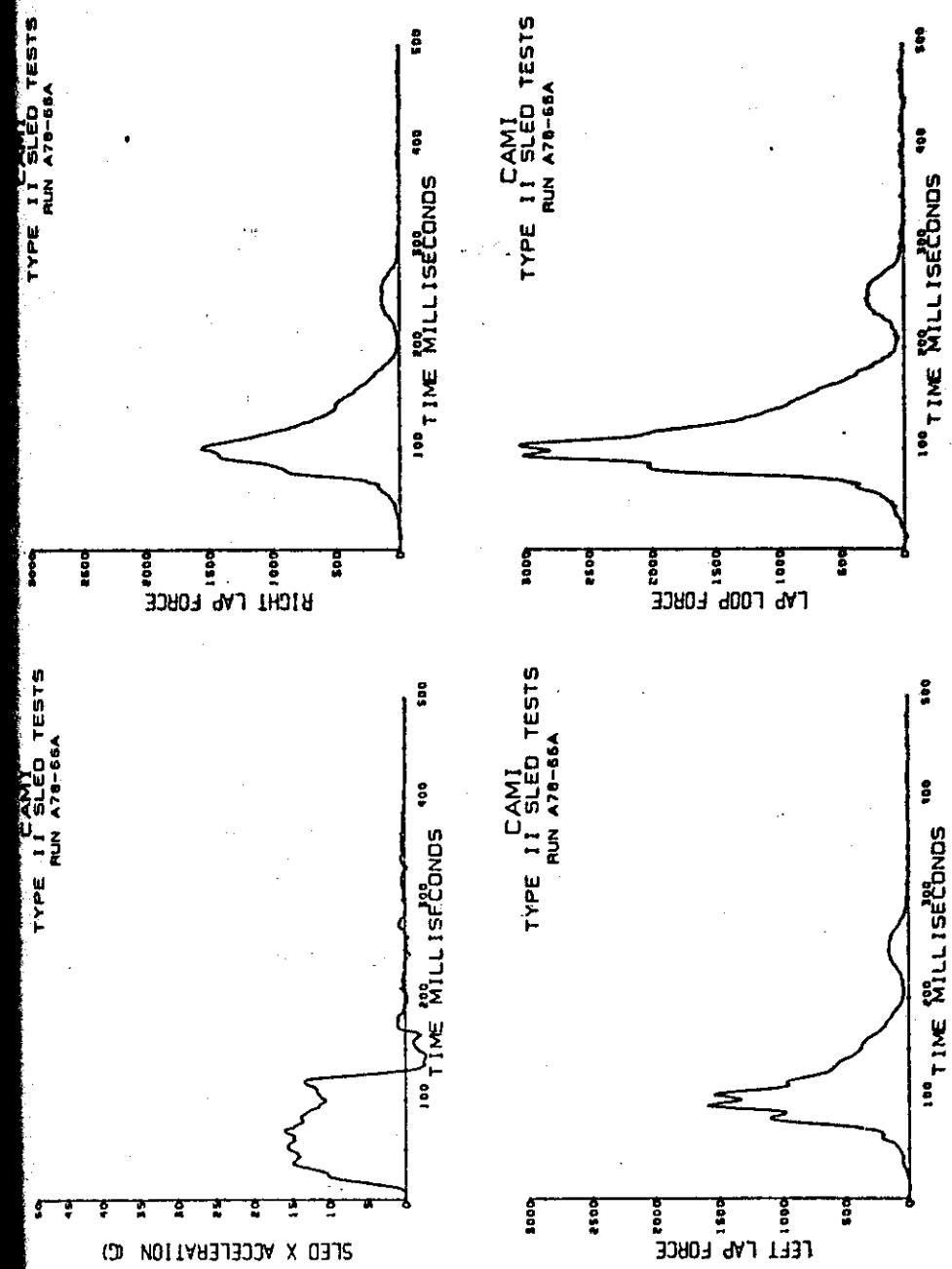


Figure B-8. 14-8 tests.  
Sled acceleration and lapbelt tests.

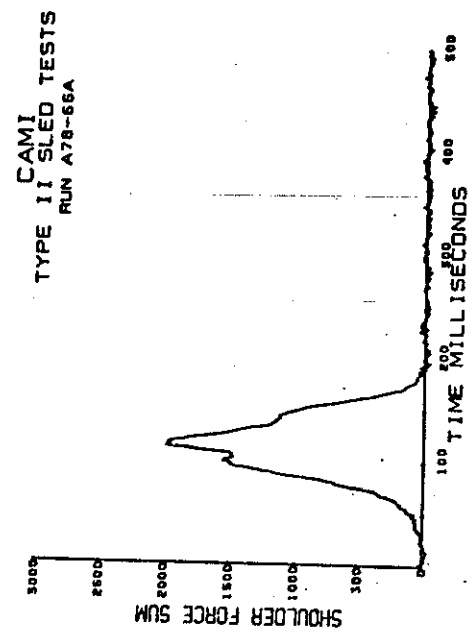
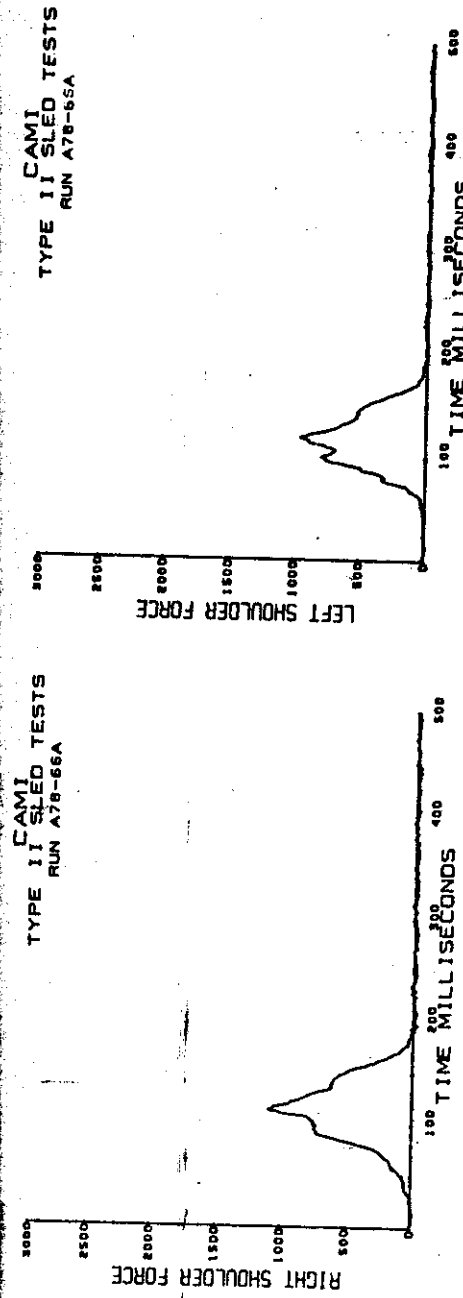
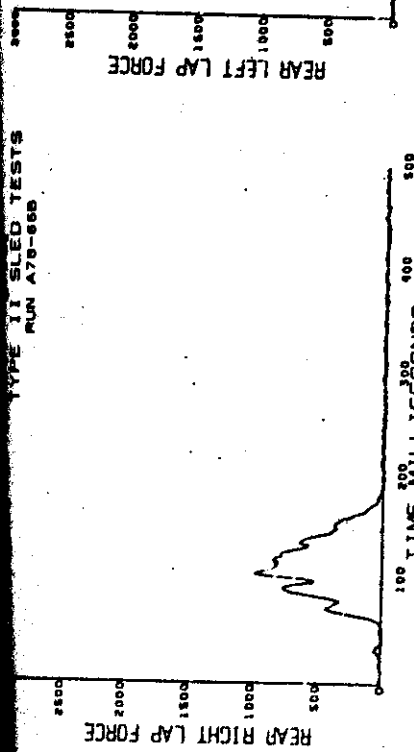


Figure B-8 (continued). Shoulder belt loads.

CAMI  
TYPE II SLED TESTS  
RUN A78-663



CAMI  
TYPE II SLED TESTS  
RUN A78-663

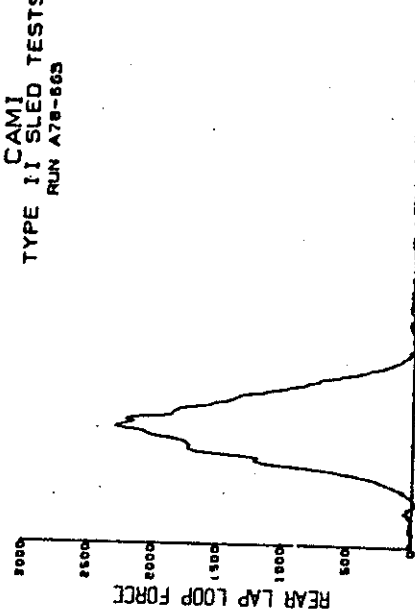


Figure B-8 (continued). Rear lapbelt loads.

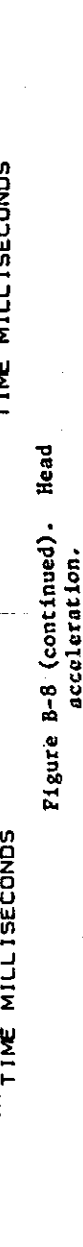
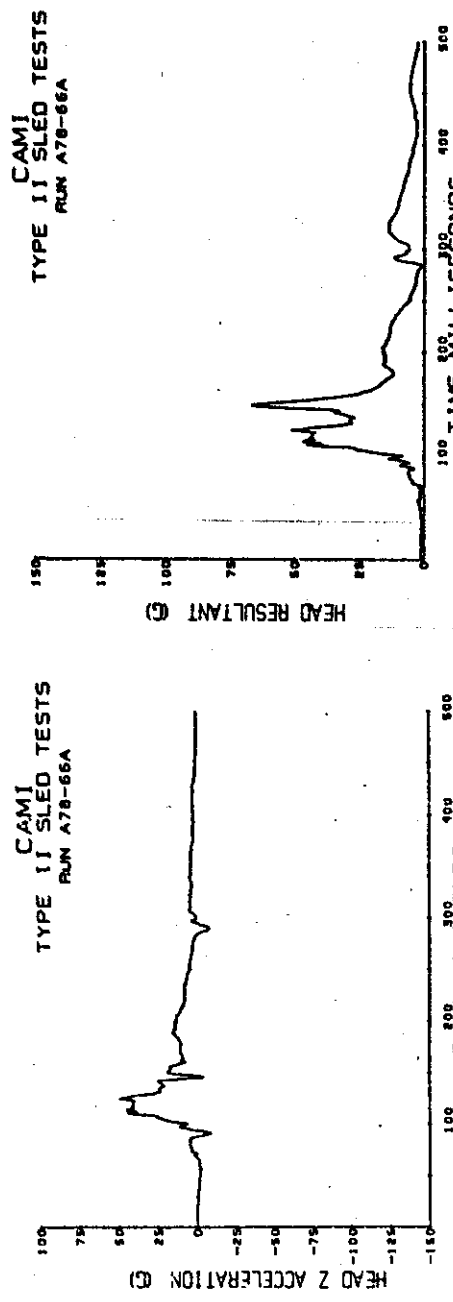
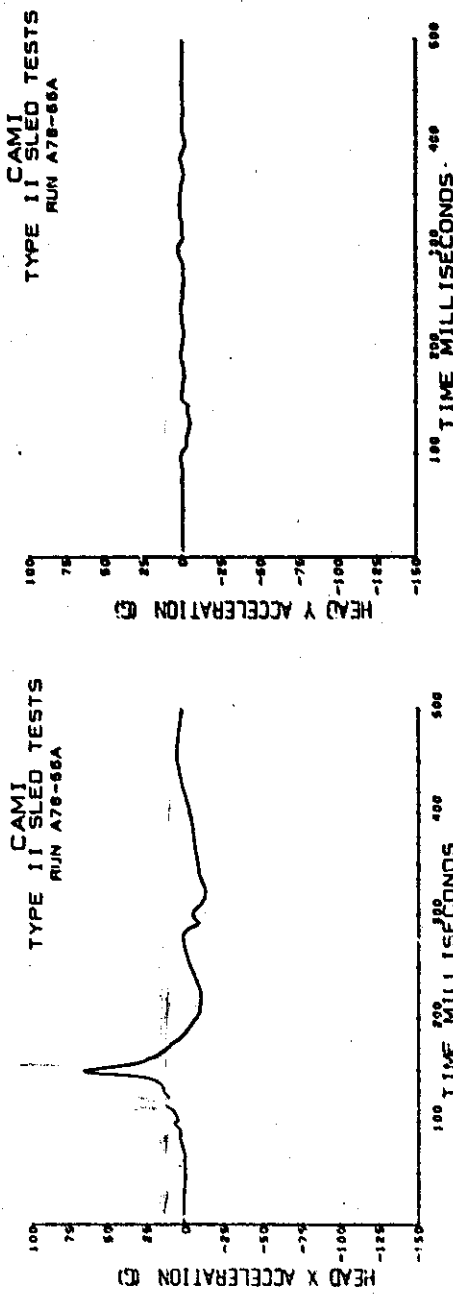


Figure B-8 (continued). Head acceleration.

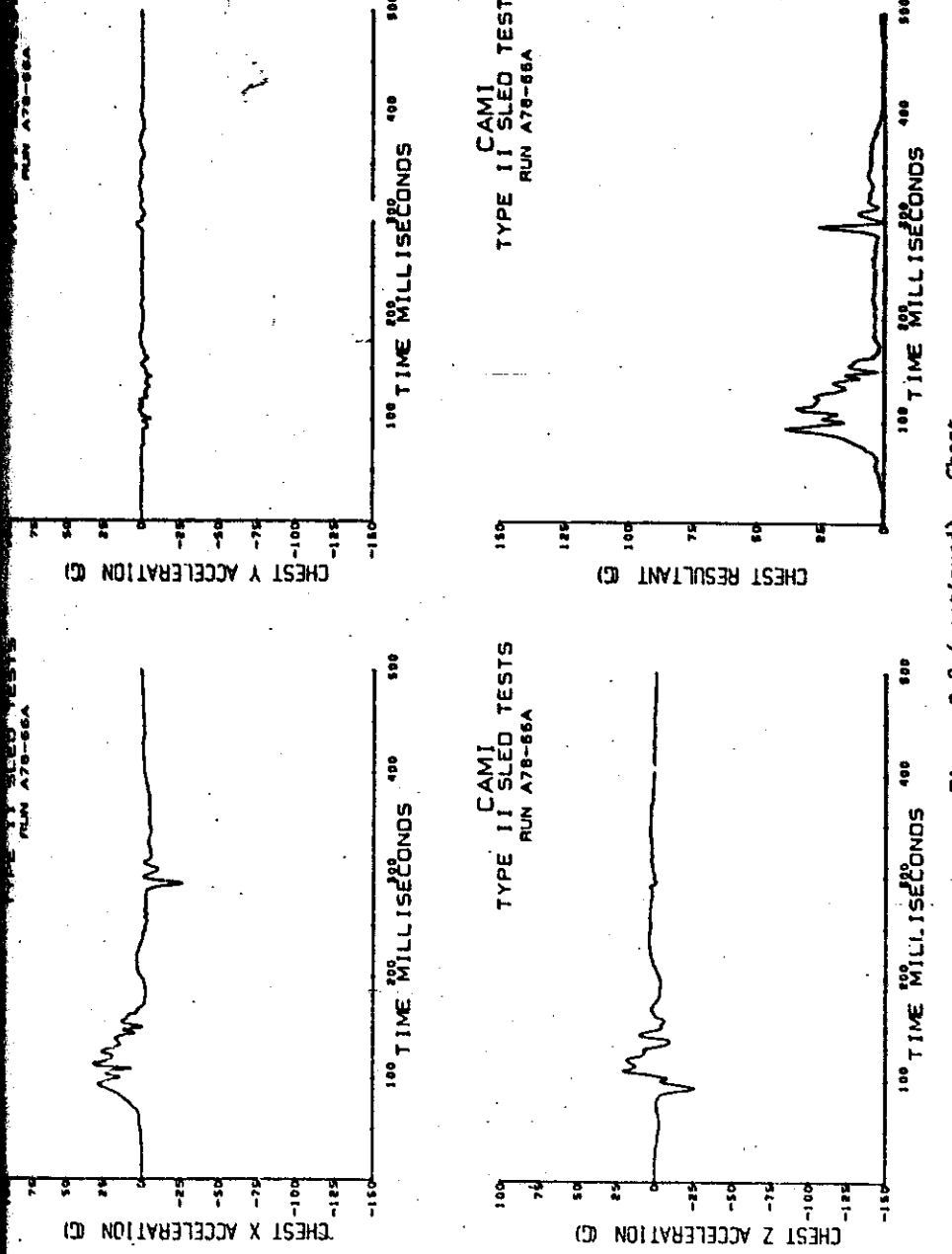
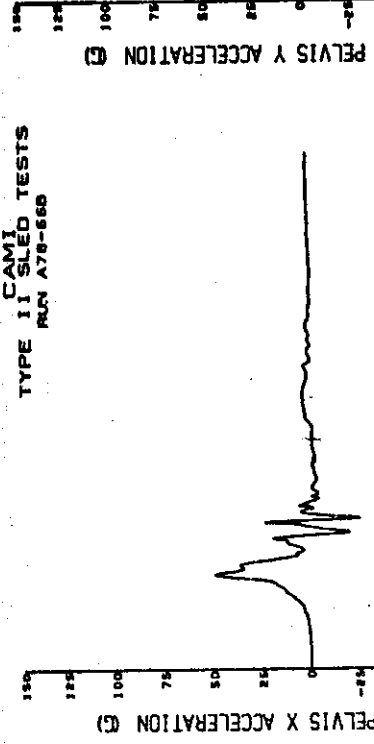
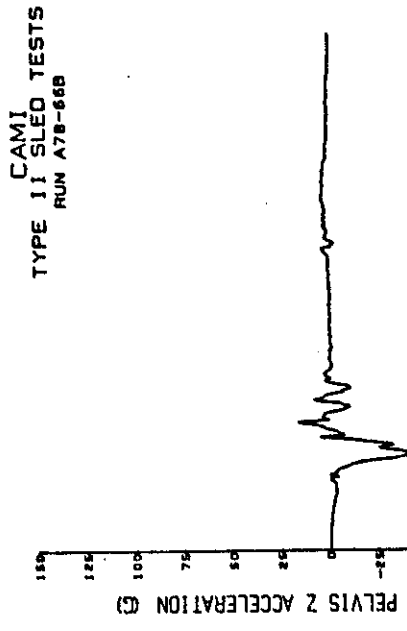


Figure B-8 (continued). Chest acceleration.

CAMI  
TYPE II SLED TESTS  
RUN A78-668



CAMI  
TYPE II SLED TESTS  
RUN A78-668



CAMI  
SUMLA SLED TESTS  
RUN A78-668

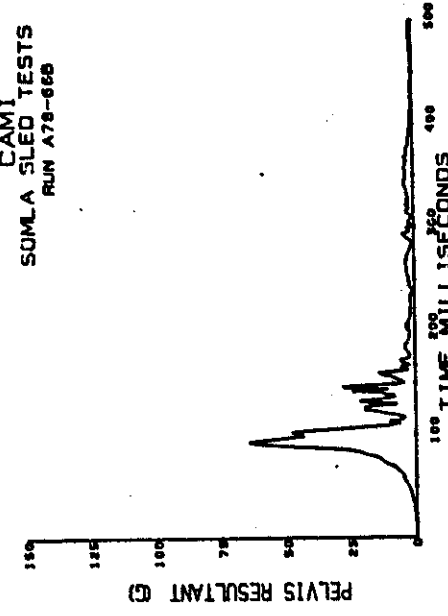


Figure B-8 (continued). Pelvis acceleration.

**APPENDIX C**

**RESULTS OF LOW-ELONGATION WEBBING EVALUATIONS**

| <u>Figure No.</u> |                    | <u>Page</u> |
|-------------------|--------------------|-------------|
| C-1               | Standard webbing.  |             |
|                   | 9-g tests.         | 151         |
|                   | 12-g tests.        | 156         |
|                   | 16-g tests.        | 161         |
|                   | 18-g tests.        | 166         |
|                   | 21-g tests.        | 171         |
| C-2               | Kevlar webbing.    |             |
|                   | 9-g tests.         | 176         |
|                   | 12-g tests.        | 181         |
|                   | 16-g tests.        | 186         |
|                   | 18-g tests.        | 191         |
|                   | 22-g tests.        | 196         |
| C-3               | Polyester webbing. |             |
|                   | 9-g tests.         | 201         |
|                   | 12-g tests.        | 206         |
|                   | 16-g tests.        | 211         |
|                   | 18-g tests.        | 216         |
|                   | 21-g tests.        | 221         |

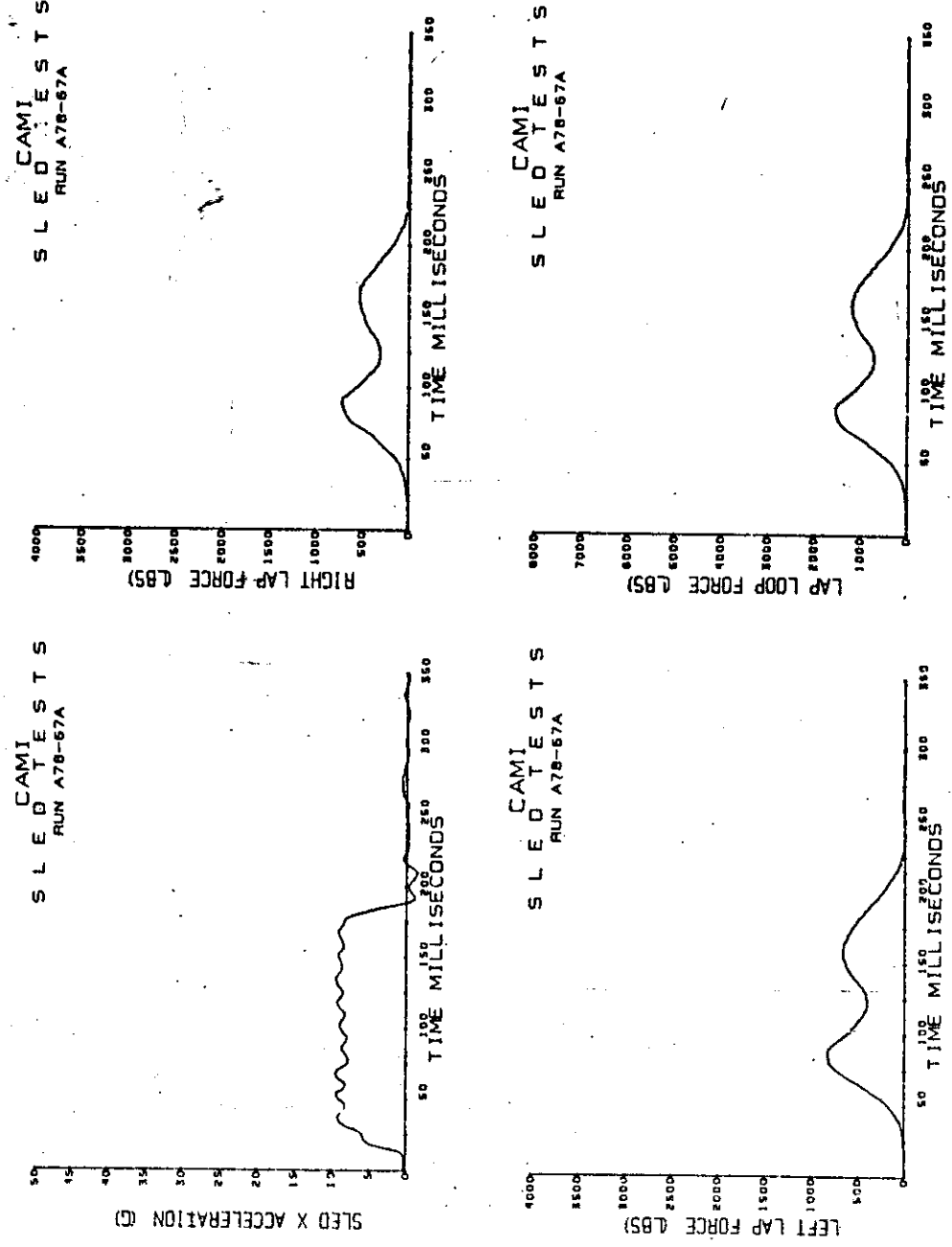


Figure C-1. Standard webbing, 9-g tests.  
Sled deceleration and lapbelt loads.

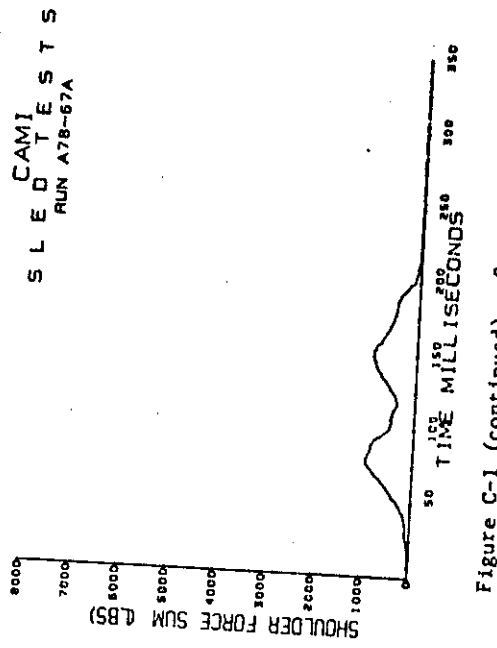
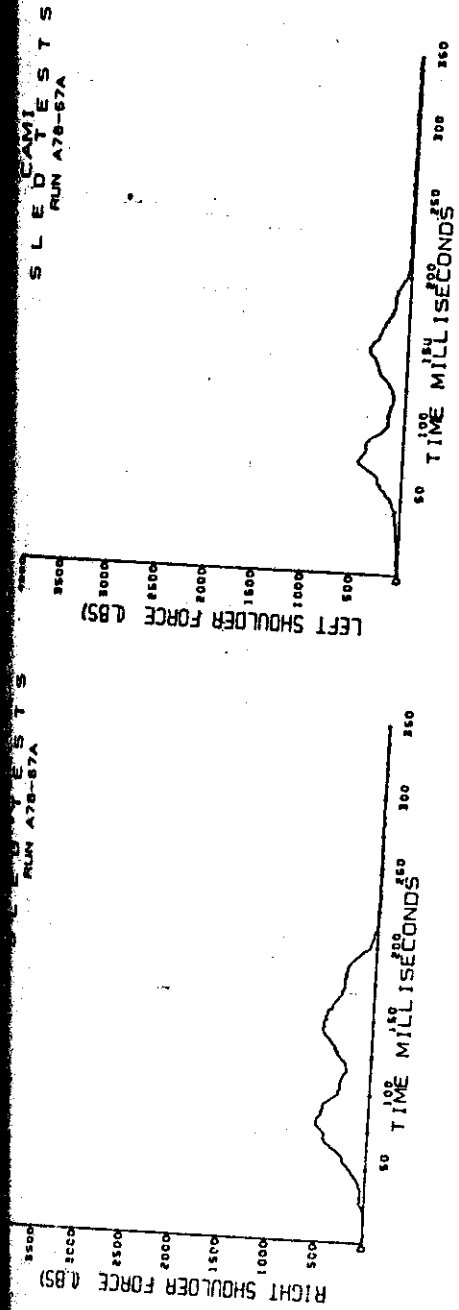


Figure C-1 (continued). 9-g tests.  
Shoulder belt loads.

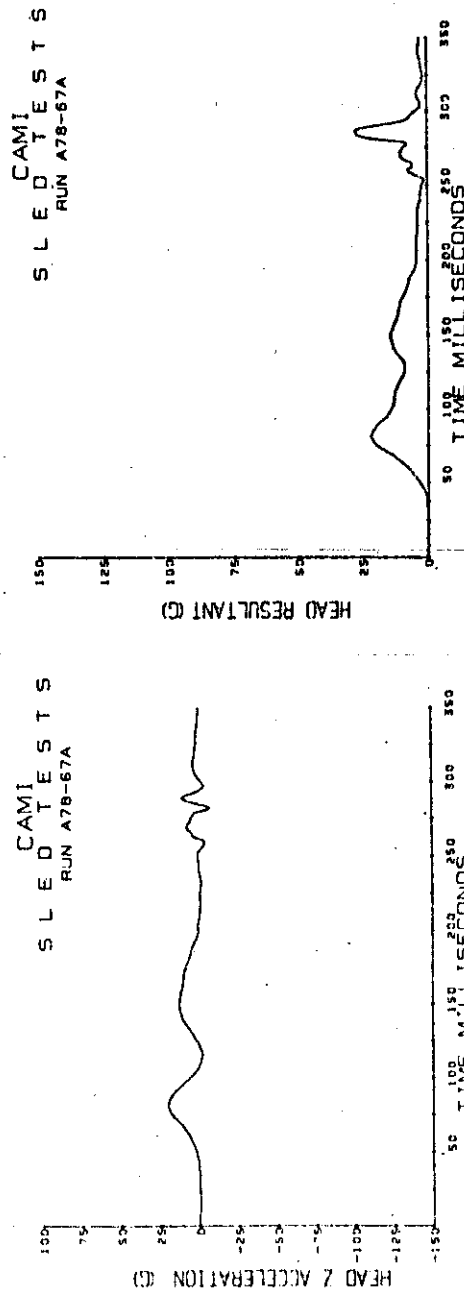
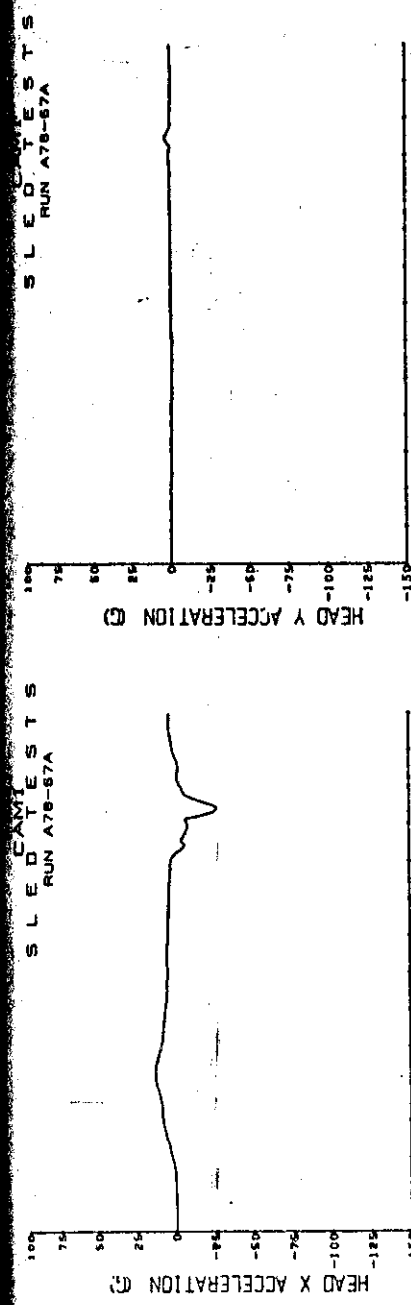


Figure C-1 (continued). 9-8 tests.  
Head acceleration.

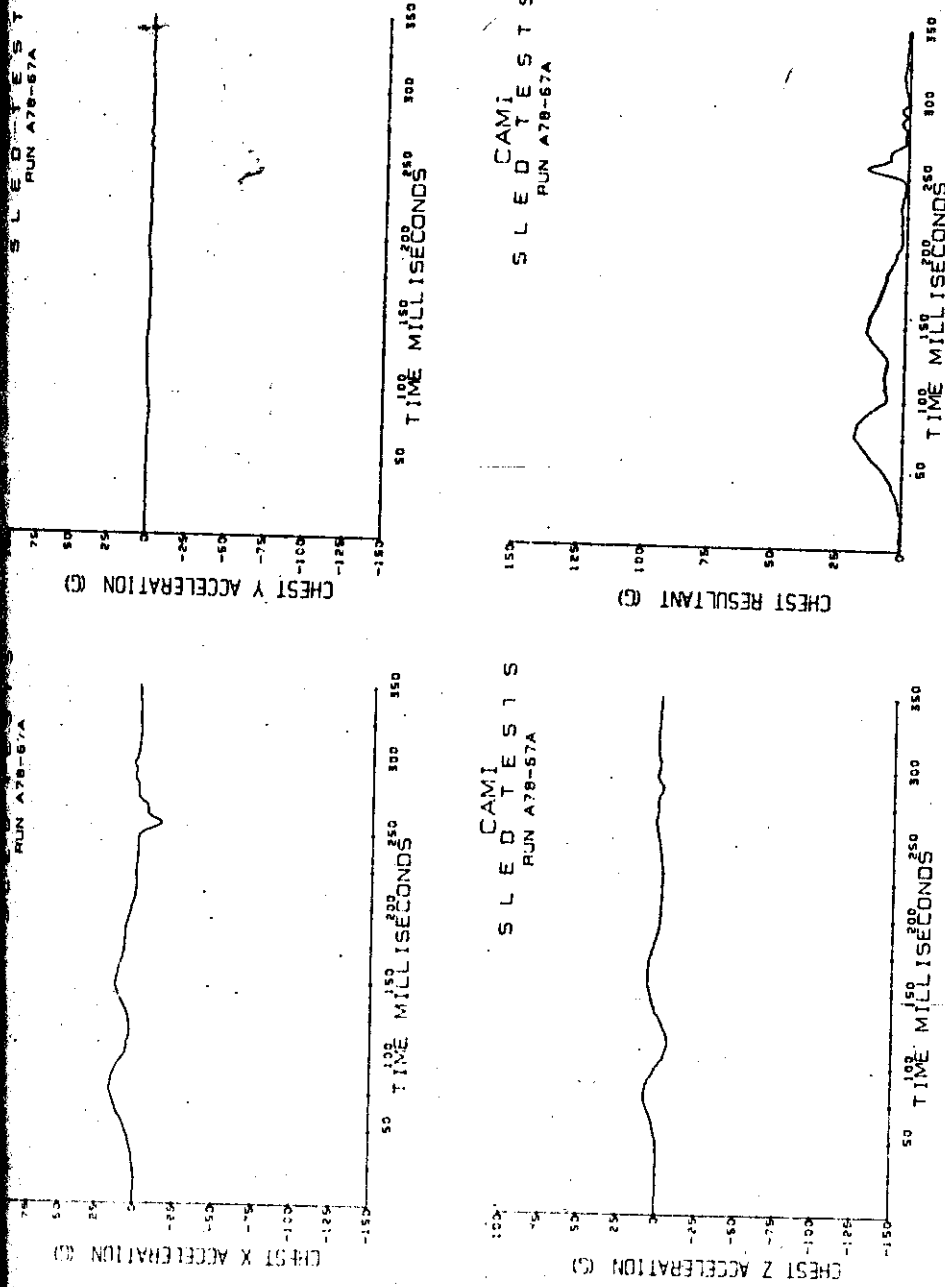
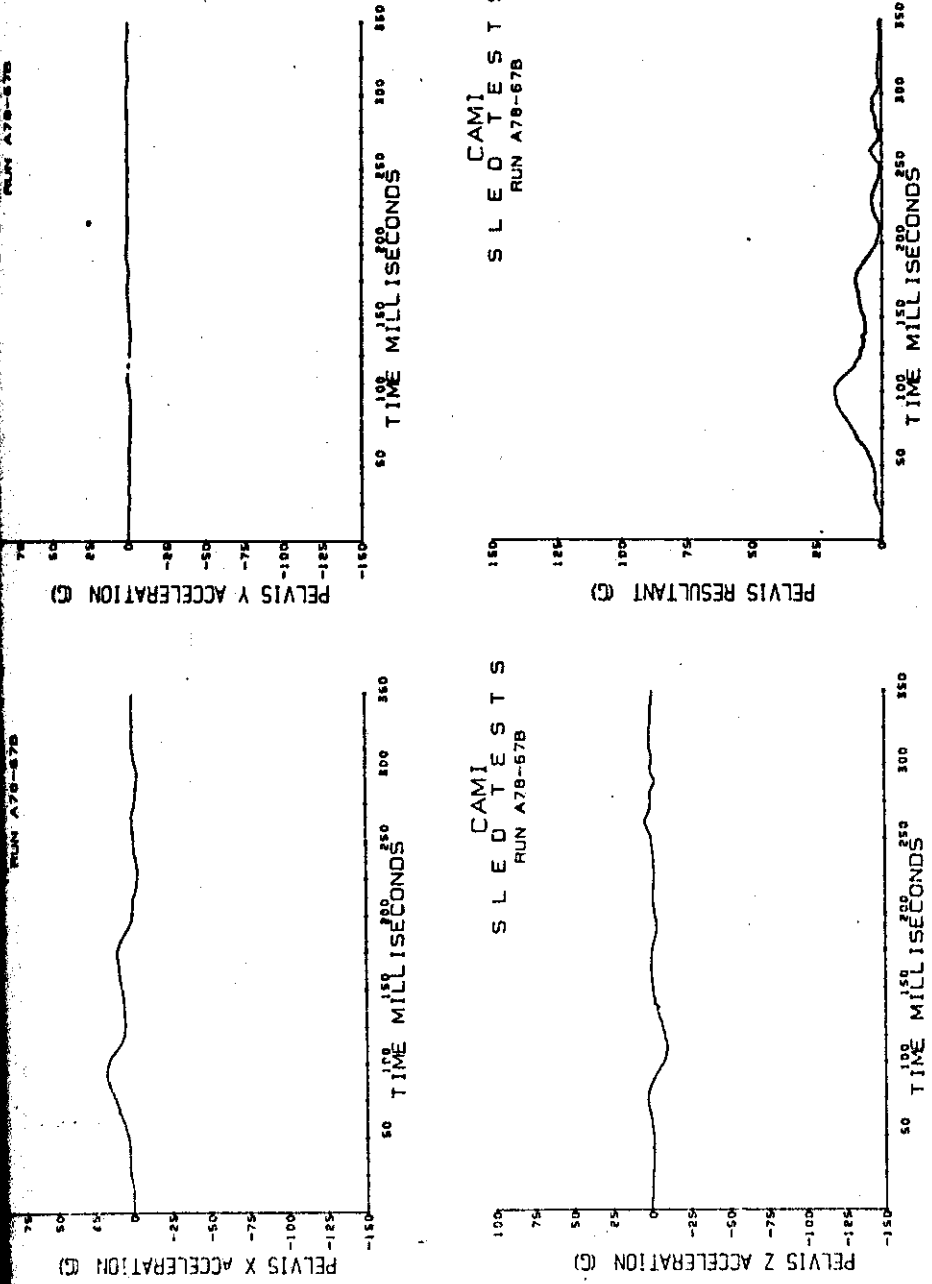


Figure C-1 (continued). 9-g tests.  
Chest acceleration.



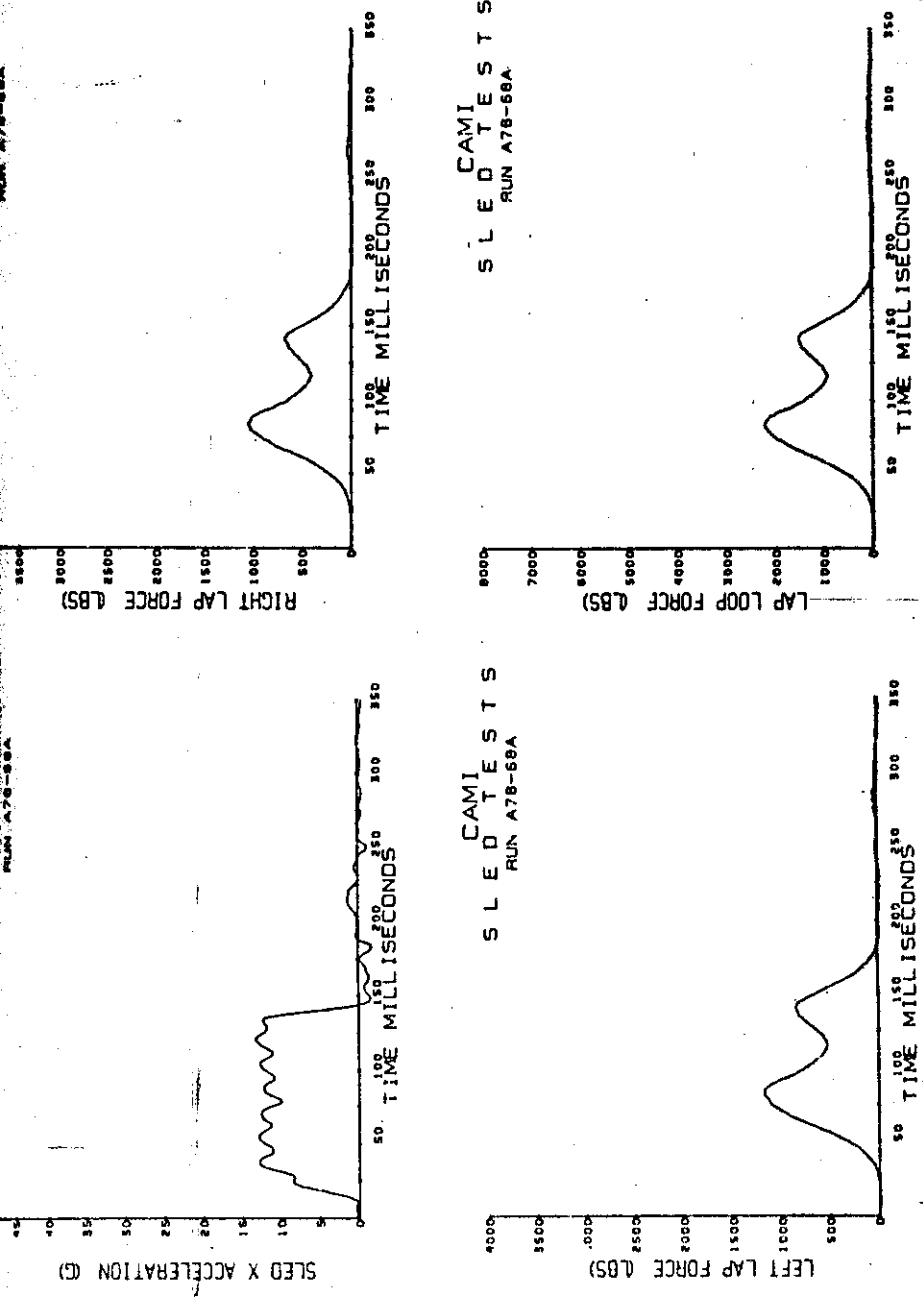


Figure C-1 (continued). 12-8 tests.  
Sled deceleration and lapbelt loads.

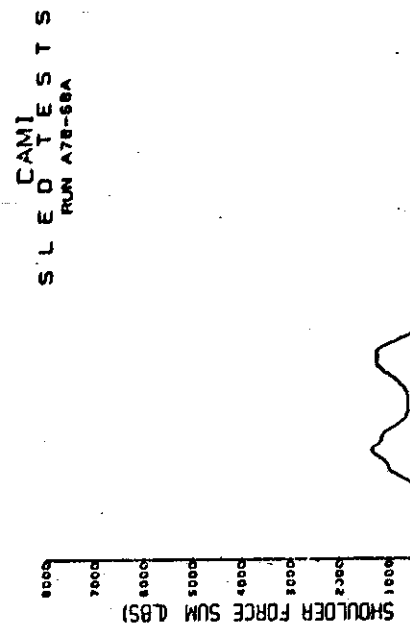
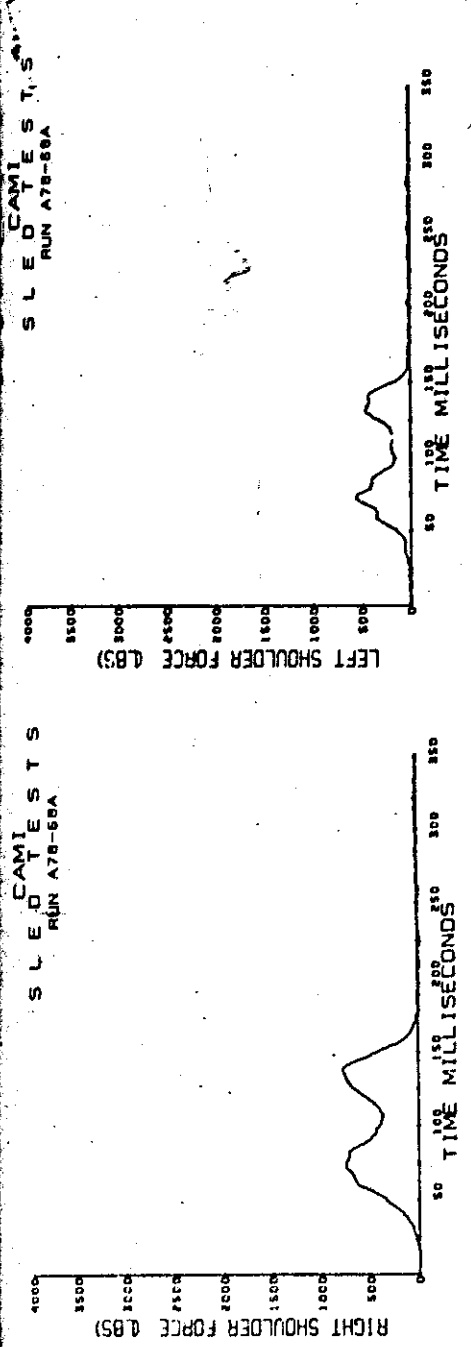
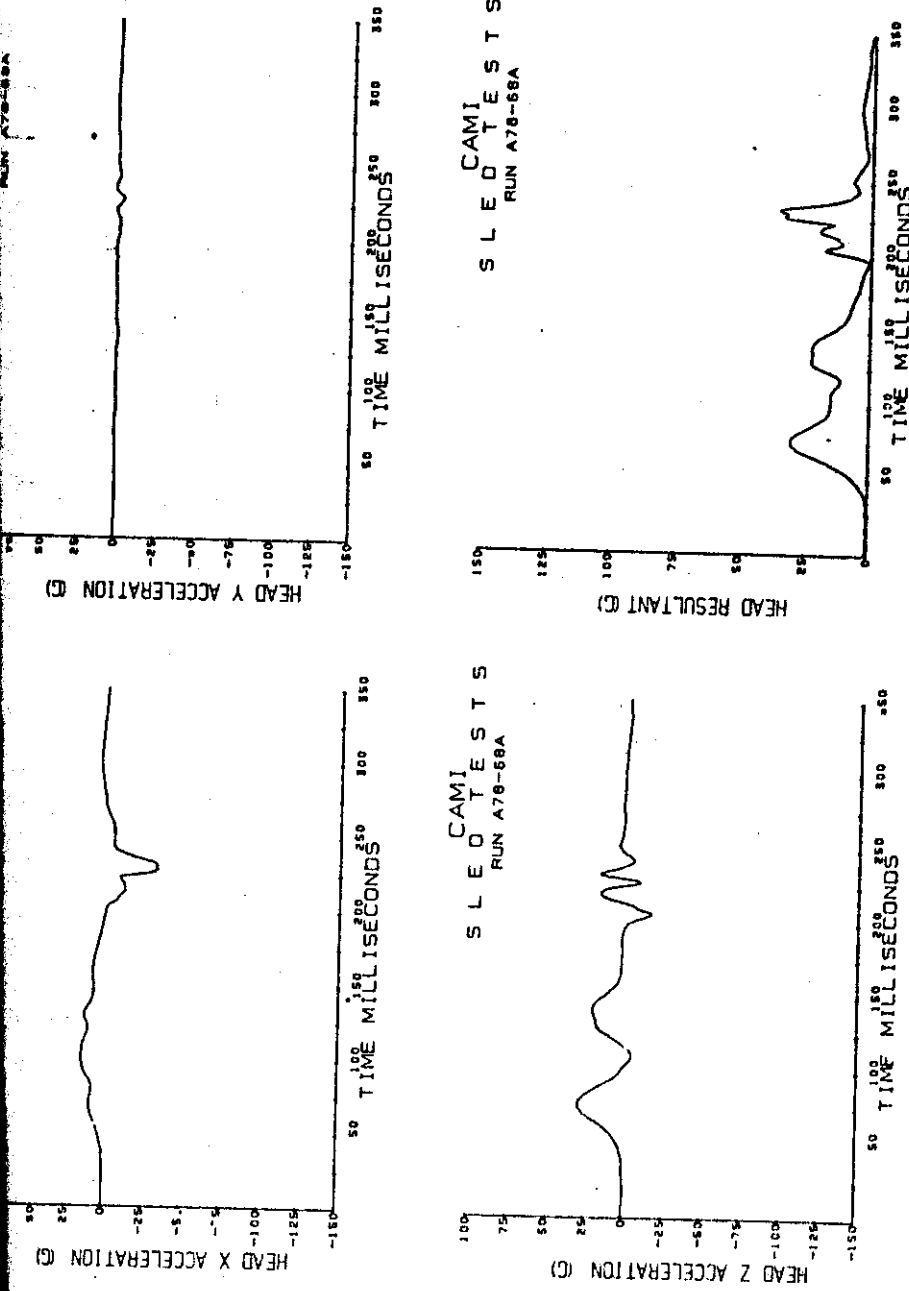


Figure C-1 (continued), 12-8 tests.  
Shoulder belt loads.



158

Figure C-1 (continued). 12-8 tests.  
Head acceleration.

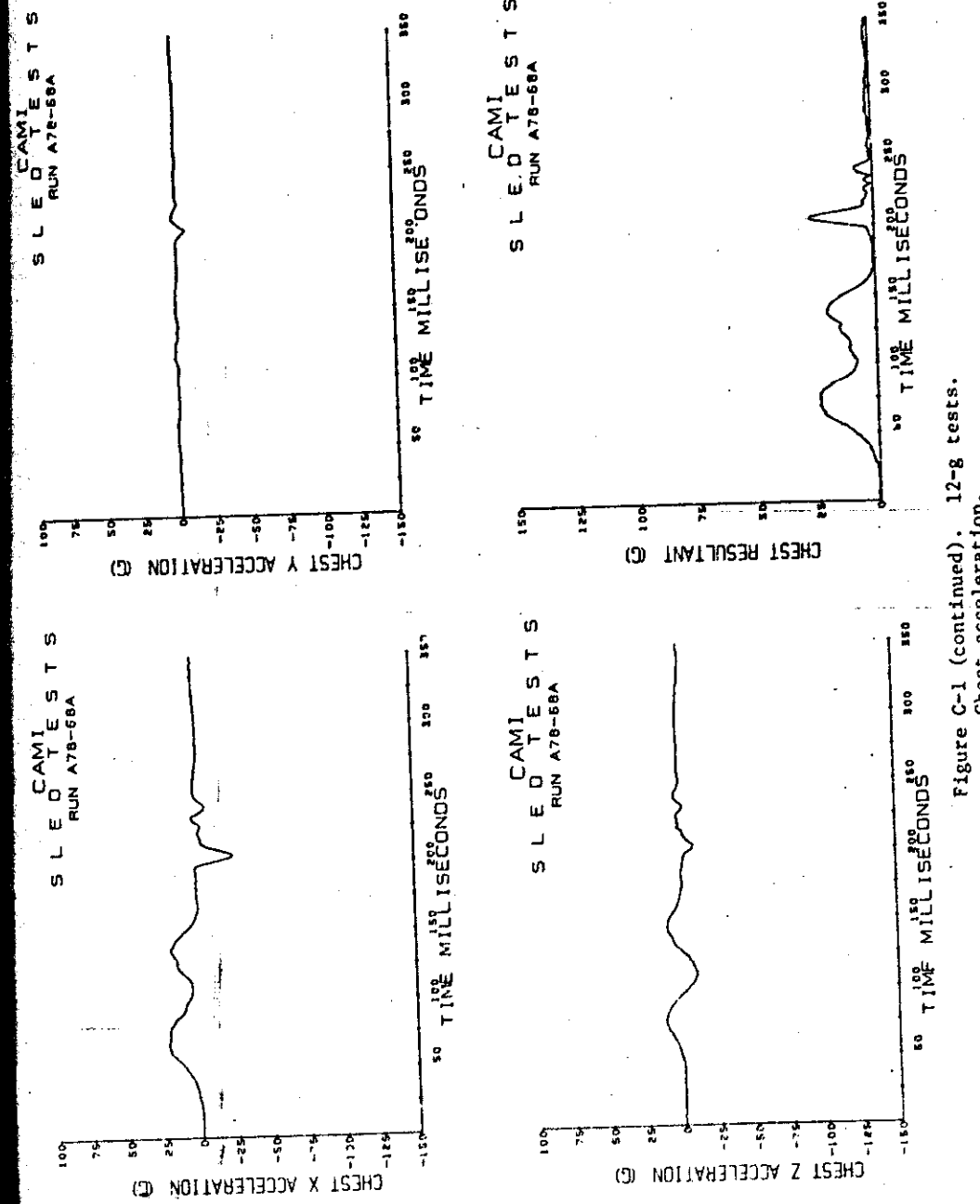


Figure C-1 (continued).  
Chest acceleration.

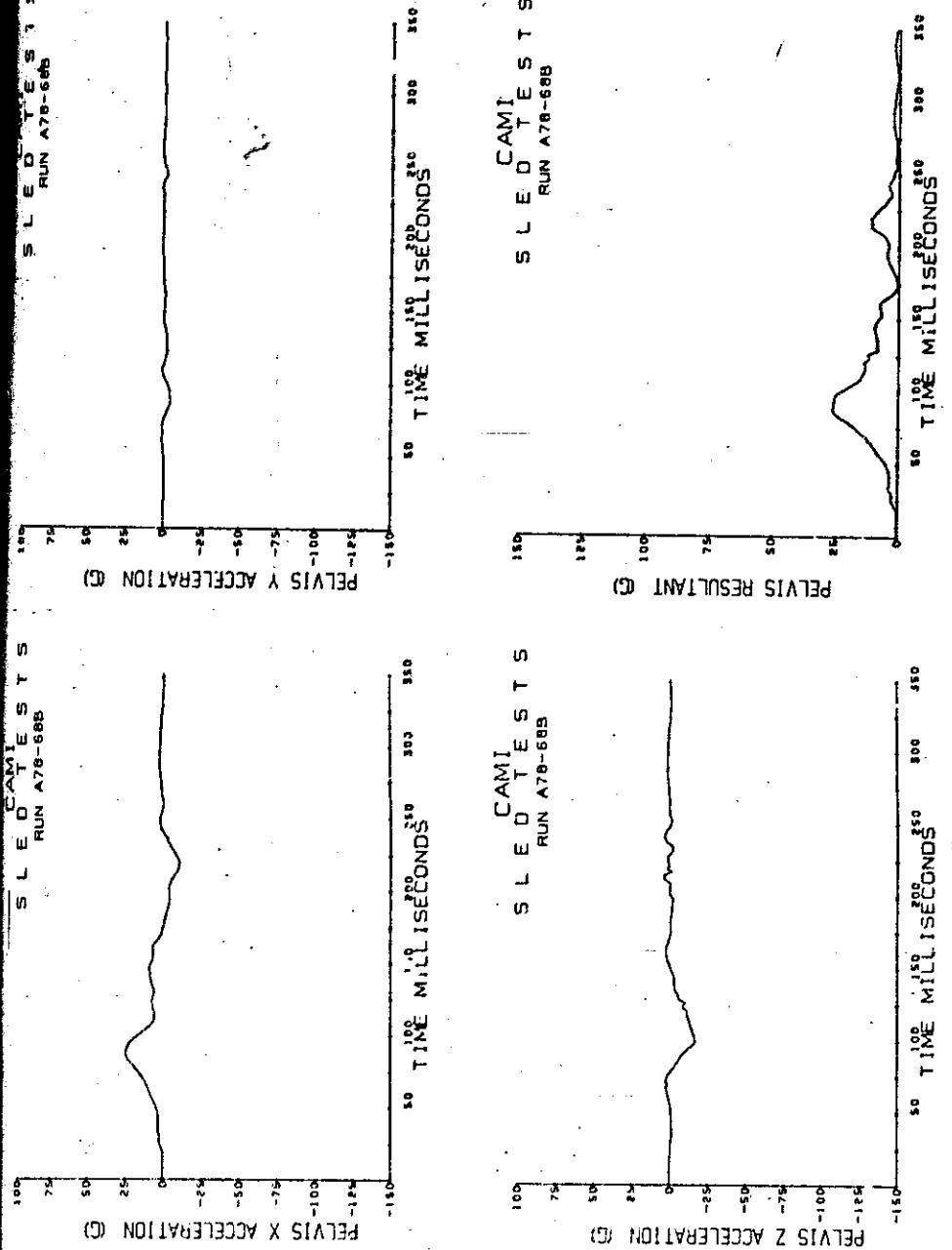


Figure C-1 (Continued). 12-8 tests.  
Pelvis acceleration.

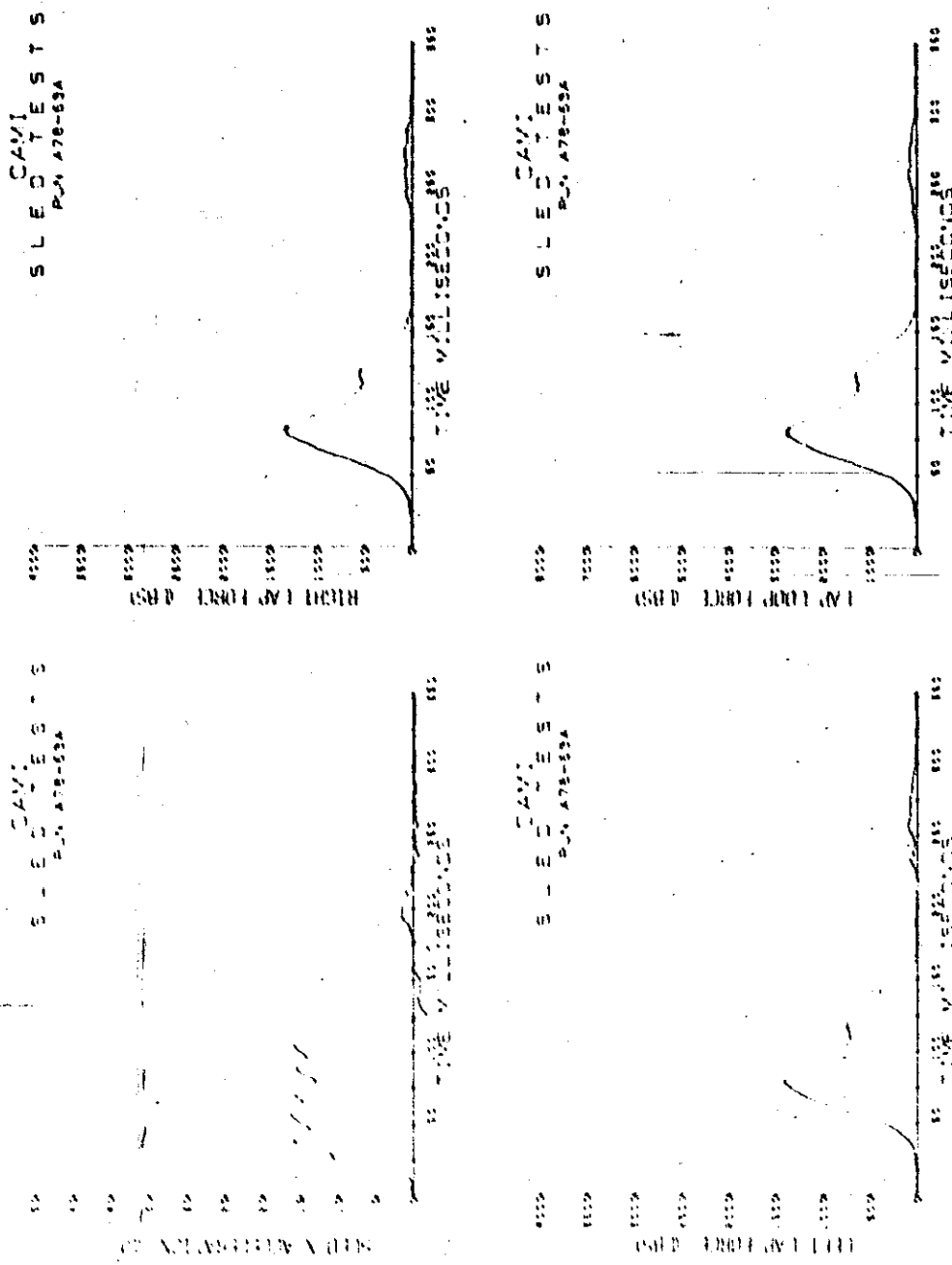
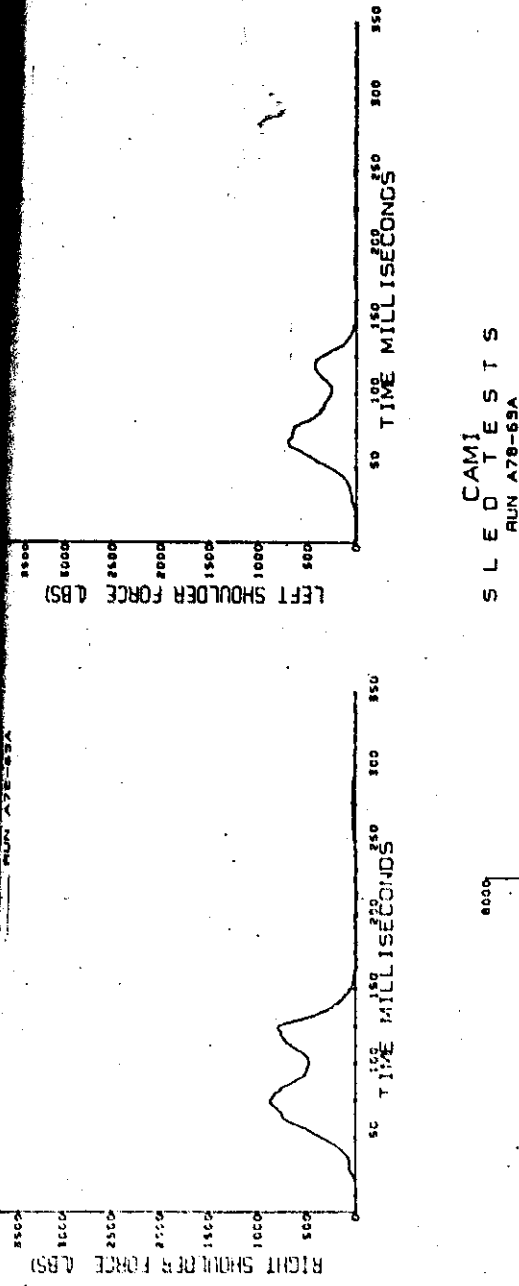


Figure C-1 (continued). 16-2 tests.  
Sled deceleration and lap belt loads.



CAMI  
SILED TESTS  
RUN A78-69A

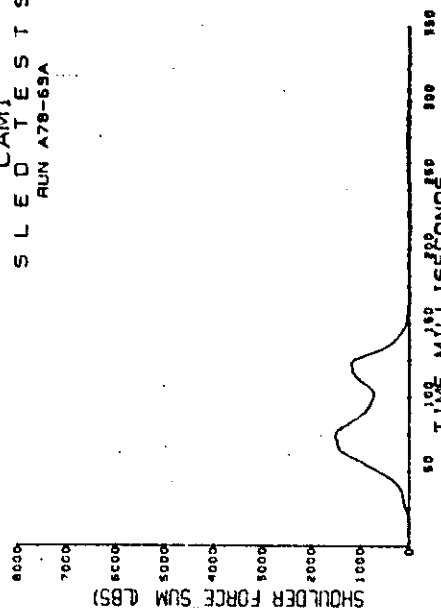


Figure C-1 (continued). 16-g tests.  
Shoulder belt loads.

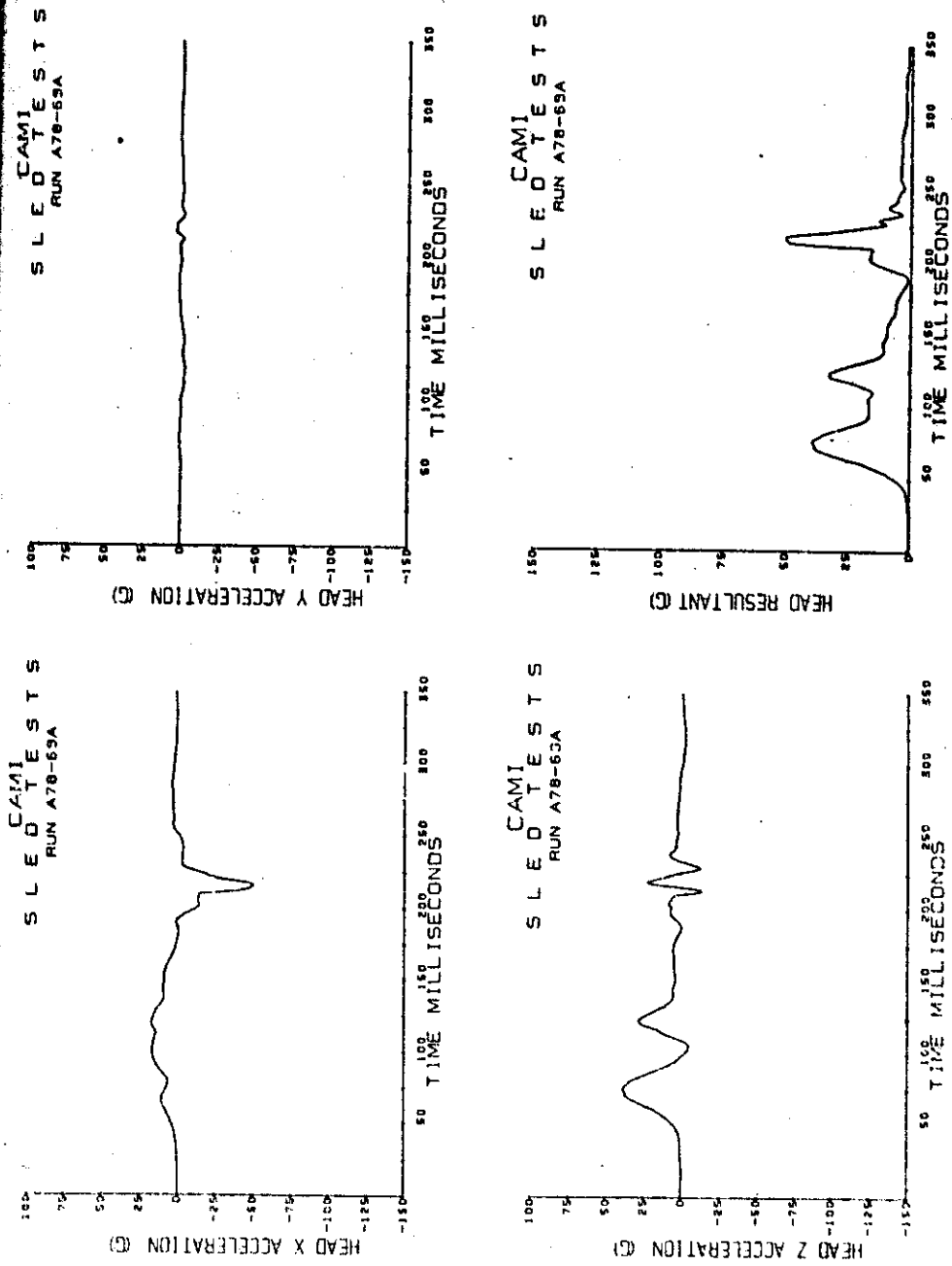


Figure C-1 (continued). 16-g tests.  
Head acceleration.

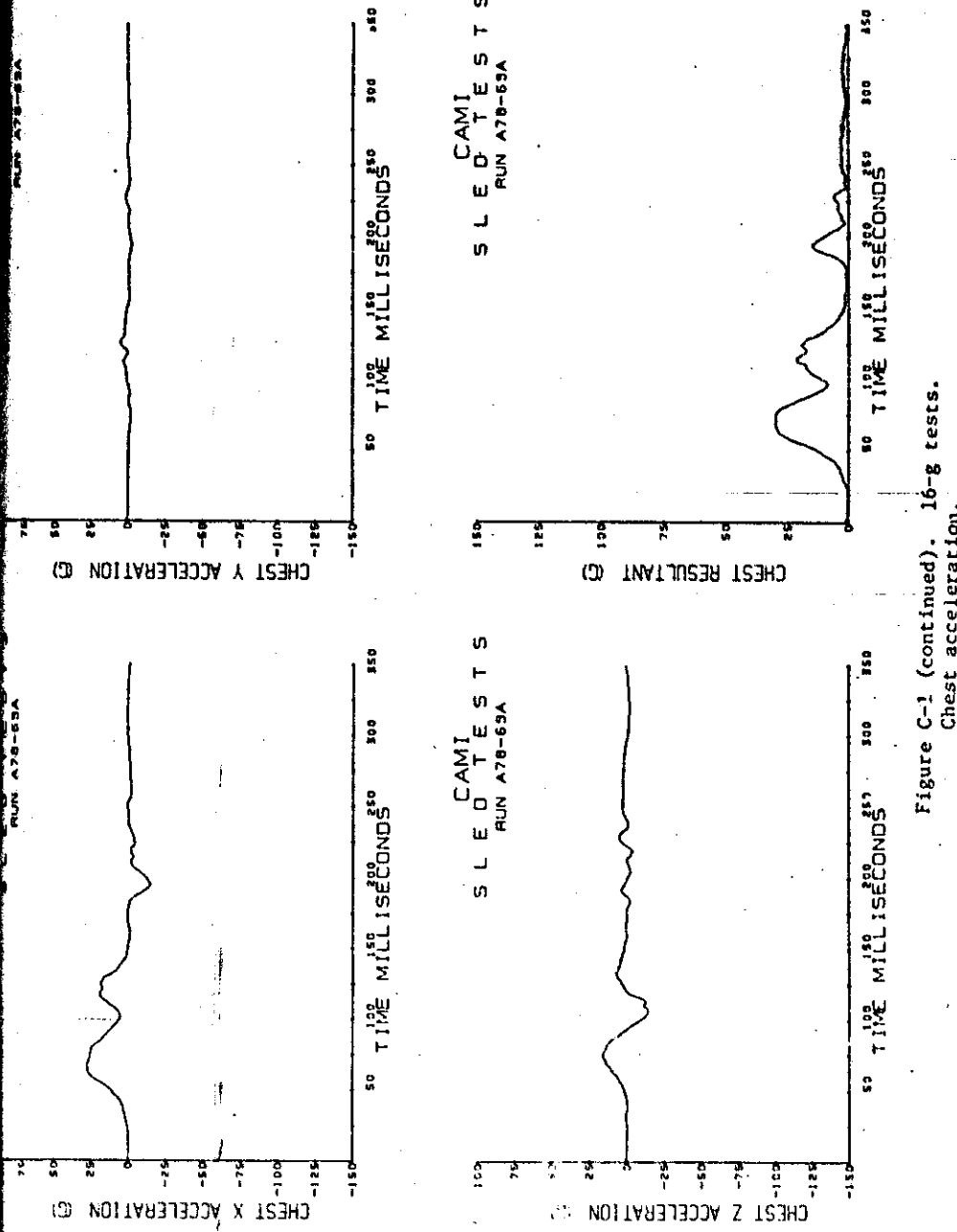


Figure C-1 (continued). 16-g tests.  
Chest acceleration.

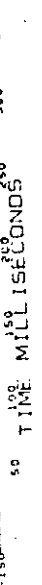
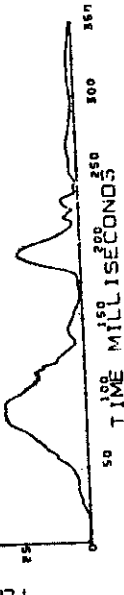
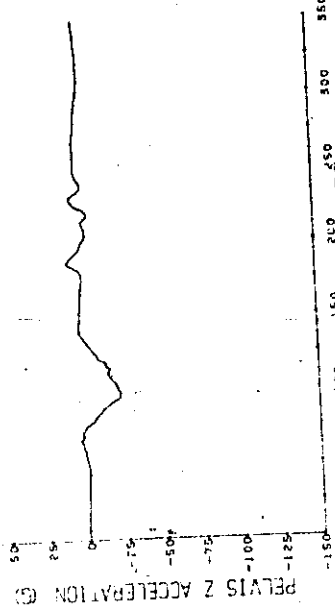
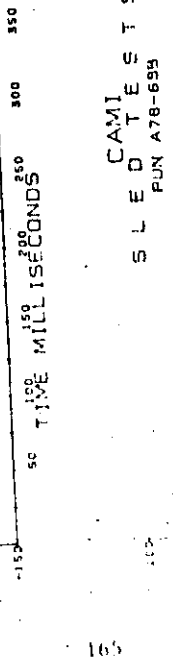
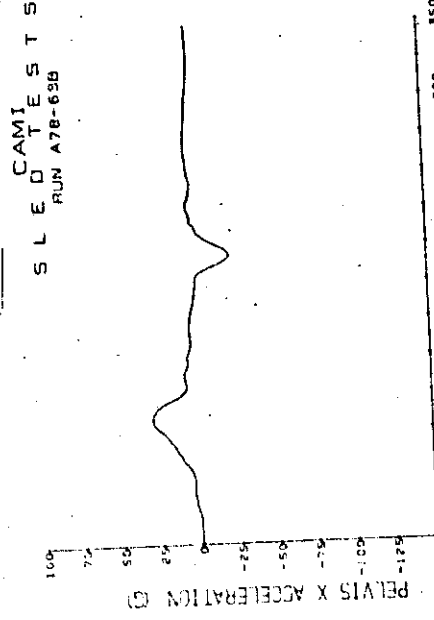


Figure C-1 (continued). 16-g tests.  
Pelvis acceleration.

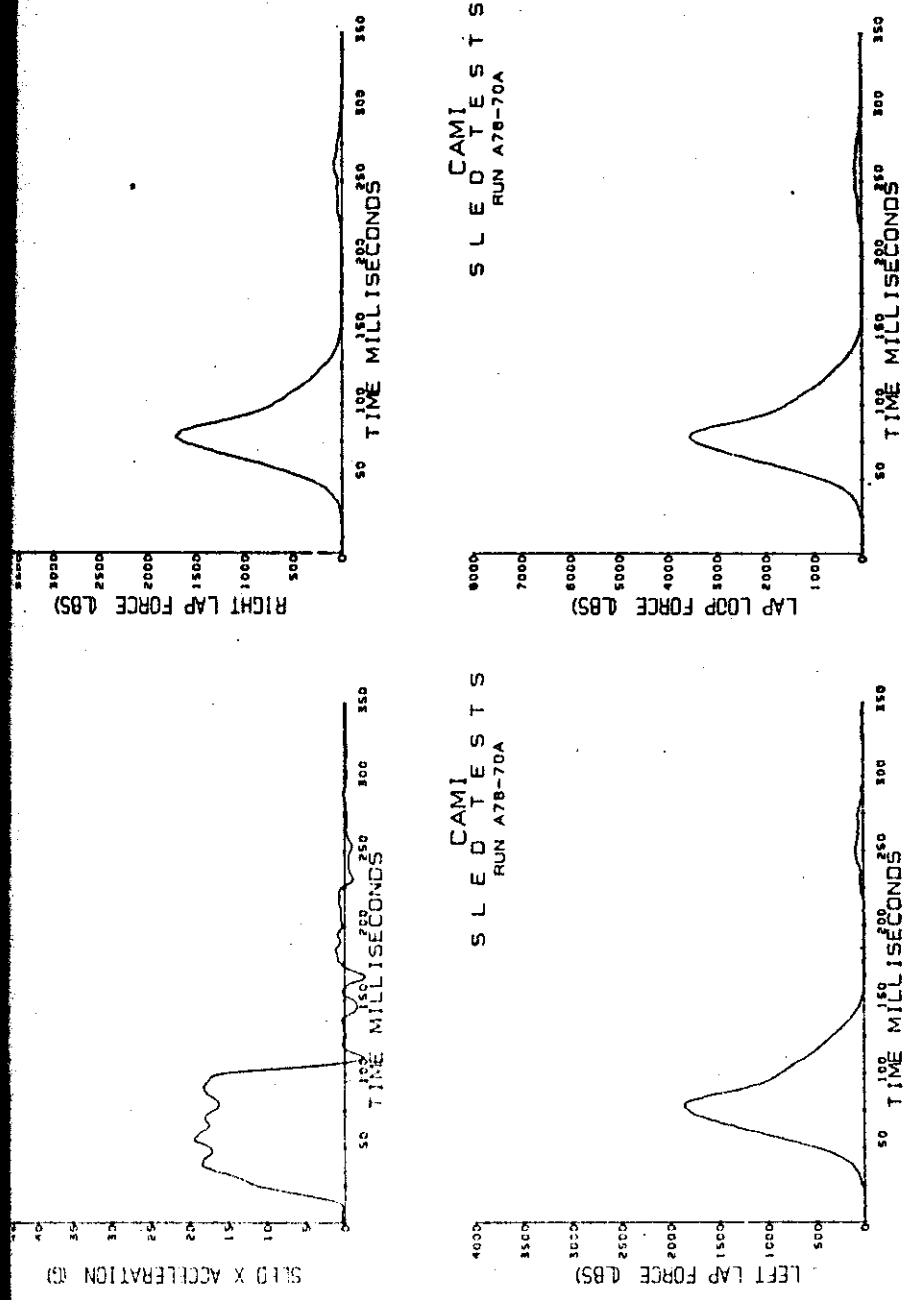


Figure C-1 (continued). 18-g tests.  
Sled deceleration and lap belt loads.

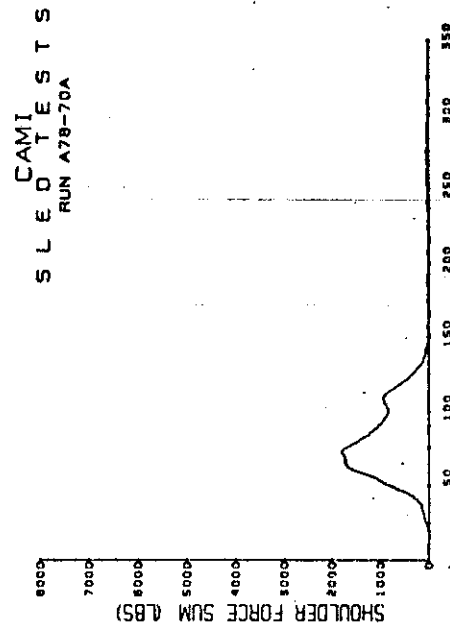
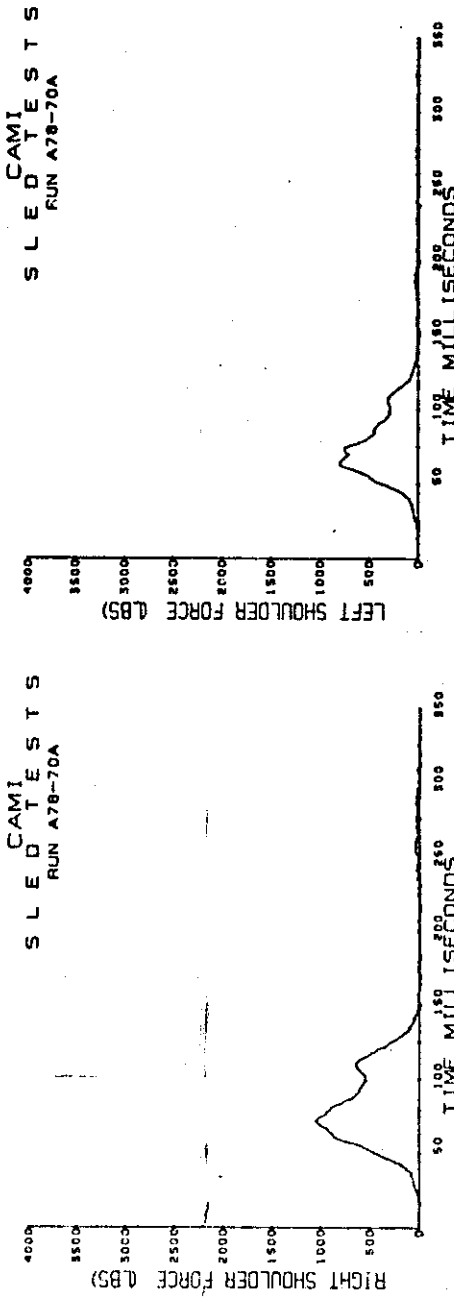


Figure C-1 (continued). 18-g tests.  
Shoulder belt loads.

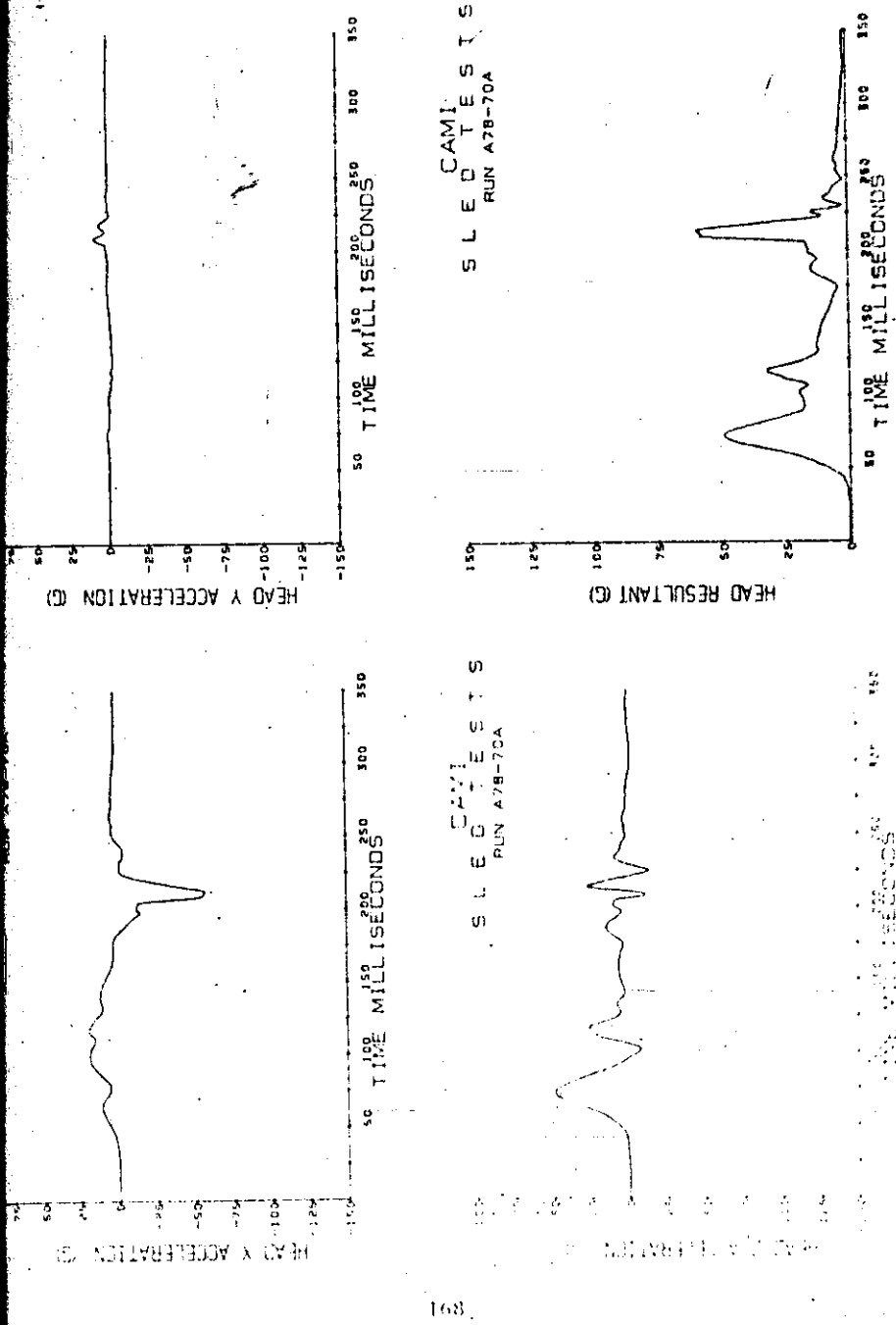


Figure C-1 (continued). 18-g tests.  
Head acceleration.

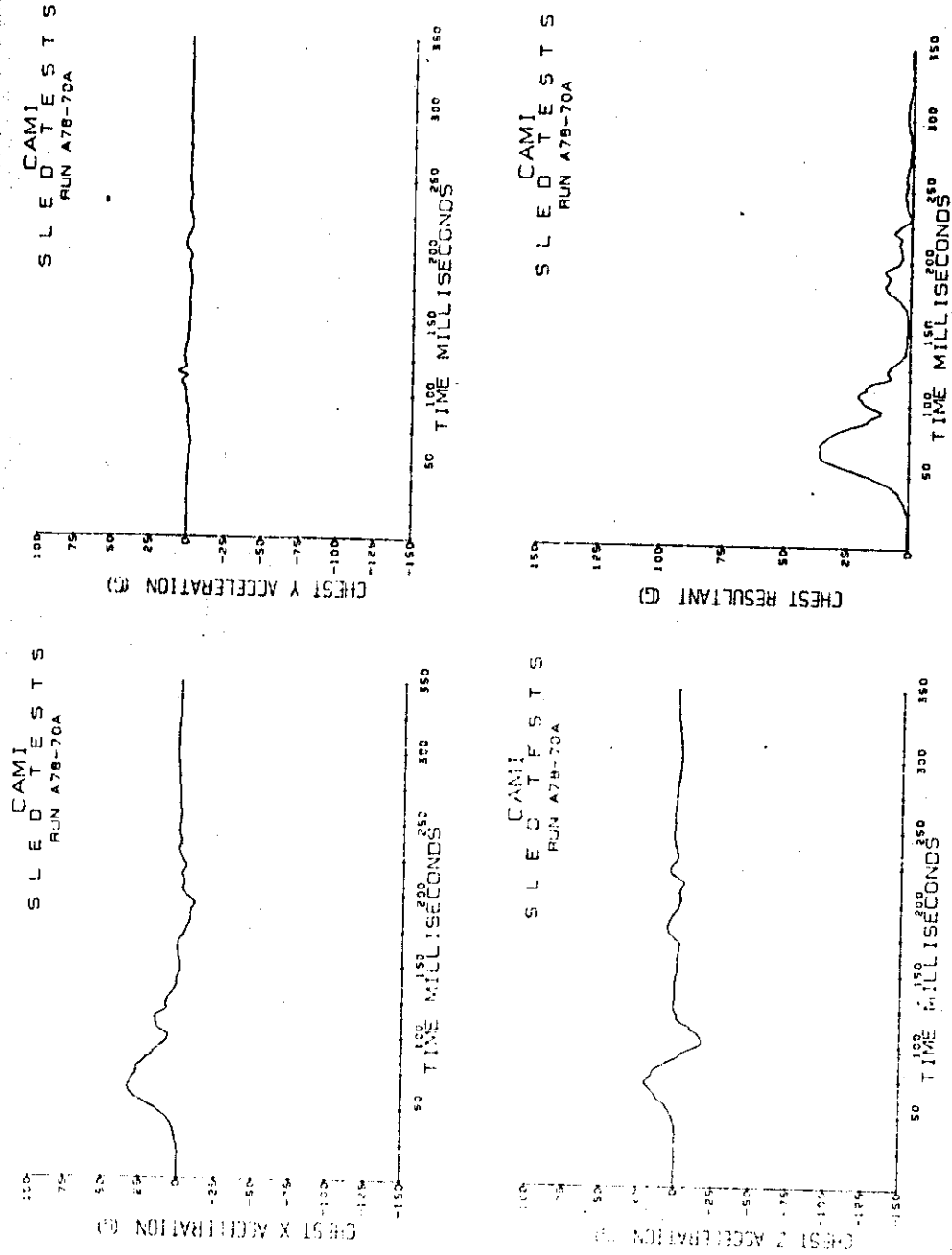


Figure C-1 (continued). 18-g tests.  
Chest acceleration.

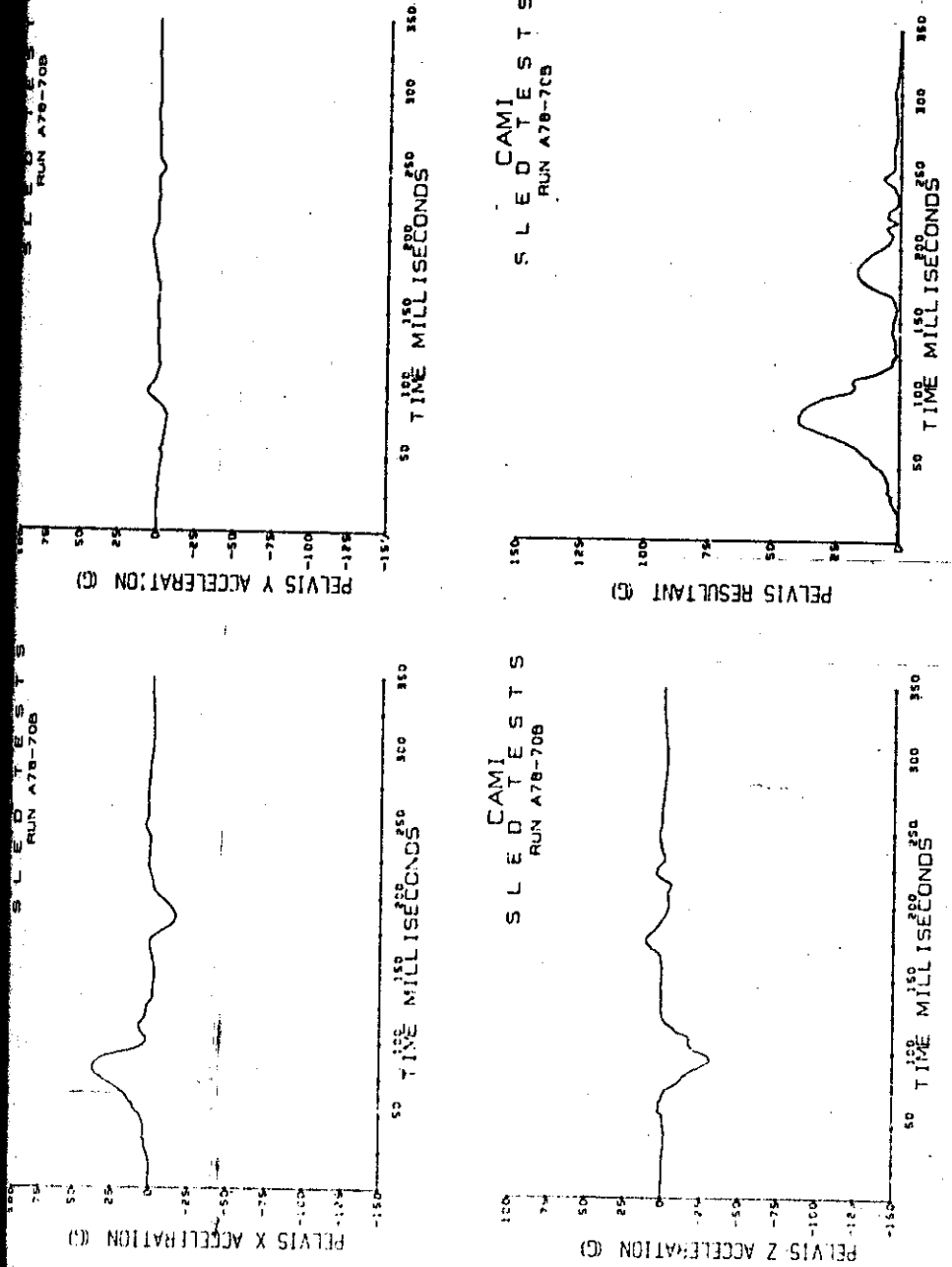


Figure C-1 (continued). 18-8 tests.  
Pelvis acceleration.

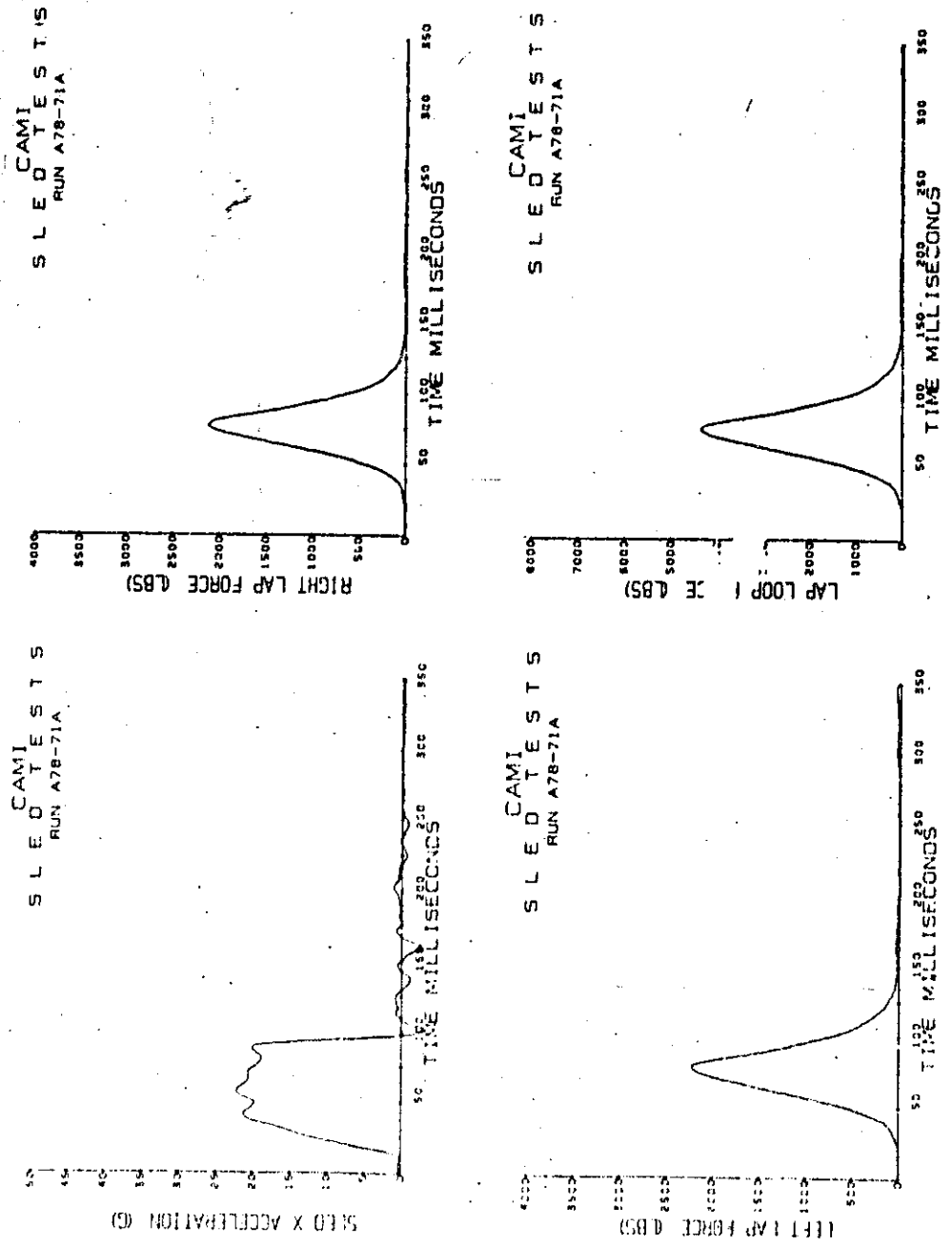


Figure C-1 (continued). 21-8 tests.  
Sled deceleration and lapbelt loads.

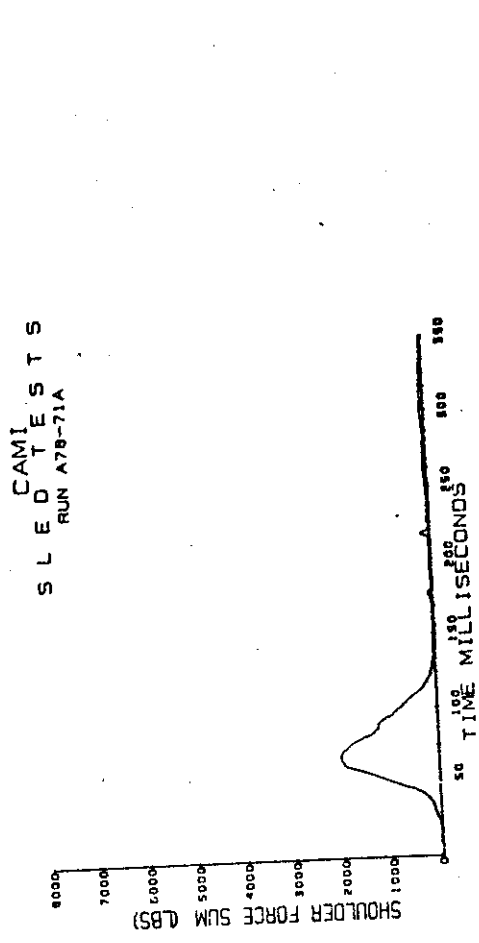
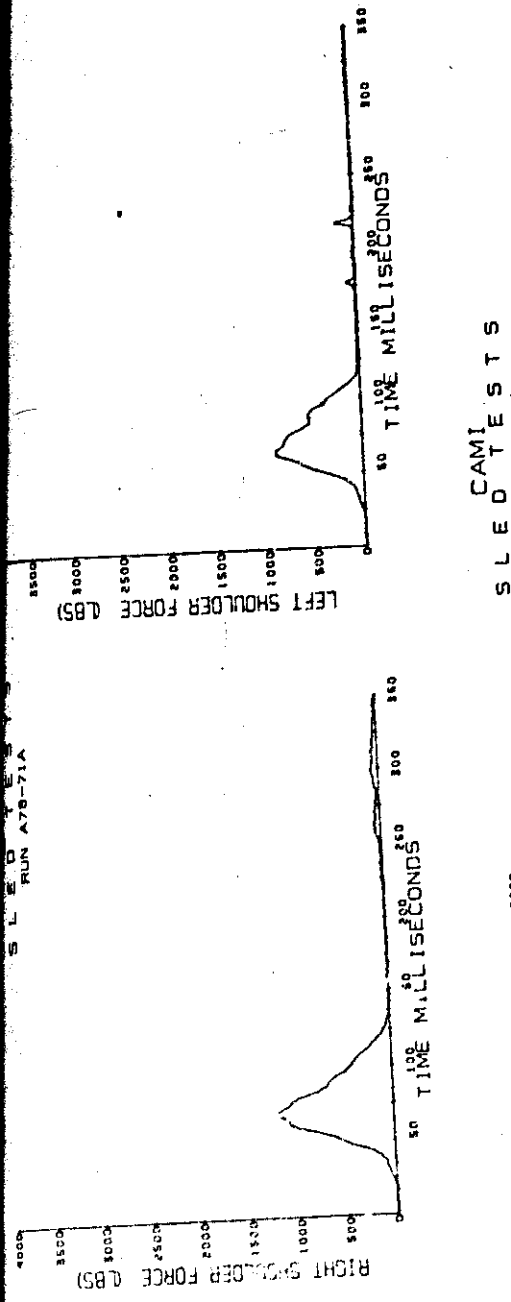


Figure C-1 (continued). 21-g tests.  
Shoulder belt loads.

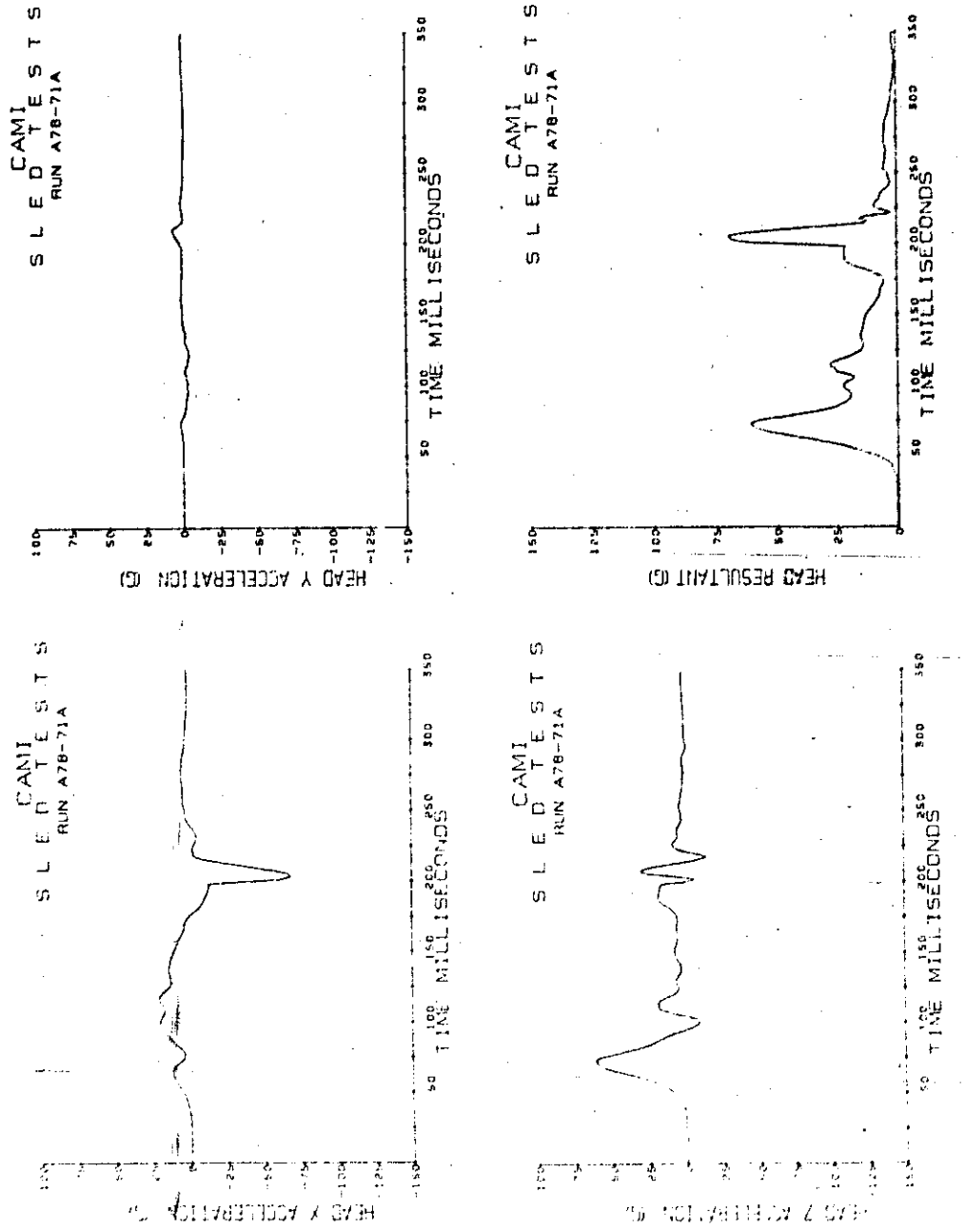


Figure C-1 (continued). 21-g tests.  
Head acceleration.

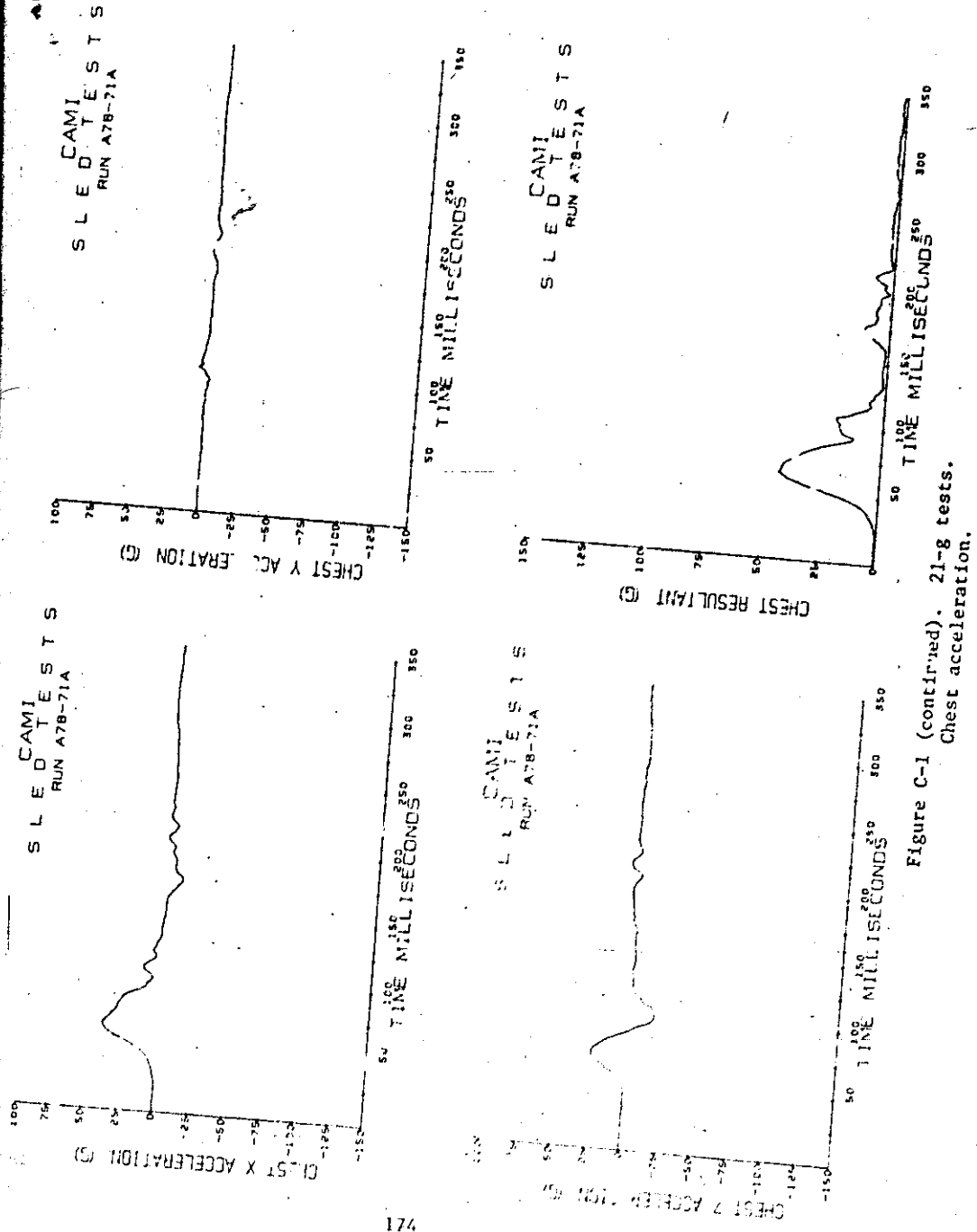


Figure C-1 (continued). 21-g tests.  
Chest acceleration.

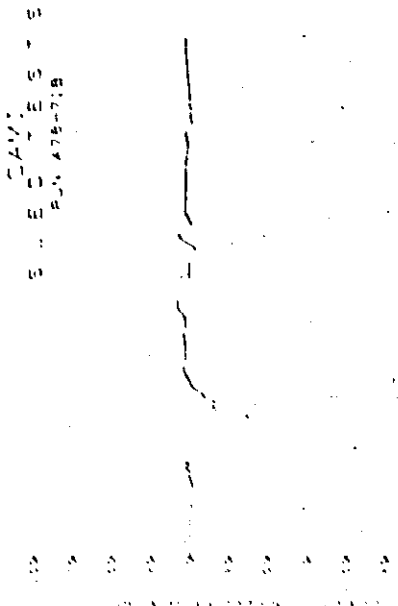
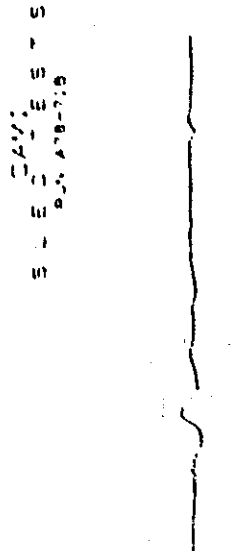
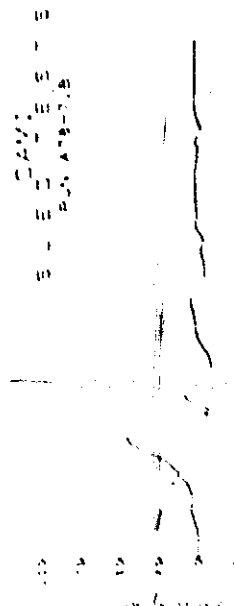


Figure 10. Concentration 21-8 tests.  
Periods acceleration.

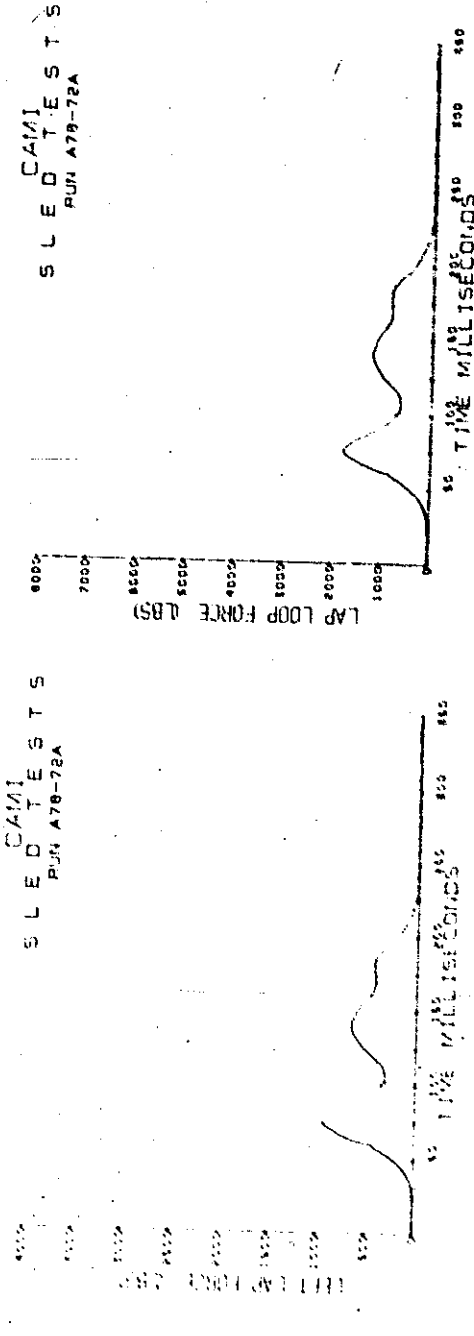
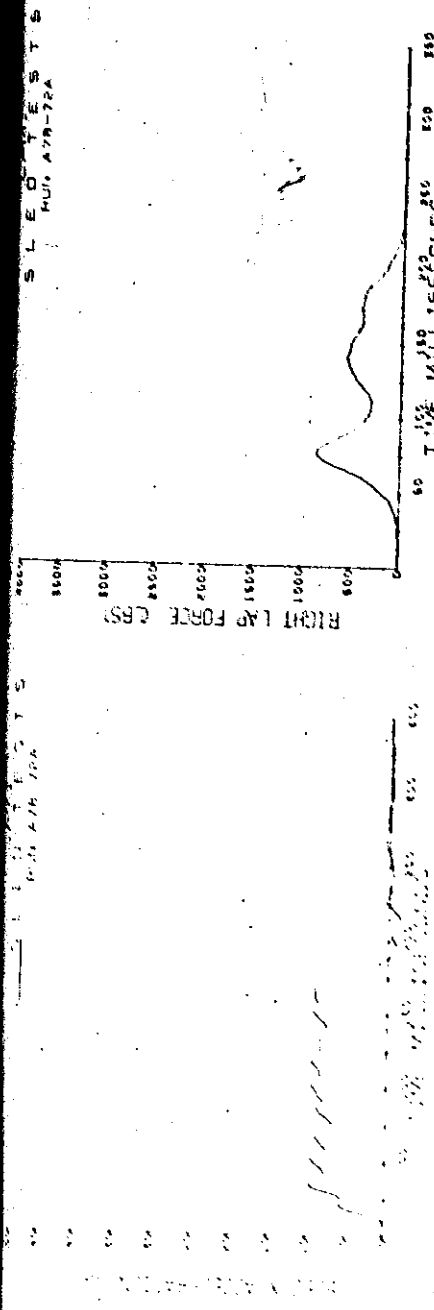


Figure C-2 Kevlar webbing. 9-g tests.  
Sled deceleration and lapbelt loads.

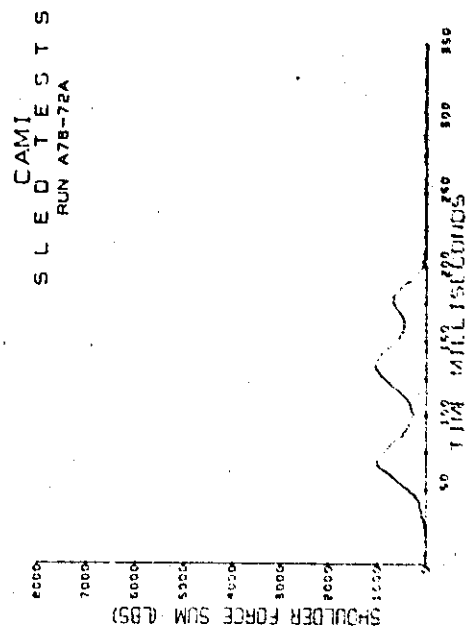
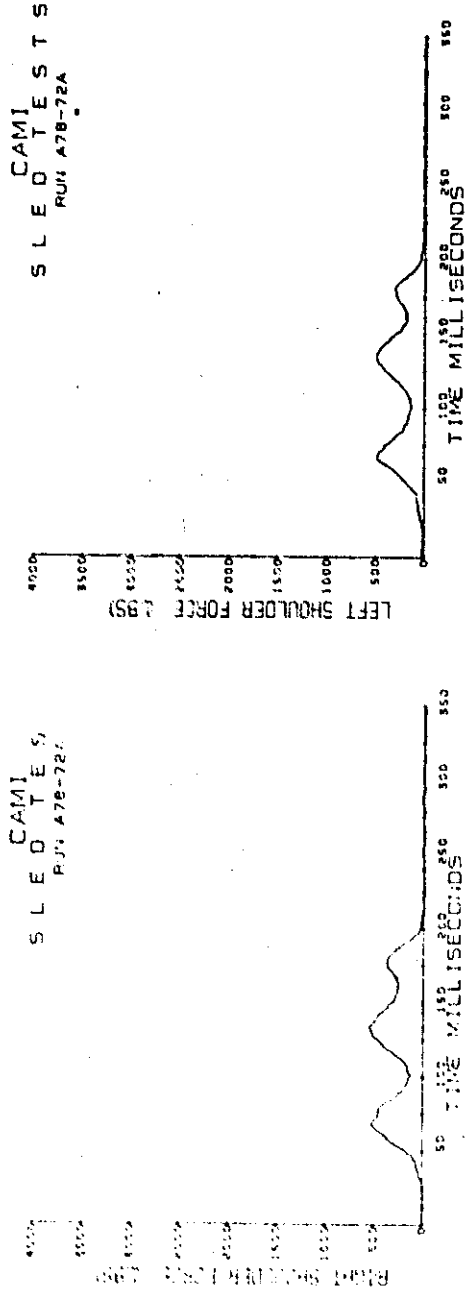


FIGURE G-2 (continued).  $g-g$  tests.  
Shoulder belt loads.

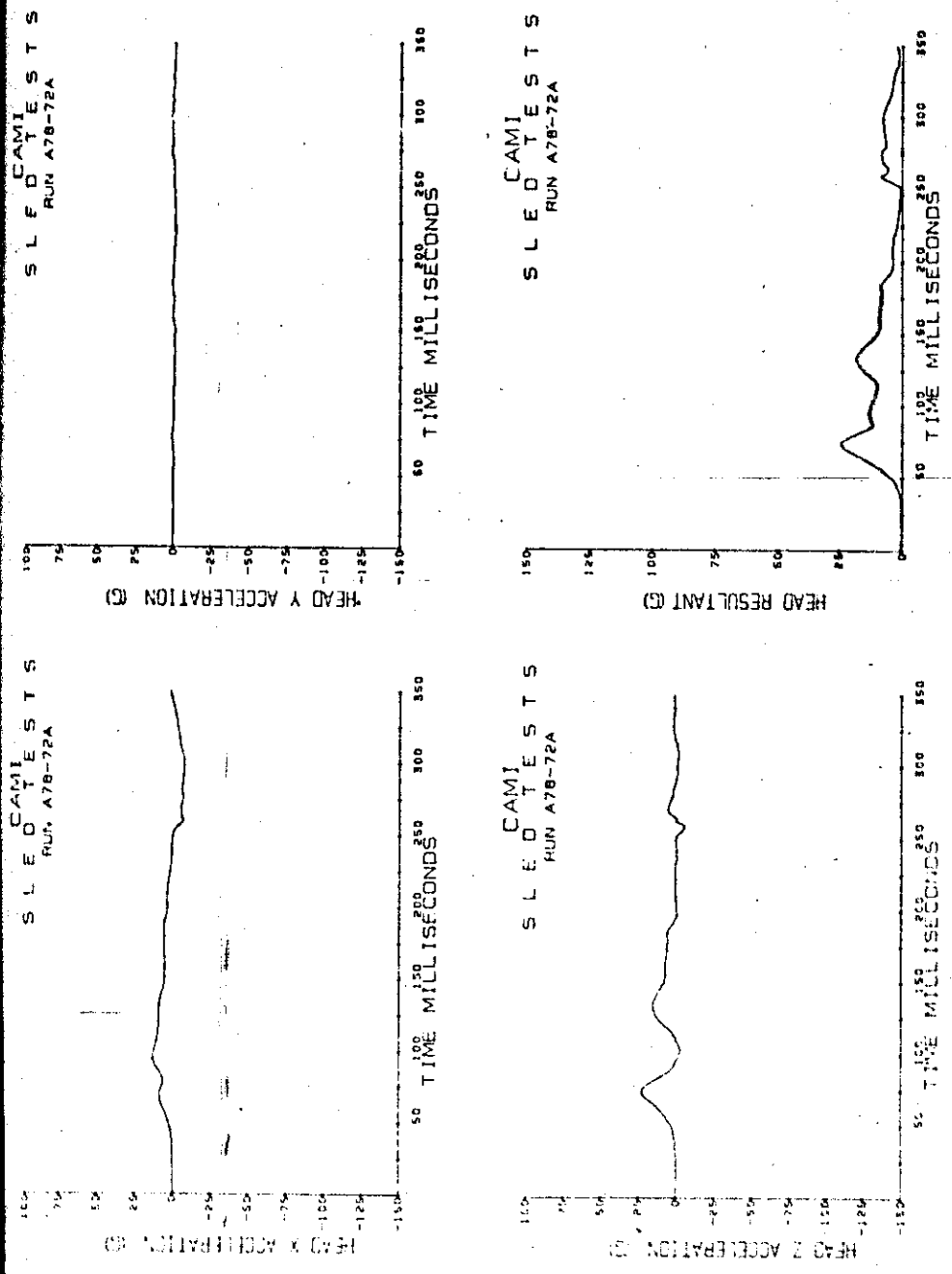


Figure C-2 (continued). 9-8 tests.  
Head acceleration.

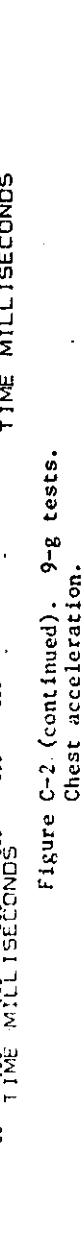
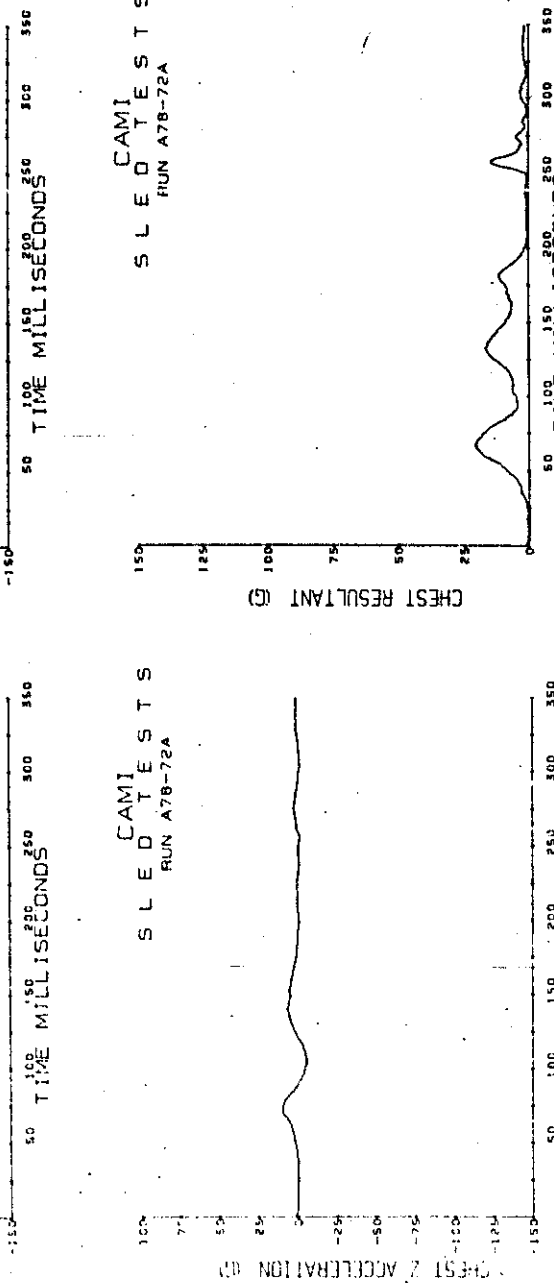
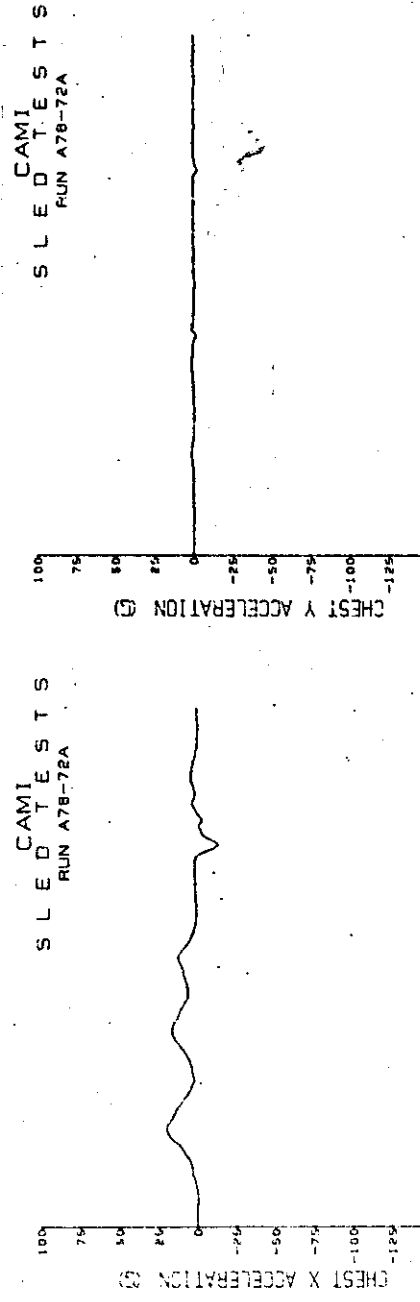


Figure C-2 (continued), 9-g tests.  
Chest acceleration.

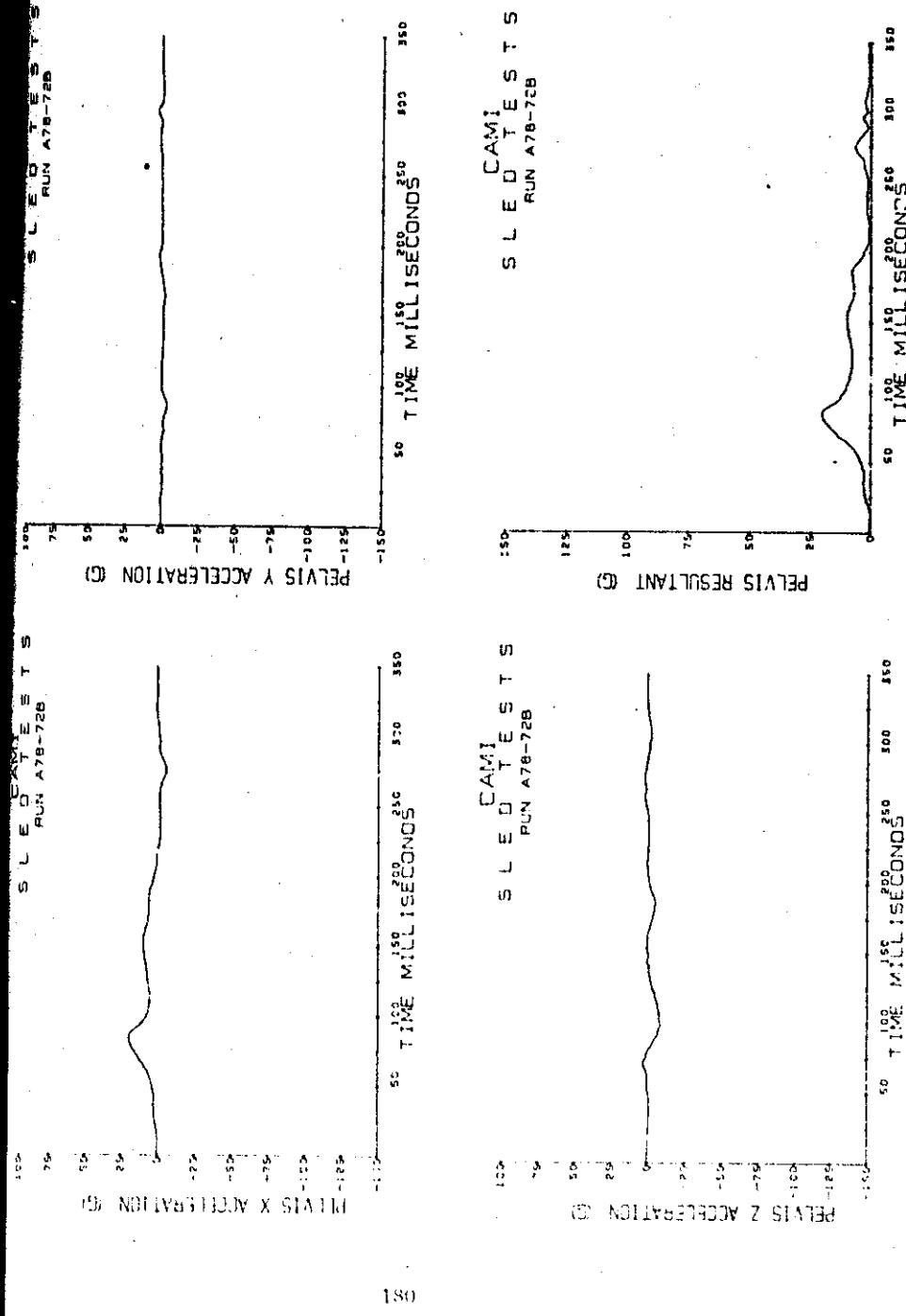


Figure C-2 (continued). 9-g tests.  
Pelvis acceleration.

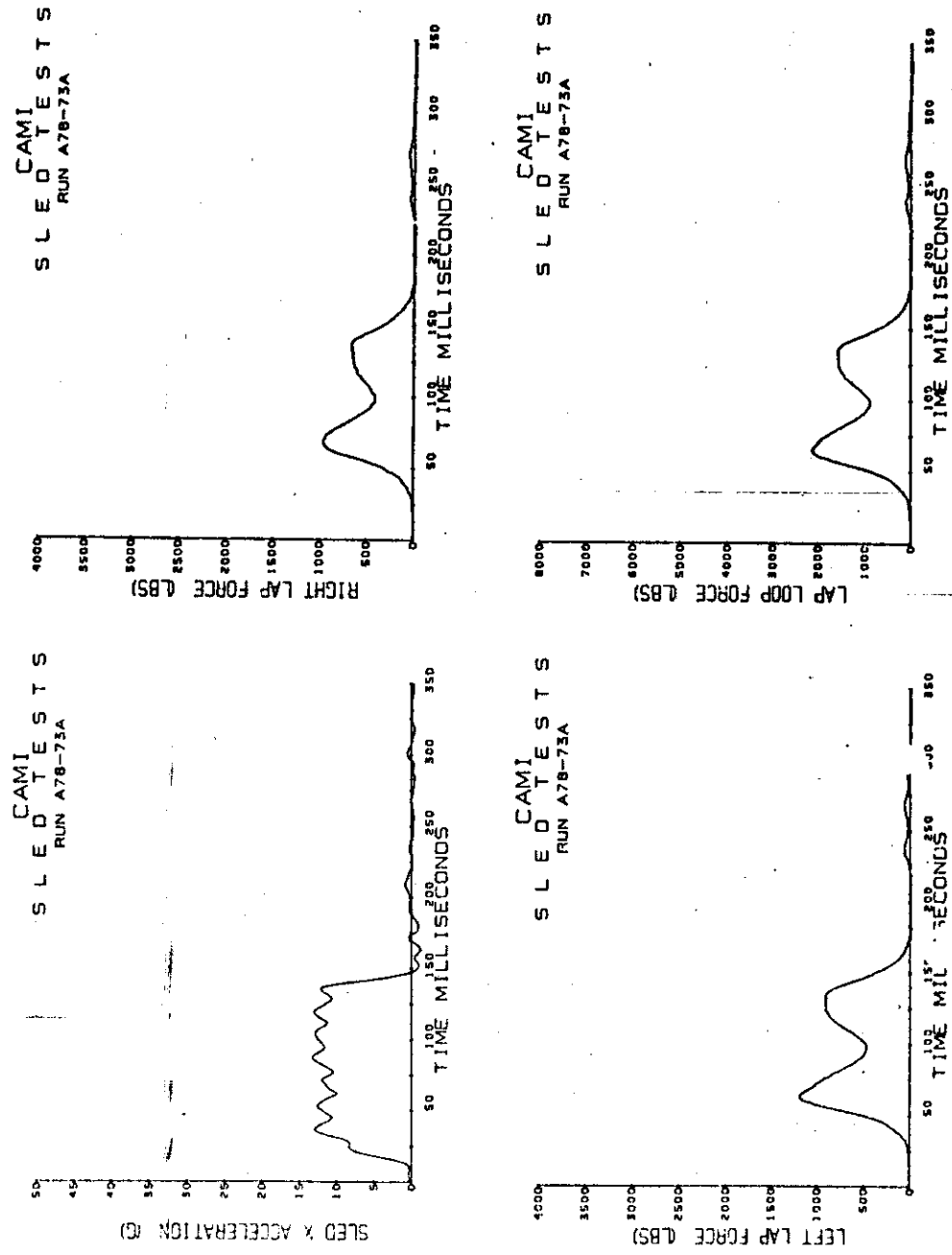


Figure C-2 (continued). 12-g tests.  
Sled deceleration and lapbelt loads.

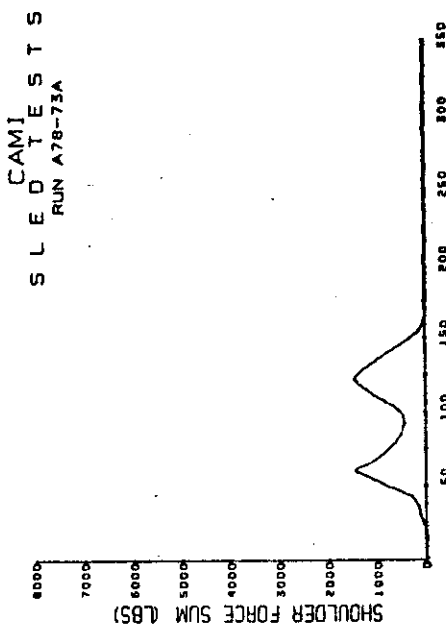
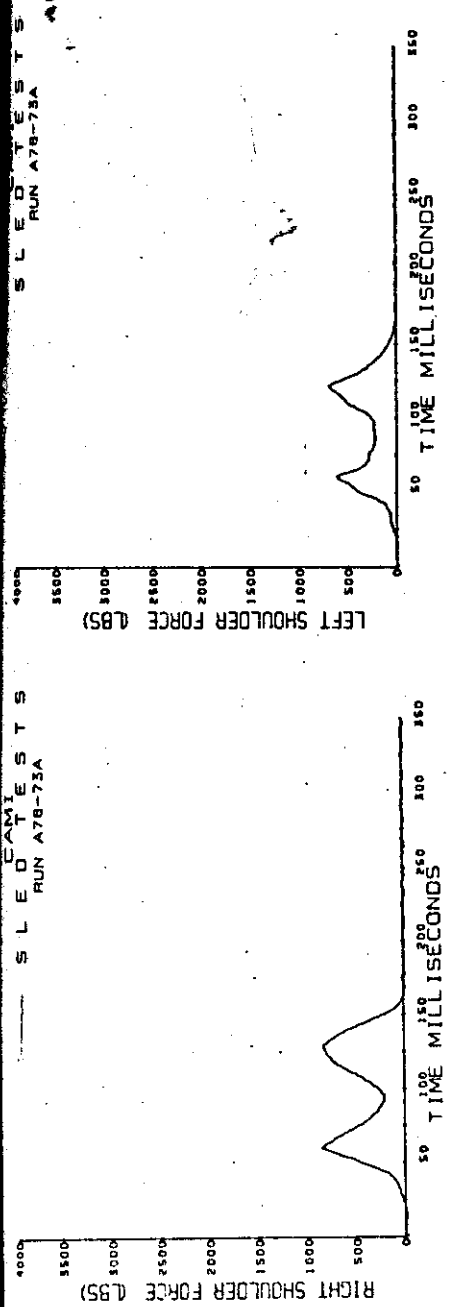


Figure C-2 (continued), 12-g tests.  
Shoulder belt loads.

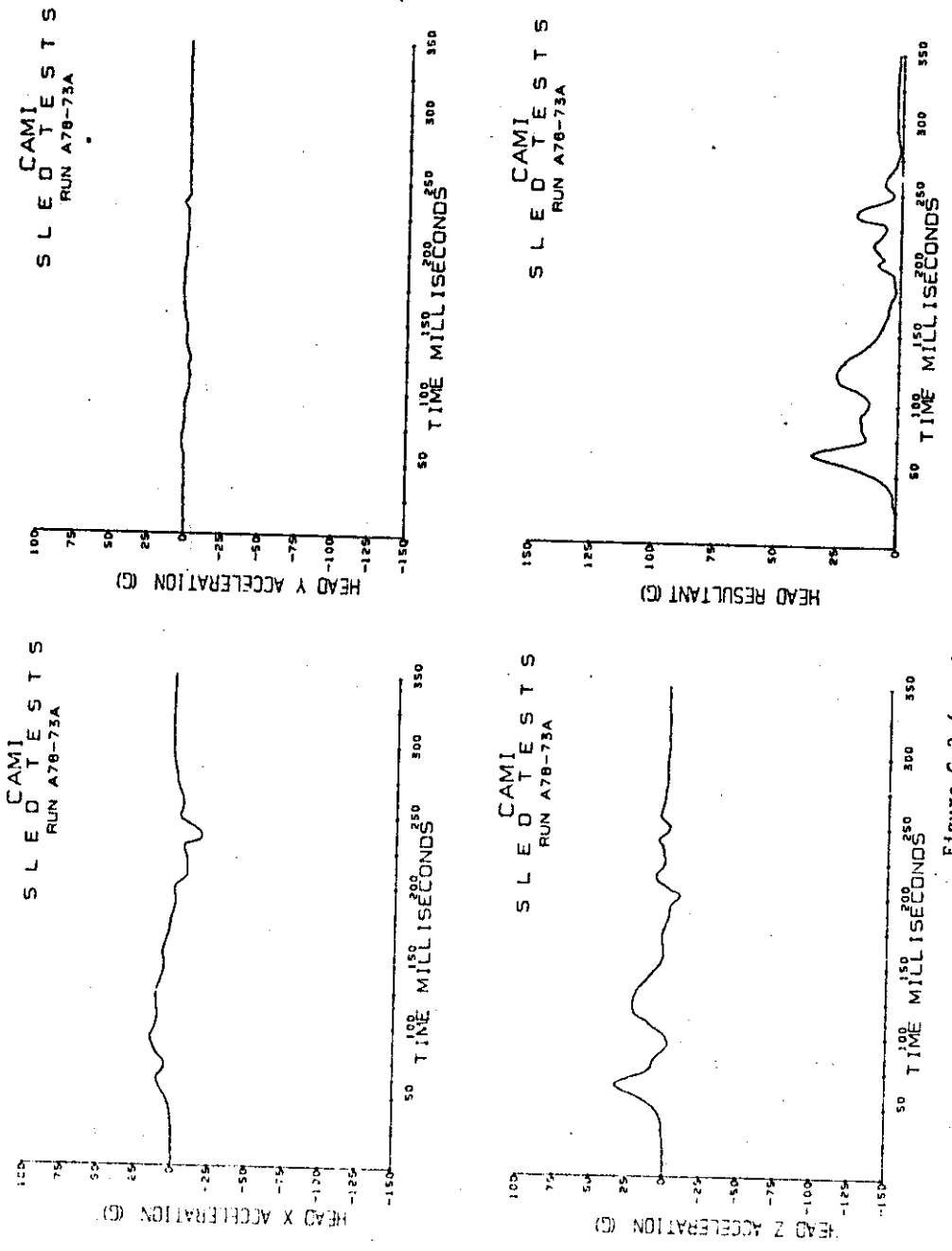


Figure C-2 (continued).  
Head acceleration.  
12-8 tests.

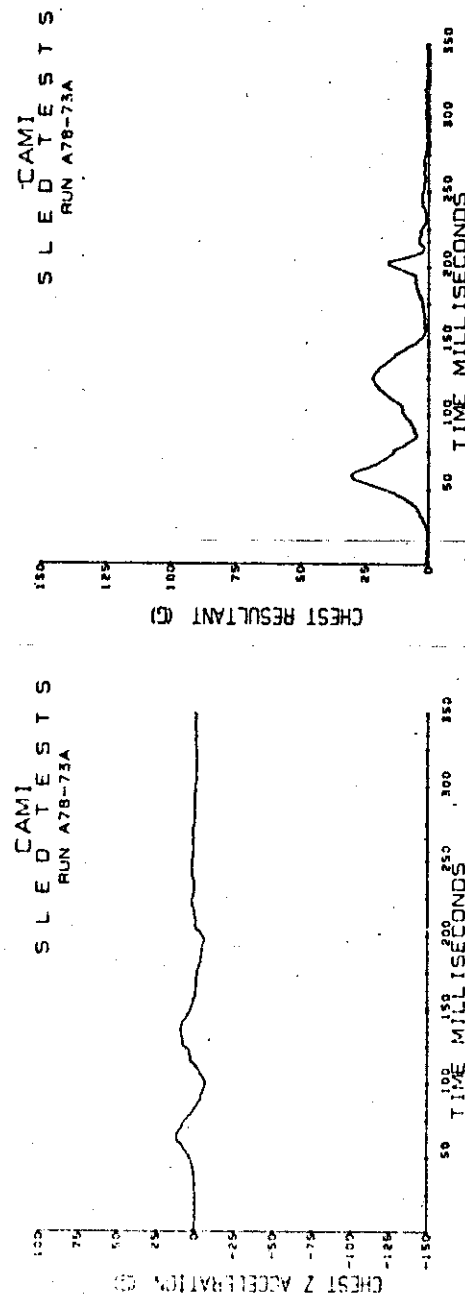
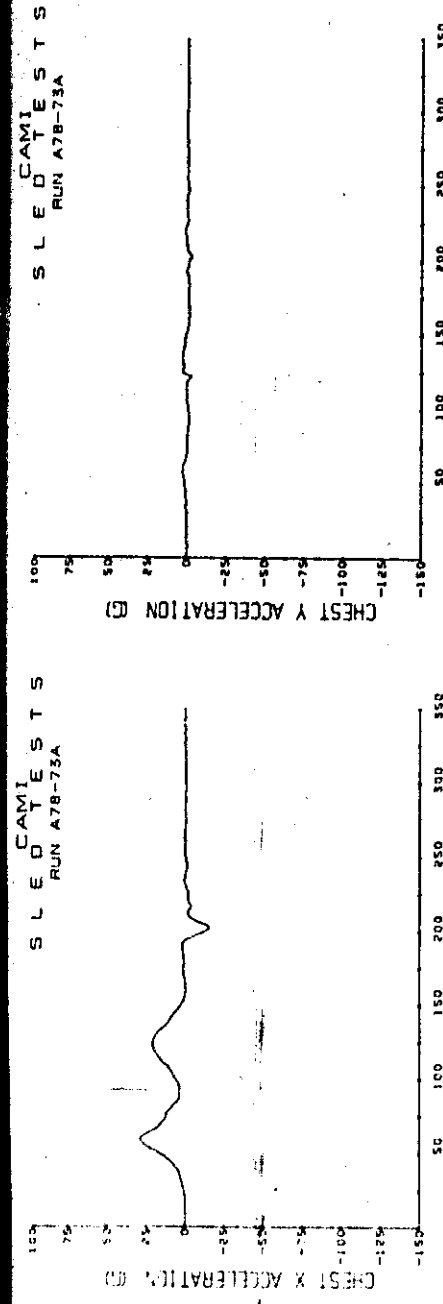


Figure C-2 (continued). 12-g tests.  
Chest acceleration.

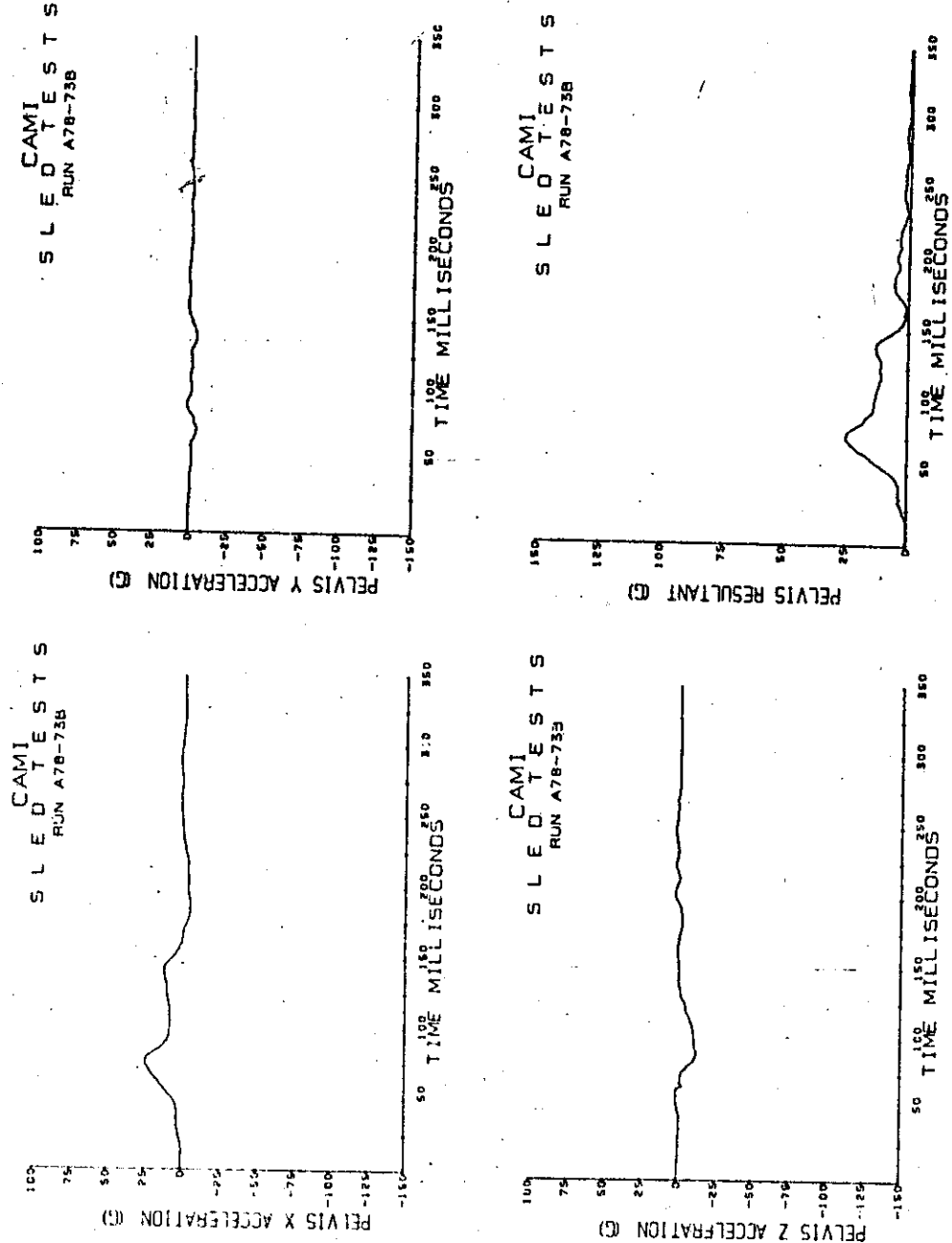


Figure C-2 (continued). 12-g tests.  
Pelvis acceleration.

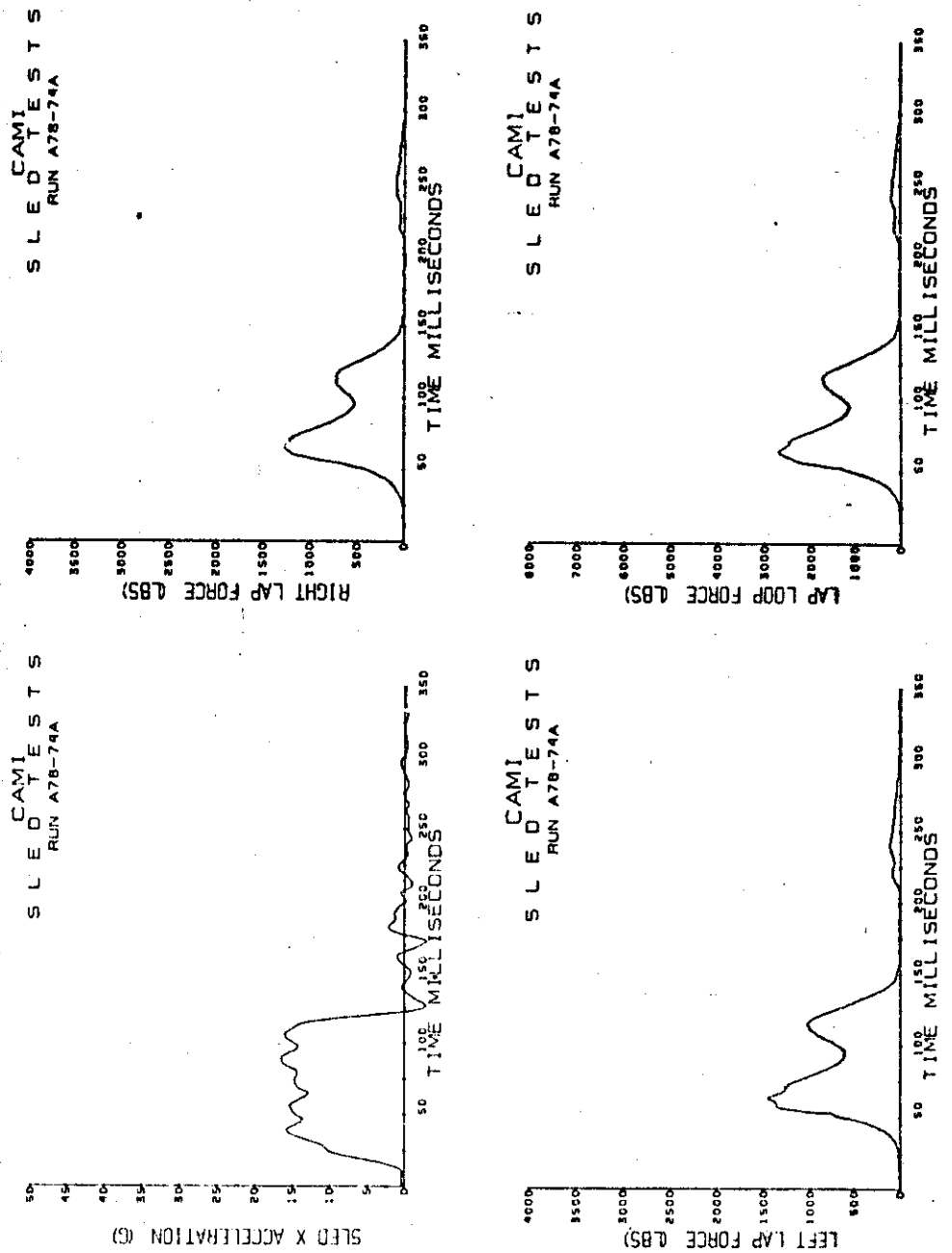
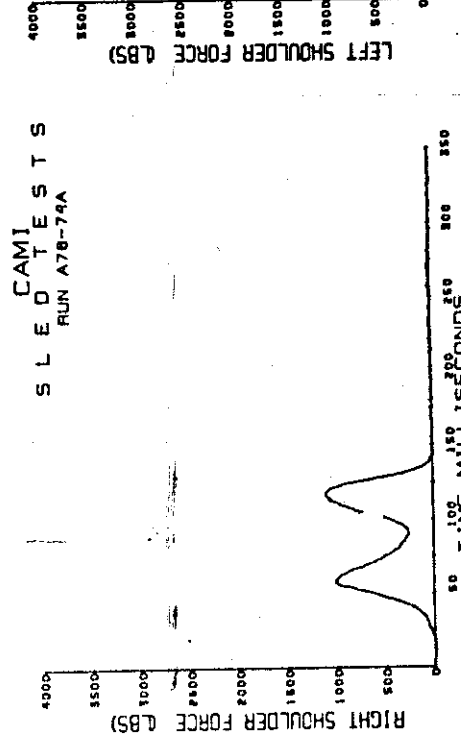
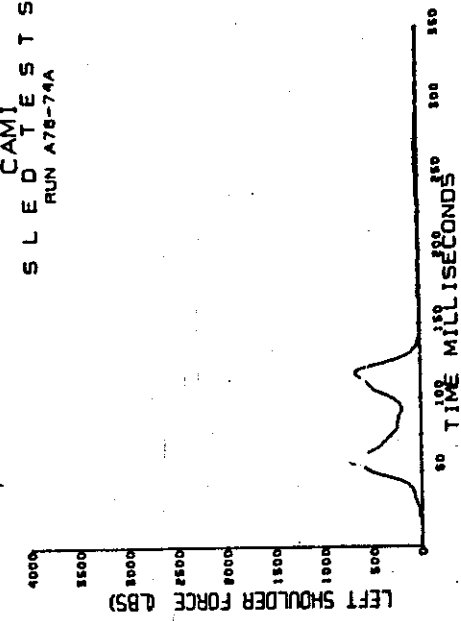


Figure C-2 (continued). 16-8 tests.  
Sled deceleration and lapbelt loads.

S L E D C A M I  
T E S T S  
R U N A 78-74A



S L E D C A M I  
T E S T S  
R U N A 78-74A



S L E D C A M I  
T E S T S  
R U N A 78-74A

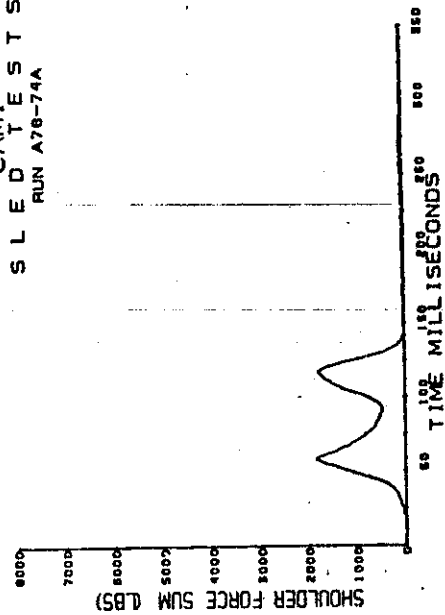


Figure C-2 (continued). 16-8 tests.  
Shoulder belt loads.

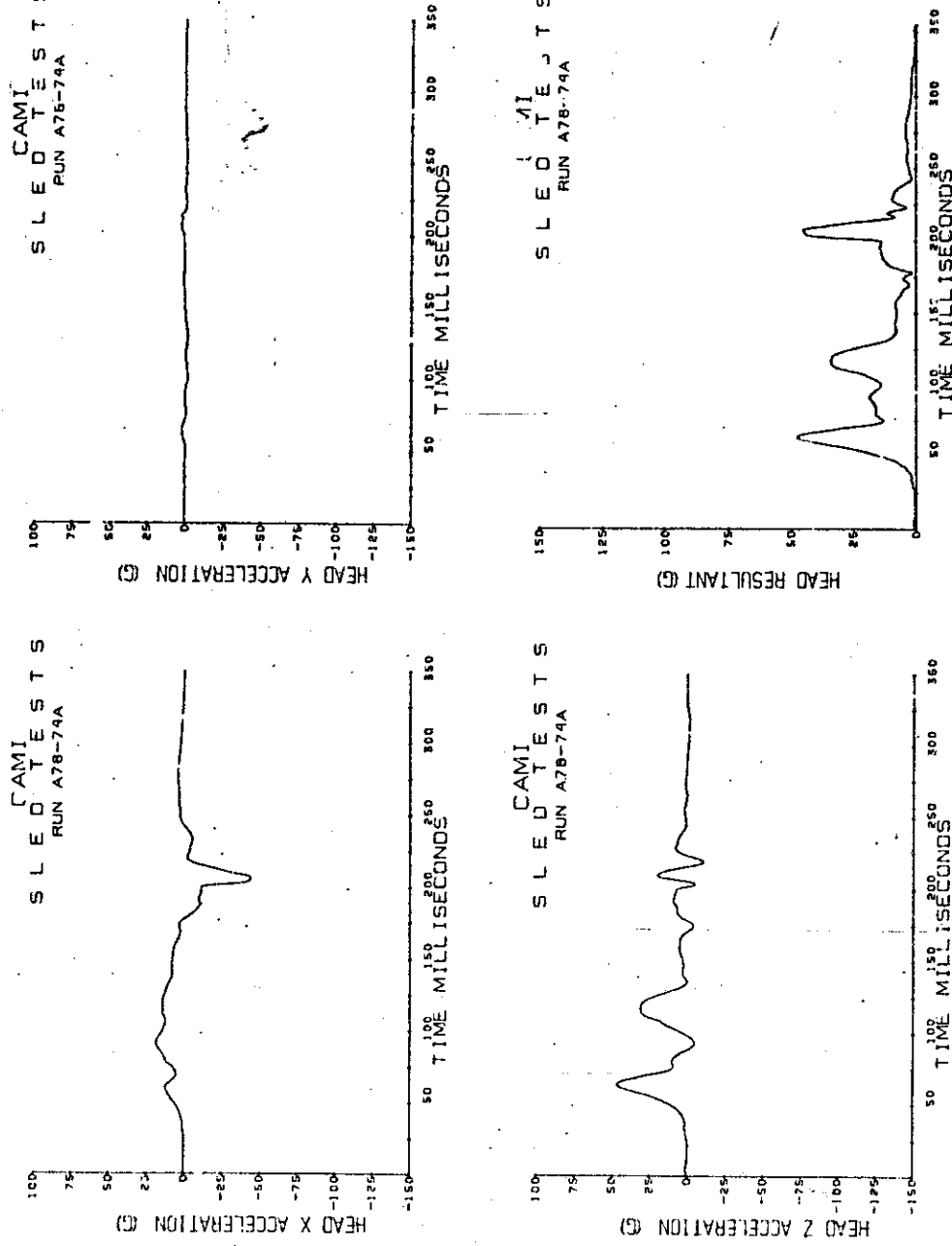


Figure C-2 (continued). 16-g tests.  
Head acceleration.

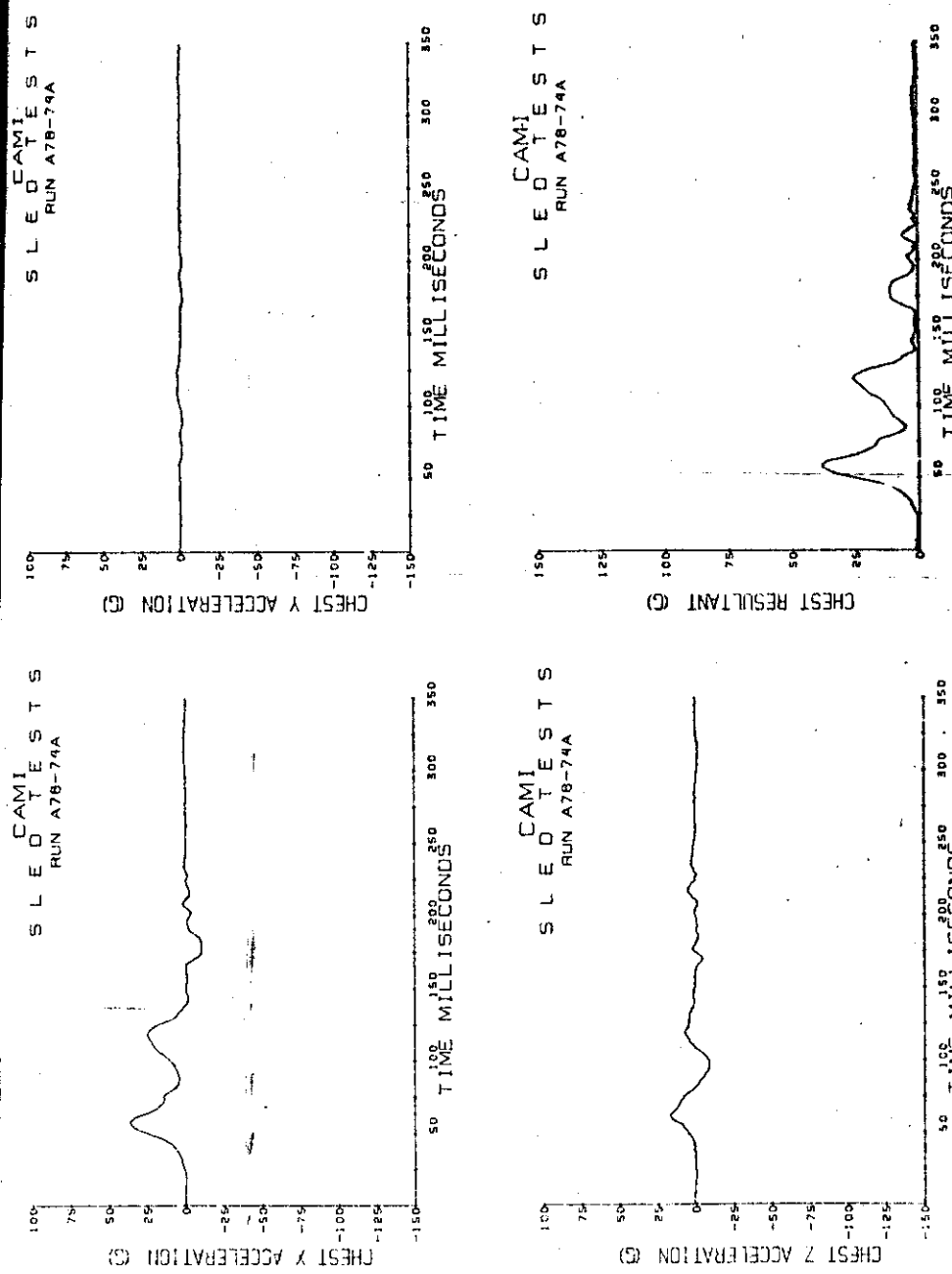


Figure C-2 (continued). 16-8 tests.  
Chest acceleration.

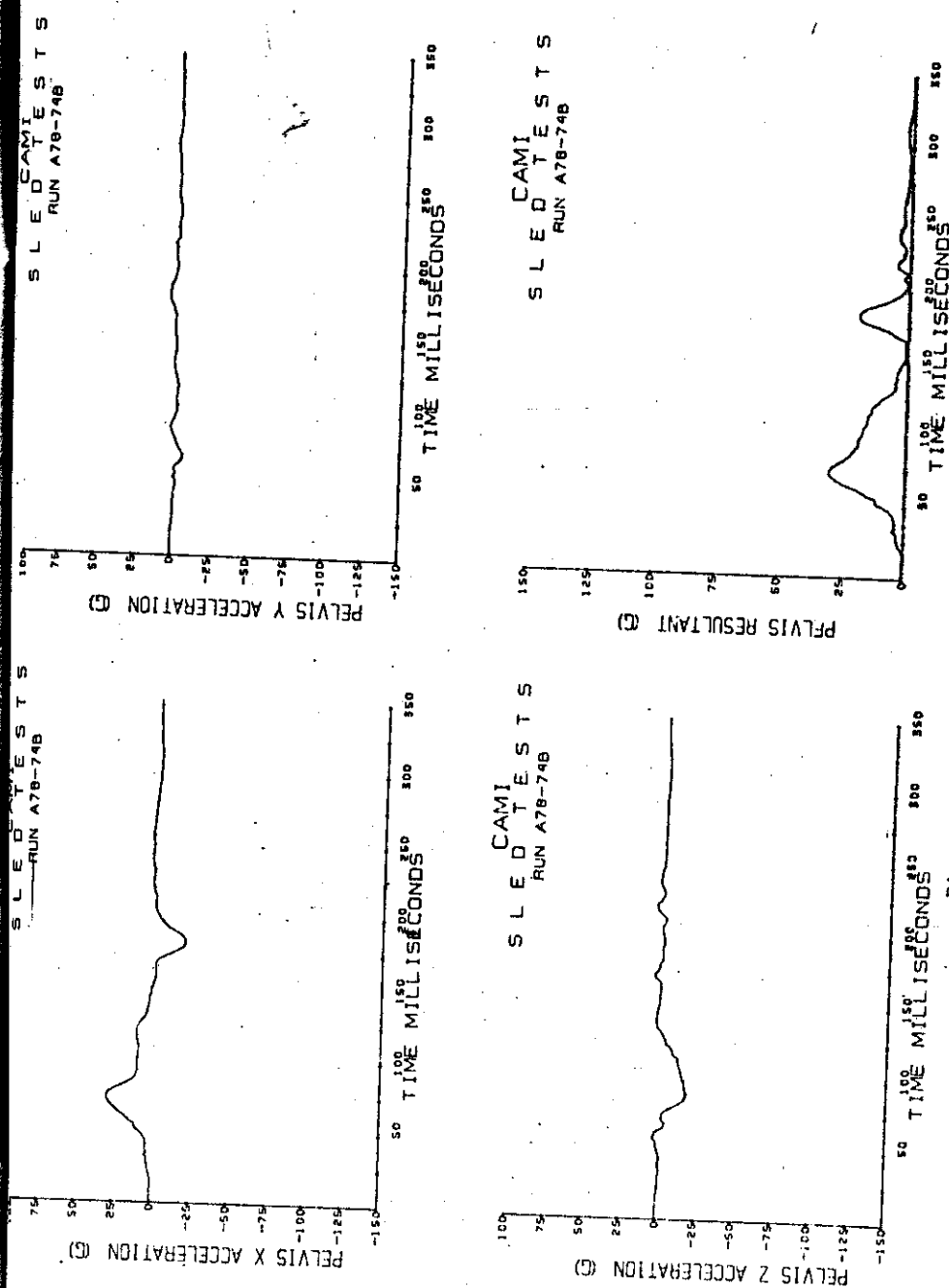


Figure C-2 (continued). 16-g tests.  
Pelvis acceleration.

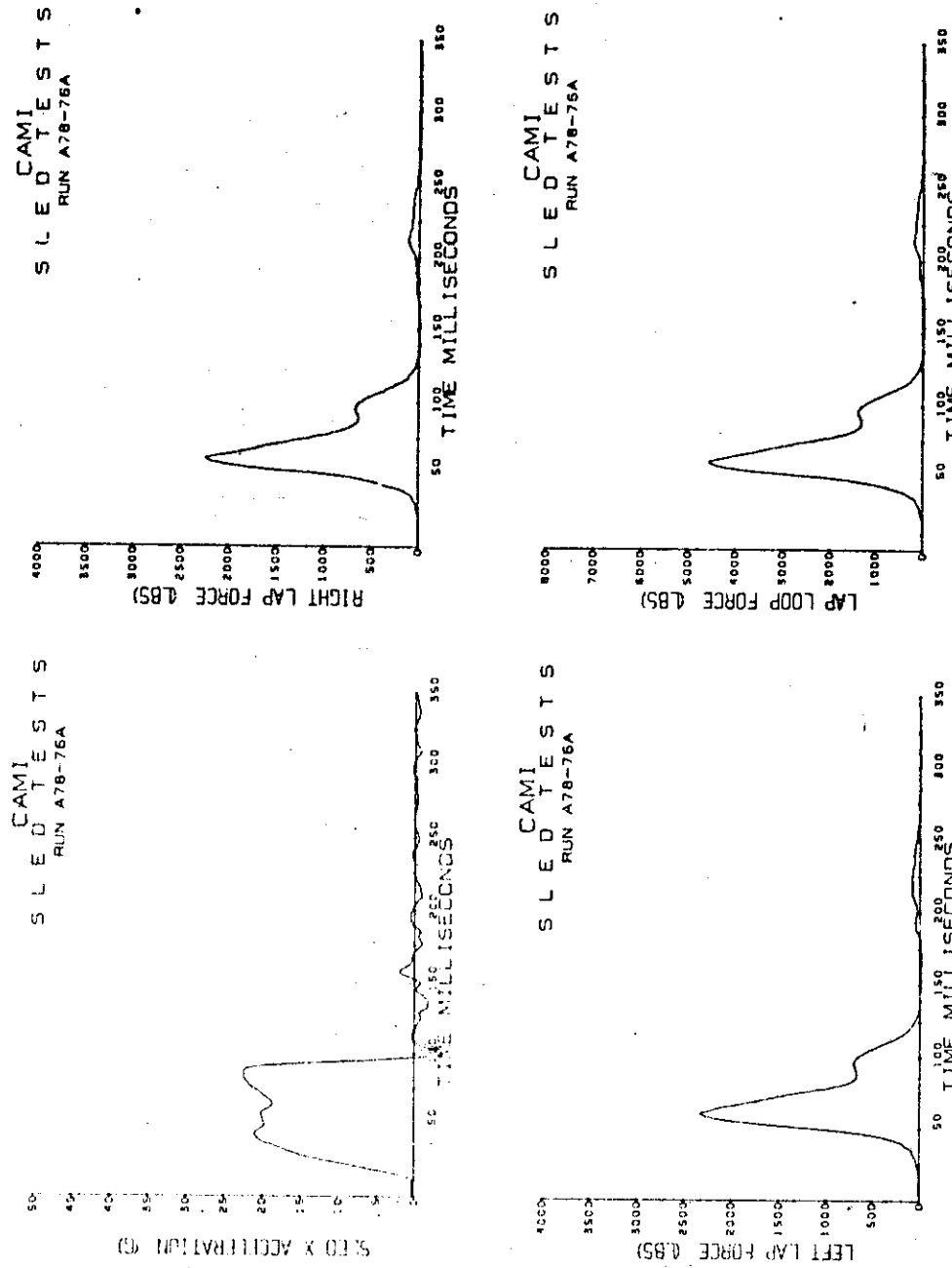


Figure C-2 (continued). 18-g tests.  
Sled deceleration and lap belt loads.

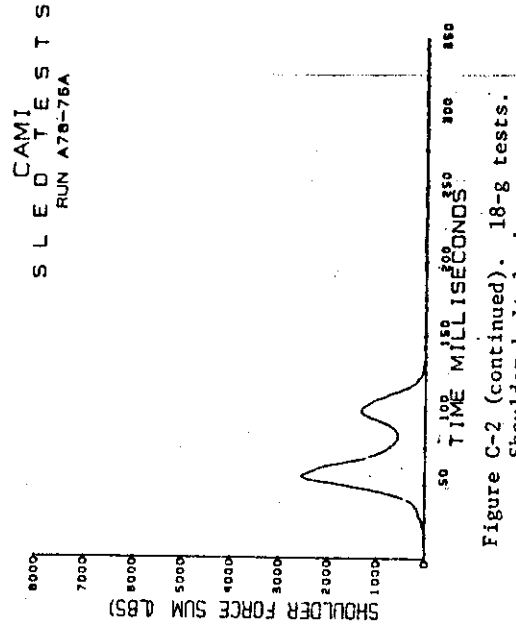
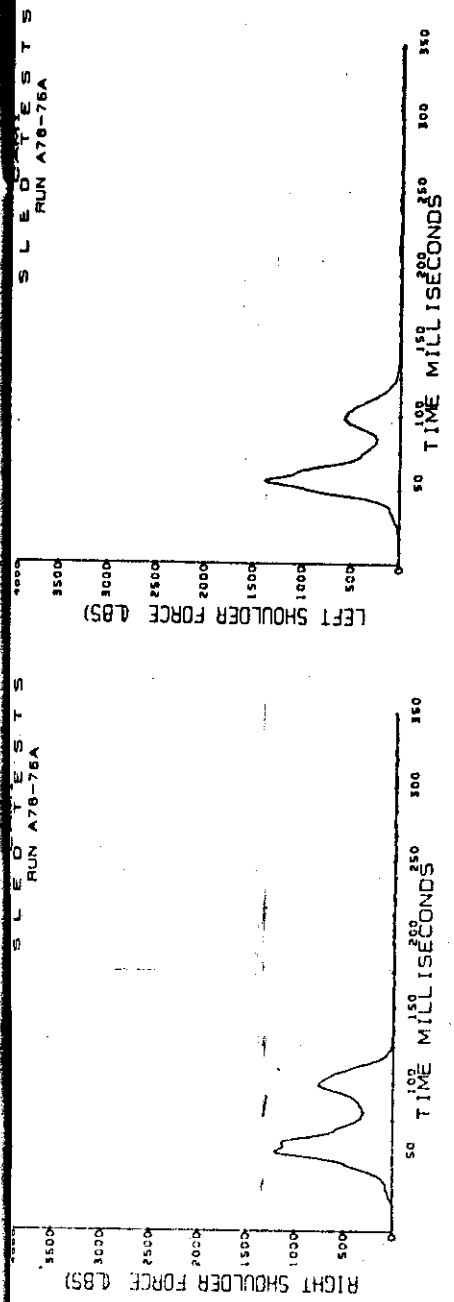


Figure C-2 (continued). 18-g tests.  
Shoulder belt loads.

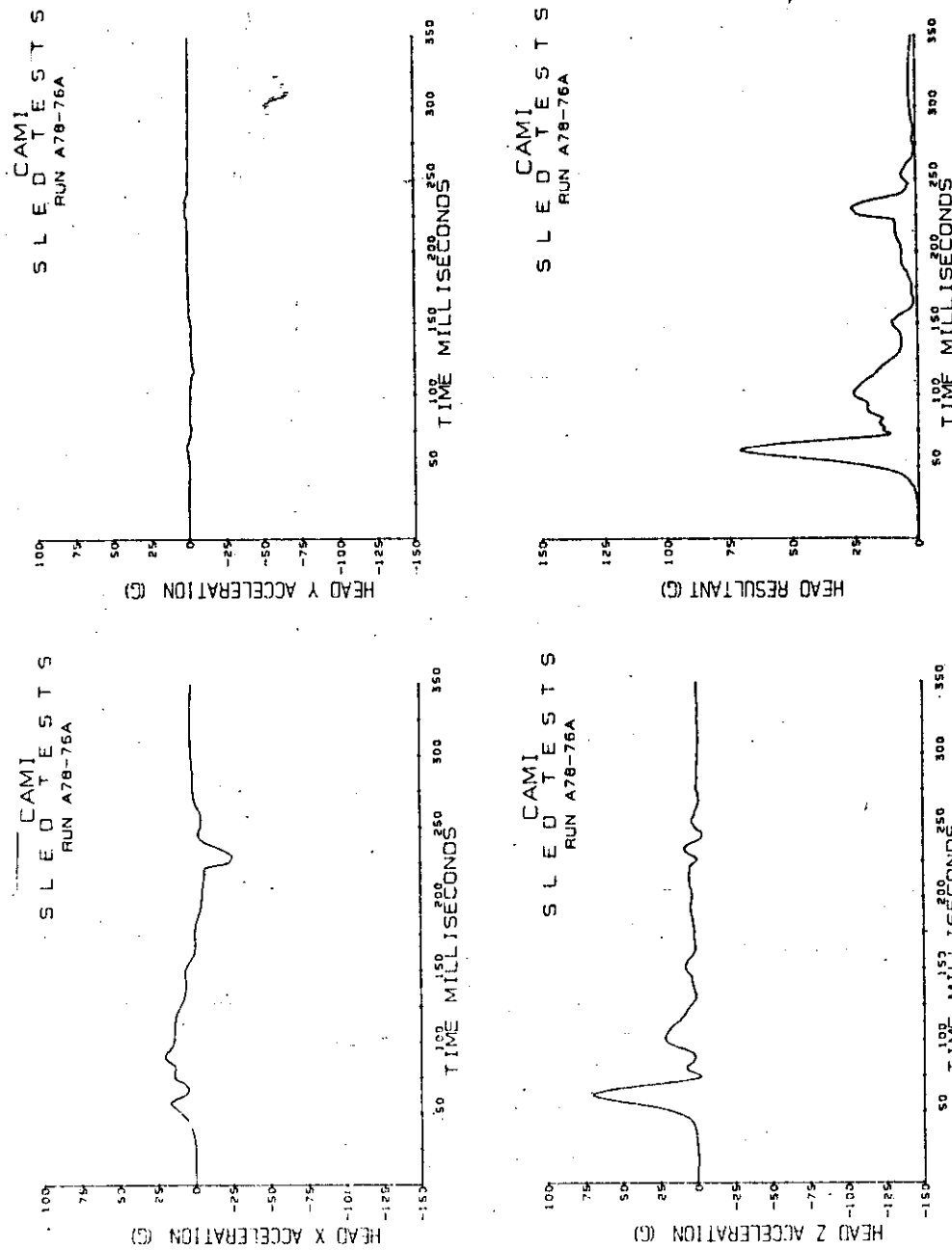


Figure C-2 (continued). 18-g tests.  
Head acceleration.

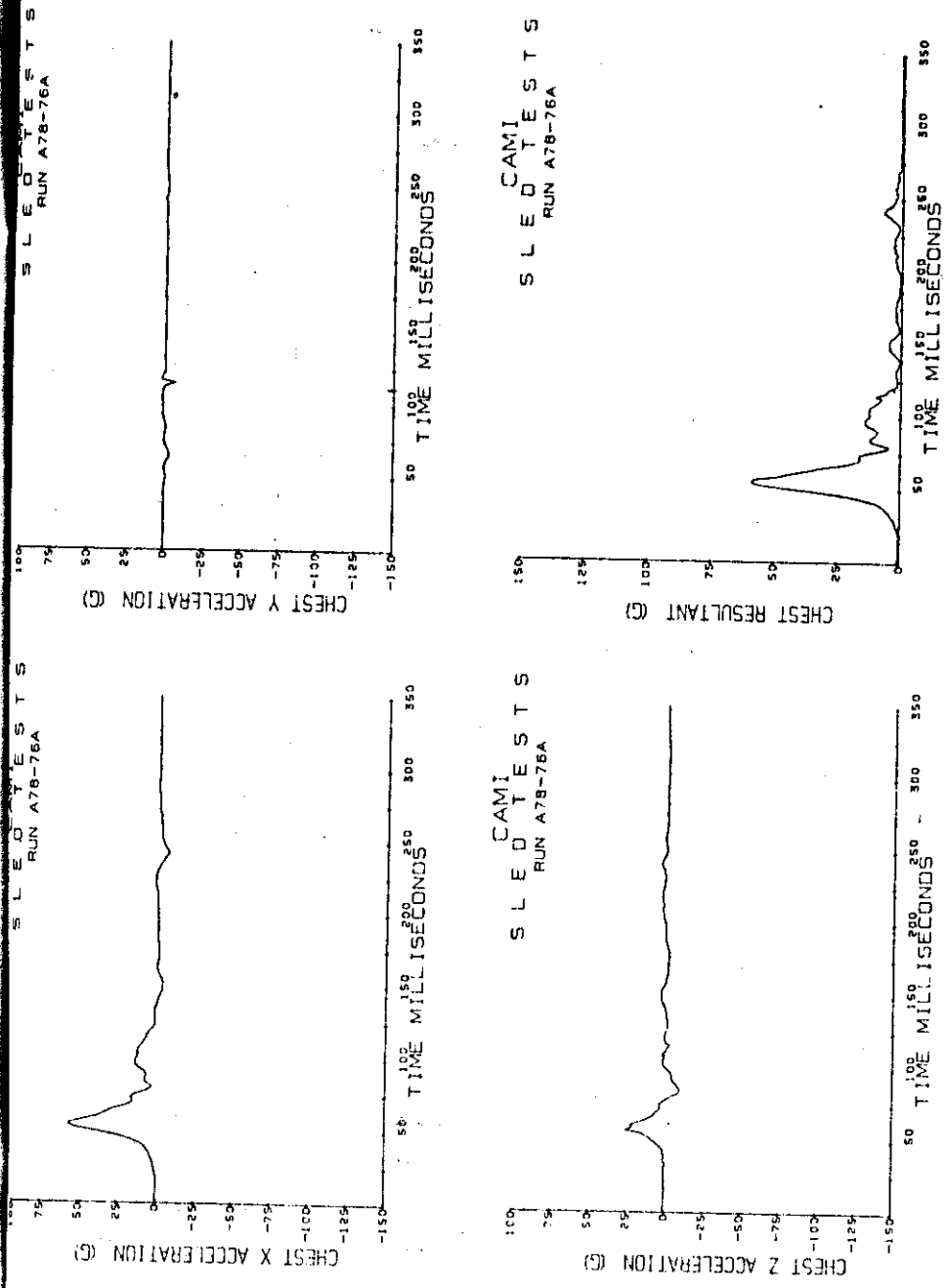


Figure C-2 (continued). 18-8 tests.  
Chest acceleration.

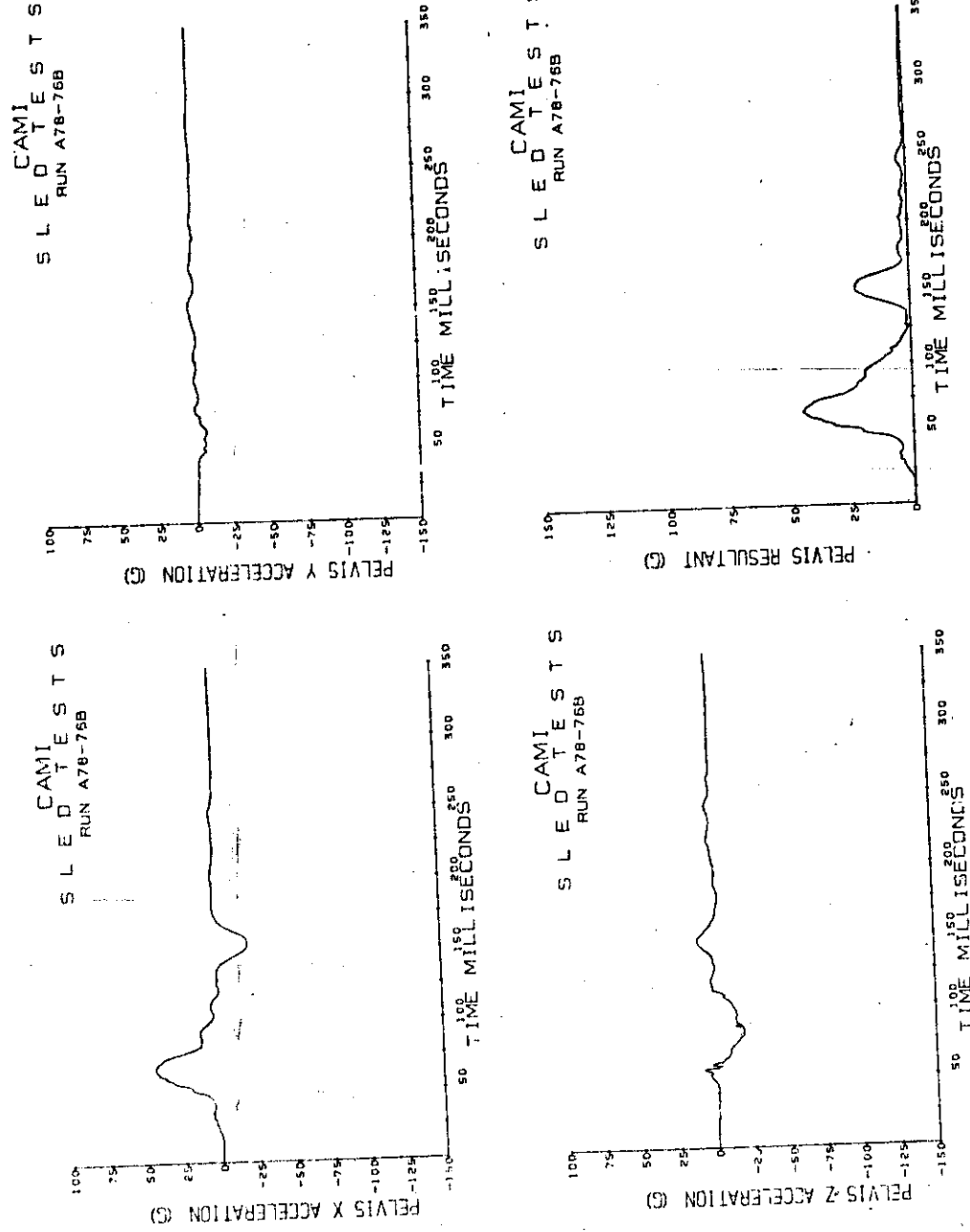


Figure C-2 (continued). 18-g tests.  
Pelvis acceleration.

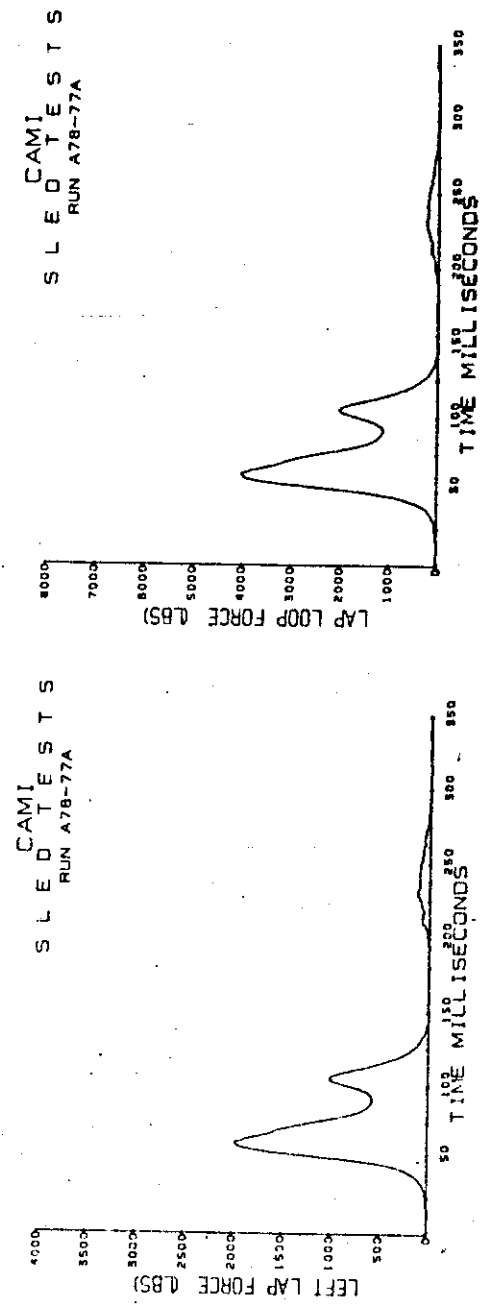
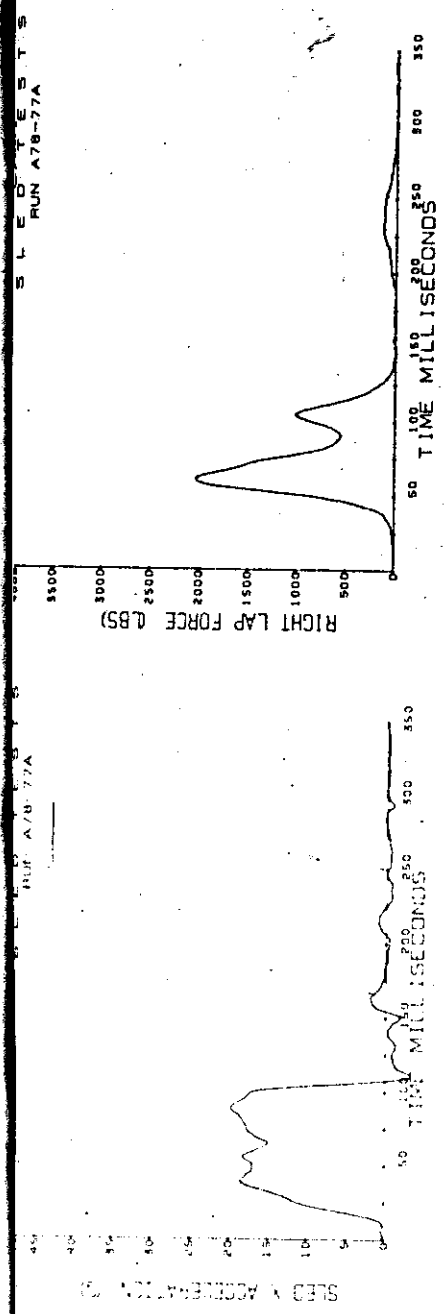


Figure C-2 (continued). 22-8 tests.  
Sled deceleration and lapbelt loads.

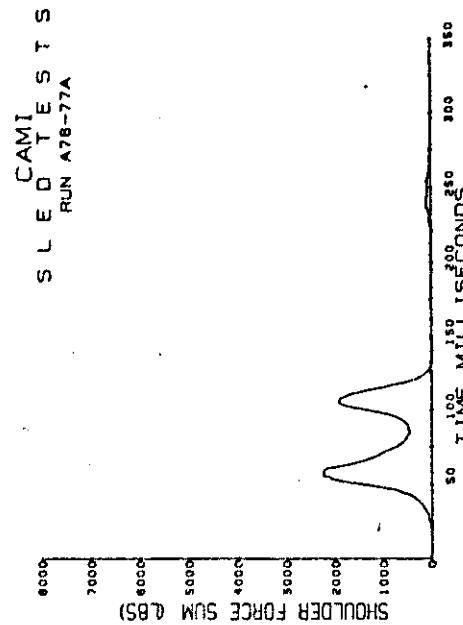
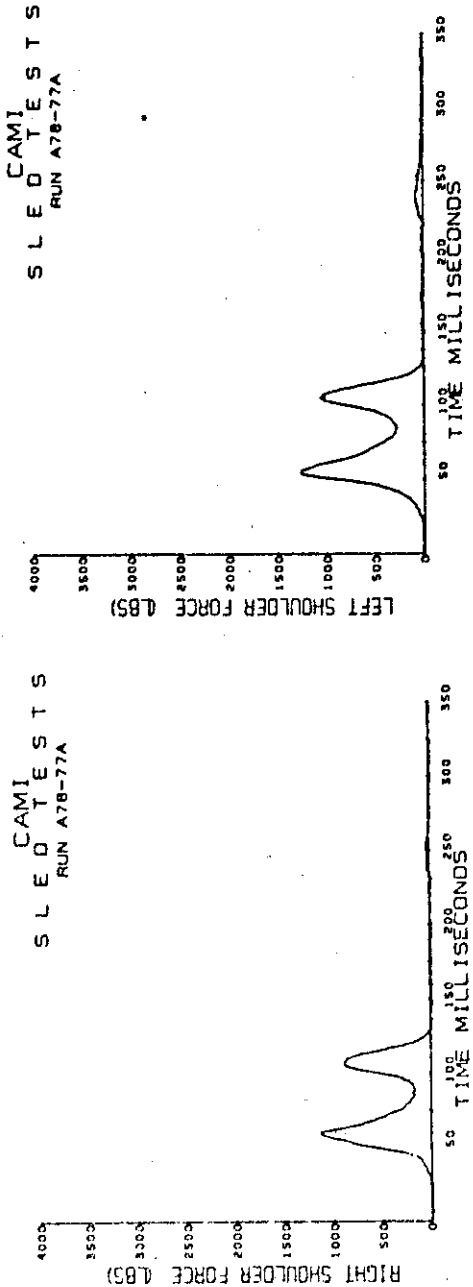


Figure C-2 (continued). 22-g tests:  
Shoulder belt loads.

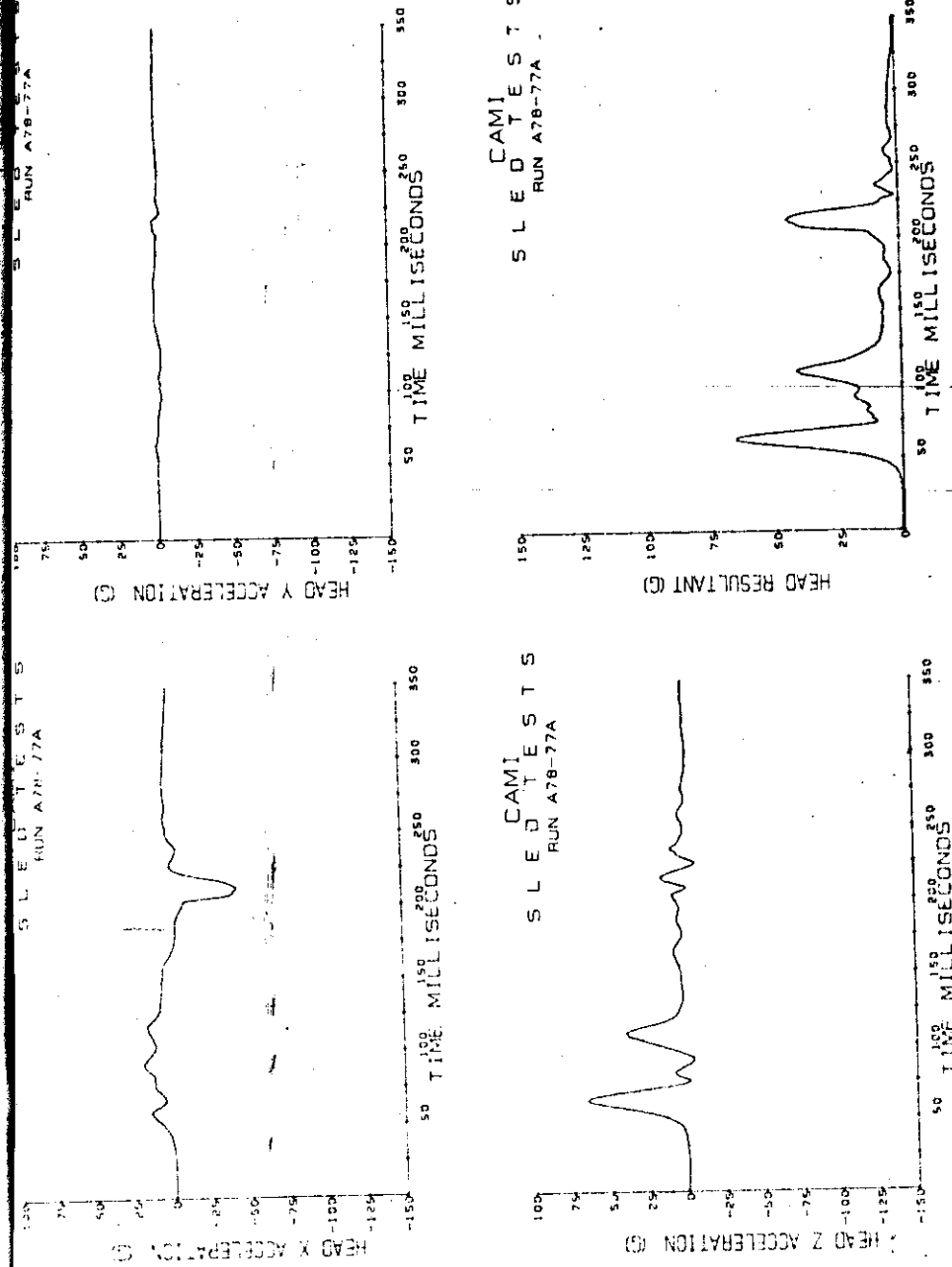


Figure C-2 (continued). 22-g tests.  
Head acceleration.

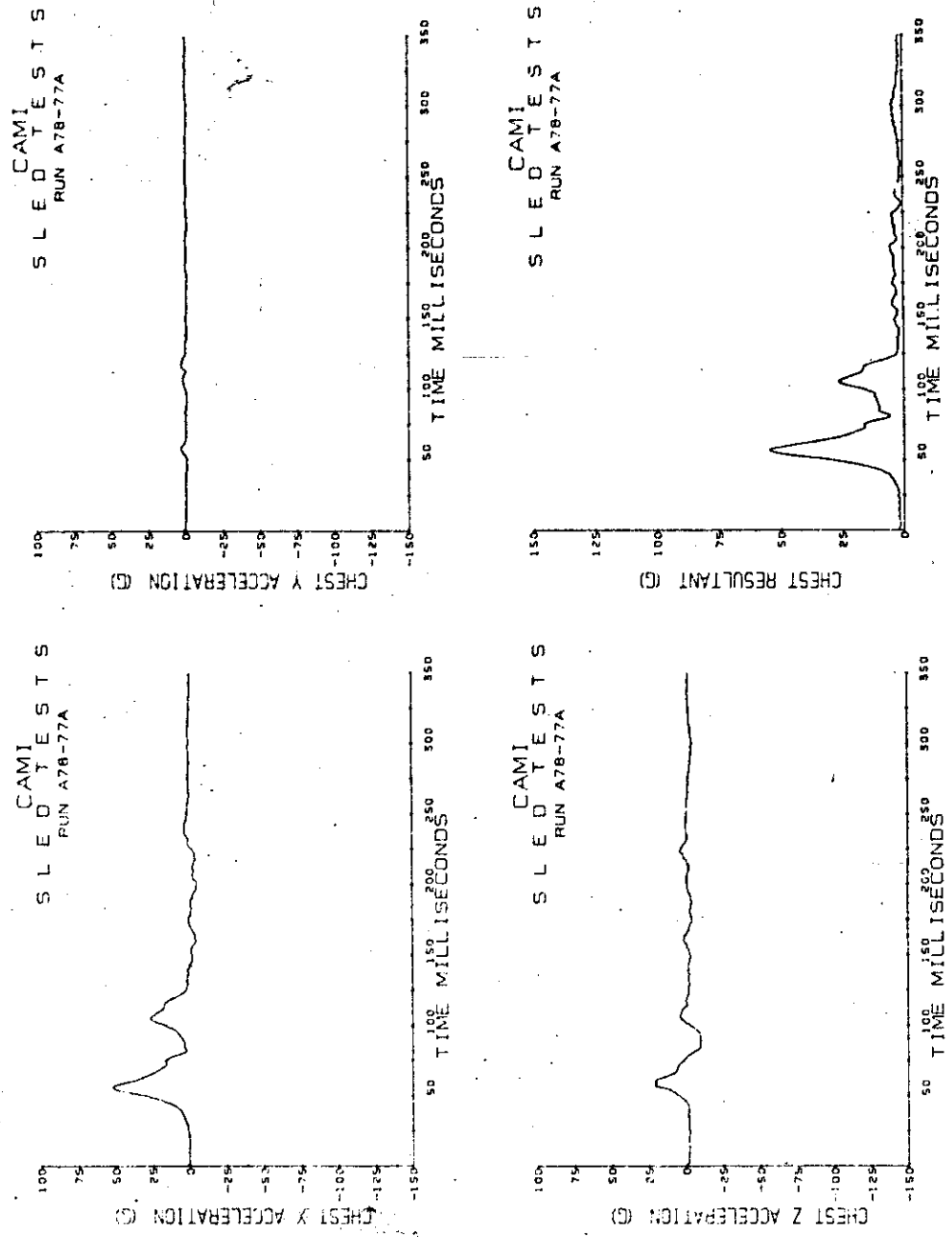


Figure C-2 (continued). 22-g tests.  
Chest acceleration.

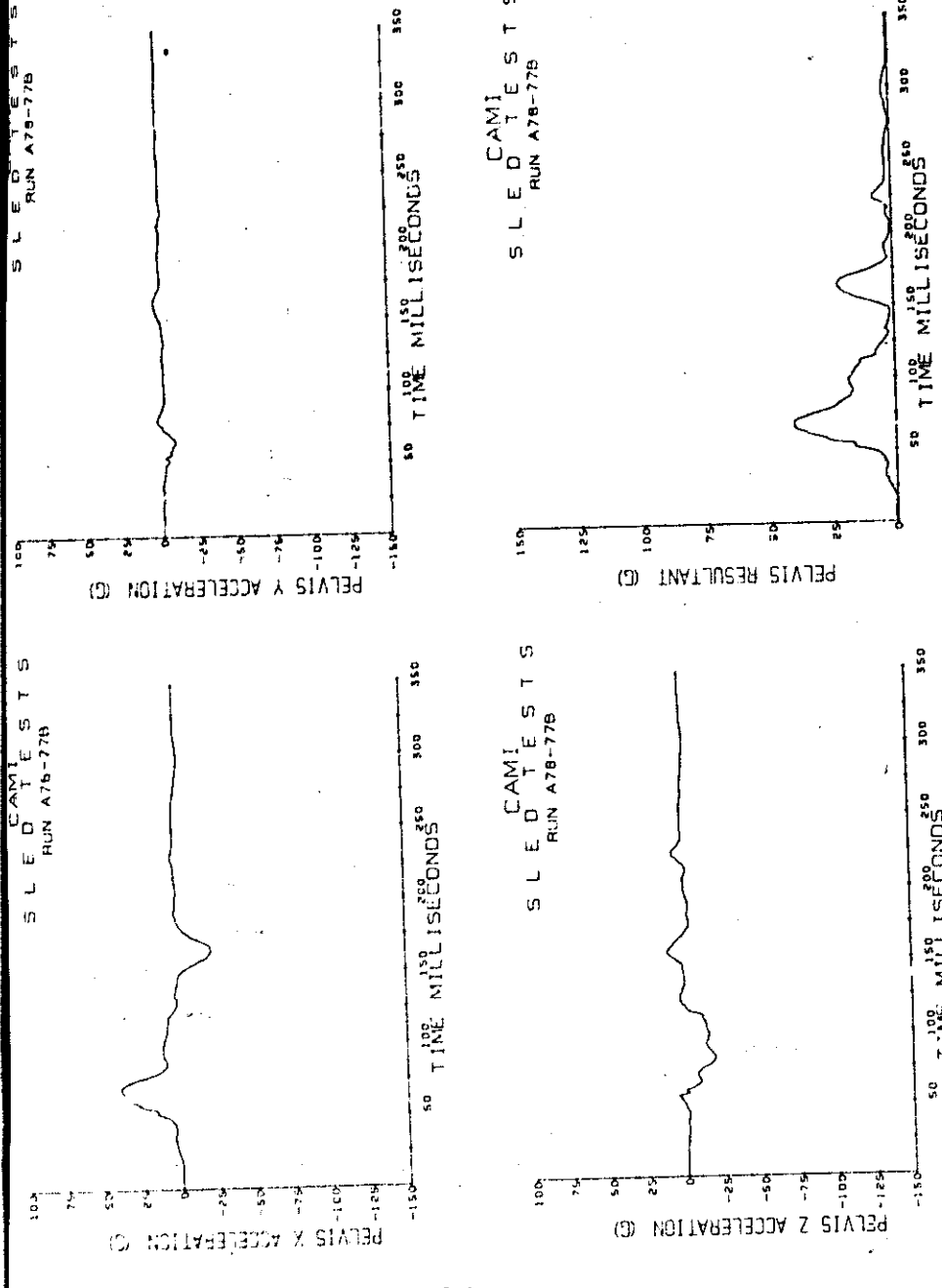


Figure C-2 (continued). 22-g tests.  
Pelvis acceleration.

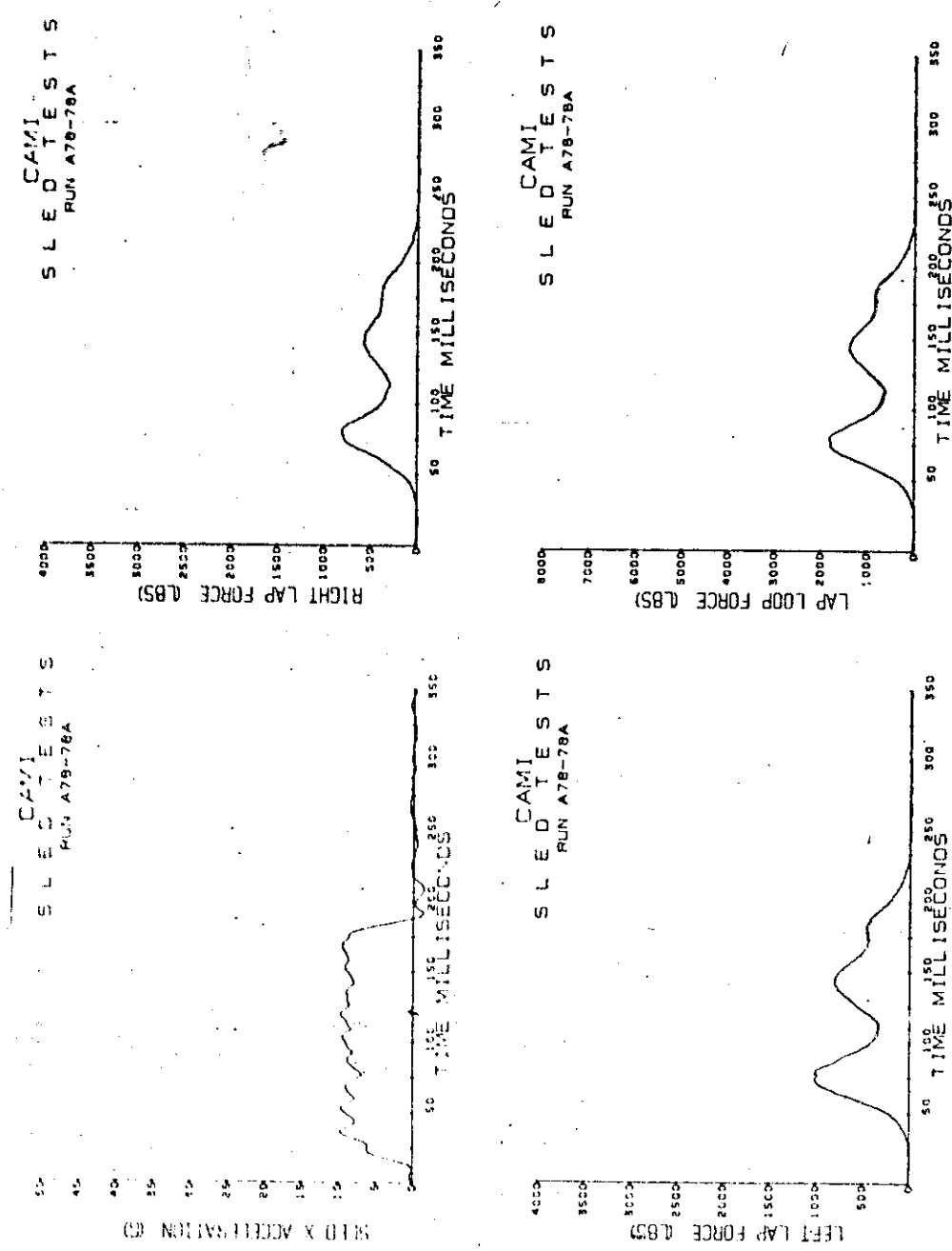


Figure C-3 Polyester webbing. 9-g tests.  
Sled deceleration and lapbelt loads.

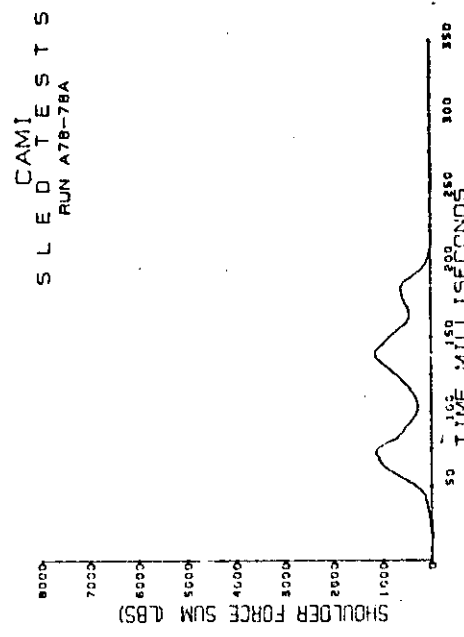
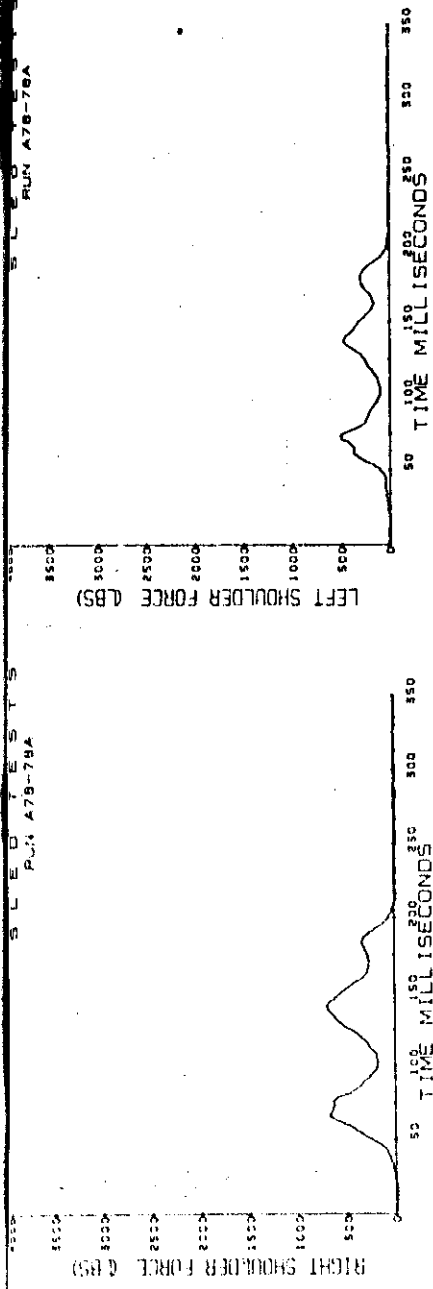


Figure C-3 (continued). 9-8 tests.  
Shoulder belt loads.

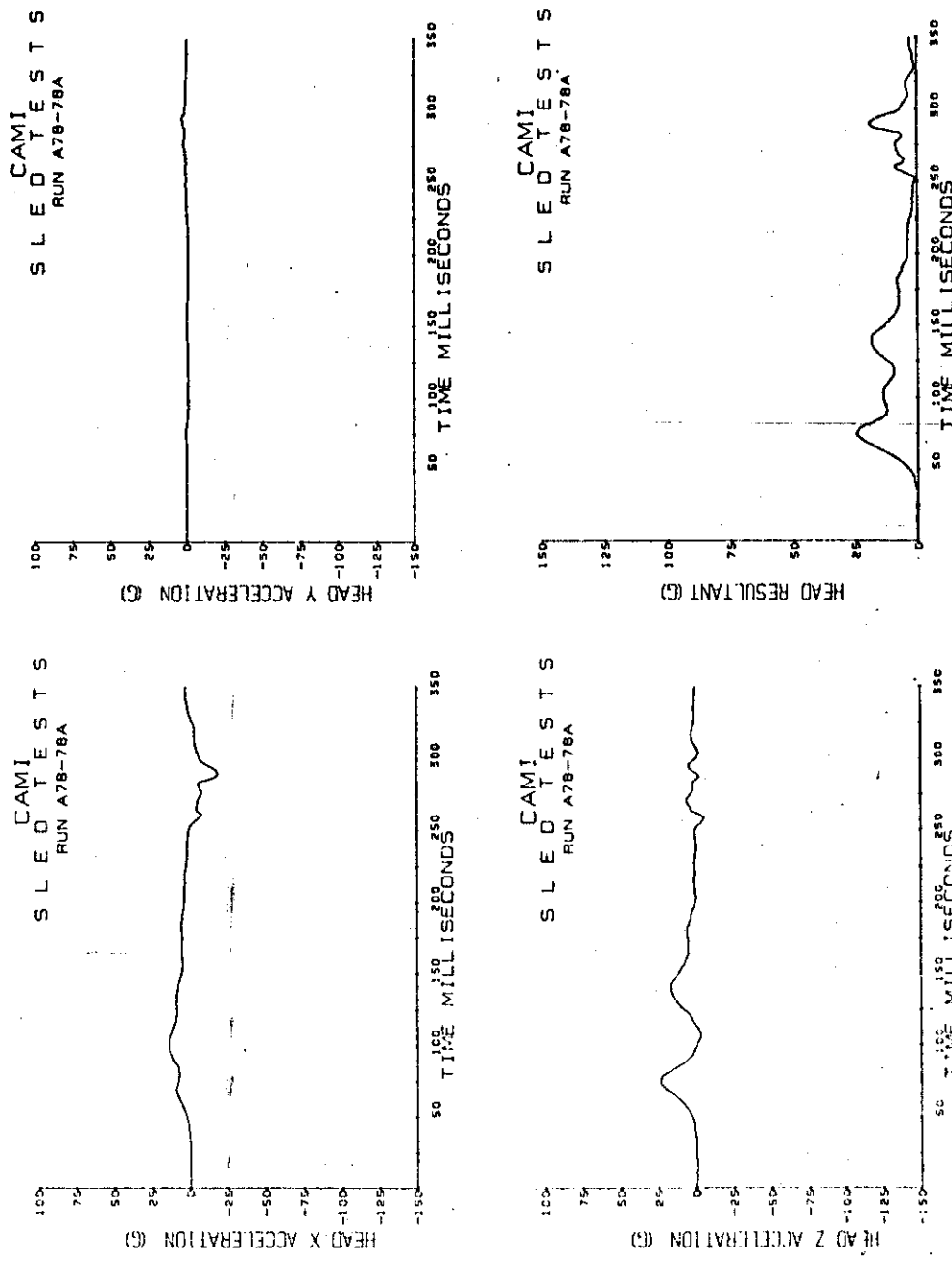


Figure C-3 (continued). 9-g tests.  
Head acceleration.

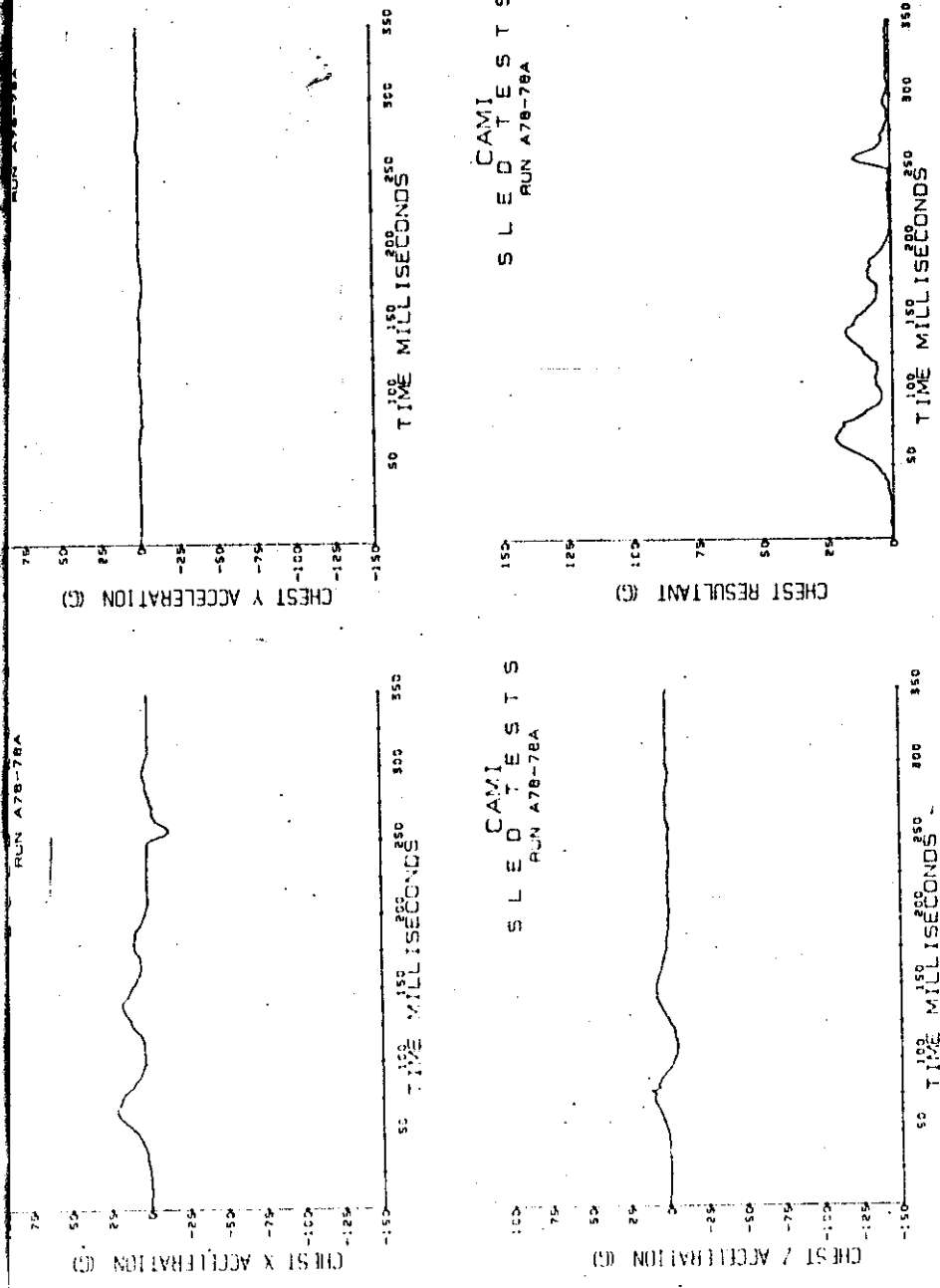
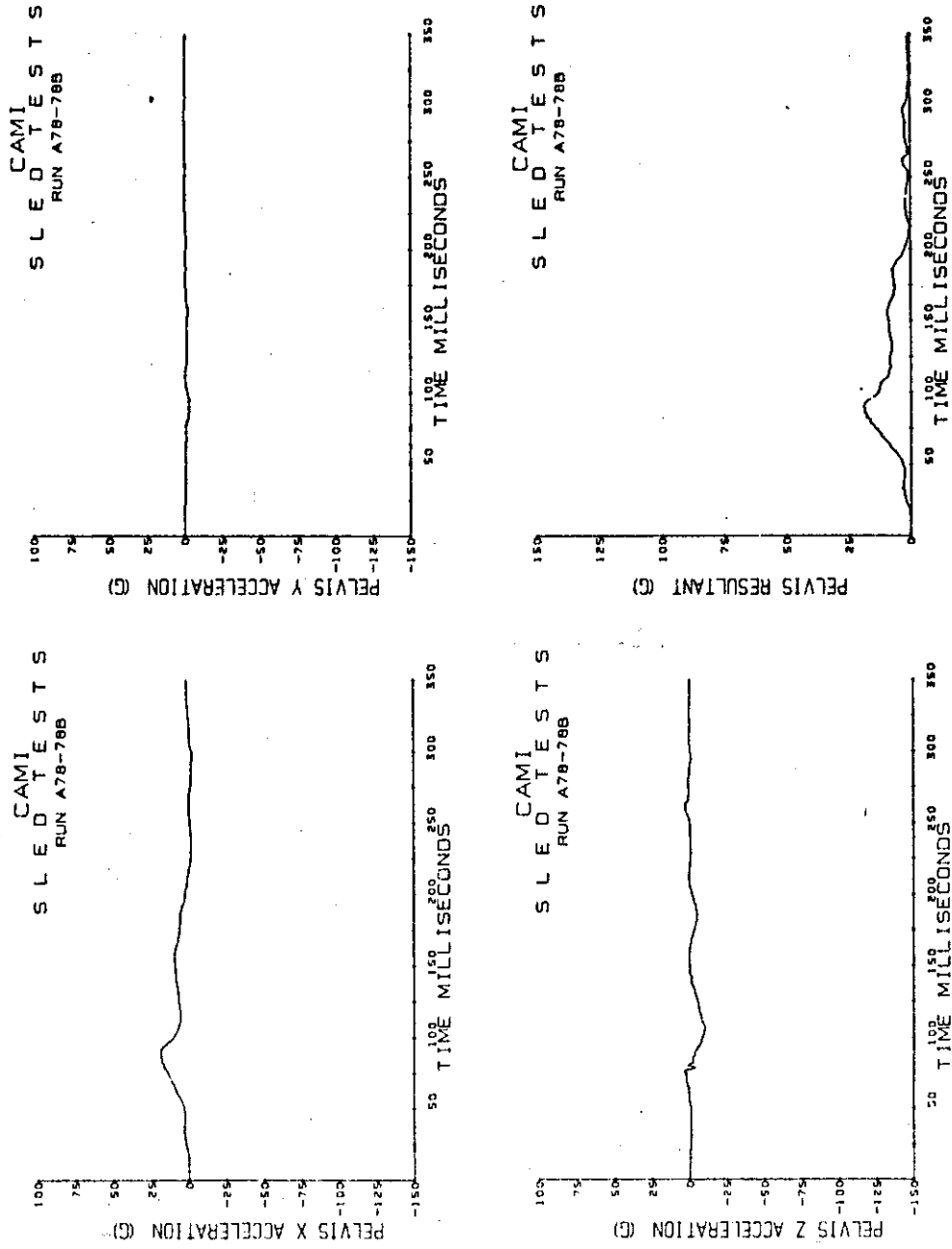


Figure C-3 (continued). 9-g tests.  
Chest acceleration.



205

Figure C-3 (continued). 9-8 tests.  
Pelvis acceleration.

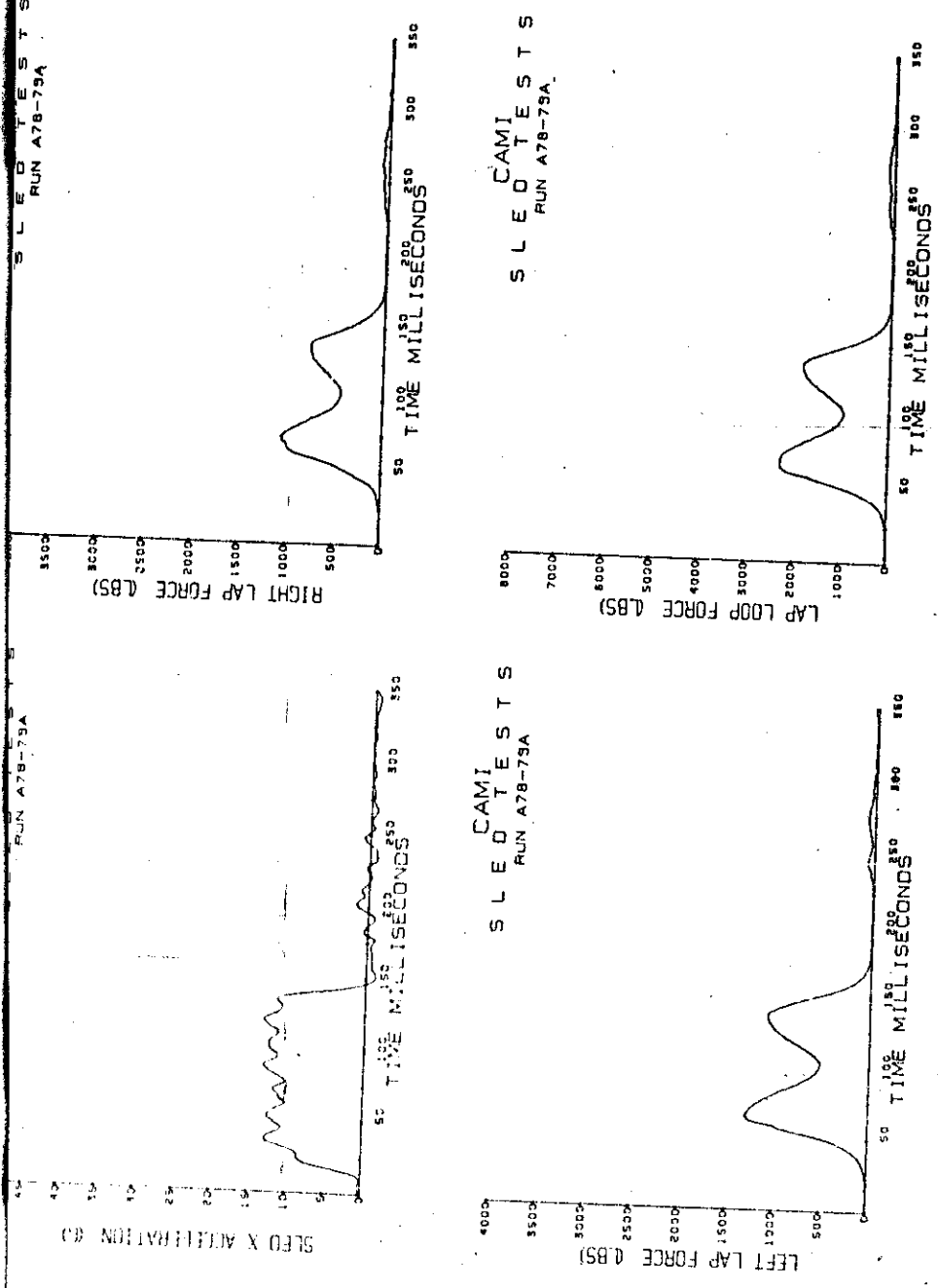


Figure C-3 (continued), 12-g tests.  
Sled deceleration and lapbelt loads.

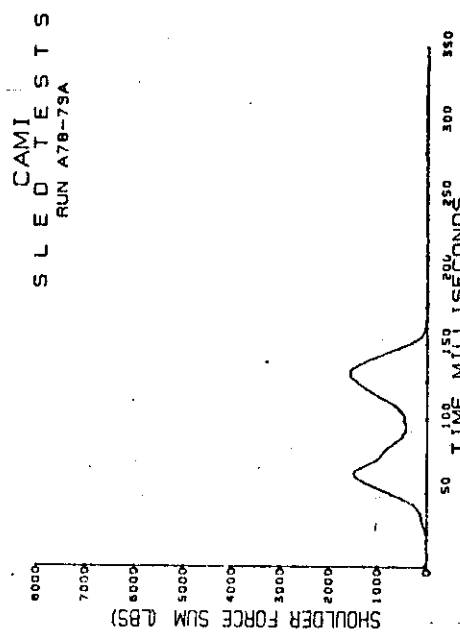
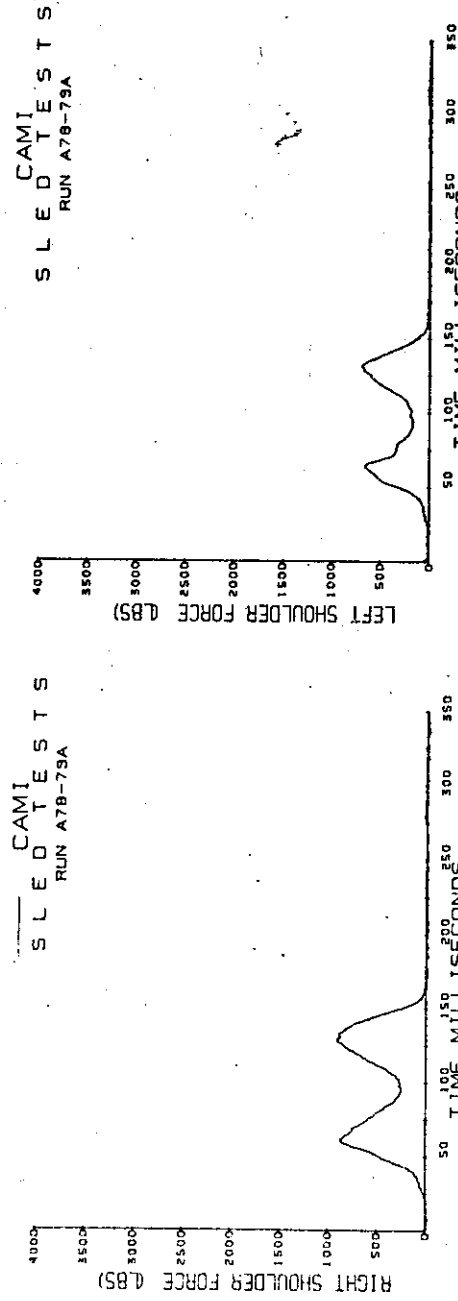


Figure C-3 (continued). 12-8 tests.  
Shoulder belt loads.

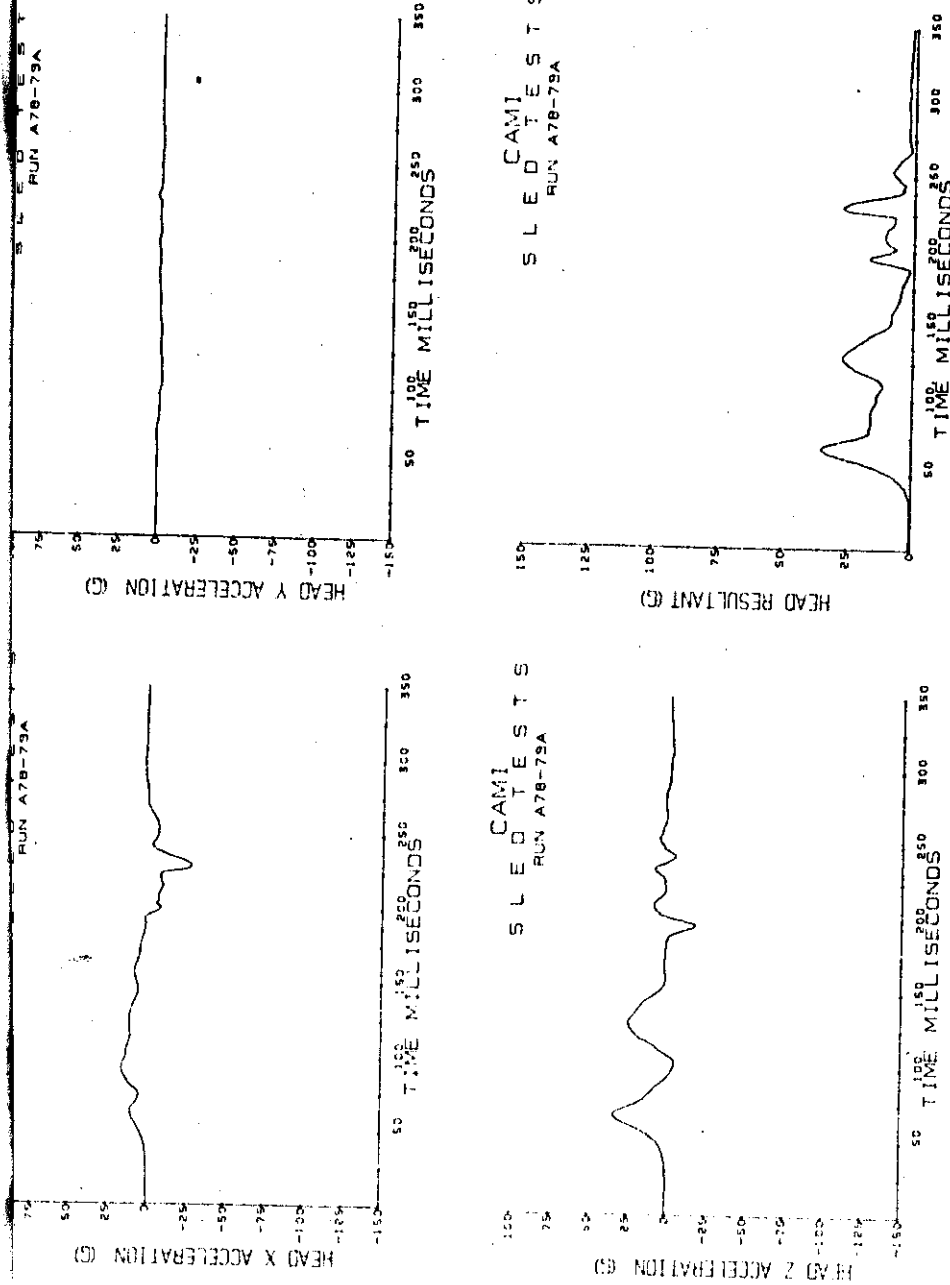


Figure C-3 (continued). 12-g tests.  
Head acceleration.

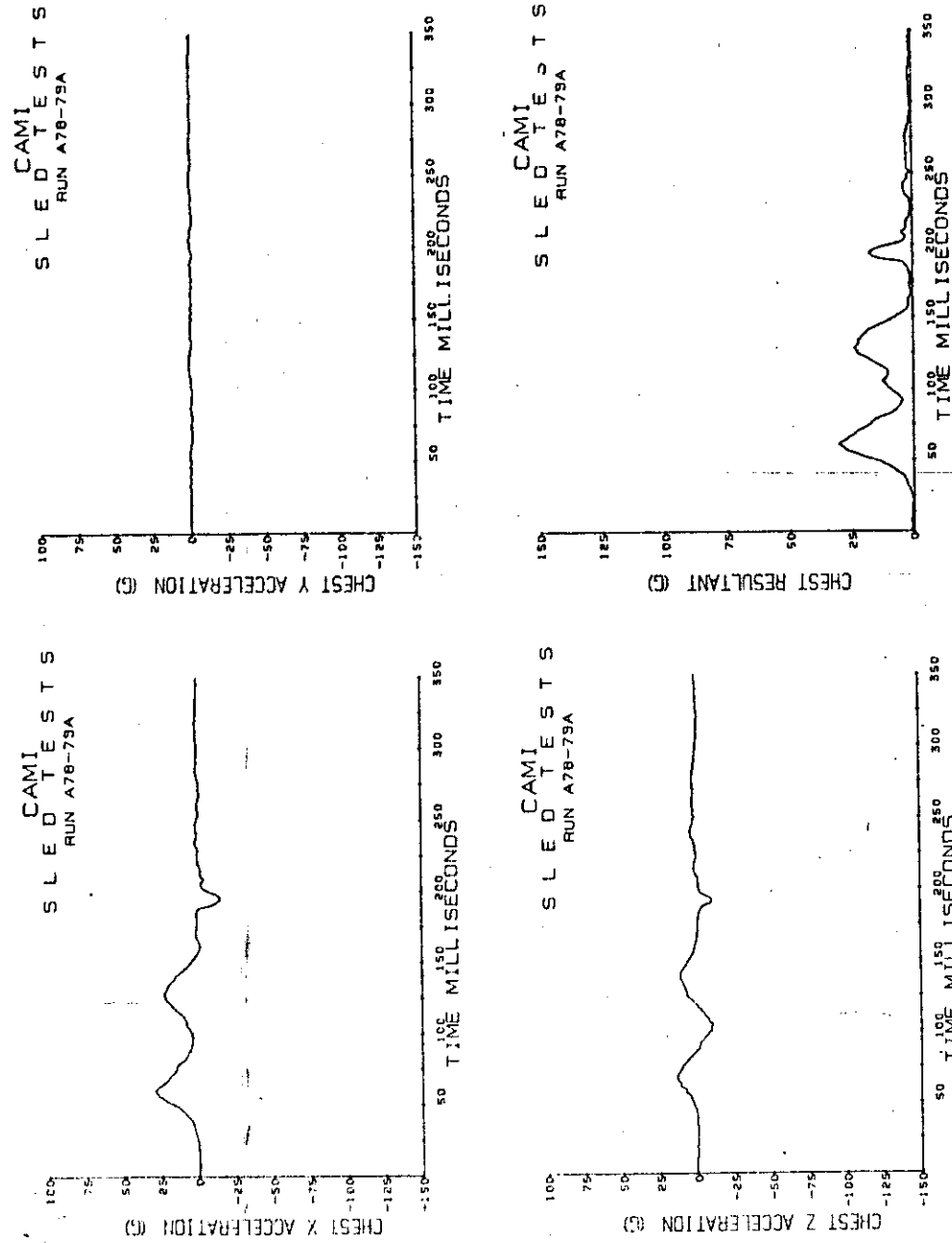
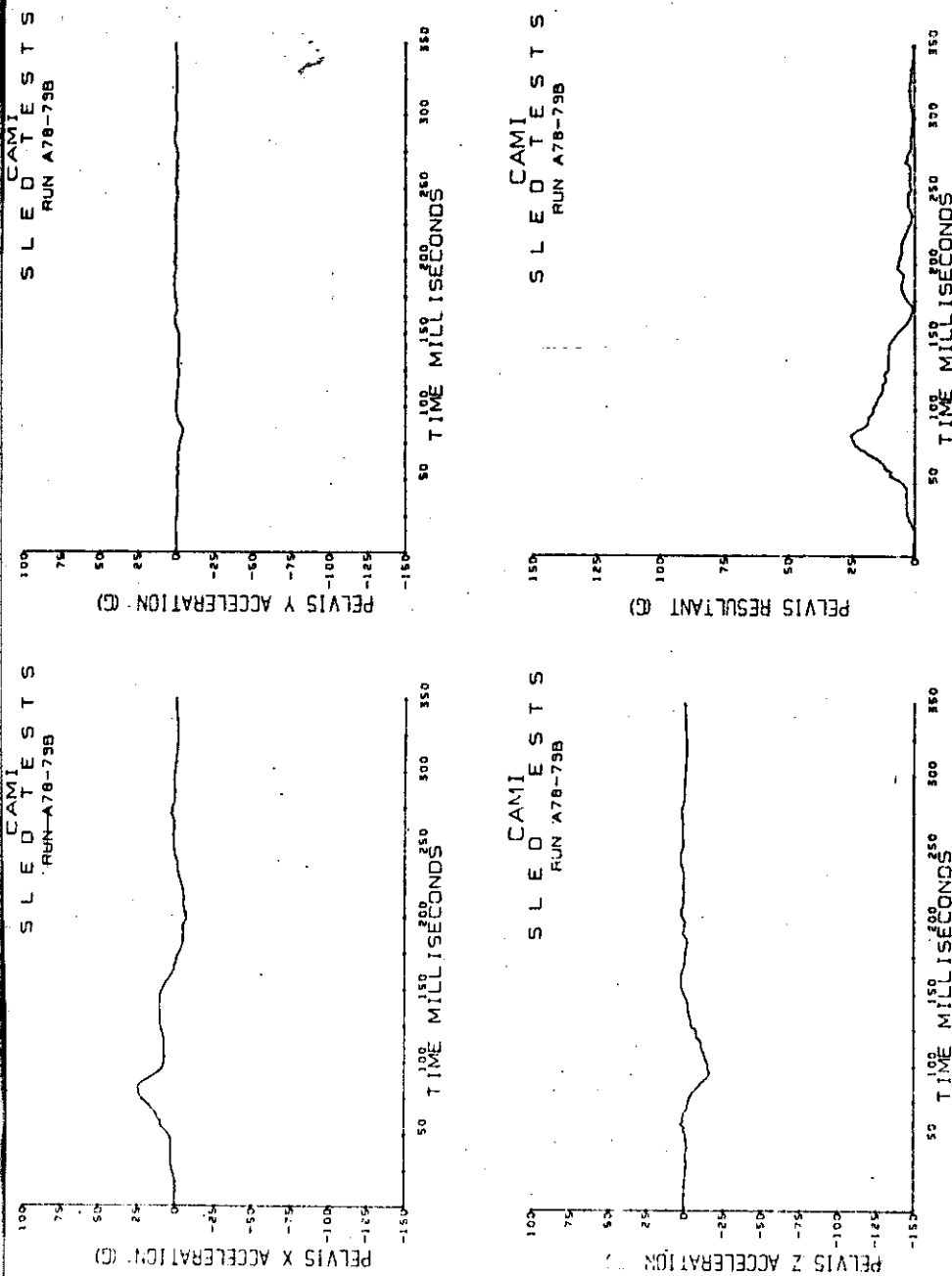


Figure C-3 (continued). 12-g tests.  
Chest acceleration.



210

Figure C-3 (continued). 12-8 tests.  
Pelvis acceleration.

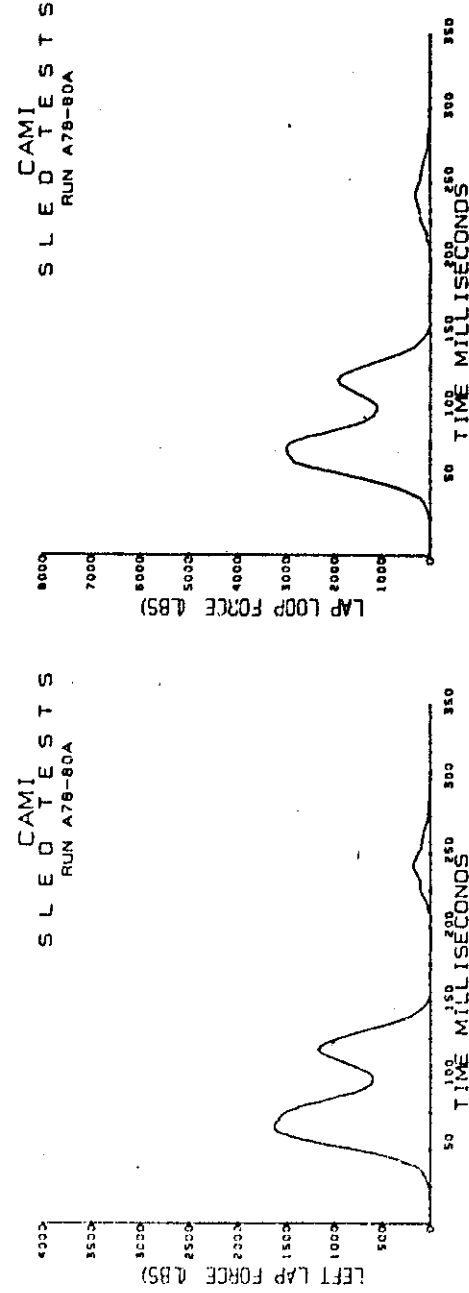
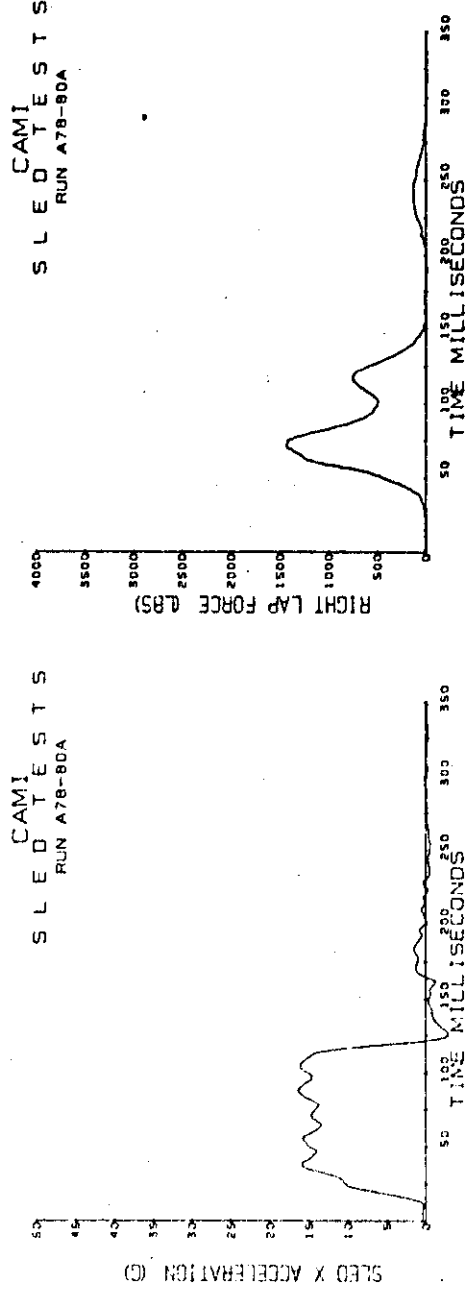


Figure C-3 (continued). 16-8 tests.  
Sled deceleration and lap belt loads.

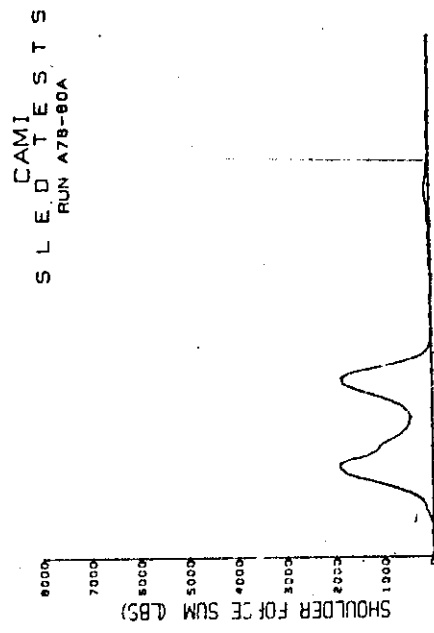
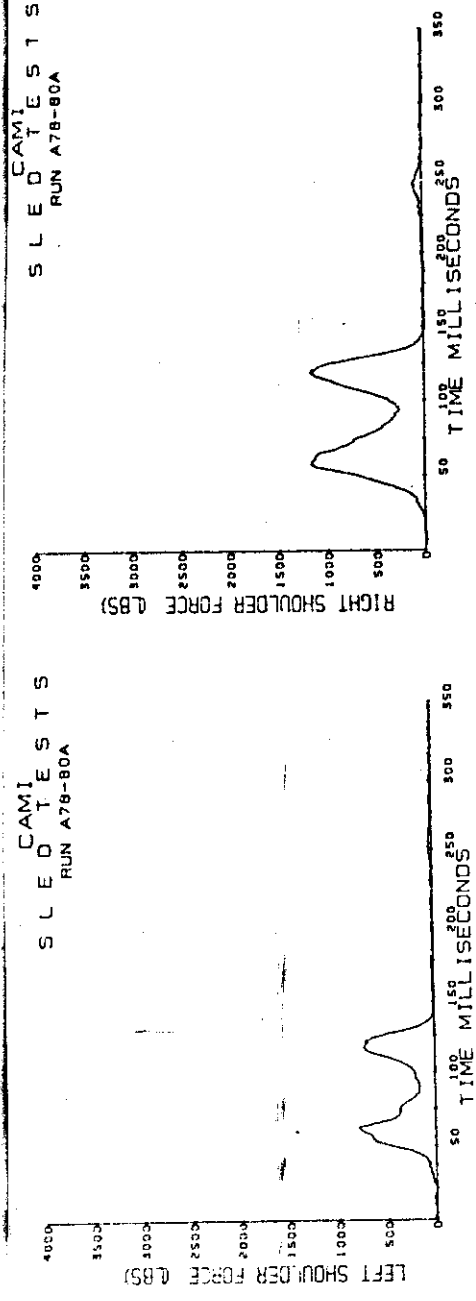


Figure C-3 (continued). 16-8 tests.  
Shoulder belt loads.

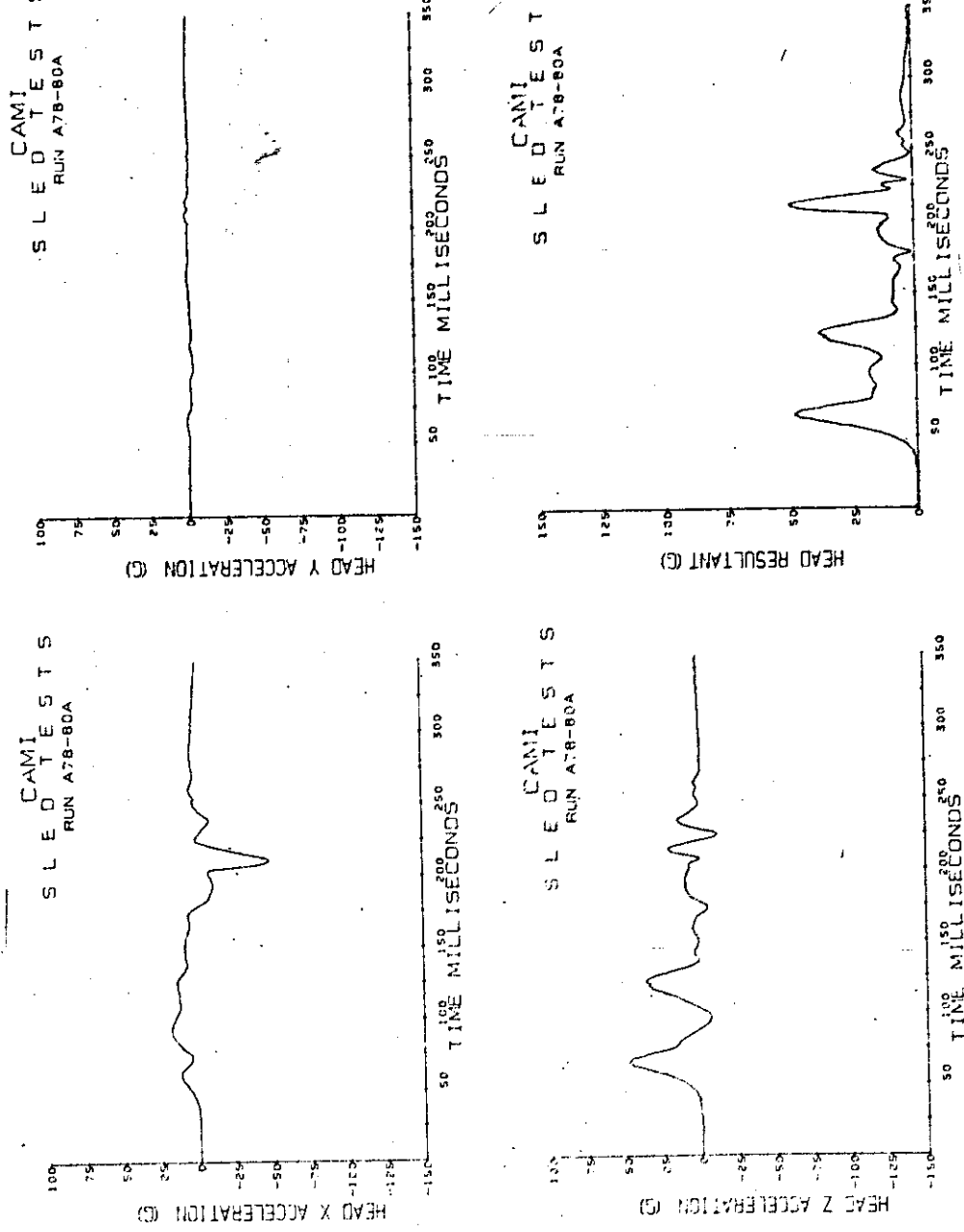


Figure C-3 (continued). 16-8 tests.  
Head acceleration.

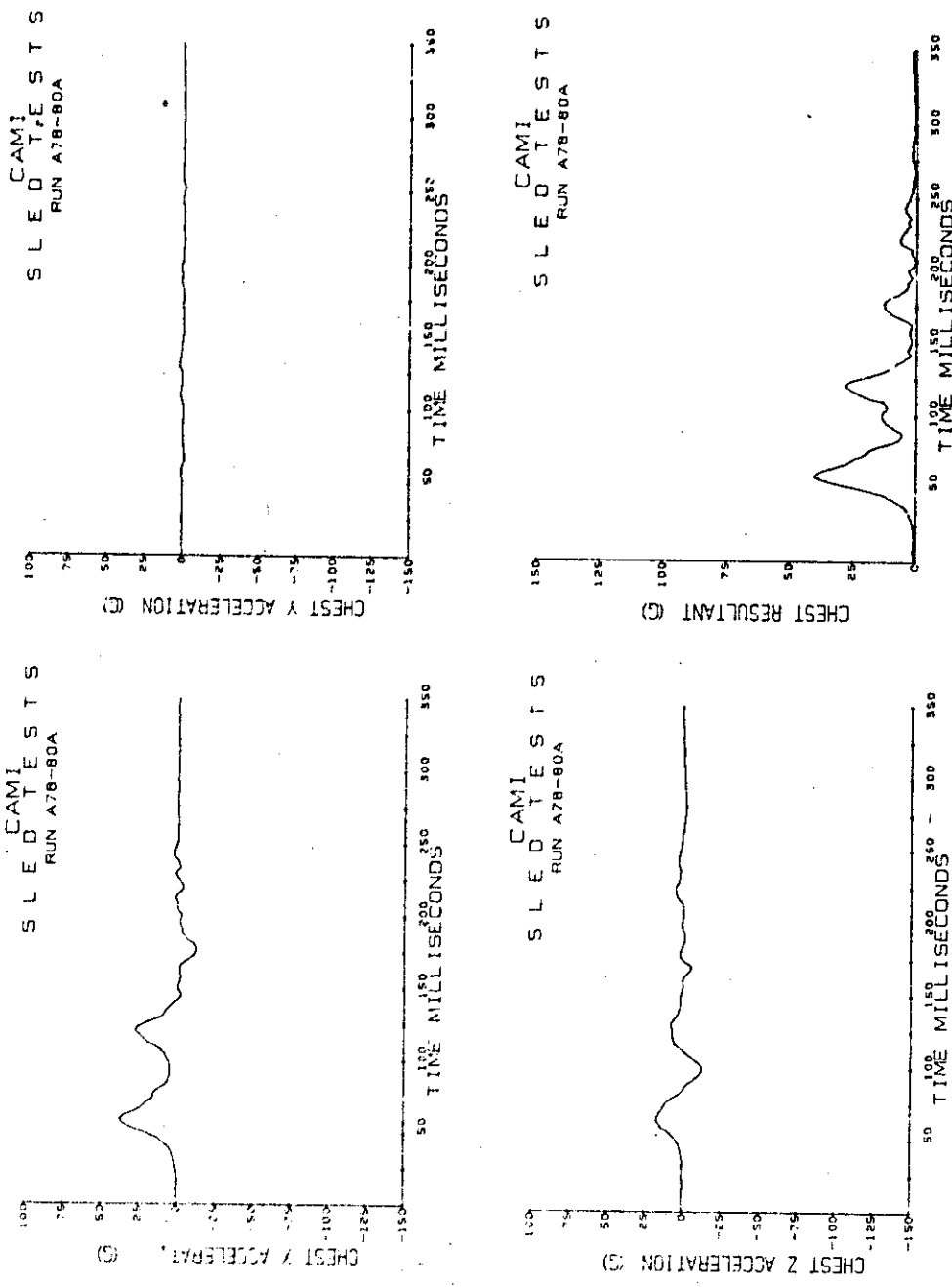


Figure C-3 (continued). 16-g tests.  
Chest acceleration.

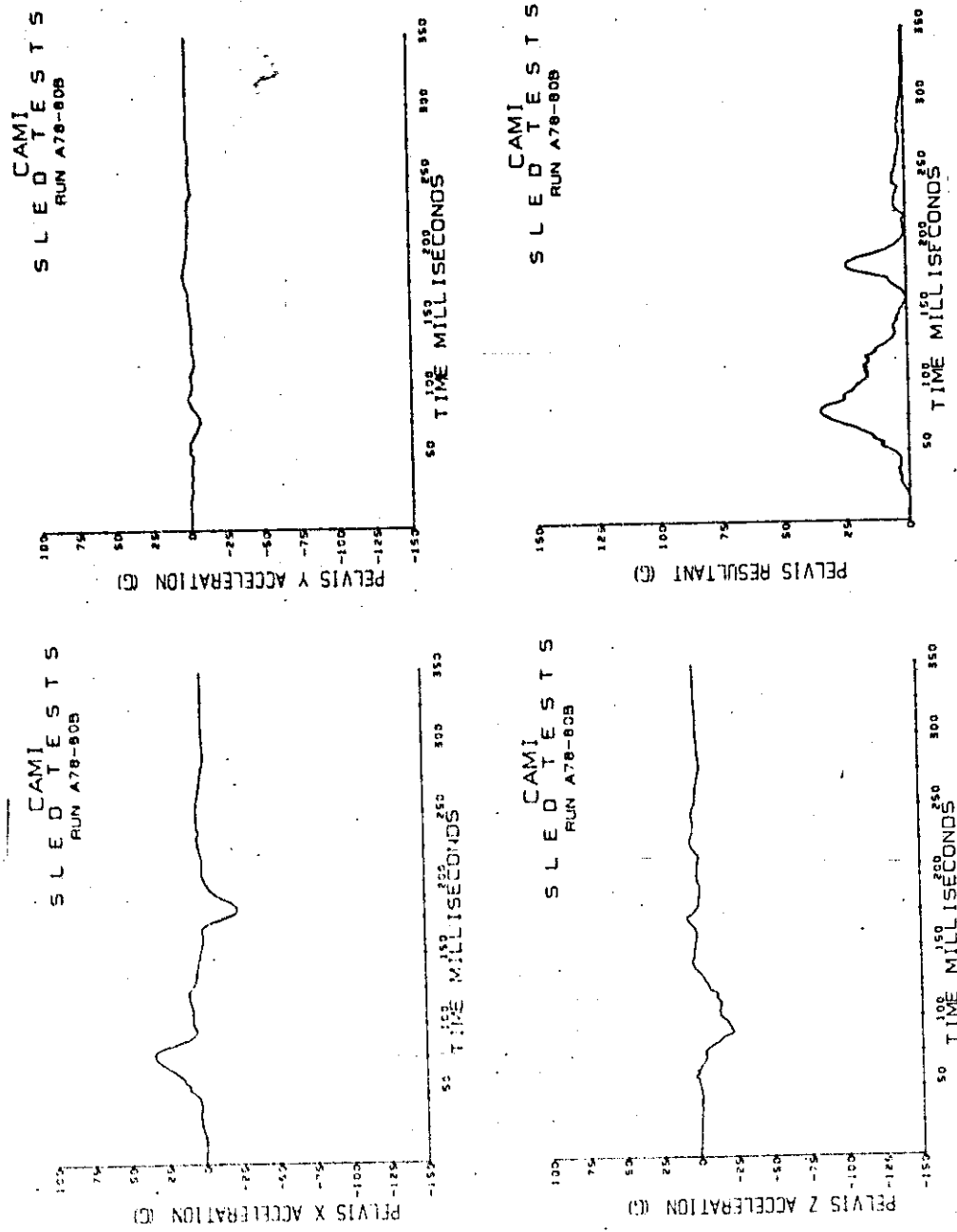


Figure C-3 (continued). 16-8 tests.  
Pelvis acceleration.

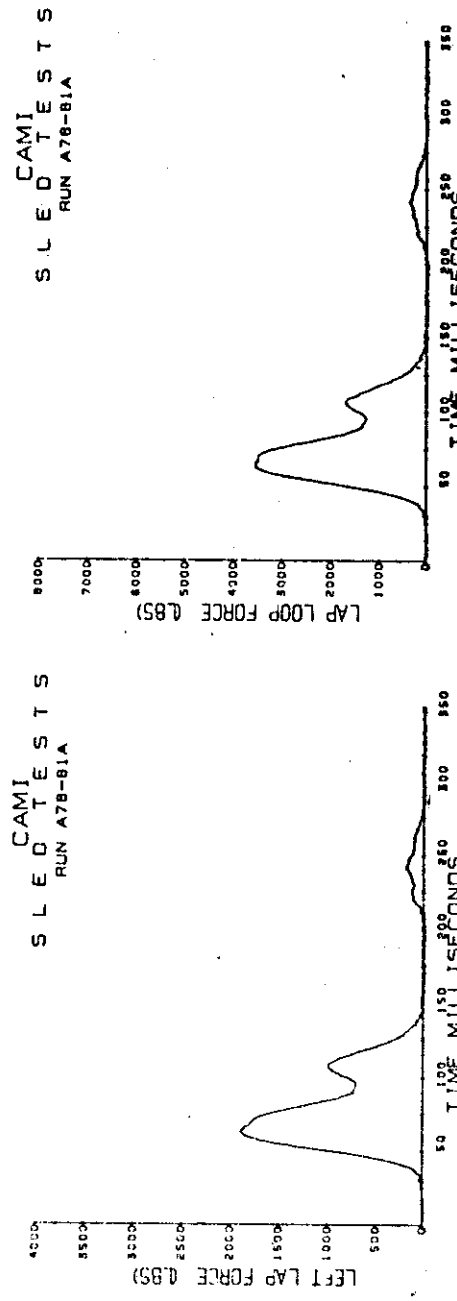
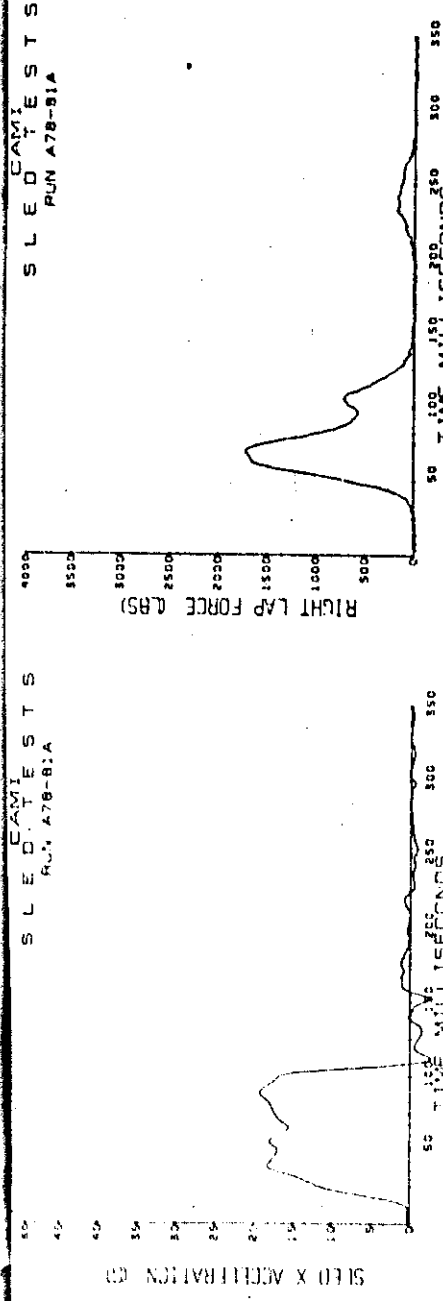


Figure C-3 (continued). 18-8 tests.  
Sled deceleration and lap belt loads.

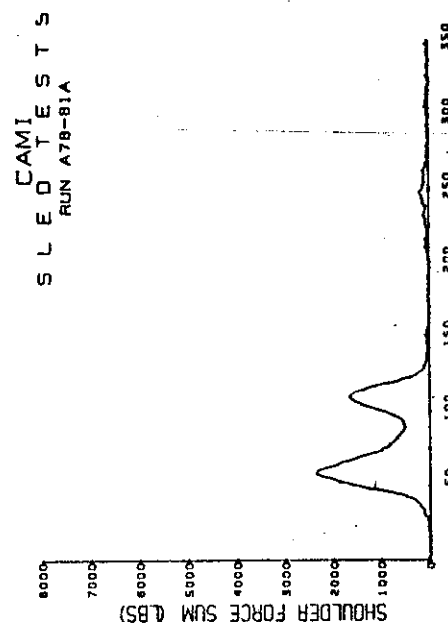
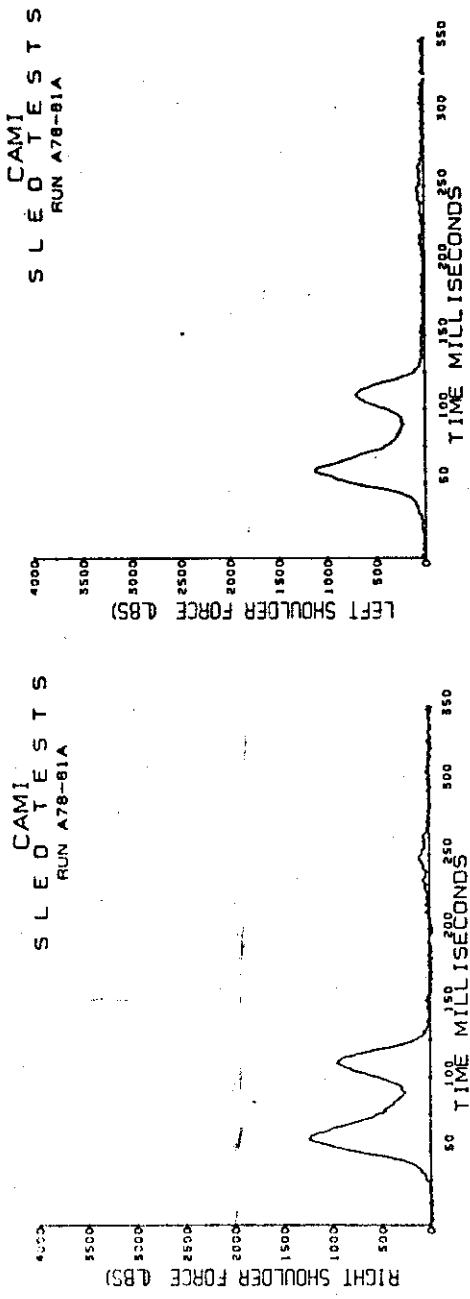


Figure C-3 (continued). 18-g tests.  
Shoulder belt loads.

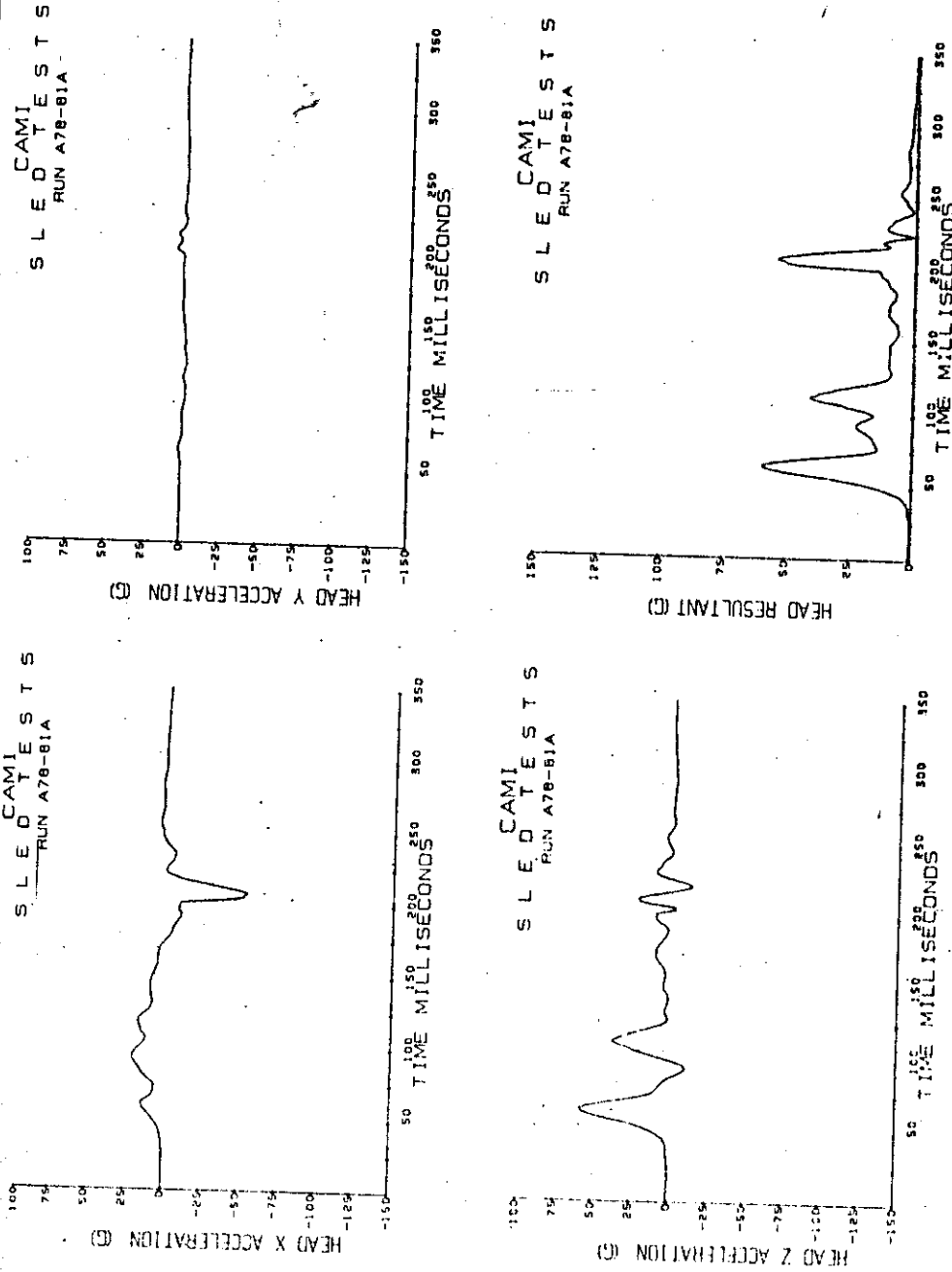


Figure C-3 (continued). 18-8 tests.  
Head acceleration.

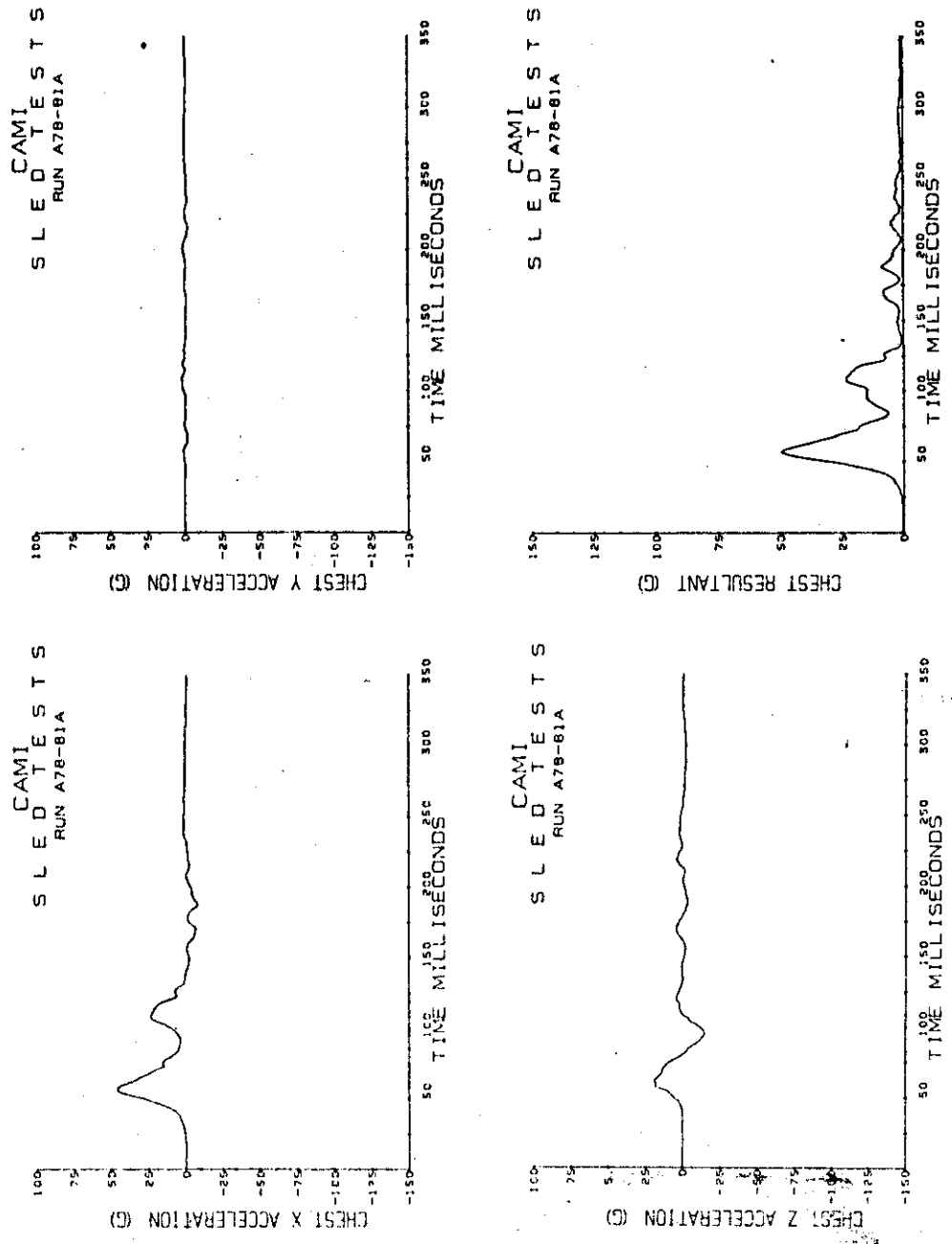


Figure C-3 (continued), 18-g tests.  
Chest acceleration.

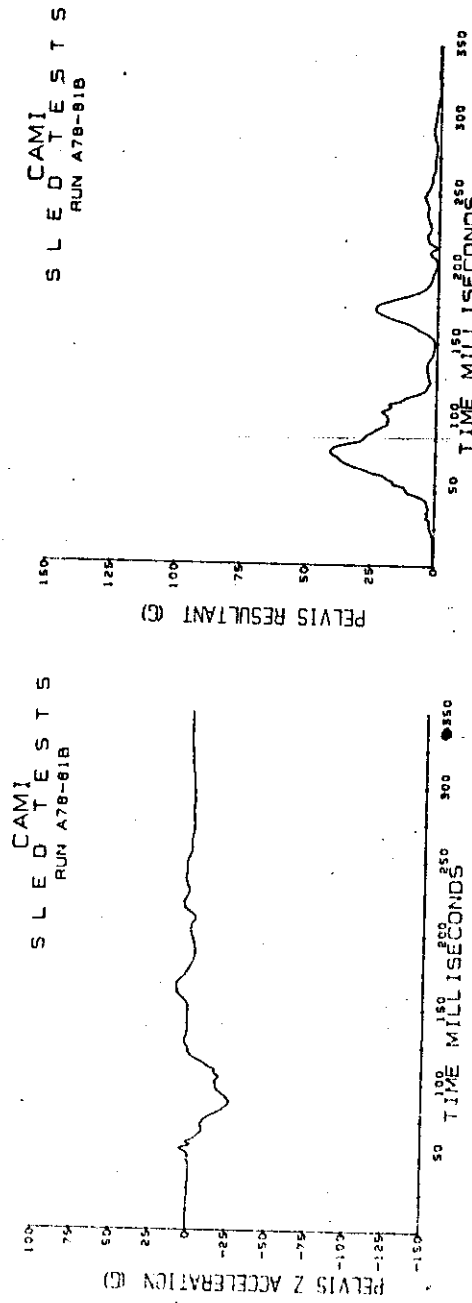
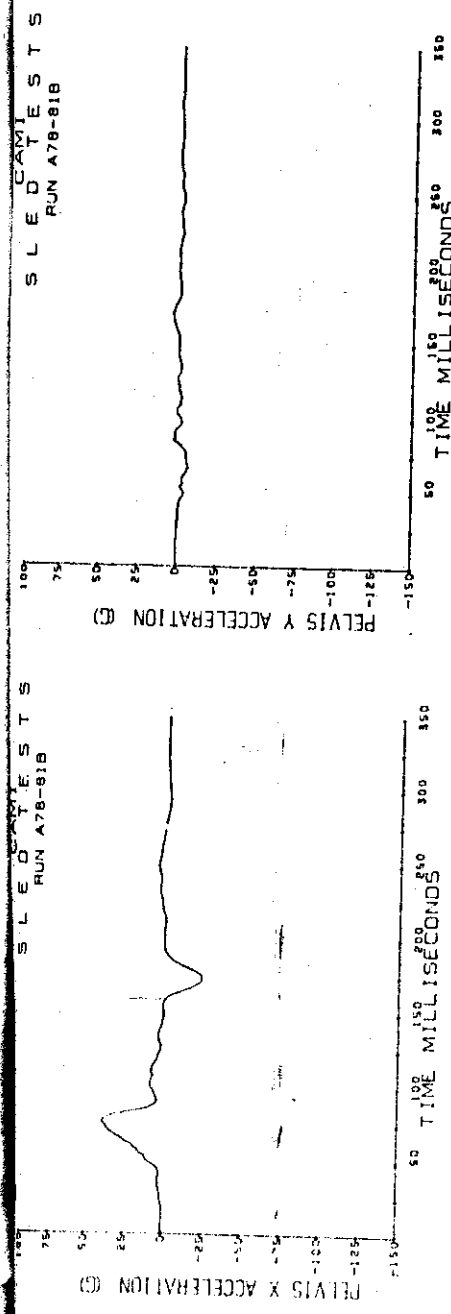


Figure C-3 (continued). 18-g tests.  
Pelvis acceleration.

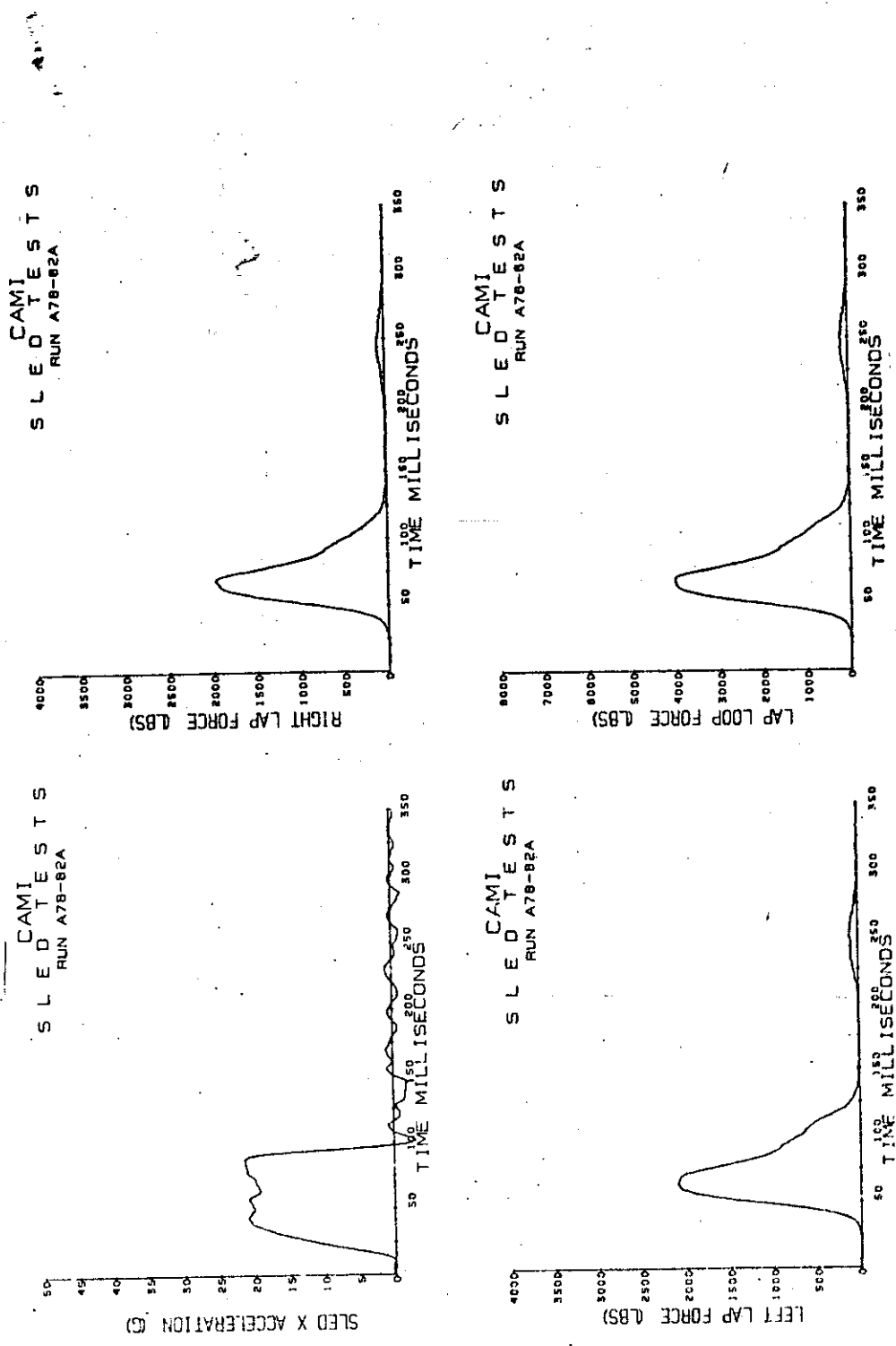


Figure C-3 (continued).  
21-g tests.  
Sled deceleration and lapbelt loads.

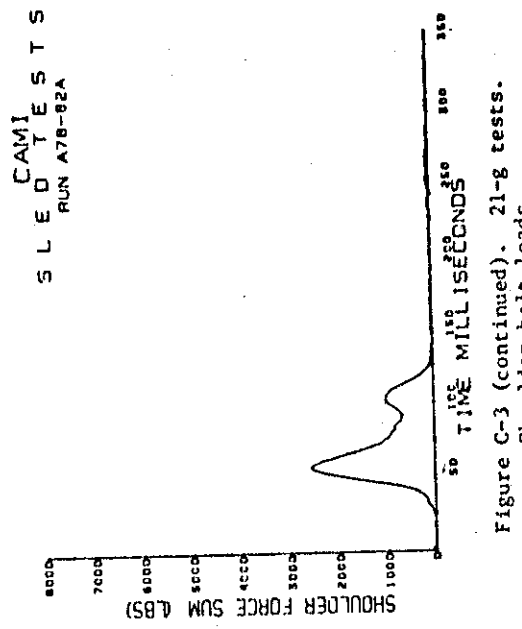
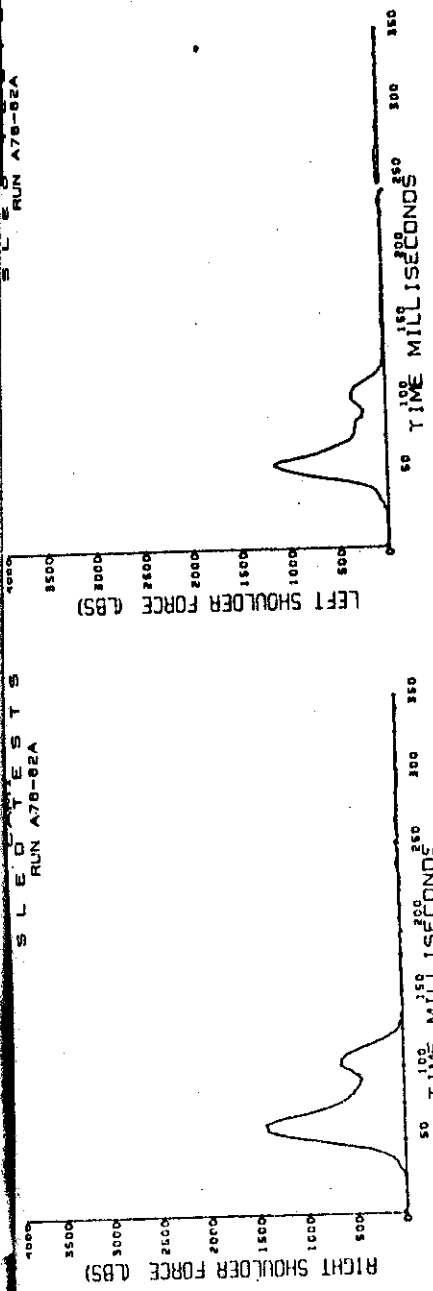


Figure C-3 (continued).  
SLE D tests.  
Shoulder belt loads.

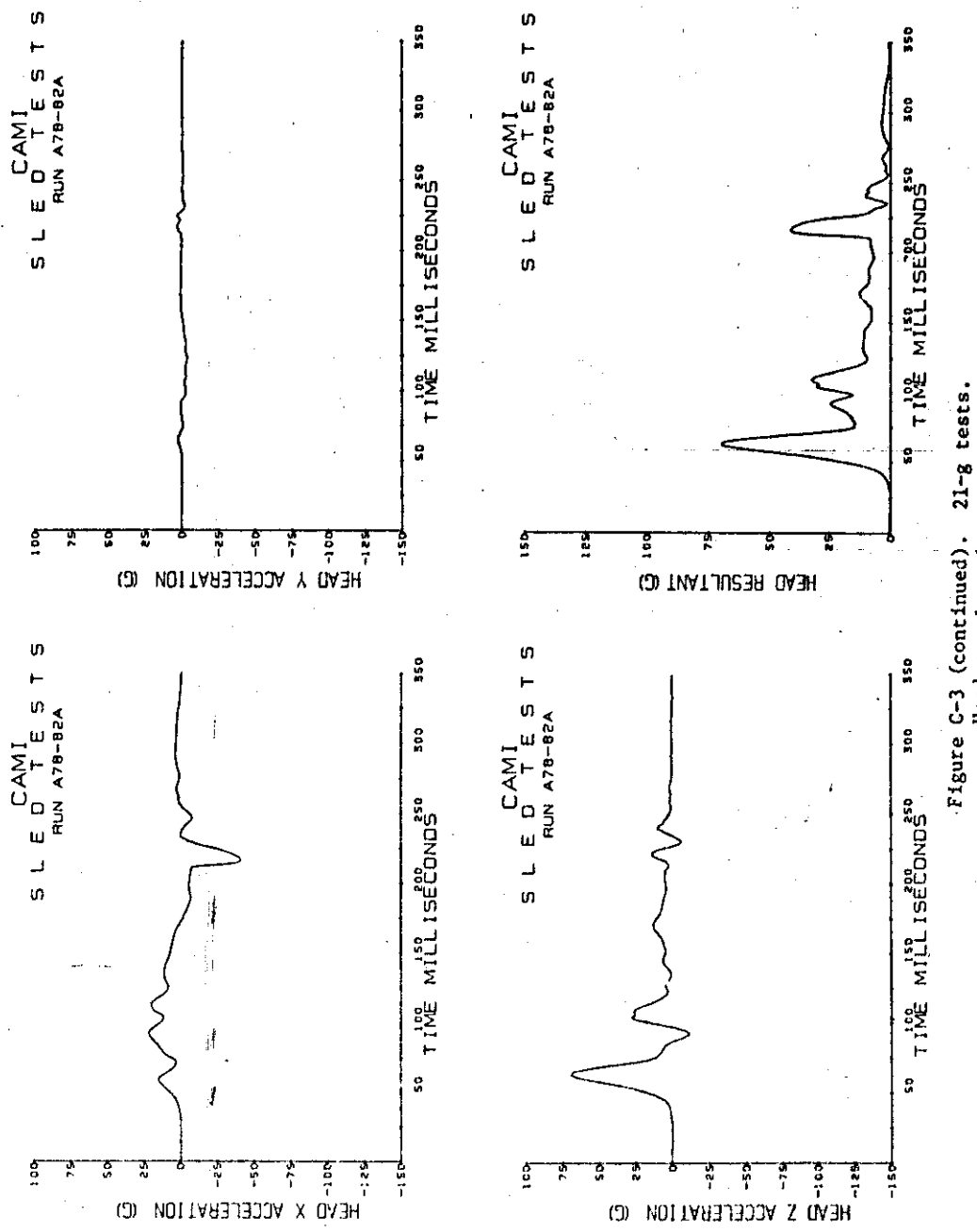


Figure C-3 (continued). 21-8 tests.  
Head acceleration.

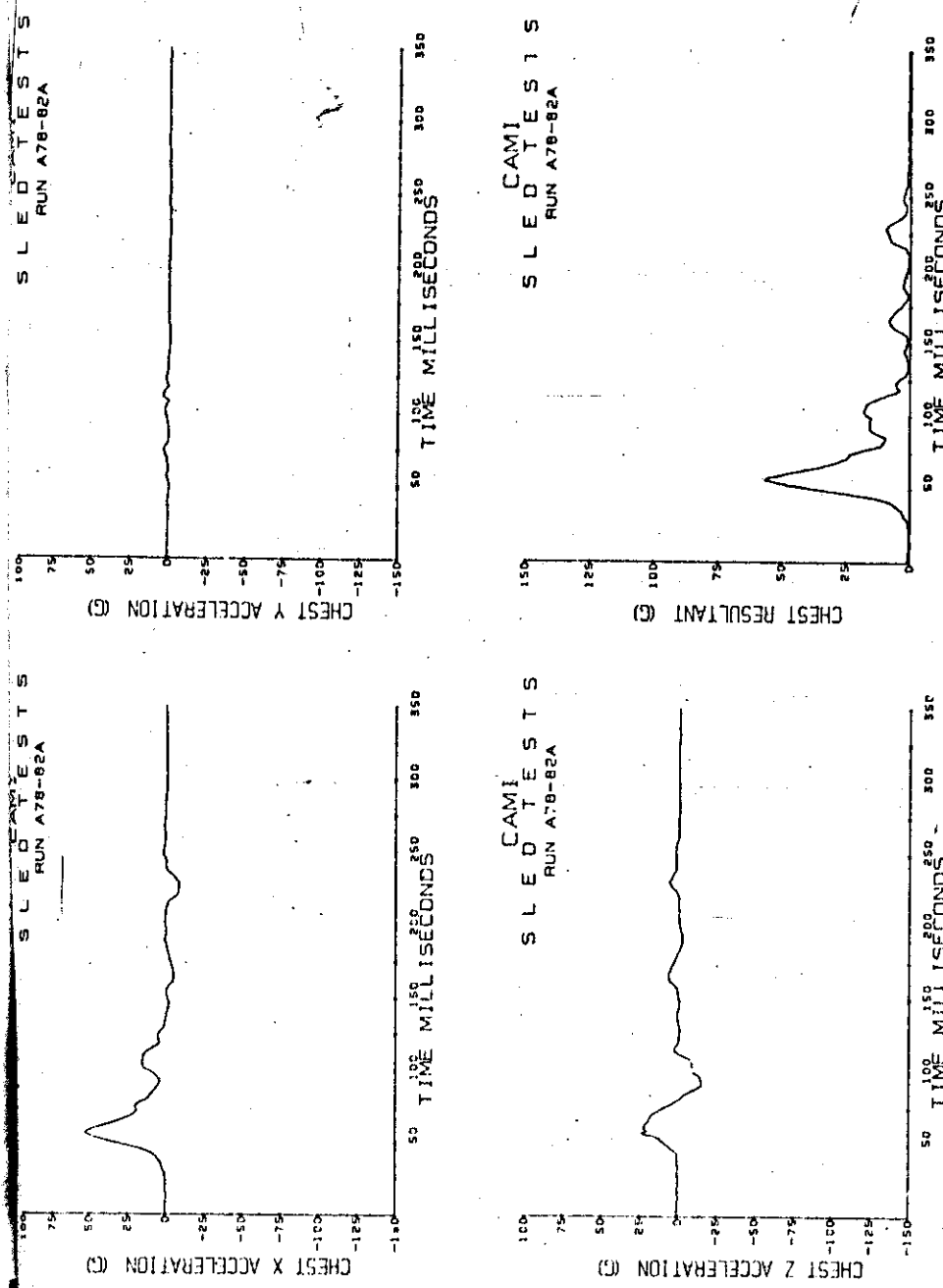


Figure C-3 (continued). 21-g tests.  
Chest acceleration.

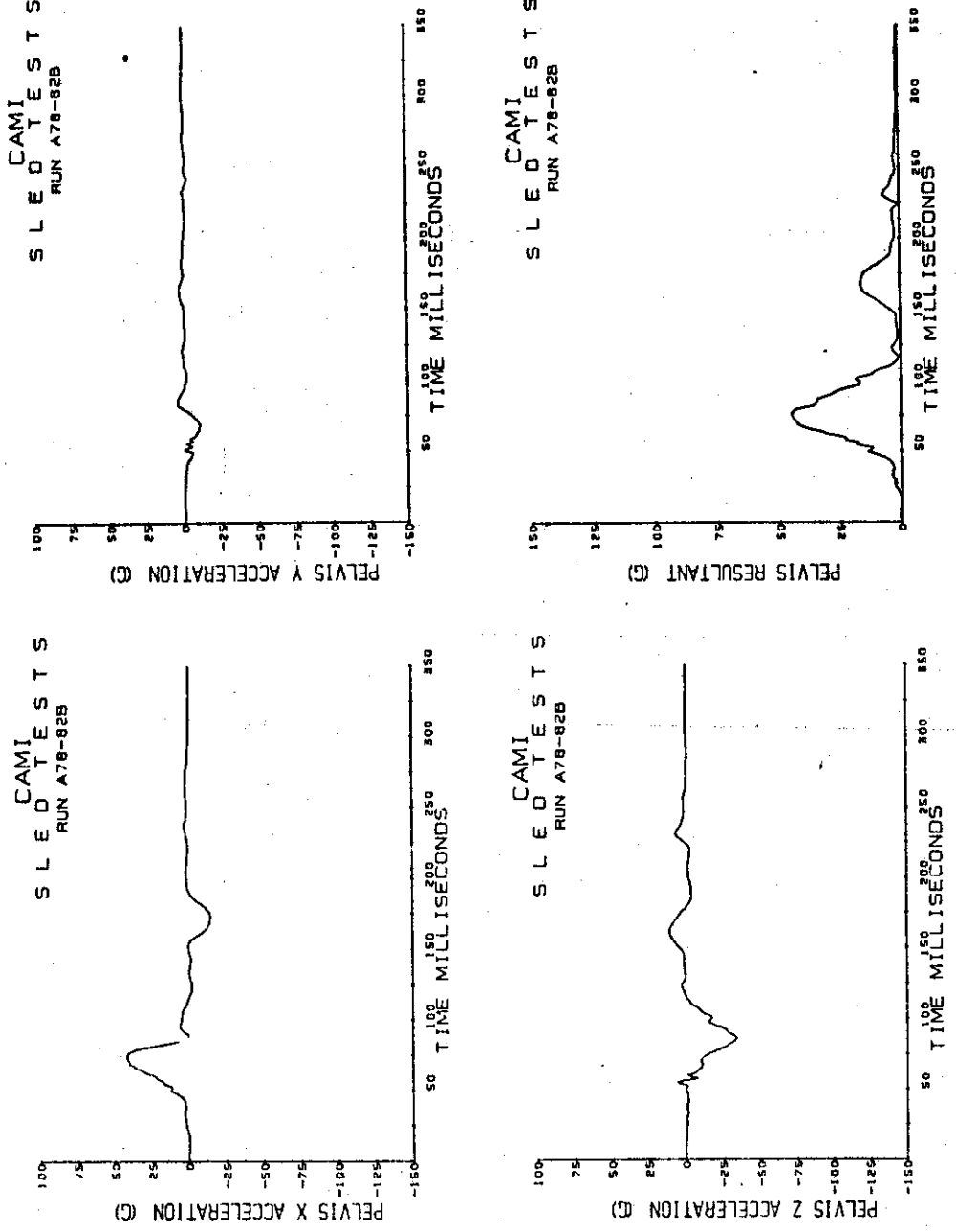


Figure C-3 (continued). 21-g tests.  
Pelvis acceleration.